

Impact of NanoBiocatalysts on *Saccharomyces cerevisiae* Metabolism for Ethanol Production: Process optimization, Kinetic studies and Preliminary scale-up

By

Isaac Adeyemi Sanusi

216075660



**Submitted in fulfilment of the academic requirements of
Doctor of Philosophy in Microbiology**

Discipline of Microbiology

School of Life Sciences

College of Agriculture, Engineering and Science

University of KwaZulu-Natal

Pietermaritzburg

South Africa

April 2021

PREFACE

The research contained in this thesis was completed by the candidate while based in the Discipline of Microbiology, School of Life Sciences of the College of Agriculture, Engineering and Science, University of KwaZulu-Natal, Pietermaritzburg campus, South Africa.

The contents of this work have not been submitted in any form to another university and, except where the work of others is acknowledged in the text, the results reported are due to investigations by the candidate.



.....
Signed: Prof. Gueguim E. B. Kana

Date: 09 April 2021

DECLARATION BY SUPERVISOR

I hereby declare that I supervised this PhD student:

Student's Full Name: Isaac Adeyemi Isaac

Student Number: 216075660

Thesis Title: Impact of Nanoparticle Biocatalysts on *Saccharomyces cerevisiae* Metabolism for Ethanol Production: Process optimization, Kinetic studies and Preliminary scale-up

Regular consultation took place between the student and me throughout the duration of this research. I advised the student to the best of my ability and approved the final document for submission to the College of Agriculture, Engineering and Science Higher Degrees Office for examination by the University appointed Examiners.

Signed:



.....
Prof E.B. Gueguim Kana (Supervisor)

Date: 09 April 2021

Declaration 1: Plagiarism

I, Isaac Adeyemi Sanusi, declare that:

- (i) The research reported in this dissertation, except where otherwise indicated or acknowledged, is my original work;
- (ii) This dissertation has not been submitted in full or in part for any degree or examination to any other university;
- (iii) This dissertation does not contain other persons' data, pictures, graphs or other information, unless specifically acknowledged as being sourced from other persons;
- (iv) This dissertation does not contain other persons' writing, unless specifically acknowledged as being sourced from other researchers. Where other written sources have been quoted, then:
 - a) Their words have been re-written but the general information attributed to them has been referenced;
 - b) Where their exact words have been used, their writing has been placed inside quotation marks, and referenced;
- (v) Where I have used material for which publications followed, I have indicated in detail my role in the work;
- (vi) This dissertation is primarily a collection of material, prepared by myself, published as journal articles or presented as a poster and oral presentations at conferences. In some cases, additional material has been included;
- (vii) This dissertation does not contain text, graphics or tables copied and pasted from the Internet, unless specifically acknowledged, and the source being detailed in the dissertation and in the References sections.



Isaac Adeyemi Sanusi (Student)

Date: 09 April 2021

Declaration 2: Publications

This thesis involves a compilation of manuscripts. Each chapter is an individual entity prepared as per the journals' specifications hence some repetition between chapters has been inevitable. The first author (student) conducted all experimental work, data collection and manuscript preparation, guided by the second and/or third (supervisor) author. The * indicates corresponding author.

Chapter 2

Isaac A. Sanusi, Yeshona Sewsynker-Sukai, E.B. Gueguim Kana*. Nanotechnology in Bioprocess Development: Applications of Nanoparticles in the Generation of Biofuels. In *Microbial Nanobiotechnology*. (2021) DOI:10.1007/978-981-33-4777-9_6. (Springer Book chapter).

Chapter 3

Isaac A. Sanusi, Funmilayo D. Faloye, Gueguim EB. Kana*. Impact of Various Metallic Oxide Nanoparticles on Ethanol Production by *Saccharomyces cerevisiae* BY4743: Screening, Kinetic Study and Validation on Potato Waste. *Catalysis Letters*. 149 (7) (2019) 2015-2031. <https://doi.org/10.1007/s10562-019-02796-6>.

Chapter 4

Isaac A. Sanusi, Terence N. Suinyuy and Gueguim EB. Kana*. Effect of nickel oxide nanoparticles on bioethanol production: Process optimization, kinetic and metabolic studies. *Process Biochemistry*. 92 (2020) 386–400. doi.org/10.1016/j.procbio.2020.01.029.

Chapter 5

Isaac A. Sanusi*, Terence N. Suinyuy, and Gueguim EB. Kana. Impact of nanoparticle inclusion on bioethanol production process kinetic and inhibitor profile. *Biotechnology Reports* 29 (2021) e00585, <https://doi.org/10.1016/j.btre.2021.e00585>.

Chapter 6

Isaac A. Sanusi*, Gueguim E. B. Kana. Preliminary scale-up studies of simultaneous saccharification and bioethanol production from waste potato peels supplemented with NiO nanoparticles. Submitted to: *Process Biochemistry*.



Signed: Isaac Adeyemi Sanusi (Student)

Date: 09 April 2021

Conference presentations

Sanusi A. Isaac and Kana E. B. Gueguim. Impact of metallic oxide nanoparticles on bioethanol production by *Saccharomyces cerevisiae* BY4743: Screening and Kinetic study. College of Agriculture, Engineering and Science Postgraduate Research and Innovation Day. Westville Campus, 26 October, 2017. Oral presentation.

Sanusi A. Isaac and Kana E. B. Gueguim. Effect of Nanoparticles Concentration, pH, Agitation on Bioethanol Production by *Saccharomyces cerevisiae* BY4743: An Optimization Study. 19th International Conference on Nanobiology (World Academic of Science Engineering and Technology Conference), 11-12 December, 2017. Kuala Lumpur, Malaysia. Oral presentation.

Sanusi A. Isaac and Kana E. B. Gueguim. Effect of NiO NP Concentration, pH, Temperature and Substrate concentration on Ethanol Production by *Saccharomyces cerevisiae* BY4743: An Optimization Study. School of Life Sciences Research Day. Pietermaritzburg Campus, 22 May, 2018. Poster presentation.

Sanusi A. Isaac and Kana E. B. Gueguim. Effect of NiO NP Concentration, pH, Temperature and Substrate concentration on Ethanol Production by *Saccharomyces cerevisiae* BY4743: An Optimization Study. College of Agriculture, Engineering and Science Postgraduate Research Innovation Symposium. Westville Campus, 25 October 2018. Poster presentation.

Sanusi A. Isaac and Kana E. B. Gueguim. Impact of various metallic oxide nanoparticles on ethanol production by *Saccharomyces cerevisiae* BY4743: Screening, kinetic study and validation on potato waste. School of Life Sciences Annual Post graduate Research Day. Westville Campus, 22 May 2019. Poster presentation.

Sanusi A. Isaac and Kana E. B. Gueguim. Preliminary scale up studies of nano-catalysed simultaneous saccharification and bioethanol production from waste potato peels. College of Agriculture, Engineering and Science Online 2020 Postgraduate Research & Innovation Symposium (PRIS). Flash presentation.


Signed: Isaac Adeyemi Sanusi (Student)

Date: 09 April 2021

Abstract

The challenges of the energy crisis and environmental pollution are vital global issues as a result of over-dependence on fossil fuels. These are driving the need to develop a renewable, sustainable, and eco-friendly energy source to replace the high dependency on fossil fuels, which are also rapidly depleting. Bioethanol has emerged as a promising alternative to fossil fuels due to its high energy content and environmentally friendly profile. However, high production cost and low yield are major obstacles to large-scale bioethanol production. Thus, a need to investigate novel strategies for improved yield and economically feasible production. These strategies involve the inclusion of nano additives in bioprocessing, process optimization, scale-up studies, and the utilisation of renewable feedstock such as agricultural residues, which are abundant and sustainable. The use of nanoparticles in bioprocessing has attracted significant attention due to their distinctive physical and chemical nature. The addition of nanoparticles could influence the process performance, which might affect the microbial metabolism (stimulates cellular and enzymatic biochemical activities) of ethanol production. This study investigates the use of different nanomaterials as a biocatalyst to enhance bioethanol production using *Saccharomyces cerevisiae* BY4743. The linear and interactive effect of nano inclusion on the key process parameters for ethanol production was optimized. Further assessment of bioethanol production at semi-pilot scale, including the geometry, rheology and hydrodynamic parameters, were investigated.

The potentials of nine nanoparticles as biocatalysts for bioethanol production were evaluated. Fermentation processes with varying nanoparticle concentrations were experimentally assessed for glucose utilisation, ethanol yield, ethanol productivity, and fermentation efficiency. The fermentation input variables consisted of nanoparticle concentration, incubating temperature, pH, glucose concentration and agitation speed. The glucose utilisation, ethanol yield, ethanol productivity and fermentation efficiency ranged from 21.95 to 99.95%, 0.03 to 0.26 g/g, 0.01 to 0.22 g/L/h and 1.27 to 50.96%, respectively. Kinetic studies showed that a maximum specific

growth rate (μ_{max}) of 0.80 h^{-1} and potential maximum ethanol concentration (P_m) of 5.24 g/L were obtained with $0.01 \text{ wt} \%$ Nickel (II) Oxide (NiO) NPs.

Moreover, response surface methodology was used to investigate the effects of NiO NPs concentration ($0\text{-}0.05 \text{ wt}\%$), temperature ($20\text{-}50 \text{ }^\circ\text{C}$), glucose concentration ($10\text{-}50 \text{ g/L}$) and pH ($4\text{-}6$) on biomass concentration and ethanol yield. The optimized process showed an increased biomass concentration and ethanol yield of 1.03 and 1.19 fold, respectively. Supplementation with NiO NPs, fostered glucose consumption affinity ($1/K_s$) (11%), cellular carbohydrate (3%) and protein accumulation (60%), with a substantial reduction in process inhibitors.

Furthermore, the inclusion of NPs at different stages in simultaneous saccharification and fermentation (NISSF) of pre-treated potato peels was carried out. The highest ethanol concentration of 36.04 g/L was obtained with NiO nanoparticle: NiO NPs ($0.02 \text{ wt}\%$) included from the pre-treatment stage, fermentation at $37 \text{ }^\circ\text{C}$, 120 rpm for 36 h . Optimum productivity and yield of 2.25 g/L/h and 0.71 g/g , an increase of 145% and 69% respectively were also observed at this nano concentration. Similarly, a two-fold reduction in the concentration of process inhibitor was observed. The kinetic study of the NISSF process was examined. The product kinetics was described using a modified Gompertz's equation. A maximum potential bioethanol concentration (P_m) of 31.84 g/L (1.46 fold increment), was obtained with NiO nanoparticle (at $0.02 \text{ wt}\%$) inclusion from the pre-treatment stage. On the other hand, the lowest bioethanol production lag time (t_L) of 1.50 h was achieved with NiO nanoparticle inclusion following the pre-treatment stage (2.04 fold lag time reduction).

Additionally, the developed NISSF process was scaled up based on constant power consumption (P/V) and impeller tip speed (V_{tip}) from 1 L to 5 L scale. The non-gassed power (P) and the impeller agitation speed (n) by an iterative process were determined for both the constant P/V and V_{tip} . Implementing constant P/V value from the 1 L scale: 95 rpm , Reynold number (Re) $5.14\text{E} + 06$, Power (P) 0.012 W , Power to Volume ratio (P/V_L) 2.4 W/m^3 ,

circulation time (t_c) 12.8 s and shear stress (γ) 950 S^{-1} , at $37 \text{ }^\circ\text{C}$, pH 5 gave the highest productivity of 1.10 g/L/h and bioethanol concentration of 25.10 g/L in the 5 L scale bioreactor. The modified Gompertz model and the logistic function were used to describe the kinetics of the scale-up process when P/V was kept constant. The logistic function was in agreement with the experimental values, showing high coefficient of determination (R^2) > 0.98 . The maximum specific growth rate (μ_{max}) and maximum biomass concentration (X_{max}) of 0.24 h^{-1} and 4.57 g/L respectively were obtained from the logistic model. Similarly, the bioethanol production data fitted the modified Gompertz model with an R^2 of 0.98. The bioethanol production lag time of 3.89 h, maximum bioethanol production rate ($r_{p,m}$) of 2.00 g/L/h and a maximum potential bioethanol concentration (P_m) of 25.29 g/L was achieved. The formation of volatile metabolic inhibitors was significantly reduced under constant P/V . These inhibitory compounds include: 5-Methyl-furfural (0.306 g/L), acetic acids (8.042 g/L), 3-methyl-pyridine (0.084 g/L) and 3-Hydroxy-6-methylpyridazine (0.039 g/L), which were reduced by 1.25, 1.67, 1.87 and 2.41 fold respectively.

This study has demonstrated the effects of metallic oxide nanoparticles on yeast metabolism of ethanol production for an improved bioethanol yield on substrate resulting from significant improvement in *S. cerevisiae* affinity for available substrate, growth rate and reduction in process inhibitors. The kinetic models were in agreement with the obtained experimental data on the utilisation of nanoparticles to improve bioethanol production. Furthermore, efficient production of bioethanol from potato waste supplemented with nanoparticle has been demonstrated.

Keywords: Bioethanol, nanoparticles, kinetic and metabolic process, scale-up, bioreactor, modelling and optimization, fermentation, inhibitor, *Saccharomyces cerevisiae* BY4743

Acknowledgements

My time at the University of KwaZulu-Natal (UKZN), Pietermaritzburg campus, South Africa has been very lovely with both cold and warm days. First and foremost, I would like to thank God Almighty for this success and also to express my sincere gratitude to my supervisor, Professor Evariste Bosco Gueguim Kana for accepting me as a PhD student and giving me the opportunity to work in an exciting interdisciplinary project.

I am thankful and forever grateful to Sanusi Clement Aderemi (a brother like a father) for all the support from the beginning of my PhD studies. I would also like to acknowledge Costech Canada Inc. for providing some financial support for the PhD studies. In this light I would likewise gratefully acknowledge the college of Agriculture, Engineering and Sciences (AES), UKZN, for the conference grant during the study period.

Special gratitude to Professor Neil Koorbanally (AES Dean of Research) for the support towards my final thesis submission.

My special thanks go to Dr Pillay Che of Genetics Department, UKZN, for the generous supply of *Saccharomyces cerevisiae* BY4743 for the PhD studies.

To Lorika Beukes and Cynthia Matyumza, sincere thanks for their help in the characterisation of synthesized nanoparticles using SEM and TEM. This would have been difficult without their professional advice and help.

Many thanks to Dr Funmilayo Faloye-Ogunubi for the advice, motivation and support right from the beginning of my studies at UKZN and for the assistance in the modelling studies and critical comments on different manuscripts. I also take the opportunity to sincerely thank the scholars in Lab 117, Rabie Saunders Building, UKZN, who supported me in the journey of this thesis: Preshanthan Moodley, Yeshona Sewsynker-Sukai, Aruwajoye Gabriel (now Doctors), Kimberly Bruce, Zanenhlanhla Gumbi, Mariam Khan, Joeline Peniston, Emmanuel Ngerem, Yulisha Naidoo and Nomfundo Shange. Indeed our academic and social interactions were superb. To Daneal Rorke thanks for been a helpful friend in numerous ways. My partnership

with Reisha Narine in nanoparticles synthesis, coating, immobilization and operation of the algae raceway reactor has been invaluable. And to the Honours' set of Lab 117 of 2016, 2017, 2018, 2019 and 2020 "high five" you have been fun to work with in spite of the countless questions from you guys.

My sincere thanks to Prof. Stefan Schmidt, Dr Charles Hunter and Dr Sumaiya Jamal-Ally for giving me the opportunity to use some of the equipment in their laboratory whenever necessary.

Many thanks to Dr Andrew Fartisinha and Abimbola Oluwalana for the assistance and sharing of knowledge on FT-IR studies. Thank you Ebenezer Nnadozie for the help with the UV characterization of my nanoparticles. Thank you to Rendani B. Bulannga for having helped with SigmaPlot.

My appreciation go as well to the reviewers who gave scientific, constructive comments and suggestions to improve the manuscripts/thesis in all aspects.

On this occasion I also wish to thank Michelle Francis and Sibongile Khuzwayo of Higher Degree Pietermaritzburg campus, UKZN, together with Dr Titi Agbaje and Ayodeji Adedoyin for their warm welcome and registration guide as a new student. Belinda Anderson, thank you very much for the conference grant and visa processing support.

Thanks to all the colleagues in School of Life Science. Especially, Heather Tredgold and Matthew G. D Van Wyngaard (the supportive duo); they are always supportive of their colleagues.

Thanks to all the staffs in School of Life Science. Thank you Celeste Clark, Diane Fowlds, Renny Noble, Natalie Jones, Tanya Karalic and Patricia Joubert for the help in fixing technical and administrative issues. And to Wilson Sikhakhane, thank you, for always putting the laboratory in order.

Many and special thanks to our Technical Manager Celeste Clark for always making the impossible possible. Celeste you are a star and an angel.

Thanks to all my friends and the Deeper Life Campus Fellowship family for the prayers, fellowship and all the different activities that made it possible to draw closer to my God and also relax outside research.

Thank you Seffie Princen (Mumsee), for being a mother throughout my stay in your house. Blessing Hutchinson, Folasade Adu, Simangele Mavundla and Rendani Bulannga, thanks for being good neighbours.

Many thanks Dr Johnson Adelokun for your brotherliness at all times, particularly for paving the way for my coming to UKZN.

Finally, I wish to express my deepest gratitude to my dearest wife, Sanusi Joy (I love you), my late parents and members of my family for all the support and encouragement during the PhD studies. Without their understanding and prayers it would have not been possible to complete my research at this time.

Table of contents

| | |
|-------------------------------------------------------------------------------------------------------------------------------------------------------|-----|
| PREFACE | i |
| DECLARATION BY SUPERVISOR | ii |
| Declaration 1: Plagiarism | iii |
| Declaration 2: Publications | iv |
| Conference presentations..... | v |
| Abstract..... | vi |
| Acknowledgements..... | ix |
| List of abbreviations..... | xiv |
| Chapter 1..... | 1 |
| 1.1 Bioethanol as a renewable energy source..... | 1 |
| 1.2 Hydrolysis and fermentation | 1 |
| Fig. 1.0: Metabolic pathway for bioethanol production from glucose by <i>Saccharomyces cerevisiae</i> under anaerobic conditions (Rorke, 2017). | 6 |
| Fig. 1.1: Bioethanol production using renewable energy sources (Rorke, 2017)..... | 6 |
| 1.3 Nanoparticles as additives in bioprocessing..... | 7 |
| 1.4 Research motivation | 8 |
| 1.5 Aims and objectives | 10 |
| 1.6 Thesis outline | 10 |
| References | 12 |
| CHAPTER 2 | 17 |
| 2.0 Introduction | 18 |
| 2.1 The use of nanotechnology in biofuel production..... | 20 |
| 2.2 Bioethanol production | 21 |
| 2.3 Biodiesel production | 23 |
| 2.4 Biohydrogen production | 26 |
| 2.5 Biogas production | 30 |
| 2.6 Nanoparticles as immobilization matrix for biofuel production..... | 33 |
| 2.7 Bioprocess modelling: optimization and kinetics | 78 |
| 2.8 Process inhibitory compounds production..... | 81 |
| 2.9 Bioprocess scale-up..... | 83 |
| References | 85 |
| CHAPTER 3 | 99 |
| CHAPTER 4 | 117 |
| CHAPTER 5 | 131 |
| CHAPTER 6 | 147 |

| | |
|--------------------------------------------------------------------------------------------------------------------------------|-----|
| 6.0 Introduction | 150 |
| 6.1 Materials and Methods..... | 153 |
| Fig. 6.0: Process scale-up schematic based on constant impeller tip speed and power consumption | 155 |
| 6.2 Analytical Methods | 160 |
| 6.3 Results and Discussion | 161 |
| Figure 6.1: Schematic description of glucose consumption from the scale-up variations using constant P/V and V_{tip} | 163 |
| Figure 6.2: pH evolution profile during the bioethanol fermentation at 1 L and 5 L scale | 164 |
| Figure 6.3: <i>Saccharomyces cerevisiae</i> biomass dry weight based on constant P/V and V_{tip} | 169 |
| Figure 6.4: Representation of bioethanol production depicting the impact of constant P/V and V_{tip} | 170 |
| 6.4 Conclusion..... | 174 |
| References | 176 |
| Chapter 7..... | 182 |
| 7.0 Conclusions and recommendations for future studies..... | 182 |
| 7.1 Recommendations for future studies | 188 |

List of abbreviations

| | |
|----------------|--------------------------------------------------------------------------|
| BP... | British Petroleum |
| EDS... | Energy dispersive spectrophotometric |
| EDX... | Energy-dispersive X-ray spectroscopy |
| EIA... | Energy Information Administration |
| EMP... | Embden-Meyerhof-Parnas pathway |
| FTIR... | Fourier Transform Infra-Red spectroscopy |
| IEA... | International Energy Agency |
| MECAD... | Middle East and Central Asia Department |
| NCEF... | Nano-catalysed ethanol fermentation |
| NISSF... | Nanoparticle inclusion in simultaneous saccharification and fermentation |
| NPs... | Nanoparticles |
| NSLSSF... | Nano + SATP + liquefaction + SSF |
| ORP... | Oxidation–reduction potential |
| <i>P/V</i> ... | constant power consumption |
| <i>Re</i> ... | Reynolds number |
| RPM... | Revolutions per Minute |
| RSM... | Response Surface Methodology |
| S:L... | Solid-to-liquid |
| SATP... | Soaking assisted thermal pretreatment |
| SEM... | Scanning electron microscopy |
| SLNSSF... | SATP + Liquefaction + Nano + SSF |
| SLSSF... | SATP + Liquefaction + SSF |
| SLSS... | SATP + Liquefaction + SS + No Fermentation |
| SNLSSF... | SATP + Nano + Liquefaction + SSF |

| | |
|---------------|------------------------------------------------|
| SPR... | Surface plasmon resonance |
| SSF... | Simultaneous saccharification and fermentation |
| TCA... | Total carbohydrate accumulation |
| TEM... | Transmission electron microscopy |
| V_{tip} ... | impeller tip speed |
| VFAs... | Volatile fatty acids |
| VICs... | Volatile inhibitory compounds |
| VMCs... | Volatile metabolic compounds |
| wt%... | Weight percent |

Chapter 1

General introduction

1.1 Bioethanol as a renewable energy source

Currently, the energy market has attracted global interest with focus on the production of renewable energy as a result of depleting crude oil reserves and the environmental effect from consumption of conventional fossil fuels. The future's commercially feasible fossil fuel substitute is bioethanol (Ge *et al.*, 2018). Bioethanol exhibits several advantages over fossil fuels, these include its renewable nature, ease of storage and transportation, higher combustible oxygen content, higher octane rating, zero sulphur and nitrogen content, lower emission of greenhouse gases and consequently, reduction in air pollution and global warming (Putra *et al.*, 2015). In addition, the global market for bioethanol fuel has grown rapidly and its production is projected to have an annual growth of over 3% (Sekoai *et al.*, 2019). World bioethanol production has been estimated at around 100, 126 and 128 billion litres in 2017, 2018 and 2019 respectively (Sekoai *et al.*, 2019, RFA, 2020). Although, ethanol can be produced by chemical processes, it is usually produced by the fermentation of simple sugars. The production of bioethanol is mainly a two-stage biochemical process of hydrolysis and fermentation, followed by product recovery through distillation (Kim and Lee, 2016).

1.2 Hydrolysis and fermentation

Hydrolysis is a chemical reaction that breaks chemical bonds between the carbohydrate molecules of polysaccharides into simple or fermentable sugars in the presence of a catalyst (Guo *et al.*, 2012). Catalysts for hydrolysis in the production of bioethanol from biomass feedstocks are usually enzymes, metal salts, acids or bases (Guo *et al.*, 2012). Enzymatic or basic hydrolysis is via the external addition of commercial enzymes or acids or by innate enzymes and acids present in the feedstock (Deenanath, 2014). The choice of hydrolysis method is dependent on the type of feedstock used for bioethanol production.

The process of fermentation to convert sugars by microorganisms to bioethanol is the oldest and the most frequently used industrial process. As early as 1750-4000BC the Egyptians and Sumerians produced dough and alcoholic beverages such as wine and beer by fermentation (Paul Ross *et al.*, 2002). However, the role of microbes in the fermentation process was unknown (Blandino *et al.*, 2003). Louis Pasteur in 1861 developed pasteurization which paved the road to the knowledge of microorganisms and their link to fermentation gradually progressed (Paul Ross *et al.*, 2002). From these theories, presently the definition of fermentation is simply a biochemical process that converts carbohydrates such as sugar into ethanol and carbon dioxide by the action of yeast enzymatic reactions (Deenanath, 2014).

Various fermentation processes such as alcoholic, lactic acid, acetic acid and alkaline are used in the production of fermented food and beverages (Blandino *et al.*, 2003). Alcoholic fermentation is the production of alcohol by *Saccharomyces cerevisiae* yeasts using cereal grains, sugarcane or fruits and presently waste lignocellulosic biomass as a substrate. Alcoholic fermentation, which is applied in bioethanol production is further classified into three types of systems, namely batch, fed-batch, continuous and solid-state fermentation. The choice of fermentation system depends on the type of raw material, desired ethanol yield and fermentation time (Deenanath, 2014).

The most widely used microorganism for ethanol fermentation is the eukaryotic, fungal organism *S. cerevisiae* (Bourdichon *et al.*, 2012). *S. cerevisiae* is the most preferred microbe for the following reasons: (1) it's easily assimilate and ferment hexose sugars to ethanol, (2) it tolerate high ethanol concentrations, (3) it growth under anaerobic, aerobic and acidic conditions, (4) it's not susceptible to bacteriophage contamination, (5) it's can be easily separated from the fermented product and re-use for subsequent fermentations, and (6) it's able to ferment at a range of temperatures from 15 – 30 °C and thermotolerant *S. cerevisiae* strains can ferment at 35 °C or greater (Deenanath, 2014). Other than yeasts, bacteria such as lactic

acid bacteria, *Zymomonas mobilis* and *Thermoanaerobacterium* are capable of ethanol fermentation (Deenanath, 2014).

During fermentation *S. cerevisiae* produces ethanol by the Embden-Meyerhof-Parnas (EMP) pathway or glycolysis (Fig. 1.0). The glucose inside the cell is converted to pyruvate and NAD⁺ is oxidized to NADH. The enzyme pyruvate decarboxylase converts pyruvate to acetaldehyde, followed by the conversion of acetaldehyde into ethanol by alcohol dehydrogenase while, NADH is re-oxidized to NAD⁺ (Mostafa, 2010, Deenanath, 2014). Usually, during bioethanol fermentation, *S. cerevisiae* and members of the genus *Zymomonas* are the two groups of microorganisms that naturally produces two moles of ethanol per mole of hexose (Mostafa, 2010). Pyruvate produced by the Embden–Meyerhoff (glycolytic) pathway in *S. cerevisiae* (Fig. 1.0) or Entner–Doudoroff pathway in *Zymomonas* is converted to alcohol via pyruvate decarboxylase/alcohol dehydrogenase enzymes (Mostafa, 2010). An indirect fermentation approaches involve the production of bioethanol by pyrolyzing/burning the starting plant material to produce syngas (CO, CO₂, and hydrogen) (Kim *et al.*, 2014, Kim and Lee, 2016). Syngas is then converted to ethanol by acetogenic bacteria. The presumably biochemistry pathway is believed to be Wood–Ljungdahl pathway. Two-carbon compounds products are produced from one-carbon compounds. Ethanol is produced instead of acetate (Mostafa, 2010). In fermentative bioethanol production, different parameters impact *S. cerevisiae* metabolic activities, that consequently determine the overall output (Rorke *et al.*, 2017). Influencing parameters during microbial biofuel production include; substrate type and concentration, pH, temperature, microbial strain, nutrient type, inclusion of additives and agitation (Rorke *et al.*, 2017).

Moreover, the vast majority of bioethanol production studies are based on biotechnological processes such pre-treatment, liquefaction, saccharification and fermentation using crops and lignocellulosic substrates (Izmirlioglu and Demirci, 2012, Kim and Lee, 2016, Moodley and

Gueguim-Kana, 2019) (Fig. 1.1). The utilisation of abundant lignocellulosic biomass is desirable both for economic and environmental reasons, as substrate suitability is one of the main cost factors taken into consideration in industrial bioethanol production (Jönsson and Martín, 2016). It is, therefore, essential that bioethanol production is carried out using cheap and carbohydrate-rich substrates (Talasila and Vechalapu, 2015). The use of pure lignocellulosic and starch-based wastes also, mitigate the threat to food security caused by food based bioethanol production (Moodley and Gueguim-Kana, 2019). Even though, bioethanol as a renewable energy resource from lignocellulosic biomass could be at the core of global shift in energy production and is projected to become the dominant form of renewable energy resource from lignocellulosic substrates, enhanced process performance and product yield is required to improve the economic viability of this biofuel compared to petroleum fuel (Sekoai *et al.*, 2019).

Furthermore, the primary biological technique for the production of bioethanol from lignocellulosic biomass is the saccharification-fermentation process, in which lignocellulosic biomass is saccharified by hydrolysis to release fermentable sugars, which is simultaneously fermented to produce bioethanol (Kim and Lee, 2016). In simultaneous saccharification and fermentation (SSF), the overall process is limited by the need to optimise enzymatic and cellular activities for maximum sugar release and subsequent bioethanol formation as well as minimise inhibitor formation during the pre-treatment and fermentation processes (Sewsynker-Sukai and Gueguim-Kana, 2018). Despite the present intensive research on fermentative bioethanol production, its low yield has become a major obstacle to its commercialization. Hence, there is a need to come up with strategies that could make the process more efficient and productive. Recent studies have examined different process enhancement techniques such as use of nutrient additives and parameter optimisation to improve the performance of saccharification-fermentation processes (Cheng *et al.*, 2017, Sewsynker-Sukai and Gueguim

Kana, 2018). Attempts to include nanoparticles as biocatalytic additives to enhance heat and mass transfer rates, buffering capacity, inhibitor control, enzymatic activities and cellular functionality in bioprocess has attracted great interest (Kim *et al.*, 2014, Cherian *et al.*, 2015, Kim and Lee, 2016). The catalysis potentials of nanoparticles (NPs) has led to significant biotechnological interest. Notwithstanding, very little is known on the bioethanol fermentation process with nanobiocatalyst inclusion at various process stages.

Nanotechnology involves the process of manipulating matter at the nanoscale level (1-100 nm) (Abdelsalam *et al.*, 2017). Nanoparticles (NPs) are usually obtained through the assembly of atoms during a chemical process or through the fragmentation of bulk materials, their size would normally depend on the process conditions and precursors used for their synthesis (Abdelsalam *et al.*, 2017). The nano size is one of the principal features of the nanoparticles especially as it confers the ability to penetrate cell membranes, thereby facilitating the uptake and transport of nutrients, creating pathways across the biological barriers which will impact the overall bioprocesses. Aside from the nano size, other properties of NPs include large surface area, high specificity, dispersibility and self-assembly (Abdelsalam *et al.*, 2017).

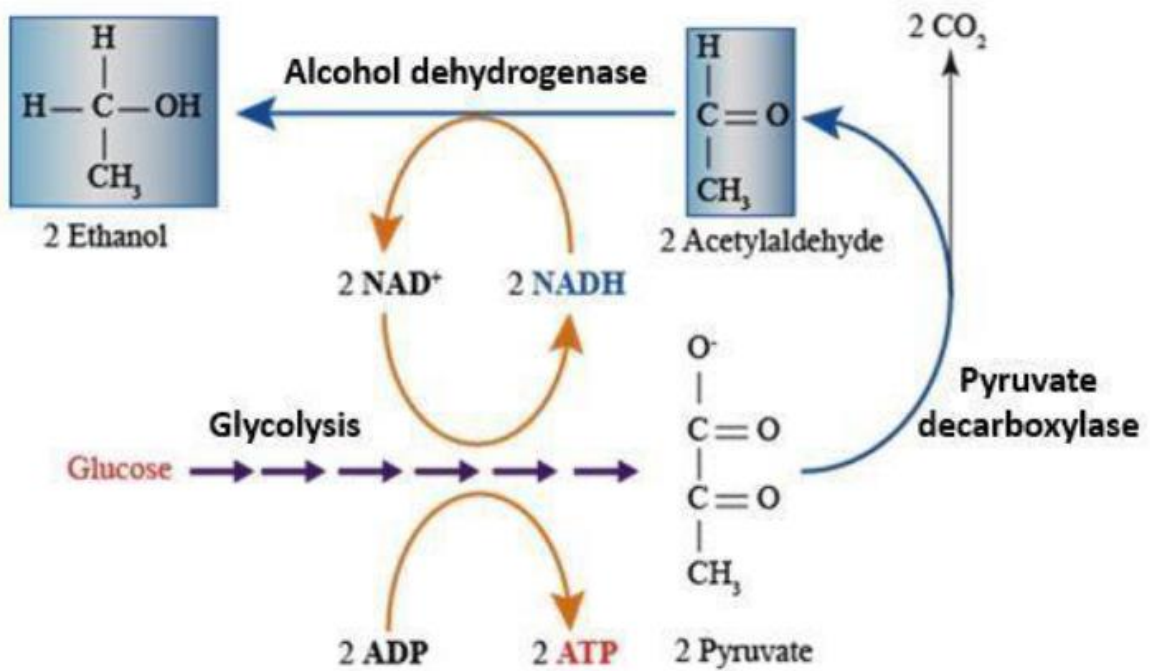


Fig. 1.0: Metabolic pathway for bioethanol production from glucose by *Saccharomyces cerevisiae* under anaerobic conditions (Rorke, 2017).

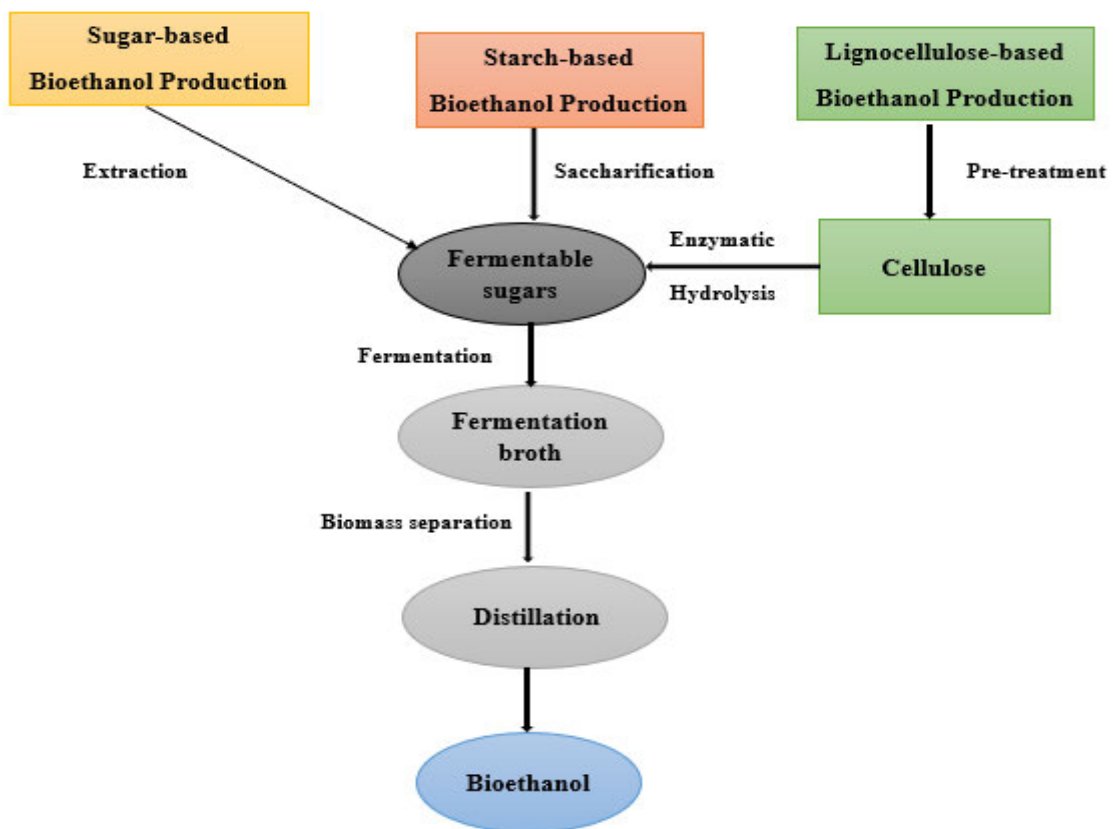


Fig. 1.1: Bioethanol production using renewable energy sources (Rorke, 2017).

1.3 Nanoparticles as additives in bioprocessing

The application of nanoparticles in bioprocessing has recently become an area of growing interest. Nanoparticles may influence the growth and proliferation of microorganisms (Ban and Paul, 2014, Usafî *et al.*, 2016). Most nanoparticles at higher concentrations have a toxic effect on microbial cells while, some have non-toxic regulatory and stimulatory effect at lower concentrations (Garcia-Saucedo, 2010). Metallic nanoparticles (NPs) in culture nutrient formulation have recently been identified as a potential catalytic technique for improving the bioactivity of ethanol-producing microorganisms and fermentation productivity (Ban and Paul, 2014). Their ability to alter the rate of reaction coupled with other biotechnological potentials have led to their increased application in many fields of research such as bioprocessing (Usafî *et al.*, 2016). Exceptional properties of nanoparticles include; chemical stability, catalytic properties, surface-to-volume ratio, interaction, magnetic separation, and specificity which can be implemented in biotechnological processes (Usafî *et al.*, 2016). Their catalytic properties generally depend on their size, shape, stabilizing agents and operating conditions (Ban and Paul, 2014). Furthermore, metals such as metallic oxide nanoparticles are essential nutrient element, that could form the metal content at the active site of enzymes, which are fundamental requirement for enzymes functionality and ultimately, the metabolic performance of enzymes and microorganisms. These enzymes catalyse various metabolic reactions during bioethanol production (Qazizada, 2016). For instance, sugar metabolism, involves hundreds of enzyme-catalysed reactions, structured (organized sequences) into ethanol metabolic pathways, for ethanol formation (Qazizada, 2016). Though, numerous studies have focused on the production of bioethanol via media composition using various nutrient supplement (Izmirlioglu and Demirci, 2016, Phukoetphim *et al.*, 2017), however, there is a dearth of studies on nutrient supplementation in bioethanol fermentation using nanoparticles.

Generally, bioethanol yields are affected by process conditions such as culture media, nutrient supplementation, pH, temperature and substrate availability (Torija *et al.*, 2003, Xu *et al.*,

2012). Only a few studies have reported on the impact of nutrient supplementation with metallic oxide nanoparticles and other operating conditions on the dynamic behaviour of bioethanol fermentation processes (Lin *et al.*, 2012). Little is known on the interactive effect of nanoparticles and these process conditions on bioethanol fermentation processes. Hence, bioethanol fermentation process optimization would be essential to optimized these operational conditions such that high productivity could be achieved.

1.4 Research motivation

A bioethanol-based economy will contribute to the mitigation of environmental pollution such as greenhouse gas emissions and help build a sustainable energy system (Ge *et al.*, 2018). Despite the merit of bioethanol as a suitable alternative to conventional fuel, some of the major challenges face the transition to bioethanol production is the sourcing of an economical and renewable feedstock as well as need to increase product yield on substrate (Talaisil and Vechalapu, 2015, Moodley and Gueguim-Kana, 2019). Lignocellulosic biomass such as potato peels is an abundant and renewable feedstock available for biofuel production both from economic and environmental point of view (Jönsson and Martín, 2016).

Potatoes (*Solanum tuberosum*) are a staple crop across the world, they are the world's third-largest staple food crop after rice and wheat (Chohan *et al.*, 2020). The increased importance of potatoes as staple food has led to the escalation in the generation of large volumes of residues in the form of peels, usually making up between 20-50% of the whole tuber (Maldonado *et al.*, 2014). Potato peels are starchy, lignocellulosic waste and suitable renewable substrate containing intricate structures composed of lignin, hemicellulose and cellulose with considerable amounts of fermentable sugar (Kristiani *et al.*, 2013). This raw material has been considered as one of the most attractive and sustainable feedstocks for biofuel production (Maldonado *et al.*, 2014). It is currently receiving great interest as its bioconversion to bioethanol fuels does not directly compete with food security. The potential of potato waste as

a feedstock for ethanol production has been reported (Hashem and Darwish, 2010, Izmirlioglu and Demirci, 2012, Khawla *et al.*, 2014). The results from these studies have not been impressive. This is due to low process performance and consequently, ineffective bioconversion of fermentable sugars to bioethanol (Rorke *et al.*, 2017). Process performances are plagued by low yields due to the formation of inhibitory compounds as well as ill-defined process parameter boundaries could hamper enzymatic hydrolysis, prevent metabolic processes and the overall fermentation processes. Overcoming these barriers is challenging, yet this knowledge is required to achieve high process yields and pave way for the establishment of a viable industrial scale bioethanol production that can compete with fossil fuels.

Therefore, to alleviate concerns regarding low bioethanol yield on substrate, the use of biotechnological tool such as nanobiocatalyst should be explored. Bioethanol yield on substrate should be considered when developing efficient fermentation strategies. This could be achieved by the implementation of nanobiocatalyst additives to enhance the process performance and RSM modelling to capture the complex interactions which link the fermentation conditions to bioethanol production as well as inhibitor generation. Furthermore, the application of nanobiocatalyst in bioethanol production should be assessed in detail. Using kinetic models such as Monod, logistic and modified Gompertz models will help to control the process and increase the quality of the bioethanol produced. These findings could therefore contribute to industrial scale productions from potato peels lignocellulosic biomass using nanobiocatalyst.

1.5 Aims and objectives

This study aimed to assess the impact of various nanoparticle biocatalysts on *Saccharomyces cerevisiae* metabolism for improve ethanol production. Additionally, the viability of a semi-pilot scale of the optimized process was evaluated.

To achieve this aim, the following specific objectives were carried out:

- (i) Screening and assessment of the catalytic potential of nine metallic oxide nanoparticles for enhanced bioethanol production.
- (ii) Assessment of the selected nanoparticles on a simultaneous saccharification and fermentation of process with pre-treated waste potato peels.
- (iii) Modelling and optimization of bioethanol response on operational parameters of nanoparticles concentration, pH, temperature and substrate concentration using the selected nanoparticle
- (iv) Preliminary assessment of bioethanol production from pre-treated waste potato peels under nano biocatalytic condition at a semi-pilot scale.

1.6 Thesis outline

This thesis comprises a literature review chapter and four experimental chapters all presented in research paper format. Each experimental chapter is independent, containing an introduction, materials and methods, results and discussion, conclusion and references. The description, assessment and application of nanoparticles as catalytic additives for the enhancement of bioethanol production are central to all chapters.

Chapter 2 presents an overview of nanoparticles as a potential additives for boosting biofuel production. It examines the different nano additives for different bioprocess as well as nano-based immobilization matrix for biofuel production.

In Chapter 3, nine nanoparticles namely Fe₃O₄ NPs, Co NPs, Ni NPs, Zn NPs, Mn NPs, Ag NPs, Cu NPs and Fe-Ag NPs, are screened for catalytic potential to enhanced fermentative ethanol production from glucose. The impact of the nano catalyst on the *Saccharomyces cerevisiae* growth and the product kinetics are assessed using logistic function and the modified Gompertz model.

Chapter 4 discusses the impact of nanoparticles inclusion in simultaneous saccharification and fermentation of pre-treated waste potato peels. Moreover, the kinetics of the batch bioethanol production to determine the process dynamics and the process inhibitory profile was undertaken.

Chapter 5 focuses on the modelling and optimization of nano concentration with key operational parameters for enhanced bioethanol production using response surface methodology. In addition, kinetic modelling of bioethanol fermentation process using *Saccharomyces cerevisiae* was undertaken to determine the dynamics and thus, predict *S. cerevisiae*'s behaviour based on factors such as the substrate utilization, specific growth rate, affinity to the fermentation substrate and maximum bioethanol production rate.

In chapter 6, a preliminary scale up process is carried out. The geometrical, rheological and hydrodynamic parameters of the bioreactors and fermentation broth were used to evaluate the viability of the process scale up based on constant power consumption and constant impeller tip speed.

The final chapter, Chapter 7, integrates the findings from the experimental chapters and provides major conclusions derived from this research. Recommendations for future studies are also provided.

References

- Abdelsalam, E., Samer, M., Attia, Y.A., Abdel-Hadi, M.A., Hassan H.E., Badr, Y., 2017. Effects of Co and Ni nanoparticles on biogas and methane production from anaerobic digestion of slurry, *Energy Conversion Management*, 141, 108-119.
- Ban, D.K., Paul, S., 2014. Zinc Oxide Nanoparticles Modulates the Production of β -Glucosidase and Protects its Functional State Under Alcoholic Condition in *Saccharomyces cerevisiae*. *Applied Biochemistry and Biotechnology*, 173, 155–166.
- Blandino, A., Al-Aseeri, M.E., Pandiella, S.S., Cantero, D. and Webb, C., 2003. Cereal-based fermented foods and beverages. *Food Research International*, 36: 527-543.
- Bourdichon, F., Casaregola, S., Farrokh, C., Frisvad, J.C., Gerds, M.L., Hammes, W.P., Harnett, J., Huys, G., Lauland, S., Ouwehand, A., Powell, I.B., Prajapati, J.B., Seto, Y., Schure, E.T., Boven, A.V., Vankerckhoven, V., Zgoda, A., Tuijtelaars, S., Hansen, E.B., 2012. Food fermentations: 241 microorganisms with technological beneficial use. *International Journal of Food Microbiology*, 154: 87-97.
- Cheng, N., Koda, K., Tamai, Y., Yamamoto, Y., Takasuka, T.E., Uraki, Y., 2017. Optimization of simultaneous saccharification and fermentation conditions with amphipathic lignin derivatives for concentrated bioethanol production. *Bioresource Technology*, 232, 126–132.
- Chohan, N.A., Aruwajoye, G.S., Sewsynker-Sukai, Y., Gueguim Kana, E.B., 2020. Valorisation of potato peel wastes for bioethanol production using simultaneous saccharification and fermentation: Process optimization and kinetic assessment. *Renewable Energy*, 146, 1031-1040.
- Deenanath, E.D., 2014. Production and Characterization of Bioethanol Derived from Cashew Apple Juice for Use in Internal Combustion Engine. *PhD Thesis*. University of the Witwatersrand, Johannesburg, South Africa.

- Garcia-Saucedo, C., 2010. Developing a Yeast Cell Assay for Measuring the Toxicity of Inorganic Oxide Nanoparticles. Chemical & Environmental Engineering Department University of Arizona. May 6th 2010. www.CitlaliGarcia_UA 5-6-10.
- Ge, S., Qiu, S., Tremblay, D., Viner, K., Champagne, P., Jessop, P.G., 2018. Centrate wastewater treatment with *Chlorella vulgaris*: Simultaneous enhancement of nutrient removal, biomass and lipid production. *Chemical Engineering Journal*, 342, 310–320.
- Guo, F., Fang, Z., Xu, C.C. and Smith Jr., R.L., 2012. Solid acid mediated hydrolysis of biomass for producing biofuels. *Progress in Energy and Combustion Science*, 38: 672-690.
- Hashem, M.S., Darwish, M.I., 2010. Production of bioethanol and associated by-products from potato starch residue stream by *Saccharomyces cerevisiae*. *Biomass and Bioenergy*, 34, 953 – 959.
- Izmirlioglu, G., Demirci A., 2012. Ethanol Production from Waste Potato Mash by Using *Saccharomyces cerevisiae*. *Applied Sciences*, 2, 738-753.
- Izmirlioglu, G., Demirci, A., 2016. Improved simultaneous saccharification and fermentation of bioethanol from industrial potato waste with co-cultures of *Aspergillus niger* and *Saccharomyces cerevisiae* by medium optimization. *Fuel*, 185, 684–691.
- Jönsson, L.J., Martín, C., 2016. Pretreatment of lignocellulose: Formation of inhibitory by-products and strategies for minimizing their effects. *Bioresource Technology*, 199, 103–112.
- Khawla, B.J., Sameh, M., Imen, G., Donyes, F., Dhouha, G., Raoudha, E.G., Oumèma. N-E., 2014. Potato peel as feedstock for bioethanol production: A comparison of acidic and enzymatic hydrolysis. *Industrial Crops and Products*, 52, 144–149.
- Kim, Y., Lee, H., 2016. Use of magnetic nanoparticles to enhance bioethanol production in syngas fermentation. *Bioresource Technology*, 204, 139–144.

- Kim, Y., Park, S.E., Lee, H., Yun, J.Y., 2014. Enhancement of bioethanol production in syngas fermentation with *Clostridium ljungdahii* using nanoparticles. *Bioresource Technology*, 159, 446 – 450.
- Kristiani, A., Abimanyu, H., Sudiyarmanto, A.H.S., Aulia, F., 2013. Effect of pretreatment process by using diluted acid to characteristic of oil palm's frond. *Energy Procedia*, 32, 183 – 189.
- Lin, Y., Zhang, W., Li, C., Sakakibara, K., Tanaka, S., Kong, H., 2012. Factors affecting ethanol fermentation using *Saccharomyces cerevisiae* BY4742. *Biomass and Bioenergy*, XXX (2012) 1-7.
- Maldonado, A.F.S., Mudge, E., Gänzle, M.G., Schieber, A., 2014. Extraction and fractionation of phenolic acids and glycoalkaloids from potato peels using acidified water/ethanol-based solvents. *Food Research International*, 65, 27–34.
- Moodley, P., Gueguim-Kana, E.B., 2019. Bioethanol production from sugarcane leaf waste: Effect of various optimized pretreatments and fermentation conditions on process kinetics. *Biotechnology Reports*, 24 xxx–xxx.
- Mostafa, S.E., 2010. Microbiological aspects of biofuel production: Current status and future directions, *Journal of Advanced Research*, 1, 103–111.
- Paul Ross, R., Morgan, S., Hill, C., 2002. Preservation and fermentation: past, present and future. *International Journal of Food Microbiology*, 79: 3-16.
- Phukoetphim, N., Salakkam, A., Laopaiboon, P., Laopaiboon, L., 2017. Kinetic models for batch ethanol production from sweet sorghum juice under normal and high gravity fermentations: logistic and modified Gompertz models. *Journal of Biotechnology*, 243, 69–75.
- Putra, M.D., Abasaed, A.E., Atiyeh, H.K., Al-Zahrani, S.M., Gaily, M.H., Sulieman, A.K., Zeinelabdeen, M.A., 2015. Kinetic Modeling and Enhanced Production of Fructose and

- Ethanol from Date Fruit Extract, *Chemical Engineering Communications*, 202, 1618–1627.
- Qazizada, M.E., 2016. Design of a batch stirred fermenter for ethanol production. *Procedia Engineering*, 149, 389 – 403.
- Renewable Fuels Association (RFA), 2020. <https://ethanolrfa.org/statistics/annual-ethanol-production/>
- Rorke DCS (2017). The potential of waste sorghum (*Sorghum bicolor*) leaves for bioethanol process development using *Saccharomyces cerevisiae* BY4743. MSc Thesis. University of KwaZulu-Natal, Pietermaritzburg, South Africa.
- Rorke, D.C.S., Kana, E.B.G., 2017. Kinetics of Bioethanol Production from Waste Sorghum Leaves Using *Saccharomyces cerevisiae* BY4743. *Fermentation*. 3, 19.
- Sekoai, P.T., Ouma, C.N.M., du Preez, S.P., Modisha, P., Engelbrecht, N., Bessarabov, D.G., Ghimire, A., 2019. Application of nanoparticles in biofuels: An overview. *Fuel*, 237, 380–397.
- Sewsynker-Sukai, Y., Gueguim-Kana, E.B., 2018. Simultaneous saccharification and bioethanol production from corn cobs: Process optimization and kinetic studies. *Bioresource Technology*, 262, 32–41.
- Talasila, U., Vechalapu, R.R., 2015. Optimization of Medium Constituents for the Production of Bioethanol from Cashew Apple Juice Using Doehlert Experimental Design. *International Journal of Fruit Science*, 15, 161–172.
- Toriija, M.J., Rozes, N., Poblet, M., Guillamon, J.M., Mas, A., 2003. Effects of fermentation temperature on the strain population of *Saccharomyces cerevisiae*. *International Journal of Food Microbiology*, 80 47-53.

- Usatîi, A., Chiselița, N., Efremova, N., 2016. The evaluation of nanoparticles ZnO and TiO₂ effects on *Saccharomyces cerevisiae* CNMN-Y-20 yeast strain *Acta Universitatis Cibiniensis Series E: Food Technology* 85 XX 1, 85-92.
- Xu, S., Liu, H., Fan, Y., Schaller, R., Jiao, J., Chaplen, F., 2012. Enhanced performance and mechanism study of microbial electrolysis cells using Fe nanoparticle decorated anodes. *Applied Microbiology and Biotechnology*, 93: 871–880.

CHAPTER 2

Nanotechnology in Bioprocess Development: Applications of Nanoparticles in the Generation of Biofuels

This chapter has been published as a book chapter (Published in *Springer*):

A. I. Sanusi, Y. Sewsynker-Sukai, E. B. Gueguim-Kana. 2021. Nanotechnology in Bioprocess Development: Applications of Nanoparticles in the Generation of Biofuels. In Microbial Nanobiotechnology. DOI:10.1007/978-981-33-4777-9_6.

Chapter 2

Literature review

2.0 Introduction

Global energy demand is rapidly increasing due to the growing human population, with the current energy sources unable to meet the staggering daily fuel consumption. More specifically, the major reliance on fossil fuels as an energy source has led to its depletion (Hirsch *et al.*, 2005; Ge *et al.*, 2018). Fossil fuels such as coal and oil are non-renewable energy sources that are most exploited globally and have been predicted to run out in the next 115 and 50 years, respectively (BP Statistical Review of World Energy, 2019). In addition to their depletion, the consumption of fossil fuels is harmful to the environment, since its combustion releases greenhouse gases such as CO₂, nitrous oxide and fluorinated oxide (Fazal *et al.*, 2018; Ge *et al.*, 2018). Consequently, the development of alternative energy sources such as biofuels that are renewable, cost-effective and environmentally friendly is attracting unprecedented research interest.

Biofuels have emerged as sustainable energy sources which could be produced *inter alia* from lignocellulosic waste, vegetable oils, animal fat and industrial wastewaters (Sekoai *et al.*, 2019). These fuels are considered 'green' since they are non-toxic, easily biodegradable, environmentally benign and sustainable in nature (Moodley and Gueguim Kana, 2019). Biofuels can be classified based on the carbohydrate sources used for their production. For example, first generation biofuels involve the use of edible feedstocks to produce biofuels (bioethanol, biodiesel and biogas) (Khawla *et al.*, 2014, Baeyens *et al.*, 2015). While first generation biofuels generate high yields, the utilisation of staple crops such as wheat, sorghum, corn and sugar cane hamper food security. Alternatively, second generation biofuels consists of non-food crops as substrates, commonly lignocellulosic materials which include rice bran, sawdust, potato waste, corncob, bagasse, and sugar cane leaves (Gueguim Kana *et al.*, 2012;

Baeyens *et al.*, 2015; Sebayang *et al.*, 2017; Sewsynker-Sukai and Gueguim Kana, 2018, and Chohan *et al.*, 2020). The third generation biofuels use various types of microalgal biomasses as feedstock for the production of biofuels (Sekoai *et al.*, 2019). In recent times, second and third generation biofuels have gained interest as advanced energy sources that can be harnessed from waste materials such as potato peels, cassava peels, sugar cane leaves, bagasse and corn cobs (Khawla *et al.*, 2014). These wastes are abundantly available via agricultural activities (Adeoye *et al.*, 2015; Elegbede and Lateef, 2018).

Currently, the bio-energy market is expanding (Renewable Fuels Association, 2018). For instance, global biodiesel production is expanding with an estimated annual increase of 7.3% to a total of US\$54.8 billion by 2025, while, the production of bioethanol is projected to have an annual growth of 3-7%. The global bioethanol production was estimated at around 100 billion litres in 2017, and is envisaged to double by 2027 (Sekoai *et al.*, 2019).

The most commonly researched biofuels that are attracting global attention include bioethanol, biodiesel, biohydrogen and biomethane – most particularly, bioethanol from lignocellulosic feedstock. The production of lignocellulosic-based bioethanol involves four phases. These include; pre-treatment, hydrolysis, fermentation and distillation processes (Deniz *et al.*, 2015; Kim *et al.*, 2016; Sewsynker-Sukai and Gueguim Kana, 2018; Moodley and Gueguim Kana, 2019). Bioethanol has been characterised as an environmentally friendly, efficient fuel with higher oxygen content and higher octane number.

Despite the merits associated with microbial biofuel production processes from lignocellulosic biomass, microalgae biomass and industrial wastewaters, several challenges plague its application at large scale. Major limitations of biofuel production may include: high cost and energy requirement; lack of a suitable substrate that can be utilised by the microbes; and low product yield (Aruwajoye *et al.*, 2017 and Sewsynker-Sukai and Gueguim Kana, 2018). In an attempt to overcome these challenges, several bioprocess optimization strategies are being

investigated, such as more cost-effective substrates, low-cost pre-treatment procedures, low energy input and the application of biocatalysts such as nano-sized biocatalysts (Kim *et al.*, 2016; Faloye *et al.*, 2014; Sewsynker *et al.*, 2015; Sewsynker-Sukai and Gueguim Kana, 2018). The use of nano-sized materials has attracted significant attention in recent decades, due to intrinsic properties that promote its application in several biotechnological fields such as bioprocessing, agriculture, biosensor, biopharmaceuticals and medicine (Lateef *et al.*, 2018; Elegbede and Lateef, 2019a, b; Shanmugam *et al.*, 2020). More specifically, nanotechnology has been employed in various bioprocesses to improve the microbial metabolic activities by their integration with metabolic intermediates and key enzyme activities, and consequently increased glycolytic rates, cell-substrate affinity, growth rate, mass transfer rate, modulation of oxidation-reduction potential (ORP), enhanced process performance and ultimately, high product yields.

2.1 The use of nanotechnology in biofuel production

In the recent years, nanoparticles have attracted significant attention due to their distinctive physical and chemical nature that has been shown to stimulate microbial and enzymatic biochemical activities in biofuel production. Previous studies have indicated that the stimulatory and catalytic properties of nanoparticles are strongly influenced by their shape, size, concentration, surface coating and operating conditions (Resham and Priyabrata, 2008). The use of biocompatible and bioactive nanomeric additives such as NiO, Fe₃O₄ and AgO nanoparticles in biofuel production processes that could significantly improve bioprocess performance and productivity are being implemented (Abdelsalam *et al.*, 2016). Nanoparticle surface properties can regulate stability, solubility and targeting of specific cellular receptors (Howarth *et al.*, 2008). Moreover, the suitability of nanoparticle additives is strongly dependent on other factors such as operating parameters, the type of substrate and additive type (Abdelsalam *et al.*, 2016). For instance, monovalent and functionalised nanomaterial might be

used to stimulate or regulate the activities of individual proteins or enzymes (Fu *et al.*, 2004; Howarth *et al.*, 2008). More specifically, for biological applications, the surface property is generally polar, which gives high aqueous solubility that prevents nanoparticles' aggregation and ultimately, their performance (Liu *et al.*, 2010). Nanomaterials can also play a vital role to improve the thermal and pH stability of enzymes (Pandurangan and Kim, 2015). Furthermore, a coated nanoparticle that is multivalent or polymeric confers high stability. Multivalent nanoparticles, bearing multiple targeting groups, can cluster receptors, which could activate cellular signalling pathways and result in stronger attachment and reactivity. Other significant properties of nanoparticles that could improve bioprocess performance include large surface-to-volume ratio, high surface reaction activity, high catalytic efficiency, strong adsorption ability and redox potential that is normally high due to small atomic size (Ansari and Husain, 2012, Abdelsalam *et al.*, 2016). Nanotechnology has been applied in the production of different biofuels such as biodiesel, bioethanol, biohydrogen and biogas, and these are subsequently discussed.

2.2 Bioethanol production

Bioethanol is produced when microbes such as *Saccharomyces cerevisiae* or *Zymomonas mobilis* metabolise fermentable sugars under microaerophilic or anaerobic conditions to produce ethanol and CO₂ (Baeyens *et al.*, 2015). Different attempts have been made to improve the bioethanol fermentation process (Kim *et al.*, 2016). These include; process optimization, microbial engineering and use of catalysis (Kim *et al.*, 2016; Sewsynker-Sukai and Gueguim Kana, 2018).

Metallic nanoparticles in fermentation process nutrient formulation have recently been identified as advantageous in stimulating and promoting the bioactivity of ethanol-producing microorganisms and fermentation productivity (Demirel and Scherer, 2011; Miazek *et al.*, 2015; Pádrová *et al.*, 2015; Kim *et al.*, 2016). Kim *et al.* (2014) supplemented six different

nanoparticles to enhance bioethanol production in syngas fermentation using *Clostridium ljungdahlii*. The aforementioned study revealed a 34.5%, 166.1%, and 29.1% increase in the levels of biomass, ethanol, and acetic acid production respectively due to supplementation with nanoparticles (Kim *et al.*, 2014). These enhancements were ascribed to enhanced gas-liquid mass transfer by methyl and isopropyl hydrophobic surface modification on the silica NPs (Kim *et al.*, 2014). The effects could also be attributed to improved metabolic and enzymatic activities, buffering capacity and oxidation-reduction potential (ORP) of the nano system. Various reports on the use of nano biocatalysts such as SiO₂-CH₃, CoFe₂O₄@SiO₂-CH₃ and metal oxides in bioethanol production are presented in Table 2.0.

Table 2.0: Nanoparticles as biostimulatory catalysts in bioethanol production

| Sources | Studies | | |
|-------------------------------|-------------------------------------------|-------------------------------------------|-----------------------------------------------------------------------------|
| | Kim <i>et al.</i> (2014) | Kim and Lee (2016) | Kim and Lee (2016) |
| Strain | <i>C. ijungdahlii</i> | <i>C. ijungdahlii</i> | <i>C. ijungdahlii</i> |
| Temperature (°C) | 30 | 37 | 37 |
| Nano supplement | 0.3 wt% SiO ₂ -CH ₃ | 0.3 wt% SiO ₂ -CH ₃ | 0.3 wt% CoFe ₂ O ₄ @SiO ₂ -CH ₃ |
| Time (h) | 24 | 60 | 60 |
| Substrate | 0.9 g Fructose | 0.9 g Fructose | 0.9 g Fructose |
| Ethanol (g/L) | - | 0.354 | 0.489 |
| Ethanol yield (% improvement) | 166.1% | 126.9% | 213.5% |
| Repeated cycle | ND | 5-Batch | 5-Batch |
| pH | 6.8 | 6.8 | 6.8 |
| Productivity (g/L/h) | ND | 0.020 | 0.027 |

ND, Not determined

2.3 Biodiesel production

Biodiesels are alkyl esters of both short- and long-chain fatty acids from either animal fats or vegetable oils. Production of biodiesel from microalgal lipids, vegetable oils and animal oils has attracted interest due to the many benefits of biodiesel, namely: feed stocks are highly abundant since they are regarded as waste; food security-wise; reduced production cost; decreased CO₂ emissions; and its degradability (Sekoai *et al.*, 2019).

Biodiesel is a clean energy source that is considered a suitable substitute for the conventional petroleum diesel. This is due to its higher energy density, enhanced lubricating property, environmental friendliness and capacity to be produced using non-edible oils (Sekoai *et al.*, 2019). Nanotechnology has been employed in biodiesel production to achieve high product yields (Lee and Lee, 2015). Chen *et al.* (2018) have reported on the impact of supplementing Fe₃O₄/ZnMg(Al)O nanoparticles in biodiesel production using microalgal oil (Table 2.1). The incorporation of Fe₃O₄/ZnMg(Al)O NPs favoured the biodiesel production, resulting in a high yield of 94% (Chen *et al.*, 2018). Similarly, Tahvildari *et al.* (2015) evaluated the catalytic and synergistic potential of CaO and MgO nanocatalysts on biodiesel production from waste cooking oil. The combination of both NPs showed an excellent catalytic efficiency, resulting in biodiesel yield of 98.95%, which was attained with 0.7 g of CaO and 0.5 g of MgO nanoparticles (Tahvildari *et al.*, 2015).

In another study, Dantas *et al.* (2017) reported on the influence of copper-magnetic nanoferrites on methyl transesterification of soybean oil and demonstrated up to 85% enhancement in the biodiesel yield. Furthermore, acid-functionalised magnetic nanocatalyst was evaluated for catalytic potential in the transesterification of glyceryl trioleate to biodiesel (Dantas *et al.*, 2017). The acid-functionalised nanoparticles (sulfamic silica-coated crystalline Fe/Fe₃O₄ core/shell magnetic nanoparticles) additives showed notable catalytic activity, with high biodiesel conversion of more than 95% (Wang *et al.*, 2015). Also, Chiang *et al.* (2015) used

functionalised nanoparticles (Fe_3O_4 @silica core-shell nanoparticles) for microalgal oil conversion to biodiesel and obtained a high percentage yield (97.1%). The use of calcite-Au nanoparticles for biodiesel production has been evaluated by Bet-Moushoul *et al.* (2016). These authors recorded a conversion value of 97.5% at 3% calcite-Au nanoparticles catalyst loading. The application of nanoparticles in biodiesel production has showed an enhanced substrate conversion, increased productivity, catalyst recovery and reusability. Various nanoparticles have been employed as biocatalysts for the enhancement of biodiesel production.

Table 2.1: Nano-additives employed in biodiesel production processes

| NPs | Feedstock | NPs (wt%) | Yield (%) | Cycle | References |
|----------------------------------------------------|-------------------------|------------------|------------------|--------------|-----------------------------------|
| Fe ₃ O ₄ /ZnMg(Al)O | Microalgal oil | ND | 94 | 7 | Chen <i>et al.</i> (2018) |
| CaO | Microalgal oil | 1.7 | 86 | ND | Pandit <i>et al.</i> (2017) |
| ZnO | Waste cooking oil | 1.5 | 96 | ND | Varghese <i>et al.</i> (2017) |
| SO ₄ ²⁻ /ZrO ₂ | Waste cooking oil | 2.9 | 94 | | Vahida <i>et al.</i> (2018) |
| Ni-ZnO | Castor oil | 11.1 | 95 | ND | Baskar <i>et al.</i> (2018) |
| CaO | <i>Bombax ceiba</i> oil | 1.5 | 96 | ND | Hebbar <i>et al.</i> (2018) |
| Calcite-Au | Sunflower oil | 0.3 | 98 | 10 | Bet-Moushoul <i>et al.</i> (2016) |
| Sulfamic silica- Fe/Fe ₃ O ₄ | Glyceryl trioleate | ND | >95 | 5 | Wang <i>et al.</i> (2015) |

ND, Not determined

2.4 Biohydrogen production

Biohydrogen is generated during the microbial fermentation of suitable substrates and it involves diverse groups of microorganisms (Han *et al.*, 2011; Faloye *et al.*, 2014). These microorganisms are able to utilise organic matter such as lignocellulosic wastes, food wastes, municipal wastes and animal manure during dark fermentation (Han *et al.*, 2011). The application of nanoparticles for the improvement of dark fermentative biohydrogen production has been reported in several studies. Many of these efforts have yielded positive and desirable results as shown in Table 2.2.

A plausible explanation for increased biohydrogen yields is due to the ability of nanoparticles to improve the process buffering capacity, which in turn stimulates and enhances the activity of hydrogenase enzymes and substrate hydrolysis (Han *et al.*, 2011). The addition of nanoparticles has been shown to enhance the hydrogen-producing metabolic pathways such as acetate and butyrate reactions and hydrolysis and acidification processes. For instance, the study by Han *et al.* (2011) supplemented hematite nanoparticles at 200 mg/L as a bioactive to a bacterial mixed culture (pH 6.0, at 35C) and this resulted in a 30% improvement in the hydrogen yield (Table 2.2). The authors attributed this increase to enhanced metabolic activities that favour hydrogen formation pathways (Han *et al.*, 2011).

Furthermore, Wimonsong and Nitisoravut (2015) investigated the activity of nano-porous activated carbon (NAC) in batch fermentative biohydrogen production (using sucrose-fed anaerobic mixed bacteria culture, at 37C). The nanoporous activated carbon resulted in low concentration of butyric acid with 77% absorption capacity, thereby increasing the buffering capacity of the system (Wimonsong and Nitisoravut, 2015). This invariably improves the physiological state and fermentative activities of biohydrogen-producing microbes that lead to high hydrogen yield in the system (Wimonsong and Nitisoravut, 2015). Moreover, the effects of silver nanoparticles concentration (0-200 nmol/L) on glucose-fed and pre-treated mixed

bacteria culture in an anaerobic batch reactor was investigated and revealed a 61.45% improvement in fermentative hydrogen production at 20 nmol/L (silver nanoparticles) (Zhao *et al.*, 2013). In another study, MCM41 nanoparticles with or without a functional group influenced syngas fermentation in a system for biohydrogen production (Haiyang *et al.*, 2010). Findings from the aforementioned study showed that biohydrogen yield was enhanced twofold in the presence of 0.6 wt% of the MCM41 nanoparticles functionalised with 5% molar ratio of mercaptopropyl group (Haiyang *et al.*, 2010). The enhanced hydrogen yield was due to improved CO-water mass transfer (water-gas shift was biologically and effectively mediated) through the addition of the functionalised MCM41 nanoparticles (Haiyang *et al.*, 2010). Similarly, in a recent study, Vi *et al.* (2017) optimized fermentative biohydrogen-producing conditions of substrate concentration, pH and FeSO₄ nanoparticle concentration. Cumulative biohydrogen yield of 3.50 g/L was achieved at optimized setpoints of 27.63 g/L, 6.10 and 0.063 g/L, for substrate concentration, pH and FeSO₄ NP concentration, respectively. Additional studies on the influence of different nanoparticles on biohydrogen production are summarised in Table 2.2 (Hydrogen yield: Highest H₂ yield in mol H₂/mol substrate, Nanoporous activated carbon: NAC, Nickel-graphene: Ni-C).

Table 2.2a: Effect of nanobiocatalyst on fermentative biohydrogen yield

| Techniques | Substrates | Inoculum | Additives | Highest H ₂ yield | References |
|------------|-----------------------|-------------------------------|------------------------------------------|------------------------------|-----------------------------------|
| Batch | Sucrose | <i>C. butyricum</i> | Hematite NPs | 3.57 | Han <i>et al.</i> (2011) |
| Batch | Starch | <i>Enterobacter aerogenes</i> | Fe ₂ O ₃ NPs | 192.40 | Lin <i>et al.</i> (2016) |
| Batch | Glucose | Sewage sludge | Gold NPs | 2.48 | Zhao <i>et al.</i> (2013) |
| Batch | Sucrose | A. sludge | NAC | 2.60 | Wimonsong and Nitorisavut, (2015) |
| Batch | Sucrose | | Fe ⁰ NPs | 4.20 | Heguang <i>et al.</i> (2014) |
| Batch | Glucose | <i>E. cloacae</i> | Iron NPs | 1.90 | Nath <i>et al.</i> (2015) |
| Batch | Glucose | A. sludge | Nickel NPs | 2.54 | Mullai <i>et al.</i> (2013) |
| Batch | Wastewater | Sewage sludge | Nickel NPs | 24.73 H ₂ /g COD | El Reedy <i>et al.</i> (2017) |
| Batch | Wastewater | Sewage sludge | Ni-C NPs | 41.28 H ₂ /g COD | El Reedy <i>et al.</i> (2017) |
| Batch | Glucose | <i>C. butyricum</i> | Silver NPs | 0.97 | Sekoai <i>et al.</i> (2019) |
| Batch | Glucose | <i>E. cloacae</i> | Copper NPs | 1.39 | Mohanraj <i>et al.</i> (2016) |
| Batch | Glucose | <i>C. butyricum</i> | Copper NPs | 1.01 | Sekoai <i>et al.</i> (2019) |
| Batch | Glucose | <i>C. butyricum</i> | Pd NPs | 0.97 | Sekoai <i>et al.</i> (2019) |
| Batch | Distillery wastewater | A. sludge | Fe ₂ O ₃ + NiO NPs | 8.83 mmol/g-COD | Gadhe <i>et al.</i> (2015a) |
| Batch | Dairy wastewater | A. sludge | Fe ₂ O ₃ + NiO NPs | 17.2 mmol/g-COD | Gadhe <i>et al.</i> (2015b) |

Footnote: Highest H₂ yield in mol H₂/mol substrate, Nanoporous activated carbon (NAC), Nickel-graphene (Ni-C), Activated carbon (A-C), Activated sludge (A. sludge), Dry weight (DW), *Clostridium butyricum* CWB11009, *Enterobacter cloacae* DH-89, *Bacillus anthracis*

Table 2.2b: Effect of nanobiocatalyst on fermentative biohydrogen yield

| Techniques | Substrates | Inoculum | Additives | Highest H ₂ yield | References |
|------------|--------------------------------|-----------------------------------|------------------------------------|------------------------------|-----------------------------|
| Batch | Glucose | <i>C. pasteurianum</i> CH5 | TiO ₂ NPs | 2.1 | Sekoai <i>et al.</i> (2019) |
| Batch | Distillery wastewater | A. sludge | NiO NPs | 6.73 mmol/g-COD | Gadhe <i>et al.</i> (2015a) |
| Batch | Dairy wastewater | A. sludge | NiO NPs | 15.7 mmol/g-COD | Gadhe <i>et al.</i> (2015b) |
| Batch | Glucose and starch | A. sludge | NiO NPs | 1.3 | Sekoai <i>et al.</i> (2019) |
| Batch | Palm oil effluent | <i>B. anthracis</i> | NiO NPs | 560 mL/g-COD | Mishra <i>et al.</i> (2018) |
| Batch | Sugar cane bagasse hydrolysate | A. sludge | Fe ₃ O ₄ NPs | 1.21 | Reddy <i>et al.</i> (2017) |
| Batch | Glucose | A. sludge | Fe ₃ O ₄ NPs | 1.53 | Sekoai <i>et al.</i> (2019) |
| Continuous | Sucrose wastewater | Sewage sludge | Fe ₂ O ₃ NPs | 300 mL/g-sucrose | Salem <i>et al.</i> (2017) |
| Batch | Distillery wastewater | A. sludge | Fe ₂ O ₃ NPs | 7.85 mmol/g-COD | Gadhe <i>et al.</i> (2015a) |
| Batch | Dairy wastewater | A. sludge | Fe ₂ O ₃ NPs | 16.75 mmol/g-COD | Gadhe <i>et al.</i> (2015b) |
| Batch | Sucrose | Cracked cereals | Fe ₂ O ₃ NPs | 3.21 | Han <i>et al.</i> (2011) |
| Batch | Glucose and starch | A. sludge | Fe ₂ O ₃ NPs | 1.92 | Sekoai <i>et al.</i> (2019) |
| Batch | Cassava starch | <i>E. aerogenes</i> ATCC13408 | Fe ₂ O ₃ NPs | 124.3 mL/g-starch | Lin <i>et al.</i> (2016) |
| Batch | Glucose | <i>E. aerogenes</i> ATCC13408 | Fe ₂ O ₃ NPs | 192.4 mL/g-glucose | Lin <i>et al.</i> (2016) |
| Batch | Glucose | <i>C. acetobutylicum</i> NCIM2337 | Fe ₂ O ₃ NPs | 2.33 | Mohanraj <i>et al.</i> 2004 |
| Batch | Palm oil effluent | <i>B. anthracis</i> | CoO NPs | 0.487 L/g-COD | Mishra <i>et al.</i> (2018) |

Footnote: Highest H₂ yield in mol H₂/mol substrate, *Clostridium pasteurianum* CH5, *Bacillus anthracis* PUNAJAN 1, *Enterobacter cloacae* 811101, *Enterobacter aerogenes* ATCC13408, *Clostridium acetobutylicum* NCIM23

2.5 Biogas production

Anaerobic digestion is one of the most important techniques used to convert organic waste biomass into renewable energy in the form of biogas (Abdelsalam *et al.*, 2016). The anaerobic digestion process is relatively slow and is carried out by a mixed consortium of microorganisms. Anaerobic digestion depends on various process parameters such as pH, temperature, hydraulic retention time and carbon/nitrogen (C/N) ratio, among others (Abdelsalam *et al.*, 2016). This process consists of a series of microbial processes that convert organic matter to biogas, which could take place under psychrophilic (<20 °C), mesophilic (25-40 °C) or thermophilic (50-65 °C) conditions (Abdelsalam *et al.*, 2017a). Biogas production from organic matter mainly depends on the contents of the substrates that can be degraded to CH₄, H₂ and CO₂. Substrate composition, biodegradability and nutrients are key factors for biogas yield. The use of catalytic, stimulatory and biochemical nanoparticles additives in anaerobic digestion processes could improve biogas production significantly and have previously recorded promising results (Table 2.3). These positive outcomes have been related to effective electron transfer (oxidation-reduction potential), cofactor of key enzymes and improved hydrolysis of organic matter. For example, the influence of zero valent iron (ZVI) and Fe₂O₃ nanoparticles on biogas production using activated waste sludge was reported by Wang *et al.* (2016). These authors indicated that ZVI NPs (10 mg/g TSS) and Fe₂O₃ NPs (100 mg/g TSS) enhanced the biogas production by 2.20-fold and 2.17-fold, respectively (Wang *et al.*, 2016). Their results demonstrate that nanoparticles inclusion has a positive effect on the activity of methanogenic archaea. Similarly, Su *et al.* (2013) assessed the effects of 0.1 wt% ZVI NPs on biogas production and methane production using activated waste sludge, and these resulted in 30% and 13.2% increase in concentration, respectively. Furthermore, Abdelsalam *et al.* (2017a) reported that the addition of Co NPs (1 mg/L) notably increased biogas and methane volume by 1.64 and 1.86 times, respectively. The same authors also observed substantial improvements in the biogas and

methane volume by 1.74 and 2.01 times, respectively, when 2 mg/L Ni NPs were included in the anaerobic digestion of livestock slurry.

On the other hand, the study by Abdelsalam *et al.* (2016) varied Co, Ni, Fe and Fe₃O₄ nanoparticle concentrations (1, 2, 20 and 20 mg/L) to assess their impacts on biogas and methane production from anaerobic digestion of livestock slurry. The aforementioned study revealed that these NPs enhanced the biogas and methane production (Abdelsalam *et al.*, 2016). Similarly, a study by Gonzalez-Estrella *et al.* (2013) revealed that Fe₃O₄ and ZVI nanoparticles enhanced biogas production by 66% and 45% respectively. This improved process productivity of nano-base anaerobic digestion can be ascribed to the proliferation of methanogens resulting from the promotion of direct interspecies electron transfer by nanoparticles (Park *et al.*, 2018). The inclusion of nanometric materials also enhances the formation of essential biogas pathway intermediates such as acetate, butyrate, formate and hydrogen, while reducing others like ethanol (Sekoai *et al.*, 2019).

In addition to the abovementioned impacts of NPs in anaerobic digestion, other catalytic effects include increased substrate conversion, which can be attributed to the large surface-area-to-volume-ratio provided by nanoparticles for microbes and enzymes to bind in active sites thereby promoting their biochemical (such as complexation, aggregation) and metabolic processes. Furthermore, nano-based anaerobic digestion provides an interdependent process condition that permits the oxidation state of nanoparticles to be altered by microorganisms acting as catalytic agents. A few studies showing the impacts of different nanoparticles on the biogas production is summarized in Table 2.3.

Table 2.3: Nanocatalysts in anaerobic digestion for biogas production

| NPs | Inoculum | Biogas (mL gas g⁻¹VS) | Methane* | References |
|--------------------------------|----------------------------|-----------------------------------------|---------------------------------------------------------|-------------------------------------|
| Ni | Livestock slurry | 615 | 362 | Abdelsalam <i>et al.</i> (2017a) |
| Co | Livestock slurry | 579 | 333 | Abdelsalam <i>et al.</i> (2017a) |
| Ni | Livestock manure | 512 | 304 | Abdelsalam <i>et al.</i> (2016) |
| Fe ₃ O ₄ | Livestock manure | 496 | 303 | Abdelsalam <i>et al.</i> (2016) |
| Fe | Livestock manure | 424 | 234 | Abdelsalam <i>et al.</i> (2016) |
| Co | Livestock manure | 491 | 281 | Abdelsalam <i>et al.</i> (2016) |
| Nzvi | Livestock manure | 513 | 286 | Abdelsalam <i>et al.</i> (2017b) |
| Fe ₃ O ₄ | Livestock manure | 584 | 352 | Abdelsalam <i>et al.</i> (2017b) |
| Nzvi | <i>Dehalococcoides sp.</i> | ND | 275 μmol | Xiu <i>et al.</i> (2010) |
| Nzvi | Waste-activated sludge | ND | 217 | Wang <i>et al.</i> (2016) |
| Fe ₂ O ₃ | Waste-activated sludge | ND | 212 | Wang <i>et al.</i> (2016) |
| CuO | Anaerobic granular sludge | ND | 6 g COD CH ₄ L ⁻¹ d ⁻¹ | Otero-Gonzalez <i>et al.</i> (2014) |

ND, Not determined; * mL gas g⁻¹VS except where otherwise stated

2.6 Nanoparticles as immobilization matrix for biofuel production

Common immobilization approaches (cells or enzymes) employ materials with sizes above the nanometre (10^{-9}) range (Nickzad *et al.*, 2012; Wiboon *et al.*, 2012; Charlimagne *et al.*, 2012; Martins *et al.*, 2013; Zhaohui *et al.*, 2016). Nevertheless, nanoparticles have been well established as an immobilization matrix and have desirable biotechnological advantages, which include large surface to volume ratios, high loading of the specific molecules targeted, easy separation from the reaction using an external magnetic field and strong adsorption ability (Han *et al.*, 2011). In addition, multivalent nanoparticles, bearing multiple targeting groups can give stronger anchoring for cells and enzymes (Willner *et al.*, 2006; Han *et al.*, 2011; Ansari and Husain, 2012).

Nanoparticles can also play a vital role in the improvement of thermal and pH stability of microbial cells and enzymes (Pandurangan and Kim, 2015). For instance, magnetic nanoparticles are suitable for lipase immobilization, due to their ability to form nanocrystals. This phenomenon increases thermal stability and reusability of the enzyme. Furthermore, the formation of nanocrystals tends to clump together, increasing the biocatalyst surface area.

The incorporation of nano-immobilized enzymes/microbes is beneficial for bioprocessing, since they enhance process costs, conversion efficiency and the overall process performance (Sekoai *et al.*, 2019). Limited studies exist on the application of nanoparticles as an immobilization matrix in biofuel production (Table 2.4). The study by Tran *et al.* (2012) immobilized lipase on magnetic nanoparticles (Fe_3O_4) coated with silica ($\text{Fe}_3\text{O}_4\text{-SiO}_2$) and demonstrated an increased tolerance to high methanol-to-oil-ratio (67:93) in an *in-situ* transesterification of *Chlorella vulgaris* lipid. Furthermore, the immobilized lipase could withstand high water content of 71% with a biodiesel conversion value of 97.3 wt% oil (Tran *et al.*, 2012). Likewise, Ivanova *et al.* (2011) assessed the effect of immobilized *S. cerevisiae* on bioethanol productivity. The immobilized cells substantially enhanced bioethanol productivity. Moreover, the entrapped cells were employed successfully over 42 days without

a significant loss of bioethanol productivity. Similarly, the study by Cherian *et al.* (2015) reported on cellulase immobilized on MnO₂ nanoparticles and found the immobilized enzyme to be more thermostable at 70 °C. Also, the reusability (after five cycles, retained 60% activity) of cellulase was significantly increased after immobilization. Studies showing the influence of various nanoparticles as immobilization agents for biofuel production are summarized in Table 2.4.

Table 2.4: Nanoparticles immobilization matrix employed in biofuel production

| NPs matrix | Cell/enzymes | Process | Biofuel produced | References |
|--------------------------------------------------|----------------------------------|---------------------------|-------------------------|--------------------------------|
| MnO ₂ | Cellulase | Sugar hydrolysis | Bioethanol | Cherian <i>et al.</i> (2015) |
| SiO ₂ | β-galactosidase | Sugar hydrolysis | Bioethanol | Beniwal <i>et al.</i> (2018) |
| Nanofiber | β-Glucosidase | Sugar hydrolysis | Bioethanol | Lee <i>et al.</i> (2010) |
| Fe ₃ O ₄ | α-amylase | Starch liquefaction | Bioethanol | Ivanova <i>et al.</i> (2011) |
| Fe ₃ O ₄ | Glucoamylase | Sugar saccharification | Bioethanol | Ivanova <i>et al.</i> (2011) |
| Fe ₃ O ₄ | <i>S. cerevisiae</i> | Fermentation | Bioethanol | Ivanova <i>et al.</i> (2011) |
| Fe ₃ O ₄ -SiO ₂ | Lipase | Lipid transesterification | Biodiesel | Tran <i>et al.</i> (2012) |
| SiO ₂ | Lipase | Lipid transesterification | Biodiesel | Babaki <i>et al.</i> (2016) |
| Fe ₃ O ₄ -SiO ₂ | Lipase | Lipid transesterification | Biodiesel | Thangaraj <i>et al.</i> (2016) |
| Modified Fe ₃ O ₄ | Lipase | Lipid transesterification | Biodiesel | Raita <i>et al.</i> (2015) |
| Modified Fe ₃ O ₄ | Lipase | Lipid transesterification | Biodiesel | Zhang <i>et al.</i> (2016) |
| Magnetic NPs | <i>Candida antarctica</i> lipase | Lipid transesterification | Biodiesel | Mehrasbi <i>et al.</i> (2017) |
| carbon nanotubes | Lipase | Lipid transesterification | Biodiesel | Fan <i>et al.</i> (2016) |

2.7 Bioprocess modelling: optimization and kinetics

The optimization of process conditions such as temperature, pH, nutrient and substrate concentration is an important factor in the development of economically feasible bioprocess, owing to their impact on the process. Process optimization aids the reduction of the cost-profit-ratio for the development of an industrial-scale production system (Faloye, 2015). Bioprocess optimization is vital to industrial production processes, in which even slight improvements can be essential for the commercialisation of a process. Process performance and product formation are influenced by many process parameters, which include the fermentation conditions, strain of fermenting microbe, substrate type and the bioreactor configuration (Qazizada, 2016; Rorke *et al.*, 2017).

The traditional method of one factor at a time is a technique that examines one variable singly, keeping the other parameters constant. The result obtained is represented on a graph to depict the effects of the single factor on the process output (Faloye, 2015). Several studies on the optimization of fermentation process focused on the method of one variable at a time method (OVAT), which is practically insufficient to accomplish appropriate optimization in a finite number of experiments (Izmirlioglu and Demirci, 2012; Betiku and Adesina, 2013; Betiku and Ajala, 2014; Adeoye *et al.*, 2015; Adeeyo *et al.*, 2016; Bamigboye *et al.*, 2019). Moreover, the OVAT technique is usually not preferred because many potential influential factors may be involved in the fermentation process and their interactive effect might not be accounted for (Faloye, 2015). Modelling and optimization have been employed with the aim of improving bioprocessing using various modelling tools. Owing to the limitations of other methods of optimization such as OVAT, statistical techniques such as Response Surface Methodology (RSM), Artificial Neural Networks (ANN) and genetic algorithm among others are progressively being used (Nikzad *et al.*, 2015; Izmirlioglu and Demirci, 2016).

The RSM allows for the identification of many factors and their interactive influences on the process yield and has been reported in the modelling and optimization of various bioprocesses (Rorke *et al.*, 2017). Response surface methodology is a blend of stepwise mathematical, statistical and empirical techniques developed to improve and optimize bioprocesses. The advantages of this technique include, minimum experimental runs, less process time, flexibility of variable assigning, closer confirmation of the output response to the target requirements, assessment of relations existing between experimental factors and the target responses (Talasila and Vechalapu, 2015).

Knowledge on the relationships that exists among the experimental variables and the set points that can produce the optimal value of the desired response are the most important features of the RSM (Izmirliloglu and Demirci, 2012). Central composite design and Box-Behnken design are examples of commonly used response surface methodology. Box-Behnken experimental design is a three-level fractional factorial model, with a two-level factorial design plus an incomplete block design. Box-Behnken design is more cost-effective to use compared to the central composite design, because of the use of few experimental factors and lack of extreme levels (too high or low levels) (Rorke *et al.*, 2017).

A second-order polynomial model is usually developed based on the data obtained from the experiments to depict the effects of the multiple factors on the target output. Response surface and contour map plots from the model display the variation of the influence of two interactive factors while keeping the other factor level constant. The plots shows the response over the different factor levels, plus the sensitivity of the response to any change in the factor. The model is lastly subjected to analysis of variance for estimation and the determination of factors with significant impact on the target response (Faloye, 2015).

Optimization is one of the essential procedures to develop a more robust process for industrial application to improve bioethanol yield (Faloye, 2015). Currently, different studies are focused

on using statistical techniques to optimize the key operational parameters such as temperature, pH, agitation speed and substrate concentration that affect the process of ethanol fermentation. Optimization of experimental design is of immense importance in fermentative bioethanol process due to the complexity and influence of many process factors; therefore, a suitable experimental design must be employed to assess the effects of these parameters. Equally, the model provides valuable suggestions for the analysis, design and operation of the bioreactor (Izmirlioglu and Demirci, 2016).

Bioprocess kinetic modelling enables assessment of the biochemical characteristics of a microbial or an enzymatic process. Kinetic modelling allows for improved productivity and product yield as well as high product quality. Similarly, this technique could help in reducing the formation of process unwanted by-products (Almquist *et al.*, 2014). These models can be used for virtual experimentation to reduce time and costs related with process development. Additionally, the implementation of these kinetic models provides a robust foundation for process design, control, optimization and ultimately lower the challenges faced during process up-scaling (Linville *et al.*, 2013).

Commonly used kinetic models in bioprocess include the Monod model, Gompertz model and logistic function model. Monod models are employed to express the relationship between biomass growth and the limiting substrate, and similarly, the changes in microbial population as a function of growth rate, initial biomass and maximum biomass concentration, and time, assuming sufficient substrate can be expressed by logistic model. At the same time, the modified Gompertz models are used to obtain vital process coefficients such as lag time, maximum product concentration and the maximum production rate (Imamoglu and Sukan, 2013; Linville *et al.*, 2013; Putra *et al.*, 2015).

2.8 Process inhibitory compounds production

The formation of inhibitory compounds and the need to reduce their effect or detoxify these compounds has been one of the challenges of high-process efficiency in bioprocessing. Numerous process-inhibitory compounds have been identified in bioprocessing. These include aldehydes, amines, amides, lactones, sulphur-containing compounds, alkanals, ketones, phenolics, aliphatic acids, alkanols and benzenoids (Han *et al.*, 2011; Rorke *et al.*, 2017). Moreover, the influence of various process inhibitors have been reported in scientific literature. For instance, Cao *et al.* (2010) reported the impact of different concentrations of inhibitory compounds such as furfural and 5-hydroxymethyl furfural (HMF) on biohydrogen production from xylose with *Thermoanaerobacterium thermosaccharolyticu* W16. The authors reported hydrogen inhibition at concentrations above 1.5, 2.0, 1.0, 2.0 and 10 g/L for furfural, HMF, syringaldehyde, vanillin and acetic acid respectively. Similarly, furfural and the HMF compounds could lower microbial enzyme activity during fermentation. Additionally, phenolic compounds will permanently disrupt microbial cell membranes (Quemeneur *et al.*, 2012). While aliphatic acids could diffuse into microbial cells, this lowers intracellular pH which impedes ethanol production as well as hampering RNA and protein synthesis and the degrading of microbial DNA molecules. Furthermore, the harsh pre-treatment conditions required to break down the lignocellulose structure often result in the formation of compounds that have been proven to inhibit the saccharification step alongside the fermentation process (Kamal *et al.*, 2011). Lignocellulosic biomass pre-treatment inhibitory by-products include compounds of aldehydes, amines, amides, lactones, phenolics, sulphur-containing compounds, alkanals, ketones, phenolics and aliphatic acids (Rorke *et al.*, 2017). These are xylose and glucose oxidation products, while, some phenolic compounds are derivative of partial lignin degradation (Cao *et al.*, 2010). These inhibitory by-products have different negative effects in bioprocessing, including furfural inhibiting bioprocesses, anaerobic growth of the microbes, causing damage to vacuole and mitochondrial membranes by the conversion of furfural to

furfuryl alcohol and the accumulation of reactive oxygen species within yeast cells (Rorke *et al.*, 2017).

Acetic acid is generated in large amounts during acid pre-treatment and fermentation process. The dissociation of acetic acid within the neutral cell environment results in a drop in pH, consequently impeding cell activity (Rorke *et al.*, 2017). Furthermore, other aliphatic acids such as formic and levulinic acid, which are furan degradation products, hamper bioethanol production by causing intracellular accumulation of anions; and an attempt to correct this by the fermenting cell results in unnecessary use of ATP, resulting in less being accessible for biomass formation.

Other important inhibitory compounds are the phenolic compounds. Although, the overall amount of phenolic compounds generated during pre-treatment is much lower than furan derivatives and carboxylic acids, the effect exerted by phenolics on bioprocesses is more pronounced (Harmsen *et al.*, 2010). The inhibitory effect of phenolic compounds include generation of reactive oxygen species, loss of cell membrane integrity, reduction in specific growth rate and lowering fermenting cell adaptation to sugars present (Harmsen *et al.*, 2010). Hence, detoxification or by-product elimination technique is essential to remove these inhibitory compounds before downstream fermentative process. The detoxification process employs chemical, physical and biological techniques. Detoxification is the removal of toxic chemical compounds such as aliphatic acids and phenolics from a process, including biological processes such as fermentation. Detoxification processes have been suggested as one of the effective approaches to reduce the concentration of fermentation inhibitory compounds (Deng and Aita, 2018). Optimization of the detoxification conditions is necessary for maximising bioproduct yields from lignocellulosic biomass.

2.9 Bioprocess scale-up

Bioethanol fermentation experiments described in scientific literature are frequently conducted at laboratory-scale while, data on scale-up bioethanol production studies are scantily reported (Ghimire *et al.*, 2015). The scale-up of a fermentation process requires several important engineering considerations which ultimately dictate process performance. Other aspects which require precise compromise between intrinsically contradictory but desirable characteristics are the metabolic processes and economic factors regarding the best economic efficiency (Qazizada, 2016).

Four techniques, namely, fundamental methods, semi fundamental methods, dimensional analysis and the rule-of-thumb are widely used in scaling up. The parameters employed in these techniques are usually correlated to reactor geometry, mass transfer, mixing activity, power consumption, bulk rheology, cell viability, substrate and products concentration, micro-conditions, nutrients' state and availability in the bioreactor (Deniz *et al.*, 2015; Qazizada, 2016). The design of an industrial-scale ethanol fermentation process depends on growth conditions, nutrient formulation, the target product, microbial strain, bioreactor geometry and fluid hydrodynamics. Therefore, for a certain product, suitable and comprehensive process parameters which are directly linked to improved productivity and scaling-up potential has to be established.

2.10 Present challenges and future perspectives on nano application in biofuel production

Fermentative production of biofuel is achieved by the bioconversion of fermentable sugars contained in organic waste through pre-treatment and fermentation processes. However, the wide application of fermentative biofuel production has always been limited on account of the need for suitable feedstock, inefficient pre-treatment regimes and low process yield. To address the low process yield in fermentative biofuel production, catalytic nano-sized materials are being employed as one of the approaches to improve biofuel productivity (Han *et al.*, 2011;

Abdelsalam *et al.*, 2016). Although, this approach has been implemented in various biofuel production projects, such as for biohydrogen, biomethane, biogas and biodiesel, there is paucity of literature on the application of this technique in bioethanol production (Han *et al.*, 2011; Ivanova *et al.*, 2011; Abdelsalam *et al.*, 2016; Abdelsalam *et al.*, 2017a; Mehrasbi *et al.*, 2017; Shanmugam *et al.*, 2020). The impact of nanoparticles in microbial fermentation include: enhanced metabolic activities leading to improved cell growth and productivity; reduction in the oxidation-reduction potential of the process; improvement of buffering capacity; reduction in organic inhibitors accumulation; and Efficient immobilisation matrix due to large surface area and modifiable surfaces (Han *et al.*, 2011; Ivanova *et al.*, 2011; Ban and Paul, 2014; Abdelsalam *et al.*, 2016; Abdelsalam *et al.*, 2017a; Thangaraj *et al.*, 2016; Beniwal *et al.*, 2018). Despite the merits of nanoparticle application in biofuel processes, several problems still plague its implementation, including the cost of synthesising the nanoparticles (achieving a cost-effective biofuel production process will require thorough considerations of the economic implications involved in the synthesis of nanomaterials), biocompatibility of nanomaterials, mechanism of action, reusability, process optimization and scalability.

References

- Abdelsalam E, Samer M, Attia YA, Abdel-Hadi MA, Hassan HE, Badr Y (2016). Comparison of nanoparticles effects on biogas and methane production from anaerobic digestion of cattle dung slurry, *Renew. Energy*, 87: 592-598.
- Abdelsalam E, Samer M, Attia YA, Abdel-Hadi MA, Hassan HE, Badr Y (2017a). Effects of Co and Ni nanoparticles on biogas and methane production from anaerobic digestion of slurry, *Energy Conversion and Management*, 141: 108-119.
- Abdelsalam E, Samer M, Attia YA, Abdel-Hadi MA, Hassan HE, Badr Y (2017b). Influence of zero valent iron nanoparticles and magnetic iron oxide nanoparticles on biogas and methane production from anaerobic digestion of manure. *Energy*, 120: 842–53.
- Adeeyo AO, Lateef A, Gueguim Kana EB (2016). Optimization of the production of extracellular polysaccharide from the Shiitake medicinal mushroom *Lentinus edodes* (Agaricomycetes) using mutation and a genetic algorithm-coupled artificial neural network (GA-ANN). *International Journal of Medicinal Mushrooms*, 18 (7): 571-581.
- Adeoye AO, Lateef A, Gueguim Kana EB (2015). Optimization of citric acid production using a mutant strain of *Aspergillus niger* on cassava peel substrate. *Biocatalysis and Agricultural Biotechnology*, 4 (4): 568-574.
- Almquist J, Cvijovic M, Hatzimanikatis V, Nielsen J, Jirstrand M (2014). Kinetic models in industrial biotechnology – Improving cell factory performance. *Metabolic Engineering*, 24: 38-60.
- Ansari SA, Husain Q (2012). Potential applications of enzymes immobilized on/in nano materials: a review. *Biotechnology Advances*, 30: 512–523.
- Aruwajoye GS, Faloye FD, Gueguim Kana EB (2017). Soaking assisted thermal pre-treatment of cassava peels wastes for fermentable sugar production: Process modelling and optimization. *Energy Conversion and Management*, 150: 558–566.

- Babaki M, Yousefi M, Habibi Z, Mohammadi M, Yousefi P, Mohammadi J (2016). .Enzymatic production of biodiesel using lipases immobilized on silica nanoparticles as highly reusable biocatalysts: effect of water, t-butanol and blue silicagel contents. *Renewable Energy*, 91:196–206.
- Baeyens J, Kang Q, Appels L, Dewil R, Lv Y, Tan T (2015). Challenges and opportunities in improving the production of bio-ethanol. *Progress in Energy and Combustion Science*, 47: 60-88.
- Bamigboye CO, Oloke JK, Dames JF, Burton M, Lateef A (2019). Process optimization for production of biomass and exopolysaccharide by King tuber oyster mushroom, *Pleurotus tuber-regium* (Agaricomycetes) for biotechnological applications. *International Journal of Medicinal Mushrooms*.
- Ban DK, Paul S (2014). Zinc Oxide Nanoparticles Modulates the Production of β -Glucosidase and Protects its Functional State Under Alcoholic Condition in *Saccharomyces cerevisiae*. *Applied Biochemistry and Biotechnology*, 173: 155–166.
- Baskar G, Selvakumari A, Aiswarya R (2018). Biodiesel production from castor oil using heterogeneous Ni doped ZnO nanocatalyst. *Bioresource Technology*, 250: 793–8.
- Beniwal A, Saini P, Kokkiligadda A, Vij S (2018). Use of silicon dioxide nanoparticles for β -galactosidase immobilization and modulated ethanol production by co-immobilized *K. marxianus* and *S. cerevisiae* in deproteinized cheese whey. *LWT – Food Science Technology*, 87: 553–61.
- Betiku E, Adesina OA (2013). Statistical approach to the optimization of citric acid production using filamentous fungus *Aspergillus niger* grown on sweet potato starch hydrolyzate. *Biomass Bioenergy*. 55: 350-4.
- Betiku E, Ajala SO (2014). Modeling and optimization of *Thevetia peruviana* (yellow oleander) oil biodiesel synthesis via *Musa paradisiacal* (plantain) peels as

- heterogeneous base catalyst: a case of artificial neural network vs. response surface methodology. *Industrial Crops and Products*, 53: 314-22.
- Bet-Moushoul E, Farhadi K, Mansourpanah Y, Nikbakht A, Molaei R, Forough M (2016). Application of CaO-based/Au nanoparticles as heterogeneous nanocatalysts in biodiesel production. *Fuel*, 164: 119–27.
- BP (2016). British Petroleum (BP) Statistical Review of World Energy 2016
- Cao GL, Ren NQ, Wang AJ, Guo WQ, Xu JF, Liu BF. (2010). Effect of lignocellulose- derived inhibitors on growth and hydrogen production by *Thermoanaerobacterium thermosaccharolyticum* W16. *International Journal of Hydrogen Energy*, 35(24):13475-80.
- Charlimagne MM, Emerson RD, Lawrence VS, Jay RTA, Rizalinda LD (2015). Continuous Bioethanol Production Using *Saccharomyces cerevisiae* Cells Immobilized in Nata De Coco (Biocellulose). 2nd International Conference on Environment and Industrial Innovation IPCBEE (2012) vol.35.
- Chen Y, Liu T, He H, Liang H (2018). Fe₃O₄/ZnMg(Al)O magnetic nanoparticles for efficient biodiesel production. *Applied Organometallic Chemistry*, 32: 1–10.
- Cherian E, Dharmendirakumar M, Baskar G. Immobilization of cellulase onto MnO₂ nanoparticles for bioethanol production by enhanced hydrolysis of agricultural waste. *Chinese Journal of Catalysis*, 2015;36:1223–9.
- Chiang Y, Dutta S, Chen C, Huang Y, Lin K, Wu J (2015). Functionalized Fe₃O₄@ silica core-shell nanoparticles as microalgae harvester and catalyst for biodiesel production. *ChemSusChem*, 8:789–94.
- Chohan NA, Aruwajoye GS, Sewsynker-Sukai Y, Gueguim Kana EB (2020). Valorisation of potato peel wastes for bioethanol production using simultaneous saccharification and

- fermentation: Process optimization and kinetic assessment. *Renewable Energy*, 146: 1031-1040.
- Dantas J, Leal E, Mapossa A, Cornejo D, Costa A (2017). Magnetic nanocatalysts of Ni_{0.5}Zn_{0.5}Fe₂O₄ doped with Cu and performance evaluation in transesterification reaction for biodiesel production. *Fuel*, 191: 463–71.
- Demirel and Scherer (2011). Trace element requirements of agricultural biogas digesters during biological conversion of renewable biomass to methane. *Biomass and Bioenergy*, 35: 992 -998.
- Deng, F., Aita, G.M., 2018. Detoxification of dilute ammonia pretreated energy cane bagasse enzymatic hydrolysate by soluble polyelectrolyte flocculants. *Industrial Crops and Products*, 112, 681–690.
- Deniz I, Imamoglu E, Vardar Sukan F (2015). Evaluation of scale-up parameters of bioethanol production from *Escherichia coli* KO11. *Turkish Journal of Biochemistry*, 40 (1): 74–80. 74–80.
- Elegbede JA, Lateef A (2018). Valorization of corn-cob by fungal isolates for production of xylanase in submerged and solid state fermentation media and potential biotechnological applications. *Waste Biomass Valorization* 9 (8): 1273-1287.
- Elegbede JA, Lateef A (2019a). Green synthesis of silver (Ag), gold (Au) and silver-gold (Ag-Au) alloy nanoparticles: A review on recent advances, trends and biomedical applications. In: Verma, D.K., Goyal, M.R., and Suleria, H.A.R. (Eds.). *Nanotechnology and Nanomaterial Applications in Food, Health and Biomedical Sciences*. <https://doi.org/10.1201/9780429425660-1>. Apple Academic Press Inc. /CRC Press, Taylor and Francis Group, Oakville, Ontario, Canada. ISBN 978-1-77188-764-9. Pp. 3-89.

- Elegbede JA, Lateef A (2019b). Green nanotechnology in Nigeria: The research landscape, challenges and prospects. *Annals of Science and Technology*, 4 (2): 6-38.
- Elreedy A, Ibrahim E, Hassan N, El-Dissouky A, Fujii M, Yoshimura C (2017). Nickel graphene nanocomposite as a novel supplement for enhancement of biohydrogen production from industrial wastewater containing mono-ethylene glycol. *Energy Conversion and Management*, 140: 133–44.
- Faloye FD (2015). Optimization of biohydrogen production inoculum development via hybrid pre-treatment techniques-semi pilot scale production assessment on agro waste. PhD Thesis. University of KwaZulu-Natal, Pietermaritzburg, South Africa.
- Faloye FD, Gueguim-Kana EG, Schmidt S (2014). Optimization of biohydrogen inoculum development via a hybrid pH and microwave treatment technique - Semi pilot scale production assessment. *International Journal of Hydrogen Energy*, 39: 5607-5616.
- Fan Y, Wu G, Su F, Li K, Xu L, Han X (2016). Lipase oriented-immobilized on dendrimer-coated magnetic multi-walled carbon nanotubes toward catalysing biodiesel production from waste vegetable oil. *Fuel*, 178: 172–8.
- Fazal T, Mushtaq A, Rehman F, Khan AU, Rashid N, Farooq W, Rehman MSU, Xu J (2018). Bioremediation of textile wastewater and successive biodiesel production using microalgae. *Renewable and Sustainable Energy Reviews*, 82: 3107–3126.
- Fu A, Micheel CM, Cha J, Chang H, Yang H, Alivisatos AP (2004). "Discrete nanostructures of quantum dots/Au with DNA". *Journal of the American Chemical Society*, 126 (35): 10832–3.
- Gadhe A, Sonawane SS, Varma MN (2015a). Influence of nickel and hematite nanoparticle powder on the production of biohydrogen from complex distillery wastewater in batch fermentation. *International Journal of Hydrogen Energy*, 40 (34): 10734-10743.

- Gadhe A, Sonawane SS, Varma MN (2015b). Enhancement effect of hematite and nickel nanoparticles on biohydrogen production from dairy wastewater. *International Journal of Hydrogen Energy*, 40 (13): 4502-4511.
- Ge S, Qiu S, Tremblay D, Viner K, Champagne P, Jessop PG (2018). Centrate wastewater treatment with *Chlorella vulgaris*: Simultaneous enhancement of nutrient removal, biomass and lipid production. *Chemical Engineering Journal*, 342: 310–320.
- Ghimire A, Frunzo L, Pirozzi F, Trably E, Escudie R, Lens PNL, Esposito G (2015). A review of dark fermentative biohydrogen production from organic biomass: Process parameters and use of by-products. *Applied Energy*, 144: 73–95.
- Gonzalez-Estrella J, Sierra-Alvarez R, Field J (2013). Toxicity assessment of inorganic nanoparticles to acetoclastic and hydrogenotrophic methanogenic activity in anaerobic granular sludge. *Journal of Hazardous Materials*, 260: 278–85.
- Gueguim-Kana EB, Oloke JK, Lateef A, Adesiyun MO (2012). Modeling and optimization of biogas production on saw dust and other co-substrates using Artificial Neural Network and Genetic Algorithm. *Renewable Energy*, 46: 276-281.
- Haiyang Z, Brent HS, Dong WC, Theodore JH (2010). Effect of functionalized MCM41 nanoparticles on syngas fermentation. *Biomass and Bioenergy*, 34: 1624 – 1627.
- Han H, Cui M, Wei L, Yang H, Shen J (2011). Enhancement effect of hematite nanoparticles on fermentative hydrogen production. *Bioresour Technol*, 102: 7903–7909.
- Harmsen PFH, Huijgen WJJ, Bermúdez López LM, Bakker RRC (2010). Literature Review of Physical and Chemical Pretreatment Processes for Lignocellulosic Biomass. *Food & Biobased Research*, 2010, Wageningen.
- Hebbar H, Math M, Yatish K (2018). Optimization and kinetic study of CaO nano-particles catalyzed biodiesel production from Bombax ceiba oil. *Energy*, 143: 25–34.

- Heguang Z, Peter S, Parker W (2014). Enhanced dark fermentative hydrogen production under the effect of zero-valent iron shavings. *International Journal of Hydrogen Energy*, 39: 19331–6.
- Hirsch RL, Bezdek RH, Wendling, RM (2005). Peaking oil production: sooner rather than later? *Issues in Science and Technology*, 21 (3): 25–30.
- Howarth M, Liu W, Puthenveetil S, Zheng Y, Marshall LF, Schmidt MM, Wittrup KD, Bawendi MG, Ting AY (2008). "Monovalent, reduced-size quantum dots for imaging receptors on living cells". *Nature Methods*, 5 (5): 397–9.
- Imamoglu E, Sukan FV (2013). Scale-up and kinetic modeling for bioethanol production. *Bioresource Technology*, 144: 311-320.
- Ivanova V, Petrova P, Hristov J (2011). Application in the Ethanol Fermentation of Immobilized Yeast Cells in Matrix of Alginate/Magnetic nanoparticles, on Chitosan Magnetite Microparticles and Cellulose-coated Magnetic nanoparticles. *International Review of Chemical Engineering*, 3: 289 – 299.
- Izmirliglu G, Demirci A (2012). Ethanol Production from Waste Potato Mash by Using *Saccharomyces Cerevisiae*. *Applied Science*, 2: 738-753.
- Izmirliglu G, Demirci A (2016). Improved simultaneous saccharification and fermentation of bioethanol from industrial potato waste with co-cultures of *Aspergillus niger* and *Saccharomyces cerevisiae* by medium optimization. *Fuel*, 185: 684–691.
- Kamal SMM, Mohamad NL, Abdullah AGL, Abdullah N (2011). Detoxification of sago trunk hydrolysate using activated charcoal for xylitol production. *Procedia Food Science*, 2011. 1: 908-913.
- Khawla BJ, Sameh M, Imen G, Donyes F, Dhouha G, Raoudha EG, Oumèma N-E (2014). Potato peel as feedstock for bioethanol production: A comparison of acidic and enzymatic hydrolysis. *Industrial Crops and Products*, 52: 144–149.

- Kim Y, Lee H (2016). Use of magnetic nanoparticles to enhance bioethanol production in syngas fermentation. *Bioresource Technology*, 204: 139–144.
- Kim Y, Park SE, Lee H, Yun JY (2014). Enhancement of bioethanol production in syngas fermentation with *Clostridium ljungdahii* using nanoparticles. *Bioresource Technology*, 159: 446 – 450.
- Lateef A, Ojo SA, Elegbede JA, Akinola PO, Akanni EO (2018). Nanomedical applications of nanoparticles for blood coagulation disorders. In: *Environmental Nanotechnology*, Volume 1. Eds: Dasgupta, N., Ranjan, S., and Lichtfouse, E. https://doi.org/10.1007/978-3-319-76090-2_8. Springer International Publishing AG, Cham, Switzerland. ISBN 978-3-319-76089-6. Pp. 243-277.
- Lee S, Jin L, Kim J, Han S, Na H, Hyeon T (2010). β -Glucosidase coating on polymer nanofibers for improved cellulosic ethanol production. *Bioprocess and Biosystems Engineering*, 33: 141–7.
- Lee Y, Lee K, Oh Y (2015). Recent nanoparticle engineering advances in microalgal cultivation and harvesting processes of biodiesel production: a review. *Bioresource Technology*, 184: 63–72.
- Lin R, Cheng J, Ding L, Song W, Liu M, Zhou J (2016). Enhanced dark hydrogen fermentation by addition of ferric oxide nanoparticles using *Enterobacter aerogenes*. *Bioresource Technology*, 207: 213–9.
- Linville JL, Rodriguez Jr M, Mielenz JR, Cox CD (2013). Kinetic modeling of batch fermentation for *Populus* hydrolysate tolerant mutant and wild type strains of *Clostridium thermocellum*. *Bioresource Technology*, 147: 605–613.
- Liu W, Greytak AB, Lee J, Wong CR, Park J, Marshall LF, Jiang W, Curtin PN, Ting AY, Nocera DG, Fukumura D, Jain RK, Bawendi MG (2010). "Compact biocompatible

- quantum dots via RAFT-mediated synthesis of imidazole-based random copolymer ligand". *Journal of the American Chemical Society*, 132 (2): 472–8.
- Martins SCS, Martins CM, Fiúza LM, Cidrão G, Santaella ST (2013). Immobilization of microbial cells: A promising tool for treatment of toxic pollutants in industrial wastewater. *African Journal of Biotechnology*, 2 (28): 4412-4418.
- Mehrasbi M, Mohammadi J, Peyda M, Mohammad M (2017). Covalent immobilization of *Candida antarctica* lipase on core-shell magnetic nanoparticles for production of biodiesel from waste cooking oil. *Renewable Energy*, 101: 596–602.
- Miazek K, Iwanek W, Remacle C, Richel A, Goffin D (2015). Effect of Metals, Metalloids and Metallic Nanoparticles on Microalgae Growth and Industrial Product Biosynthesis: A Review. *International Journal of Molecular Science*, 16: 23929-23969.
- Mishra P, Thakur S, Mahapatra DM, AbWahid Z, Liu H, Singh L (2018). Impacts of nano-metal oxides on hydrogen production in anaerobic digestion of palm oil mill effluent – A novel approach. *International Journal of Hydrogen Energy*, 43 (5): 2666-2676.
- Mohanraj S, Anbalagan K, Rajaguru P, Pugalenti V (2016). Effects of phyto-genic copper nanoparticles on fermentative hydrogen production by *Enterobacter cloacae* and *Clostridium acetobutylicum*. *International Journal of Hydrogen Energy*, 41: 10639–45.
- Mohanraj S, Anbalagan K, Rajaguru P, Pugalenti V (2016). Effects of phyto-genic copper nanoparticles on fermentative hydrogen production by *Enterobacter cloacae* and *Clostridium acetobutylicum*. *International Journal of Hydrogen Energy*, 41:10639–45.
- Moodley P, Gueguim-Kana EB (2019). Bioethanol production from sugarcane leaf waste: Effect of various optimized pretreatments and fermentation conditions on process kinetics. *Biotechnology Reports*, 22: e00329.

- Mullai P, Yogeswari MK, Sridevi K (2013). Optimisation and enhancement of biohydrogen production using nickel nanoparticles – a novel approach. *Bioresource Technology*, 141: 212–9.
- Nath D, Manhar A, Gupta K, Saikia D, Das S, Mandal M (2015). Phytosynthesized iron nanoparticles: effects on fermentative hydrogen production by *Enterobacter cloacae* DH-89. *Bulletin of Materials Science*, 38: 1533–8.
- Nikzad M, Movaghernajed K, Talebnia F, Mighani M (2015). Modeling of Alkali Pre-treatment of Rice Husk Using Response Surface Methodology and Artificial Neural Network. *Chemical Engineering Communications*, 202 (6): 728-738.
- Otero-Gonzalez L, Field J, Sierra-Alvarez R (2014). Inhibition of anaerobic wastewater treatment after long-term exposure to low levels of CuO nanoparticles. *Water Research*, 58: 160–8.
- Pádrová K, Lukavský J, Nedbalová L, Čejková A, Cajthaml T, Sigler K, Vítová M, Řezanka T (2015). Trace concentrations of iron nanoparticles cause over production of biomass and lipids during cultivation of cyanobacteria and microalgae. *Journal of Applied Phycology*, 27: 1443–1451.
- Pandit P, Fulekar M (2017). Egg shell waste as heterogeneous nanocatalyst for biodiesel production: Optimized by response surface methodology. *Journal of Environmental Management*, 198: 319–29.
- Pandurangan M, Kim DH (2015). ZnO nanoparticles augment ALT, AST, ALP and LDH expressions in C2C12 cells. *Saudi Journal of Biological Sciences*, 22: 679–684.
- Park J-H, Kang H-J, Park K-H, Park H-D (2018). Direct interspecies electron transfer via conductive materials: a perspective for anaerobic digestion applications. *Bioresource Technology*, 254: 300–11.

- Putra MD, Abasaeed AE, Atiyeh HK, Al-Zahrani SM, Gaily MH, Sulieman AK, Zeinelabdeen MA (2015). Kinetic Modeling and Enhanced Production of Fructose and Ethanol from Date Fruit Extract. *Chemical Engineering Communications*, 202: 1618–1627.
- Qazizada ME (2016). Design of a batch stirred fermenter for ethanol production. *Procedia Engineering*, 149: 389 – 403.
- Quemeneur M, Hamelin J, Barakat A, Steyer JP, Carrere H, Trably E. (2012). Inhibition of fermentative hydrogen production by lignocellulose-derived compounds in mixed cultures. *International Journal of Hydrogen Energy*, 37(4): 3150-9.
- Raita M, Arnthong J, Champreda V, Laosiripojana N (2015). Modification of magnetic nanoparticle lipase designs for biodiesel production from palm oil. *Fuel Processing Technology*, 134: 189–97.
- Reddy K, Nasr M, Kumari S, Kumar S, Gupta S, Enitan A (2017). Biohydrogen production from sugarcane bagasse hydrolysate: effects of pH, S/X, Fe²⁺, and magnetite nanoparticles. *Environmental Science and Pollution Research*, 24:8790–804.
- Resham B, Priyabrata M (2008). Biological properties of “naked” metal nanoparticles. *Advance Drug Delivery Reviews*, 60: 1289–1306.
- Rorke DCS, Gueguim Kana EB (2017). Kinetics of Bioethanol Production from Waste Sorghum Leaves Using *Saccharomyces cerevisiae* BY4743. *Fermentation*, 3: 19.
- Salem AH, Mietzel T, Brunstermann R, Widmann R (2017). Effect of cell immobilization, hematite nanoparticles and formation of hydrogen-producing granules on biohydrogen production from sucrose wastewater. *International Journal of Hydrogen Energy*, 42 (40): 25225-25233.
- Sebayang AH, Masjuki HH, Ong HC, Dharma S, Silitonga AS, Kusumo F, Milano J (2017). Optimization of bioethanol production from sorghum grains using artificial neural networks integrated with ant colony. *Industrial Crops and Products*, 97: 146–155.

- Sekoai PT, Ouma CNM, du Preez SP, Modisha P, Engelbrecht N, Bessarabov DG, Ghimire A (2019). Application of nanoparticles in biofuels: An overview. *Fuel*, 237: 380–397.
- Sewsynker Y, Gueguim-Kana EB, Lateef A (2015). Modelling of biohydrogen generation in microbial electrolysis cells (MECs) using a committee of artificial neural networks (ANNs). *Biotechnology & Biotechnological Equipment*, 29 (6): 1208-1215.
- Sewsynker-Sukai Y, Gueguim-Kana EB (2018). Simultaneous saccharification and bioethanol production from corn cobs: Process optimization and kinetic studies. *Bioresource Technology*, 262: 32–41.
- Shanmugam S, Hari A, Pandey A, Mathimani T, Felix L, Pugazhendhi A (2020). Comprehensive review on the application of inorganic and organic nanoparticles for enhancing biohydrogen production. *Fuel*, 270: 117453.
- Su L, Shi X, Guo G, Zhao A, Zhao Y (2013). Stabilization of sewage sludge in the presence of nanoscale zero-valent iron (nZVI): abatement of odor and improvement of biogas production. *Journal of Material Cycles and Waste Management*, 15: 461–8.
- Tahvildari K, Anaraki Y, Fazaeli R, Mirpanji S, Delrish E (2015). The study of CaO and MgO heterogenic nano-catalyst coupling on transesterification reaction efficacy in the production of biodiesel from recycled cooking oil. *Journal of Environmental Health Science and Engineering*, 13: 73–81.
- Talasila U, Vechalapu RR (2015). Optimization of Medium Constituents for the Production of Bioethanol from Cashew Apple Juice Using Doehlert Experimental Design, *International Journal of Fruit Science*, 15 (2): 161-172.
- Thangaraj B, Jia Z, Dai L, Liu D, Du W (2016). Effect of silica coating on Fe₃O₄ magnetic nanoparticles for lipase immobilization and their application for biodiesel production. *Arabian Journal of Chemistry*, 2016. <https://doi.org/10.1016/j.arabjc.2016.09.004>.

- Tran D, Chen C, Chang J (2012). Immobilization of *Burkholderia* sp. lipase on a ferric silica nanocomposite for biodiesel production. *Journal of Biotechnology*, 158: 112–9.
- Vahida B, Saghatoleslami N, Nayebzadeh H, Toghiani J (2018). Effect of alumina loading on the properties and activity of $\text{SO}_4^{2-}/\text{ZrO}_2$ for biodiesel production: process optimization via response surface methodology. *Journal of the Taiwan Institute of Chemical Engineers*, 83: 115–23.
- Varghese R, Henry J, Irudayaraj J (2017). Ultrasonication-assisted transesterification for biodiesel production by using heterogeneous ZnO nanocatalyst. *Environmental Progress & Sustainable Energy*, 37: 1176–82.
- Vi L, Salakkam A, Reungsang M (2017). Optimization of key factors affecting bio-hydrogen production from sweet potato starch. *Energy Procedia*, 41: 973–8.
- Wang H, Covarrubias J, Prock H, Wu X, Wang D, Bossmann S (2015). Acid-functionalized magnetic nanoparticle as heterogeneous catalysts for biodiesel synthesis. *The Journal of Physical Chemistry C*. 119: 26020–8.
- Wang T, Zhang D, Dai L, Chen Y, Dai X (2016). Effects of metal nanoparticles on methane production from waste-activated sludge and microorganism community shift in anaerobic granular sludge. *Scientific Reports*, 6:1–10.
- Wiboon R, Maneewan S, Poonsuk P (2012). Application of palm pressed fiber as a carrier for ethanol production by *Candida shehatae* TISTR5843. *Electron Journal Biotechnology*, 15 (6) ISSN: 0717-3458. <http://dx.doi.org/10.2225/vol15-issue6-fulltext-1>.
- Willner I, Baron R, Willer B (2006). Growing metal nanoparticles by enzymes. *Advanced Materials*, 18:1109–1120.
- Wimonsong P, Nitisoravut R (2015). Comparison of Different Catalysts for Fermentative Hydrogen Production. *Journal of Clean Energy Technologies*, 3 (2): 128–131.

- Xiu Z, Jin Z, Li T, Mahendra S, Lowry G, Alvarez P (2010). Effects of nano-scale zerovalent iron particles on a mixed culture dechlorinating trichloroethylene. *Bioresource Technology*, 101: 1141–6.
- Zhao W, Zhang Y, Du B, Wei D, Wei Q, Zhao Y (2013). Enhancement effect of silver nanoparticles on fermentative biohydrogen production using mixed bacteria. *Bioresource Technology*, 142: 240–245.
- Zhaohui X, Qi Z, Xueyi S, Yan L (2016). Saccharomyces Cerevisiae Immobilized in Alginate for Continuous Fermentation. *Journal of Clean Energy Technologies*, 4 (1): 48 – 51.

CHAPTER 3

Impact of various metallic oxide nanoparticles on ethanol production by *Saccharomyces cerevisiae* BY4743: Screening, kinetic study and validation on potato waste

This chapter has been published with the title: Impact of various metallic oxide nanoparticles on ethanol production by *Saccharomyces cerevisiae* BY4743: Screening, kinetic study and validation on potato waste in *Catalysis Letters* (149 (7) (2019) 2015-2031). The published paper is presented in the following pages.



Impact of Various Metallic Oxide Nanoparticles on Ethanol Production by *Saccharomyces cerevisiae* BY4743: Screening, Kinetic Study and Validation on Potato Waste

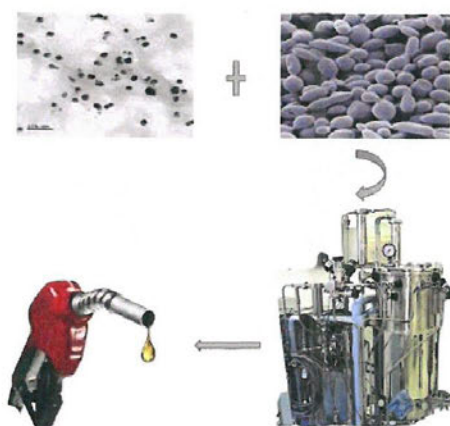
Isaac A. Sanusi¹ · Funmilayo D. Faloye¹ · E. B. Gueguim Kana¹

Received: 24 January 2019 / Accepted: 14 April 2019
© Springer Science+Business Media, LLC, part of Springer Nature 2019

Abstract

This study investigates the impact of nine (9) metallic oxide nanoparticles (NPs) on ethanol production by *Saccharomyces cerevisiae* BY4743. Ethanol concentrations decreased at higher NPs (above 0.02 wt%) for all the NPs studied. Ethanol production was mainly enhanced by Fe₃O₄ NPs with a maximum ethanol yield of 0.26 g/g, glucose utilization of 99.95%, 0.22 g/L/h ethanol productivity and 51% fermentation efficiency at 0.01 wt%. The logistic and modified Gompertz kinetic models gave R^2 values ≥ 0.88 . The highest maximum specific growth rate (μ_{max}), potential maximum ethanol concentration (P_m) and maximum production rate of 0.80 h⁻¹, 5.24 g/L and 0.72 g/L/h were obtained with 0.01 wt% NiO NPs and Fe–Ag NPs respectively. Nano inclusion in a simultaneous saccharification and fermentation (NISFF) process enhanced ethanol production from potato peels by 1.60-fold and 1.13-fold using NiO and Fe₃O₄ NPs respectively. These findings demonstrated the suitability of NiO and Fe₃O₄ NPs biocatalyst for their application in bioethanol production from agro waste such as potato peels.

Graphical Abstract



Electronic supplementary material The online version of this article (<https://doi.org/10.1007/s10562-019-02796-6>) contains supplementary material, which is available to authorized users.

Extended author information available on the last page of the article

Published online: 04 May 2019

Springer

Keywords Nanobiocatalyst · Ethanol · Fermentation · Kinetics model · Potato waste

1 Introduction

The last few decades, have witness an increasing demand for alternative sources of fuels due to the excessive consumption of fossil fuels globally and their environmental impacts. Thus, alternative and sustainable energy sources, such as bioethanol may reside in the production of renewable energies [1]. Bioethanol exhibits several advantages over fossil fuel, which include its renewable nature, ease of storage, higher combustible oxygen content, higher octane rating, zero sulfur and nitrogen content. Additionally, it reduces greenhouse gas emissions, thus alleviating air pollution and global warming [2]. Unlike other prospective renewable energy sources such as biohydrogen and biogas, bioethanol storage, transportation, and utilization are compatible with existing infrastructure for fossil fuel products thus making it a suitable replacement for conventional fossil fuels [3]. However, a sustainable, renewable supply of bioethanol to meet present energy requirements is not available. Though, the present bioethanol technologies offer potential for practical application but are still faced with many challenges [4]. These include the need for enhancing the bioactivity and stress tolerance of ethanol-producing microorganisms [5, 6], cost-effective fermentation process that will result in high ethanol yield, efficient utilization of substrate and shorter fermentation time [5]. Several research efforts have been made to enhance the bioactivity of ethanol-producing yeast, and to improve the conversion efficiency of substrate to ethanol [5, 7, 8]. High conversion efficiency of substrates and satisfactory ethanol yield has remained a challenge. Attempts to improve the bioactivity of ethanol-producing yeast in a fermentation process through the administration of micronutrient has been reported [9, 10]. These micronutrients are required in low concentration and their deficiency can impact on the production of enzymes, coenzymes and growth factors required for metabolism and ultimately reduces metabolic activity [11]. The impacts of micronutrient deficiency on fermentation process include; increase in volatile fatty acids formation and accumulation, weak buffering capacity and poor enzymatic activities [10]. Micronutrients are vital constituents of cofactors and enzymes and their addition to fermentation process has the potential to stimulate and enhance bioethanol process performance [5, 12]. Micronutrients form the metal component at the active site of enzymes that catalyze many metabolic processes such as alcohol dehydrogenase and pyruvate decarboxylase that catalyze the conversion of pyruvic acid to ethanol [13]. Besides acting as a cofactor for many enzymes, they are also required for the structural stability of many proteins such as the regulatory proteins as well as structural proteins, many

of which exert important controls on cellular metabolic processes and eventually process performance [5]. For example, micronutrients such as iron (Fe), nickel (Ni), cobalt (Co), zinc (Zn), silicon (Si) are essential for cell growth and product formation and have been reported to enhance bioprocess performance [4, 14].

The increasing application of Nano chemistry in biotechnology has the potential to enhance the bioactivities of ethanol-producing yeast and bioethanol conversion. Nanomaterials have unique physical and chemical properties and are gaining prominence in areas such as biomedical science, environmental science biotechnology, optics, magnetics, catalysis and energy science [4, 15, 16]. Some of the bioprocessing applications of nanoparticles have been reported for enzyme encapsulation [17], DNA transfection [18] and biosensors [19]. The catalytic potentials of these particles largely depend on their sizes, shapes, stabilizing agents and operating conditions. Furthermore, some nanoparticles have shown that they can improve the kinetics of bioprocess through the capacity to react rapidly with electron donors and enhance the bioactivity of microbes as biocatalysts [20]. Similarly, some microorganisms in the presence of nanoparticles especially under anaerobic condition, transfer more efficiently electrons to acceptors [21]. Many new catalytic systems with nanoparticles as biocatalyst are now being explored [22]. Abdelsalam et al. [23], achieved improvement in biomethane production when substrates were treated with 1 mg/L Co NPs. Similarly, an enhancement in biohydrogen yield by 200% was observed with the addition of 0.6 wt% functionalized MCM41 nanoparticles during syngas fermentation [22]. Zhang and Shen [24], also reported that the addition of 5 nm gold-nanoparticle improved the efficiency of biohydrogen fermentation substantially, and the maximum increase of hydrogen yield reached 36% compared with the control experiment. There is a dearth of knowledge on the impact of nanoparticles in bioethanol processes using agricultural waste substrates [5, 25, 26]. Supplementary nanoparticles' inclusion approach can promote fermentative ethanol production at certain concentrations as well as modify the microorganism metabolic pathway to favour ethanol production [4, 15]. Nevertheless, nanoparticles at high concentrations can also inhibit the activity of ethanol-producing microbes through various mechanisms including membrane disruption [27]. Therefore, the paradox effect of metallic oxide nanoparticles on the fermentative utilisation and conversion of substrates makes it an attractive area of research. Moreover, there is a scarcity of information regarding the impact of metallic oxide nanoparticles on the bioactivity

of *S. cerevisiae* BY4743 and the kinetics assessment of the fermentation efficiency of substrates for biofuel production.

Kinetic modelling is required in bioprocesses development for industrial scale application [28]. These models define the production process under different process conditions which can help improve the product yield, quality, productivity and reduce undesirable by-products. Logistic function models describe the changes in microbial growth as a function of cell growth rate, initial and maximum biomass concentration and time [29]. The modified Gompertz model elucidates the production lag time, maximum product production rate, and maximum product concentration on a given substrate [30].

The specific objectives of this work was to: (1) screen nine different metallic oxide nanoparticles on batch bioethanol production, (2) study the kinetics of yeast growth and bioethanol formation under nanobiocatalytic conditions, and (3) assess the impact of nanoparticles on simultaneous saccharification and fermentation (SSF) using potato peels as substrate.

2 Materials and Methods

2.1 Experimental Setup

2.1.1 Nanoparticle Preparation

Nine nanoparticles were used in this study and were prepared using the following chemicals: iron(III) chloride (FeCl_3), iron(II) sulphate heptahydrate ($\text{FeSO}_4 \cdot 7\text{H}_2\text{O}$), copper sulphate pentahydrate ($\text{CuSO}_4 \cdot 5\text{H}_2\text{O}$), manganous sulphate monohydrate ($\text{MnSO}_4 \cdot \text{H}_2\text{O}$), cobalt(II) chloride hexahydrate ($\text{CoCl}_2 \cdot 6\text{H}_2\text{O}$), nickel(II) chloride hexahydrate ($\text{NiCl}_2 \cdot 6\text{H}_2\text{O}$), silver nitrate (AgNO_3), zinc chloride (ZnCl_2), sodium hydroxide (NaOH) and ammonia (NH_3) sterile distilled water was used throughout the experiment. All chemicals (purchased from Merck, South Africa) were of reagent grade and used without further purification. The nanoparticles used in this study are listed as follow; iron(II) oxide (Fe NPs), iron(III) oxide (Fe_3O_4 NPs), cobalt oxide (Co NPs), nickel oxide (Ni NPs), zinc oxide (Zn NPs), manganese oxide (Mn NPs), silver oxide (Ag NPs), copper oxide (Cu NPs) and iron(III) oxide–silver doped (Fe–Ag NPs). These nanoparticles were prepared using the co-precipitation method. For microwave radiation, the treatment was carried at 800 W using a microwave oven (Samsung, Model: ME9114S1, South Africa) Calcination was done using a muffle furnace (LABCON, TYPE RM4). The nanoparticles were thereafter characterized using Fourier transform infra-red spectroscopy (FTIR), scanning electron microscopy (SEM) and transmission electron microscopy (TEM).

2.1.1.1 Preparation of Fe_2O_3 Nanoparticles (Fe NPs) Fe_2O_3 NPs was prepared according to the method of Khaghani and Ghanbari [31]. 3.24 g of FeCl_3 was dissolved in 20 mL of sterile distilled water after which the ammonia solution was slowly added to the mixture. The pH was adjusted to 12 and treated with microwave radiation (700 W, 30 s on, 60 s off) for 4 min. The red-brown precipitate was then centrifuged at 1000 rpm for 10 min and rinsed with distilled water. Fe NPs obtained was dried at 70 °C for 12 h.

2.1.1.2 Preparation of ZnO Nanoparticles (ZnO NPs) An amount of 15 g of starch was completely dissolved in 65 wt% ZnCl_2 aqueous solution at 80 °C with constant stirring at 500 r/min. This was followed by the addition of 15 wt% NaOH aqueous solution drop-wisely to the starch-zinc chloride solution and constantly stirred at 500 r/min to achieve a final pH value of 8.4. The nanocomposite was then allowed to age for 30 min with constant stirring at 80 °C. The ZnO nanoparticles were obtained by calcining the dried ZnO–starch nanocomposite at 575 °C for 1 h after which it was grounded using the laboratory crucible [32].

2.1.1.3 Preparation of Iron(III) Oxide Nanoparticles (Fe_3O_4 NPs) One gram of $\text{FeSO}_4 \cdot 7\text{H}_2\text{O}$ was dissolved in 100 mL of distilled water after which 1 M NaOH solution was dropped slowly to adjust the pH to 12, and the volume made up to 200 mL. The solution was subjected to microwave radiation (700 W) for 10 min for complete reaction and precipitation. The black magnetic iron(III) oxide nanoparticles (Fe_3O_4 NPs) product was then rinsed with distilled water and oven dried at 70 °C [33].

2.1.1.4 Preparation of $\text{Fe}_3\text{O}_4/\text{Ag}$ Nanoparticles (Fe–Ag NPs) Fe_3O_4 doped Ag NPs was prepared by the co-precipitation of iron(II) sulphate heptahydrate and Tollens' reagent ($[\text{Ag}(\text{NH}_3)_2]^+$). 20 mL of $[\text{Ag}(\text{NH}_3)_2]^+$ solution was added to 80 mL of $\text{FeSO}_4 \cdot \text{H}_2\text{O}$ solution (1 g of $\text{FeSO}_4 \cdot 7\text{H}_2\text{O}$ dissolved in 100 mL of water) with constant stirring. The pH of the solution was adjusted to 12 with 1 M NaOH and the volume was made up to 200 mL. The reaction mixture was then exposed to microwave irradiation (700 W, 10 min). The Fe–Ag NPs obtained was dried in the oven at 70 °C for 12 h [34].

2.1.1.5 Preparation of Ag_2O Nanoparticles (Ag NPs) An amount of 20 mL of 0.02 M solution of AgNO_3 was made to react with 1.5 M NaOH drop-wisely until the pH of the solution reached to 10. The mixture was subjected to microwave radiation at 700 W for 30 s on, 60 s off for 4 min. The precipitates obtained were washed several times with distilled water. The greyish brown precipitates

of Ag NPs were then dried in an oven at 70 °C followed by SEM and TEM characterization [34].

2.1.1.6 Preparation of CoO Nanoparticles (CoO NPs) The five-step preparation scheme for cobalt nanoparticles started with dissolving 4.76 g of cobalt(II) chloride hexahydrate ($\text{CoCl}_2 \cdot 6\text{H}_2\text{O}$), in 20 mL distilled water to obtain a greenish solution. This was followed by the addition of ammonia to a pH of 11.3. The mixture was then subjected to a microwave irradiation for 3 min at 700 W. In the fourth step, the obtained precipitate was washed three times after which the deep dull green Co NPs was dried in an oven at 100 °C for 6 h [23].

2.1.1.7 Preparation of NiO Nanoparticles (NiO NPs) The preparation of NiO NPs were carried out by dissolving 4.75 g of Nickel chloride hexahydrate ($\text{NiCl}_2 \cdot 6\text{H}_2\text{O}$) in 20 mL distilled water. This was followed by drop-wise slow addition of ammonia to the solution until the pH reached 10. The mixture was subjected to microwave irradiation (700 W, 3 min) and the formation of light green precipitate signalled the completion of the reaction. The NiO NPs obtained were washed three times and dried at 100 °C in an oven for 6 h [23].

2.1.1.8 Preparation of MnO_2 Nanoparticles (MnO_2 NPs) The MnO_2 NPs were prepared using the co-precipitation method. 6.76 g of $\text{MnSO}_4 \cdot \text{H}_2\text{O}$ was dissolved in 40 mL distilled water, after which ammonia was added drop-wisely to achieve pH 11, with continuous stirring at 60 °C for 2 h to precipitate the Mn NPs. The resulting brownish precipitated particles were then washed thrice with distilled water and dried in a hot air oven at 70 °C for 12 h [26].

2.1.1.9 Preparation of CuO Nanoparticles (CuO NPs) The CuO nanoparticles were prepared using copper salt and a reducing agent. 0.04 M of Copper sulphate pentahydrate ($\text{CuSO}_4 \cdot 5\text{H}_2\text{O}$) was mixed with 1 M NaOH drop-wisely with continuous stirring to achieve pH 12.7. The mixture was then subjected to microwave irradiation (700 W, 2.5 min). A black-grey precipitate was formed, which was then washed with distilled water and dried overnight at 70 °C.

2.2 Nanoparticles Characterization

The elemental composition, particle size and the functional binding of the nine NPs were evaluated using the scanning electron microscope (SEM), transmission electron microscope (TEM) and Fourier infra-red spectroscopy (FIR) respectively. The SEM-EDX images were obtained using the scanning electron microscope (ZEISS, Model ZEISS-EVO/LS15, UK). SEM was operated using

EDX detector (Oxford I, X-Max 80 mm^2), the variable pressure of 100 μ , dead time 15–30%, accelerating voltage 5.00 kV and beam current of 95–105%. Prior to the image and elemental analysis, the samples were mounted on aluminium grid coated with carbon INCA x-stream-2 (Oxford, United Kingdom) for Energy-dispersive X-ray spectroscopy (EDX) analysis.

The transmission electron microscopy (TEM) images of the nanoparticles were obtained with a transmission electron microscope JEM-1400 (JEOL, USA) operating at 120 kV. TEM samples were prepared by dispersing NPs in ethanol/acetone for 15 min in a sonicator (DAWE Instrument, England). The solution was withdrawn using hypothermal syringe after which a drop of the solution was placed on a formvar-coated copper grid and left to dry for 15 min. The dry grid was then mounted and inserted into the electron microscope for viewing and further analysis.

The Fourier transform infra-red spectra of the nanoparticles were obtained to ascertain the purity and the nature of the nanoparticles using FT-IR spectrometer (Spectrum 100, PerkinElmer, USA). Fourier transform infra-red spectroscopy spectra were recorded between 450 and 4000 cm^{-1} for the dry nanoparticle's samples.

2.3 Ethanol Fermentation

2.3.1 Screening of Metallic Oxide Nanoparticles

A preliminary screening was undertaken to assess the influence of the nine metallic oxide nanoparticles at different concentrations on ethanol fermentation. Batch fermentation experiments were carried out at controlled process set points of initial pH 5, incubating temperature of 30 °C, agitation speed of 120 rpm and a process time of 72 h. The nanoparticles concentrations in the experimental set-up range from 0 to 0.08 wt%. The detailed experimental set up for the preliminary screening is presented in Table 1.

2.3.2 Strain and Inoculum Preparation

Saccharomyces cerevisiae BY4743 obtained from the Department of Genetics, University of KwaZulu-Natal, Pietermaritzburg Campus, South Africa was used in this study. The yeast was inoculated into a 250 mL Erlenmeyer flask containing 100 mL of the Yeast Peptone Dextrose (YPD) medium for inoculum development. The medium contained (g/L); Yeast extract: 10, Peptone: 20 and Glucose: 20. The strain was incubated at 120 rpm, 30 °C for 12 h until the exponential growth phase was reached. The culture was then used as the inoculum for subsequent fermentation.

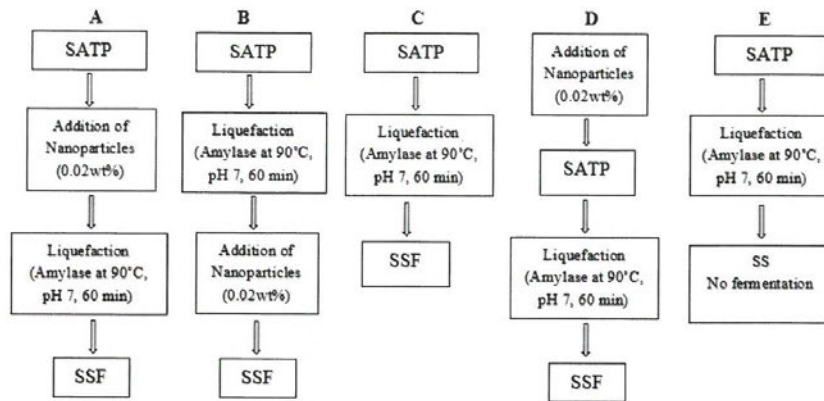


Fig. 2 Process flow diagram for NISSF process modes

Table 2 Performance of glucose utilisation, fermentation efficiency, ethanol yield and productivity at different NPs concentration

| NPs type | NPs concentration (wt%) | | | | | | | |
|------------------------------------|-------------------------|-------|---------------------|------|------------------------------|------|-----------------------------|-------|
| | Glucose utilisation (%) | | Ethanol yield (g/g) | | Ethanol productivity (g/L/h) | | Fermentation efficiency (%) | |
| | 0.01 | 0.02 | 0.01 | 0.02 | 0.01 | 0.02 | 0.01 | 0.02 |
| Control | 99.80 | 99.80 | 0.23 | 0.23 | 0.19 | 0.19 | 45.58 | 45.58 |
| Cu NPs | 99.40 | 96.80 | 0.25 | 0.23 | 0.21 | 0.18 | 49.40 | 42.58 |
| Mn NPs | 99.50 | 99.95 | 0.22 | 0.21 | 0.18 | 0.18 | 43.08 | 41.14 |
| Ni NPs | 99.95 | 99.90 | 0.25 | 0.22 | 0.21 | 0.18 | 48.83 | 42.07 |
| Fe NPs | 99.80 | 99.80 | 0.19 | 0.18 | 0.16 | 0.15 | 37.42 | 35.73 |
| Fe ₃ O ₄ NPs | 99.95 | 99.95 | 0.26 | 0.25 | 0.22 | 0.20 | 50.96 | 47.78 |
| Fe–Ag NPs | 99.70 | 99.85 | 0.20 | 0.19 | 0.17 | 0.16 | 39.03 | 37.91 |
| Zn NPs | 99.75 | 99.75 | 0.24 | 0.22 | 0.20 | 0.18 | 47.59 | 41.89 |
| Ag NPs | 92.20 | 21.95 | 0.15 | 0.03 | 0.11 | 0.01 | 26.69 | 01.27 |
| Co NPs | 98.40 | 98.45 | 0.24 | 0.21 | 0.20 | 0.17 | 45.74 | 39.57 |

NPs nanoparticles, Cu NPs copper(II) oxide, Mn NPs manganese oxide, Ni NPs nickel oxide, Fe NPs iron(II) oxide, Fe₃O₄ NPs iron(III) oxide, Fe–Ag NPs iron(III) oxide–silver doped, Zn NPs zinc oxide, Co NPs cobalt oxide, Ag NPs silver oxide

average of two repeats. Experimental data for *S. cerevisiae* BY4743 growth and ethanol formation were used to fit the logistic and modified Gompertz using the least squares method (Curve Expert V1.5.5).

2.4 Analytical Methods

The ethanol concentration was determined using an ethanol vapour sensor (LABQUEST[®]2, Vernier, USA). The fermentation broth was centrifuged at 10,000 rpm for 5 min and the residual glucose concentration in the supernatant was determined using the DNS method [36]. Biomass

concentration was measured as a function of the cell dry weight and the optical density. The optical density was measured at 600 nm using a SpectroVis plus Spectrophotometer (Vernier Software & Technology, USA). The cell dry weight was determined by sedimenting the cell pellets after centrifugation at 8000 rpm at 4 °C for 10 min. Subsequently, the correlation between the optical density and the cell dry weight was extrapolated using a standard calibration curve [14]. While cell biomass in the NISSF was quantified by using the cell count as a function of the concentration of yeast cells.

Table 1 Preliminary screening of nanoparticles for ethanol production

| NPs | Ethanol concentration (g/L) | | | | |
|------------------------------------|-----------------------------|------|------|------|------|
| | Treatments (wt%) | | | | |
| | Control | 0.01 | 0.02 | 0.04 | 0.08 |
| Cu NPs | 4.50 | 4.86 | 4.40 | 2.55 | 1.40 |
| Mn NPs | 4.50 | 4.34 | 4.23 | 4.29 | 4.17 |
| Ni NPs | 4.50 | 4.68 | 4.12 | 3.91 | 3.59 |
| Fe NPs | 4.50 | 4.12 | 3.77 | 3.67 | 3.63 |
| Fe ₃ O ₄ NPs | 4.50 | 5.03 | 4.76 | 3.98 | 3.49 |
| Fe–Ag NPs | 4.50 | 4.43 | 4.22 | 4.20 | 4.14 |
| Zn NPs | 4.50 | 4.81 | 2.94 | 2.83 | 2.76 |
| Co NPs | 4.50 | 4.99 | 4.42 | 3.86 | 3.27 |
| Ag NPs | 4.50 | 2.51 | 0.24 | 0.19 | 0.18 |

NPs nanoparticles, Cu NPs copper(II) oxide, Mn NPs manganese oxide, Ni NPs nickel oxide, Fe NPs iron(II) oxide, Fe₃O₄ NPs iron(III) oxide, Fe–Ag NPs iron(III) oxide–silver doped, Zn NPs zinc oxide, Co NPs cobalt oxide, Ag NPs silver oxide

2.3.3 Batch Fermentation

The fermentation medium used in this study contained per litre; glucose, 20 g; yeast extract: 5 g, (NH₄)₂SO₄: 1 g, KH₂PO₄: 2 g and MgSO₄: 1 g and was autoclaved at 121 °C for 15 min. The fermentation processes were carried out in sterile 250 mL Erlenmeyer flasks with a total working volume of 100 mL. Aliquots of 10 mL of the inoculum, and nanoparticles (type and concentration specified in Table 1) were aseptically added to each fermentation flasks. The process set points of initial pH 5, incubating temperature of 30 °C, agitation of 120 rpm were used [8] and the fermentation broth was sampled every 3 h for 24 h. All experiments were performed in duplicate and samples were taken at regular interval during the fermentation to determine the ethanol concentration. A control experiment was set up in which there was no NP supplementation. The kinetic studies of the best NPs concentrations were further studied.

2.3.4 Soaking Assisted Thermal Pretreatment (SATP) of Potato Waste

SATP was carried out as described by [35]. Analysis of the milled potato peels (Fig. 1) gave starch (20%), structural carbohydrate (14%), cellulose (4%), hemicellulose (10%) and lignin (6%). The milled potato waste was soaked in dilute hydrochloric acid (0.92 mL) in a water bath at 69.7 °C for 2.34 h and followed by 5 min autoclave thermal treatment (121 °C).

2.3.5 Nano Inclusion Simultaneous Saccharification and Fermentation (NISSF)

Hydrolysate from the SATP stage was used. The NISSF process (50 mL) contained: pretreated potatoes waste with solid loading (10%), enzyme loading; 0.212 FPU/g amylase for liquefaction (at 90 °C, pH 7, for 60 min), 0.295 FPU/g amyloglucosidase for saccharification and nutrients (5 g/L yeast extract, 2 g/L KH₂PO₄, 1 g/L MgSO₄, 1 g/L (NH₄)₂SO₄). Ten percent *S. cerevisiae* BY4743 inoculum broth was then added. After inoculation, the different NISSF experiments were incubated at 37 °C and 120 rpm over 24 h. For sample analysis, 0.5 mL aliquots were extracted every four hours. The NISSF designs with 0.02 wt% of Nano type supplement are listed below (Fig. 2). NiO and Fe₃O₄ nanoparticles administered were chosen based on their performance in the preliminary study. The various fermentation setup modes assessed are illustrated in the flowchart below:

2.3.6 Kinetic Study

The nanoparticles type and concentration used in the fermentation kinetic study were selected based on preliminary screening experiments (Sect. 2.4.3). The NPs concentration ranged from 0 to 0.02 wt% and the detailed experimental design is presented in Table 2. The fermentation broth was analyzed for biomass concentration, pH, sugar degradation and ethanol production. Data were calculated from the

Fig. 1 Flowchart of fresh, dried and milled potato waste used for the SATP



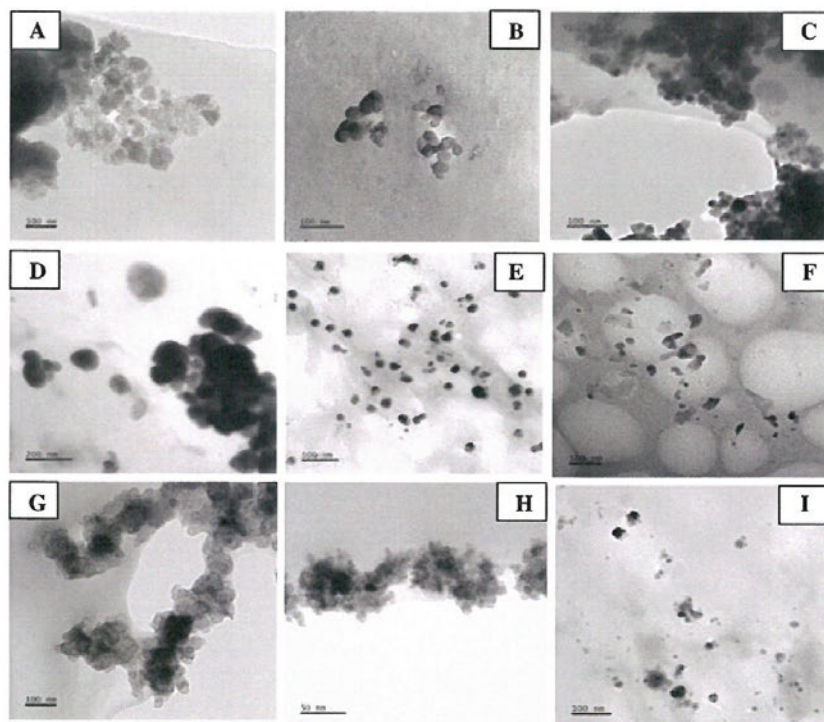


Fig. 3 TEM images showing **a** Fe NPs, **b** Zn NPs, **c** Fe₃O₄ NPs, **d** Fe–Ag NPs, **e** Ag NPs, **f** Co NPs, **g** Ni NPs, **h** Mn NPs, **i** Cu NPs

study, Fe–Ag NPs (61 nm) had the highest particle size, which may be attributed to its doped nature. Similar TEM micrographs of Fe₃O₄/Ag NPs with a spherical shape and an average diameter of 50 nm was reported by Zheng et al. [34]. The variation in the average diameter may be attributed to differences in microwave treatment, precursors used and precipitation rate.

3.1.3 Nanoparticles Characterization by FTIR

In this study, Mn–O, Co–O, Cu–O, Ag–O, Zn–O and Fe₃O₄ absorption band were observed at 860, 659, 845, 797, 715 and 664 cm⁻¹ respectively. NiO NPs and Fe NPs had an absorption band below 650 cm⁻¹. Oxides and hydroxides of metal nanoparticles generally give absorption peak below the wavelength of 1000 nm in the fingerprint region. This arises from inter-atomic vibrations [38, 40]. Other peaks observed indicated the presence of functional groups, with different stretching vibrations of –CH₃, –CH₂, =C–H, –C–H,

C=O, –OH and NH groups [41]. These absorption peaks range from 3628 to 1031 cm⁻¹. These peaks at different points on each NPs spectrum could be attributed to the absorbed atmospheric moisture, CO₂ and precursor remains [38, 41]. Kumar et al. [40], also observed an absorption band of 515 and 480 cm⁻¹ which corresponds to the Mn–O bond of manganese oxide (MnO₂) nanoparticles. The authors likewise opined that absorption peak observed above 1000 cm⁻¹ may be due to stretching vibration of –CH₃, –CH₂, =C–H, and –C–H.

3.2 Screening of Nanoparticles for Ethanol Production

The results of the preliminary screening for the nine NPs on ethanol production are presented in Table 1. The ranges of ethanol concentration observed were, 2.21–5.03 g/L (0.01 wt%), 0.24–4.76 g/L (0.02 wt%), 0.02–4.47 g/L (0.04 wt%) and 0.02–4.45 g/L (0.08 wt%).

2.4.1 Yield and Productivity Calculation

Sugar utilisation, fermentation efficiency, ethanol yield and ethanol productivity were determined as stated in the following Eqs. (1)–(4) respectively.

$$\text{Sugar utilisation (\%)} = \frac{\text{Initial sugar content} - \text{final sugar content}}{\text{Initial sugar content}} \times 100 \quad (1)$$

$$\text{Fermentation efficiency (\%)} = \frac{\text{Actual ethanol yield (g/l)}}{\text{Theoretical yield of ethanol (g/l)}} \times 100 \quad (2)$$

$$\text{Ethanol yield (g/g)} = \frac{\text{Maximum ethanol concentration (g/l)}}{\text{Utilized glucose (g/l)}} \quad (3)$$

$$\text{Ethanol productivity (g/l/h)} = \frac{\text{Maximum ethanol concentration (g/l)}}{\text{Fermentation period (h)}} \quad (4)$$

2.5 Kinetic Calculations

The average specific growth rates (μ) of the yeast during the fermentation process was calculated using Eq. (5). The specific growth rate values (μ) and the substrate concentration data were subsequently used to estimate the maximum specific growth rate (μ_{\max}).

$$\text{Specific growth rate } (\mu) = \frac{\ln X_2 - \ln X_1}{t_2 - t_1} \quad (5)$$

where X_2 and X_1 are biomass concentrations (g/L) at time instants t_2 and t_1 respectively.

Experimental data for *S. cerevisiae* BY4743 growth were used to fit the logistic model (Eq. 6). This equation represents both the exponential and the stationary phase:

$$X = \frac{X_0 \cdot \exp(\mu_{\max} \cdot t)}{1 - \left(\frac{X_0}{X_{\max}}\right) \cdot (1 - \exp(\mu_{\max} \cdot t))} \quad (6)$$

where X_0 is the initial yeast cell mass concentration (g/L), X_m is the maximum attainable yeast cell mass concentration (g/L) and μ_m is the maximum specific yeast cell growth rate (h^{-1}).

Data of ethanol production over time were used to fit the modified Gompertz model. This model describes the lag time, the maximum ethanol production rate, and the potential maximum product concentration as presented in Eq. (7).

$$P = P_m \cdot \exp\left\{-\exp\left[\frac{r_{p,m} \cdot \exp(1)}{P_m} \cdot (t_L - t) + 1\right]\right\} \quad (7)$$

where P is the ethanol concentration (g/L), P_m is the potential maximum ethanol concentration (g/L), $r_{p,m}$ is the maximum ethanol production rate (g/L/h) and t_L is the time (lag phase) from the beginning of fermentation to exponential ethanol production (h).

3 Results and Discussion

3.1 Nanoparticles Characterization

3.1.1 SEM Characterization

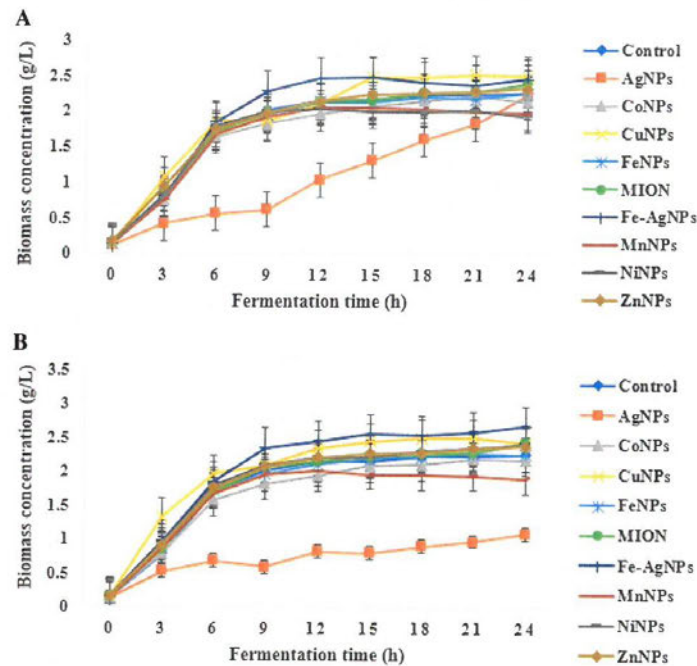
The elemental composition of the nine NPs were characterised by SEM-EDS. The Energy dispersive spectrophotometric (EDS) confirmed the presence of the desired elements, the metallic and oxygen unit in each of the nine NPs, as well as their level of purity. All the NPs shows a strong signal of the metal and the oxygen unit, confirming the existence of metallic oxide. Some other elements such as carbon, sulphur, chlorine, silicon, aluminium were found in the NPs, due to the trace amount of precursor used in the preparation of the NPs and the grid used in the SEM analysis (aluminium grid coated with carbon).

3.1.2 TEM Characterization

The Transmission Electron Microscopy (TEM) images describe the shape and the particle size of each nanoparticle (NPs). All the synthesized nanoparticles had a rough spherical shape, except Co NPs which was irregular in shape, with Ag NPs, Co NPs, and Cu NPs having a weak agglomeration (Fig. 3). The particle size analysis shows the size distribution of each NPs. An average diameter of 8, 12, 15, 23, 29, 30, 31, 47 and 61 nm was recorded for Mn NPs, Co NPs, Cu NPs, Ag NPs, Ni NPs, Zn NPs, Fe_3O_4 NPs, Fe NPs and Fe–Ag NPs respectively. The results indicated that the nanoparticles are of varying sizes within nano-range, with a narrow size distribution.

Co NPs and Cu NPs had particles sizes in the range of 8–17 and 8–19 nm respectively, while, Fe_3O_4 NPs, Ni NPs and Ag NPs had particles sizes in the range of 18–37, 23–37 and 21–25 nm, which were comparable to those obtained in other reported studies [37]. Similar to our findings, Li et al. [38], obtained NiO nanoparticles with a spherical shape and these authors further reported a small particle size of 13 nm and a narrow size distribution (ranging from 8 to 18 nm) after calcination at 400 °C for an hour. Also, a particle size of 30 nm was reported for NiO prepared via a rapid microwave-assisted method [39]. Furthermore, in this

Fig. 5 Cell dry weight of *S. cerevisiae* BY4743 in the NPs administered culture at different concentrations **a** 0.01 wt%, **b** 0.02 wt%



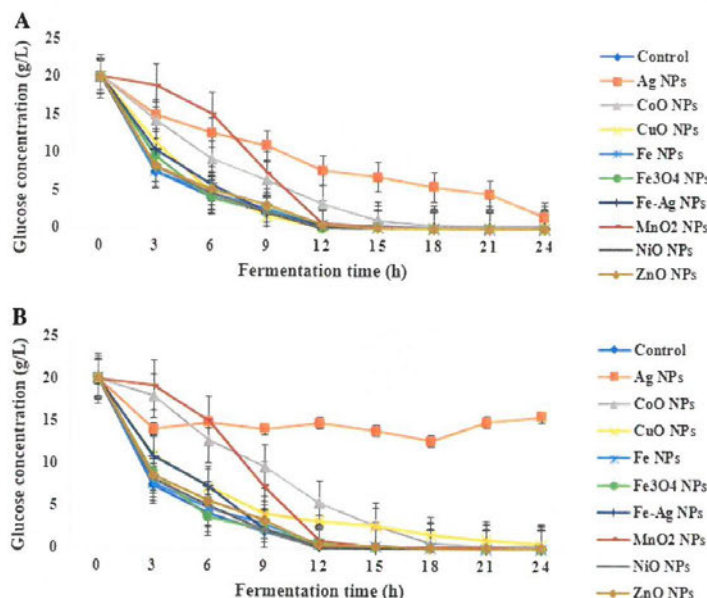
against 99.80% for the control experiment (Table 2). The glucose utilization profiles during ethanol fermentation with the nine NPs are presented in Fig. 4a, b. The substrate utilisation efficiency above 92.20% suggests that the substrate affinity in the presence of metallic oxide nanoparticles was not drastically affected. In other words, *S. cerevisiae* BY4743 was able to metabolize the glucose without difficulty with the administered NPs except with Ag NPs at both concentrations. Substrate utilization depends on cell type, biomass concentration, media composition which then determines the productivity of a fermentation system. Nanoparticles with their high surface area to volume ratio are good catalysts. This catalytic potential probably improved the contact and the interaction between the glucose and the yeast cells during fermentation in this study. El-Kemary et al. [44], concluded that the possible interaction was that the hydrophobic part of glucose was adsorbed onto the surface layers of NPs by van der Waals interactions and the hydrophilic part of the OH⁻ is oriented toward the aqueous phase. This interaction between the NPs and the glucose might have enhanced the rate of glucose uptake by *S. cerevisiae* BY4743 which in turn enhanced ethanol formation as evident in this study. The rate of glucose uptake has been indicated as a limiting step in the optimum functioning of the Embden–Meyerhof–Parnas

pathway (EMP), consequently, the rate of glucose utilisation may affect the efficiency of the ethanol fermentation system.

3.3.2 Effect of Nanoparticles on Biomass Accumulation

The biomass concentration (g/L) increased rapidly in the first 3–9 h of fermentation and then progressed slightly until the 24 h mark (Fig. 5a, b). The cell dry weights obtained after 24 h for 0.01 wt% Cu NPs, Fe–Ag NPs, and Zn NPs were 2.53, 2.49, 2.40 and 2.34 g/L which corresponded to 11.47, 9.66, 6.05 and 3.13% improvement respectively over the control experiment (2.27 g/L). The results also revealed that the biomass concentration was enhanced by 0.04, 5.47, 6.93, 7.46, 11.21 and 18.27% at 0.02 wt% for Fe NPs, Zn NPs, Ni NPs, Fe₃O₄ NPs, Cu NPs and Fe–Ag NPs respectively over the control. This increment was probably due to the improvement in the metabolic activities of *S. cerevisiae* BY4743 as a result of the biocatalytic effect of these NPs. Metal-biomass interactions depend on the chemical, biological and physical processes occurring at and near the biological interface in controlling trace metal bioavailability through shifts in the limiting bio-uptake fluxes. Many cellular processes are catalysed by transported ions and mineral elements, which help to improve metabolic activities such as

Fig. 4 Effect of nine metallic oxide NPs on glucose utilisation during fermentation at a 0.01 wt% inclusion, **b** 0.02 wt% inclusion



Ethanol concentration was enhanced mainly by Fe_3O_4 NPs (5.03 g/L), Co NPs (4.99 g/L), Cu NPs (4.86 g/L), Zn NPs (4.81 g/L) and Ni NPs (4.68 g/L) at 0.01 wt% supplementation, which corresponds to 11.78, 10.89, 8.00, 6.89 and 4.00% improvement over the control experiment (4.50 g/L) respectively. At 0.02 wt% inclusion, only Fe_3O_4 NPs culture showed ethanol concentration (4.76 g/L) higher than the control experiment. The inclusion of nanoparticles might have triggered changes in the cellular membrane and cytoplasmic activities which in turn influences cell growth and metabolic processes. In addition, the variation in the ethanol concentration observed could be attributed to the differences in types, sizes, and shapes of the NPs, which confers on them unique chemical and physical properties.

At NPs concentration above 0.02 wt%, a drastic decrease in ethanol concentration was observed for all the nine NPs. Ethanol concentration decreased with an increase in the concentration of NPs from 0.04 to 0.08 wt% for all the metallic oxide nanoparticles tested.

The above results indicated that the bioactivity of ethanol-producing yeast can be promoted by the supplement of nanoparticles, but excess nanoparticles is harmful to ethanol-producing activity of *S. cerevisiae* in this work. Other possible reasons for the negative impact with higher NPs concentration includes (1) cell toxicity or cell inhibition, (2) inhibition of the ethanol production pathway, and (3) promotion of other pathways apart from the ethanol production pathway. In addition,

the antimicrobial mechanism of these NPs at higher concentration may involve the formation of reactive oxygen species (ROS), lipid peroxidation and the alkaline effect ultimately resulting in cell death. The release of ions from the surface of nanoparticles has been reported to cause bacterial death by binding to the cell membrane.

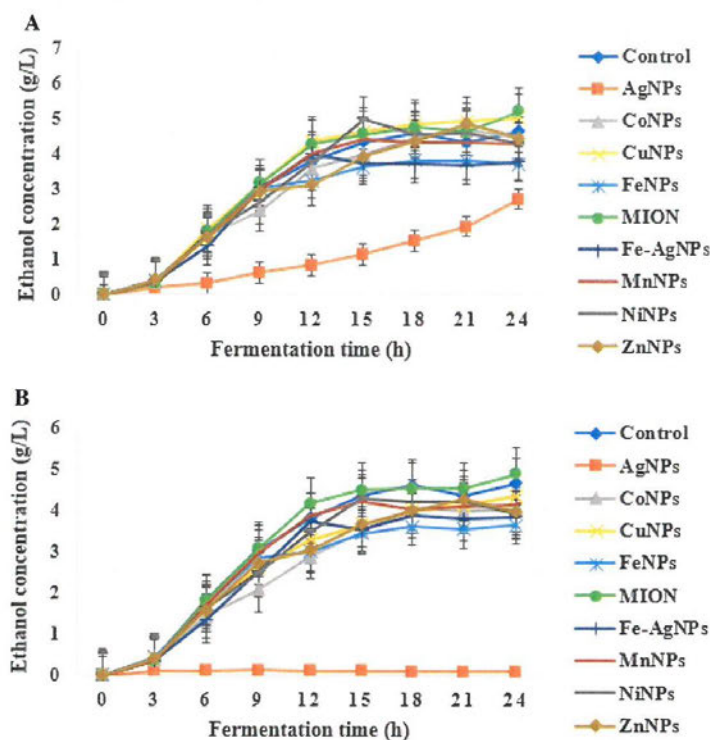
However, Lower concentrations of NPs have been shown to possess catalytic effect on some microbial cells [23, 42]. In a recent study by Ban and Paul [43], ZnO NPs with an average diameter of 5 nm was reported to support yeast cell growth while 10 and 15 mM resulted in the inhibition of yeast growth. Based on the observation from the preliminary study, 0.01 and 0.02 wt% inclusion was selected for further studies.

3.3 Effect of Nanoparticles Concentration on Fermentation Characteristics

3.3.1 Effect of Nanoparticles on Glucose Utilisation

In this study, *S. cerevisiae* BY4743 was able to utilise over 92.20% glucose within 24 h of fermentation in all the cultures, with the exception of 0.02 wt% Ag NPs which had 21.95% glucose utilization. The maximum glucose utilization of 99.95% was observed at 0.01 and 0.02 wt% Fe_3O_4 NPs administered cultures, while the minimum glucose utilization of 21.95% was observed at 0.02 wt% Ag NPs as

Fig. 7 Time course of ethanol production showing the effect of metallic oxide NPs at different concentrations a 0.01 wt%, b 0.02 wt%



fermentation have been known to be pH dependent, a buffering effect will keep them in the optimum physiological state for optimum activities. Ban and Paul [43], reported that yeast culture administered with 5 mM ZnO NP enhanced the intracellular β -glucosidase (BGL) activity for up to 28% with a simultaneous increase in cell growth compared to the control.

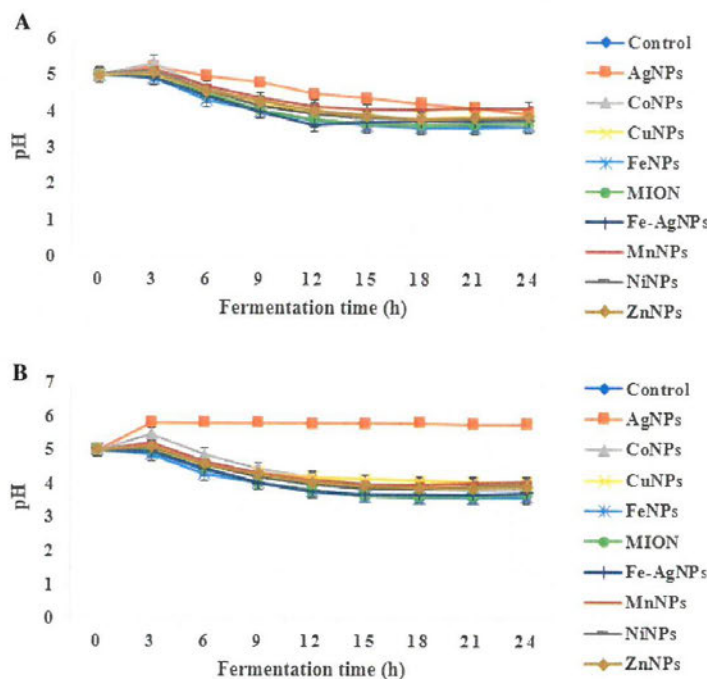
The pH was relatively stable in the nano-administered culture with the final pH value above 3.66 and 3.70 at 0.01 and 0.02 wt% inclusion respectively. This is with the exception of Fe NPs (0.01 wt% = 3.59, 0.02 wt% = 3.61). This result suggests the buffering effect of the NPs resulting in pH stability during fermentation. Additionally, NPs directly influenced *S. cerevisiae* BY4743 metabolism towards less acidic metabolites formation or a chemical interaction between the NPs and these acidic metabolites which thus, reduces the effect of these metabolites on the pH during the fermentation process [26, 46]. Furthermore, volatile metabolic compounds (VMCs) have chelating capacities due to their functional groups such as carboxylates, hydroxyls, phenols, sulfhydryls, and amines. These chelating groups can

perform as ligands and complex most of the metals available during fermentation. Suggesting that natural chelating agents such as VMCs formed in the bioprocessing play an important role in metal ions bioavailability to microorganisms and consequently the process performance.

3.3.4 Effect of NPs on Ethanol Formation

The observed ethanol concentration for the two experimental set up (0.01 and 0.02 wt%) with the nine NPs are presented in Fig. 7a and b respectively. Ethanol concentration increased from 0 h till the 24 h, after which there was a decline in the concentration of ethanol for all the cultures (< 3.60 g/L). The decline in ethanol concentration could be attributed to the depletion of glucose, nutrient, formation of metabolites and decrease in the pH of the medium. Ethanol concentrations of 2.73, 3.83, 3.99, 4.41, 4.68, 4.87, 5.00, 5.05 and 5.21 g/L were obtained at 0.01 wt% inclusion for Ag NPs, Fe NPs, Fe-Ag NPs, Mn NPs, Co NPs, Zn NPs, Ni NPs, Cu NPs and Fe₃O₄ NPs respectively (Fig. 5a), while 0.10, 3.66, 3.88, 4.05, 4.15, 4.29, 4.30, 4.36 and 4.89 g/L

Fig. 6 pH profile during ethanol fermentation at different NPs concentrations **a** 0.01 wt%, **b** 0.02 wt%



cell division, protein synthesis, and transportation of materials across the plasma membrane which in turn will enhance cell proliferation [23].

Table 2 shows the specific growth rate of yeast cell for the nine NPs. At 0.01 wt%, 0.23, 0.23, 0.22, 0.23, 0.22, 0.24, 0.21, 0.12 and 0.20 h^{-1} was obtained for Cu NP, Mn NP, Ni NP, Fe NP, Fe_3O_4 NP, Fe-Ag NP, Zn NP, Ag NP and Co NP respectively, while 0.23, 0.23, 0.22, 0.22, 0.23, 0.21, 0.23, 0.22, 0.08 and 0.21 h^{-1} was recorded for Cu NP, Mn NP, Ni NP, Fe NP, Fe_3O_4 NP, Fe-Ag NP, Zn NP, Ag NP and Co NP respectively at 0.02 wt%. The results also show that the highest specific growth rate of 0.24 h^{-1} was obtained with 0.01 wt% Fe-Ag NPs. Ag NPs administered cultures at both concentrations had the lowest specific growth rate of 0.122 h^{-1} (0.01 wt%) and 0.084 h^{-1} (0.02 wt%). This is believed to be influenced by the silver nanoparticles antimicrobial activities. Ban and Paul [43], reported a higher specific growth rate of 0.54 h^{-1} of *S. cerevisiae* with 5 mM ZnO NP. Although there was no appreciable effect of metallic oxide NPs on the specific growth rate of *S. cerevisiae* BY4743, however, the results suggest that the NPs have the potential to improve the growth rate of *S. cerevisiae* BY4743 under the optimum process conditions.

3.3.3 Effect of Nanoparticles on Culture pH

The pH profiles during ethanol fermentation are shown in Fig. 6a, b. A slight decrease in the pH was observed in the first 3 h of fermentation, which then gradually continued till the 24 h mark in all the cultures. For instance, with Zn NPs at 0.01 wt%, the pH gradually declines from 5.00 to 4.01 after 12 h and remained at 3.8 by the 24 h mark (Fig. 5a). Likewise, Ag NPs and Mn NPs, at 0.01 wt%, recorded a decline from pH 5.00 to 4.49 and 5.00 to 4.15 respectively at the 12 h mark and was stable at pH 4.00 by the 24 h mark. On the other hand, the control experiment declined sharply to 3.79 after 12 h and reached pH 3.65 by the 24 h.

Higher ethanol yields were achieved at pH 3.65–3.84, which occurred between the 15 h and 24 h at 0.01 wt% NPs inclusion. At pH above 4.00, ethanol yields were lower as evident with 0.02 wt% Ag NPs, which recorded the lowest ethanol yield of 0.03 g/g at pH above 5.00. The highest ethanol yield of 0.26 g/g was obtained at pH 3.72 with 0.01 wt% Fe_3O_4 NPs. Perhaps, the conversion of glucose to ethanol and other metabolic activities of *S. cerevisiae* BY4743 was improved at this pH range, which in turn enhanced ethanol yield [45]. For instance, enzyme activities during microbial

Table 3 Kinetic parameters for cell growth and ethanol production under different NPs types and concentrations

| NPs (wt%) | Logistic function parameters | | | | | Modified Gompertz parameters | | | |
|----------------------------------------|------------------------------|-----------------|--------------------|--------------------------|-------|------------------------------|-------------------|-----------|-------|
| | X_0 (g/L) | X_{max} (g/L) | μ (h^{-1}) | μ_{max} (h^{-1}) | R^2 | P_m (g/L) | $r_{p,m}$ (g/L/h) | t_l (h) | R^2 |
| Cu NPs | | | | | | | | | |
| 0.01 | 0.40 | 2.43 | 0.23 | 0.41 | 0.950 | 5.01 | 0.54 | 2.67 | 0.998 |
| 0.02 | 0.34 | 2.41 | 0.23 | 0.60 | 0.970 | 4.29 | 0.37 | 1.90 | 0.997 |
| Fe₃O₄ NPs | | | | | | | | | |
| 0.01 | 0.22 | 2.25 | 0.22 | 0.54 | 0.988 | 4.94 | 0.56 | 2.89 | 0.995 |
| 0.02 | 0.23 | 2.28 | 0.21 | 0.54 | 0.991 | 4.74 | 0.54 | 2.71 | 0.997 |
| Ni NPs | | | | | | | | | |
| 0.01 | 0.12 | 2.00 | 0.22 | 0.80 | 0.998 | 5.24 | 0.47 | 2.71 | 0.989 |
| 0.02 | 0.25 | 2.30 | 0.22 | 0.57 | 0.991 | 4.47 | 0.42 | 2.50 | 0.993 |
| Zn NPs | | | | | | | | | |
| 0.01 | 0.27 | 2.25 | 0.21 | 0.53 | 0.989 | 5.02 | 0.35 | 1.61 | 0.987 |
| 0.02 | 0.24 | 2.30 | 0.22 | 0.55 | 0.994 | 4.43 | 0.35 | 1.77 | 0.992 |
| Co NPs | | | | | | | | | |
| 0.01 | 0.22 | 2.11 | 0.20 | 0.53 | 0.985 | 4.71 | 0.40 | 2.28 | 0.993 |
| 0.02 | 0.25 | 2.11 | 0.21 | 0.49 | 0.987 | 4.26 | 0.32 | 2.08 | 0.994 |
| Fe NPs | | | | | | | | | |
| 0.01 | 0.19 | 2.17 | 0.23 | 0.62 | 0.993 | 3.77 | 0.49 | 2.43 | 0.996 |
| 0.02 | 0.22 | 2.20 | 0.23 | 0.57 | 0.991 | 3.60 | 0.43 | 2.07 | 0.995 |
| Fe–Ag NPs | | | | | | | | | |
| 0.01 | 0.17 | 2.44 | 0.24 | 0.63 | 0.998 | 3.81 | 0.72 | 3.97 | 0.986 |
| 0.02 | 0.26 | 2.57 | 0.23 | 0.53 | 0.994 | 3.89 | 0.49 | 3.16 | 0.990 |
| Mn NPs | | | | | | | | | |
| 0.01 | 0.14 | 2.02 | 0.23 | 0.70 | 0.998 | 4.41 | 0.56 | 3.00 | 0.997 |
| 0.02 | 0.16 | 1.96 | 0.22 | 0.73 | 0.997 | 4.18 | 0.54 | 2.80 | 0.997 |
| Ag NPs | | | | | | | | | |
| 0.01 | 0.24 | 2.99 | 0.12 | 0.14 | 0.989 | 25.03 | 0.33 | 18.58 | 0.993 |
| 0.02 | 0.31 | 1.06 | 0.08 | 0.17 | 0.877 | 0.12 | 1.03 | 1.97 | 0.999 |
| Control | 0.18 | 2.21 | 0.23 | 0.60 | 0.996 | 4.61 | 0.49 | 2.45 | 0.997 |

NPs nanoparticles, Cu NPs copper(II) oxide, Mn NPs manganese oxide, Ni NPs nickel oxide, Fe NPs iron(II) oxide, Fe₃O₄ NPs iron(III) oxide, Fe–Ag NPs iron(III) oxide-silver doped, Zn NPs zinc oxide, Co NPs cobalt oxide, Ag NPs silver oxide

0.084 h^{-1} using *S. cerevisiae* in a fermentation process with 240 g/L initial glucose concentration. Aside the variation that might be due the inclusion or exclusion of nanoparticles, other factors such as substrate type and concentration, yeast strain and process operating conditions might have led to the differences in the specific growth rate (μ) values.

3.4.2 Ethanol Production

The ethanol formation during fermentation of glucose is shown in Fig. 7a, b. The experimental data fitted excellently the modified Gompertz model (Table 3), with a coefficient of determination ($R^2 \geq 0.99$ for all the NPs tested). This shows the adequacy of the model to describe the formation of ethanol by *S. cerevisiae* BY4743 in the presence of these metallic oxides.

Maximum ethanol production rate ($r_{p,m}$) of 0.54, 0.56, 0.47, 0.35, 0.40, 0.49, 0.72, 0.56 and 0.33 g/L/h were obtained for Cu, Fe₃O₄, Ni, Zn, Co, Fe, Fe–Ag, Mn and Ag NPs with 0.01 wt% inclusion respectively. While the maximum ethanol production rate ($r_{p,m}$) obtained at 0.02 wt% inclusion was 0.37, 0.54, 0.42, 0.35, 0.32, 0.43, 0.49 and 0.54 g/L/h for Cu, Fe₃O₄, Ni, Zn, Co, Fe, Fe–Ag and Mn NPs respectively. Most of the processes with 0.01 wt% inclusion demonstrated higher $r_{p,m}$ values compared to the 0.02 wt% inclusion and the control experiment (0.49 g/L/h). Fe–Ag NPs at 0.01 wt% had the highest $r_{p,m}$ value (0.72 g/L/h), which did not translate to higher ethanol production, primarily because of the long lag time (3.97 h) observed for ethanol production in the process. This was caused by the long adaption time by the yeast to the Fe–Ag NPs.

were recorded for Ag NPs, Fe NPs, Fe–Ag NPs, Co NPs, Mn NPs, Zn NPs, Ni NPs, Cu NPs and Fe₃O₄ NPs at 0.02 wt% inclusion respectively (Fig. 5b). Cultures with Co NPs, Zn NPs, Ni NPs, Cu NPs and Fe₃O₄ NPs at 0.01 wt% enhanced ethanol yield with 0.43, 4.51, 7.30, 8.37 and 11.80% improvement in the ethanol concentration observed from the control experiment (4.66 g/L).

Kim and Lee [5], obtained 0.35 g/L and 0.49 g/L ethanol in syngas fructose fermentation by *Clostridium ljungdahlii* (ATCC 55383) using SiO₂–CH₃ and CoFe₂O₄@SiO₂–CH₃ nanoparticles respectively. A maximum glucose utilisation of 99.95%, ethanol yield of 0.26 g/g, ethanol productivity of 0.22 g/L/h and fermentation efficiency of 50.96% was achieved with Fe₃O₄ NPs at 0.01 wt%. Ethanol yield, productivity and fermentation efficiency at 0.01 wt% Fe₃O₄ NPs, Cu NPs, Ni NPs, Zn NPs and Co NPs were found to be higher than other NPs and the control at both concentrations tested (Table 2). These results indicated that ethanol production was best impacted at 0.01 wt% NPs. Metal ions could act as an enzyme cofactor/enzyme activator, growth factor, chelating agent, enzyme stabilizer and cell growth stimulator to enhance microbial metabolic activities. Furthermore, these metallic ions are important in stimulating the formation of cytochromes and ferroxins (Fd) which are vital for cell energy metabolism, hence product formation during fermentation. The correlation between ethanol production, biomass concentration and metabolic activity during fermentation has been reported by other authors [14]. This, however, may depend on the yeast strain, culture conditions, the physiological properties of the metal and its interaction with other metal ions in the medium [23].

The variation in ethanol response under various NPs may be attributed to differences in the NPs' shape, diameter and particle size. For example, spherically shaped Fe₃O₄ NPs with an average diameter of 31 nm had the highest impact on ethanol production. Zn NPs (30 nm), Ni NPs (29 nm), and Cu NPs (15 nm) which were also spherical in shape, similarly impacted ethanol production positively. On the other hand, Co NPs (12 nm), with an irregular shape had the least positive impact (0.43% improvement over the control) on ethanol production. The NPs with a positive effect on ethanol production in this study ranged from 12 to 31 nm in average diameter, except for Ag NPs (23 nm). A similar bio-stimulatory effect was reported with spherically shaped Co and Ni NPs within the range of 17–28 nm which resulted to an improved biogas and methane production during anaerobic digestion of slurry [23]. Also, Verma and Stellacci [47] in their study on the effect of surface properties on nanoparticles–cell interactions, opined that the shape and size of nanoparticles significantly influence cellular uptake.

On the other hand, Fe–Ag NPs (61 nm), Fe NPs (47 nm), Ag NPs (23 nm) and Mn NPs (8 nm), showed a lower ethanol concentration at 0.01 and 0.02 wt%. Besides the possibility of a toxic effect by these nanoparticles, the larger particle size of these NPs could have also affected the ethanol metabolic pathway. Nano-size is a principal property that influences the NPs interaction with biological systems as it determines the ability to penetrate the cell membrane, thus facilitating the passage across biological barriers, uptake, absorption, distribution and metabolism of biological material.

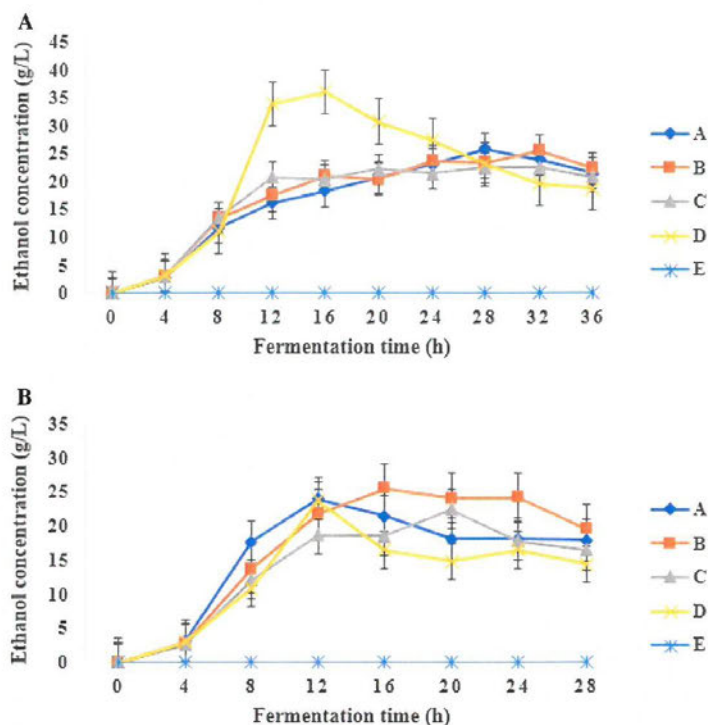
3.4 Kinetic Studies

3.4.1 Biomass Growth

The kinetic parameters of *S. cerevisiae* growth were estimated by fitting the experimental data into the logistic equation (Eq. 6). The experimental data fitted the model with $R^2 \geq 0.88$ (Table 3). This suggests that the model's predictions could explain over 88% of the total variations observed with the *S. cerevisiae* BY4743 growth in the nano-administered processes [45]. According to the fitted growth model, the values for the maximum biomass concentration (X_m) were mostly higher in the nano-administered processes compared to the control experiment (2.21 g/L). On the other hand, the estimated values of maximum specific growth rate (μ_{max}) were lower in the nanoparticles supplemented processes in comparison to the control process (0.60 h⁻¹) except for Cu NPs (0.02 wt%), Fe NPs (0.01 wt%), Fe–Ag NPs (0.01 wt%), Mn NPs (0.01 wt%), Mn NPs (0.02 wt%) and Ni NPs (0.01 wt%), which were 0.60, 0.62, 0.63, 0.70, 0.73 and 0.80 h⁻¹ respectively. Based on the μ_{max} , the results indicated that NPs supplementation has a potential to significantly improve the specific growth rate of *S. cerevisiae* during fermentation.

The lowest specific growth rate of 0.14 and 0.17 h⁻¹ were observed with 0.01 and 0.02 wt% Ag NPs respectively. The lower specific growth rate (μ) values obtained for some of the NPs supplemented processes may be due to the longer lag phase and the need for the yeast cells to adapt to the administered NPs. Therefore, an inoculum development stage with the metallic oxide nanoparticles prior to fermentation might be crucial to improve the specific growth rate of the yeast. Previous kinetic studies on ethanol production, though without nanoparticles supplementation gave a correlated μ_{max} values. For instance, Ortiz-Muniz et al. [48], studied the kinetics of *S. cerevisiae* ITV-01 on sugarcane molasses with initial glucose concentrations ranging from 100 to 250 g/L and reported μ_{max} values of 0.26 to 0.23 h⁻¹. Similarly, Ahmad et al. [49], recorded a μ_{max} value of

Fig. 8 Time course of ethanol production in Nano inclusion in a simultaneous saccharification fermentation (NISSF) process **a** NiO SSF, **b** Fe₃O₄ SSF. **A** SATP → Nano → liquefaction → SSF. **B** SATP → liquefaction → Nano → SSF. **C** SATP → liquefaction → SSF (control). **D** Nano → SATP → liquefaction → SSF. **E** SATP → liquefaction → SS → no fermentation



Lag time (t_l) obtained for the processes at 0.01 wt% were 2.67, 2.89, 2.71, 1.61, 2.28, 2.43, 3.97, 3.00 and 18.58 h for Cu, Fe₃O₄, Ni, Zn, Co, Fe, Fe–Ag, Mn and Ag NPs respectively while at 0.02 wt% lag time of 1.90, 2.71, 2.50, 1.77, 2.08, 2.07, 3.16, 2.80 and 1.97 h for Cu, Fe₃O₄, Ni, Zn, Co, Fe, Fe–Ag, Mn and Ag NPs respectively. The long adapting time for the yeast to the administered NPs and the antimicrobial activities of Ag NPs accounts for the longer lag time observed in the nano-administered processes. However, Zn NPs had the shortest lag phase of 1.61 h at 0.01 wt% inclusion compared to the other NPs administered processes and the control experiment (2.45 h). This led to the high P_m (5.02 g/L) obtained.

High maximum potential ethanol concentration (P_m) of 5.01, 4.94, 5.24, 5.02 and 4.71 g/L at 0.01 wt% inclusion for Cu, Fe₃O₄, Ni, Zn and Co NPs respectively were obtained compared to 0.02 wt% inclusion and the control process (4.61 g/L). This observation can be attributed to high maximum ethanol production rate and shorter lag time observed in these set ups.

4 Effect of Nano on SSF of Potato Waste

Bioethanol evolution under the nanoparticles inclusion in a simultaneous saccharification and fermentation (Fig. 8a, b) processes conditions revealed a short lag phase (4 h) for all four NISSF processes. An increase in the ethanol concentration up to 25.85, 25.63, 22.53 and 36.04 g/L were observed for SSF NiO NPs inclusion processes Mode A, B, C and D respectively. The SSF Fe₃O₄ NPs inclusion processes also showed increases in the bioethanol concentration up to 23.99, 25.49, 22.49 and 23.75 g/L for NISSF processes Mode A, B, C and D respectively. Maximum bioethanol concentration occurred during the exponential growth phase in all the NISSF processes and were associated with a rapid conversion of glucose to ethanol. The high production of fermentable sugars and bioethanol in NISSF processes were due to increased hydrolysis and glucose conversion rates at improved enzymatic activities. A previous study by Ban and Paul [43], also reported increase in intracellular β -glucosidase (BGL) activity up to 28% with 5 mM

Table 4 Fermentation performance in Nano inclusion simultaneous saccharification fermentation (NISSF) process

| | A | B | C | D |
|---------------------------------------------|------|------|------|------|
| NiO NPs SSF mode | | | | |
| Sugar utilization (%) | 96 | 100 | 100 | 99 |
| Ethanol yield (g/g) | 0.48 | 0.48 | 0.42 | 0.71 |
| Ethanol productivity (g/L/h) | 0.92 | 0.80 | 0.92 | 2.25 |
| Fe ₃ O ₄ NPs SSF mode | | | | |
| Sugar utilization (%) | 97 | 100 | 100 | 96 |
| Ethanol yield (g/g) | 0.93 | 0.58 | 0.46 | 0.79 |
| Ethanol productivity (g/L/h) | 2.00 | 1.59 | 0.92 | 1.98 |

ZnO NP process inclusion. This can be attributed to the nanoparticle's presence, which provides excellent reactive sites for several enzymes such as alcohol dehydrogenase [43]. Similarly, the metallic nanoparticles act as a bridge between the substrate and enzyme thus, increasing the binding energy. Maximum glucose utilisation of 96, 100, 100 and 99% were observed for the SSF NiO NPs inclusion processes Mode A, B, C and D respectively, while 97, 100, 100 and 94% maximum glucose utilisation were observed for the processes Mode A, B, C and D SSF Fe₃O₄ NPs inclusion respectively. These suggest the presence of the NPs did not affect glucose utilization. The yield, and the productivity of bioethanol production increased noticeably. The highest ethanol productivity (2.25 g/L/h) and ethanol yield (0.93 g/g) were obtained at the process design D with NiO NPs and process design A with Fe₃O₄ NPs respectively. These were 146% and 102% respectively improvement over the control experiment (Table 4). Nanoparticles bio-stimulatory potentials and enhancement of metabolic activities have been reported [43, 47]. For instance, they are important in stimulating the formation of cytochromes and ferroxins (Fd) which are vital for cell energy metabolism. Additionally, the surface free energy of particles increases as the dimensions decrease, which enables the strong ability of small-sized particles to interact with electrons, enhancing efficiently electrons to acceptors transfer, this is of benefit to bioprocessing [19]. Verma and Stellacci [47], reported effect of surface properties on nanoparticles–cell interactions which significantly influenced cellular activity.

5 Conclusion

This study investigated the impacts of nine metallic oxide NPs on ethanol production with *S. cerevisiae* BY4743. The results indicated that ethanol production was best impacted at 0.01 wt% Fe₃O₄ NPs. A maximum glucose utilisation of 99.95%, ethanol yield of 0.26 g/g, ethanol productivity

of 0.22 g/L/h and fermentation efficiency of 50.96% were achieved with Fe₃O₄ NPs at 0.01 wt%. The Logistic model ($R^2 \geq 0.88$) and the modified Gompertz model ($R^2 \geq 0.99$) fitted the experimental data excellently. Nano inclusion in a simultaneous saccharification and fermentation (NISSF) process conditions favoured ethanol production from potato peels up to 60%. The present study demonstrate the use of metallic oxide NPs as a biocatalyst to enhance substrate conversion efficiency and ethanol yield.

Acknowledgements The authors thankfully acknowledge Dr. Che Pillay of the Discipline of Genetics, University of KwaZulu-Natal for the generous supply of *S. cerevisiae* BY4743 used in this study.

Compliance with Ethical Standards

Conflict of interest The authors declare that there was no conflict of interest in this work.

References

- Ivanova V, Petrova P, Hristov J (2011) *Int Rev Chem Eng* 3:289–299
- Putra MD, Abasaeed AE, Atiyeh HK, Al-Zahrani SM, Gaily MH, Sulicman AK, Zcinelabdeen MA (2015) *Chem Eng Commun* 202:1618–1627
- Mostafa SE (2019) *J Adv Res* 1:103–111
- Kim Y, Lee H (2016) *Bioresour Technol* 204:139–144
- Zhao X-Q, Bai F-W (2012) *J Biotechnol* 158:176–183
- Talasila U, Vechalapu RR (2015) *Int J Fruit Sci* 15:161–172
- Laopaiboon L, Nuanpeng S, Srinophakun P, Klarit P, Laopaiboon P (2008) *Biotechnology* 7:493–498
- Lin Y, Zhang W, Li C, Sakakibara K, Tanaka S, Kong H (2012) *Biomass Bioenerg* 47:395–401
- Moestedt J, Nordell E, Yekta SS, Lundgren J, Marti M, Sundberg C, Ejlerstsson J, Svensson BH, Björn A (2016) *Waste Manag* 47:11–20
- Thanh PM, Ketheesan B, Yan Z, Stuckey D (2016) *Biotechnol Adv* 34:122–136
- Steinle ED, Mitchell DT, Wirtz M, Lee SB, Young VY, Martin CR (2002) *Anal Chem* 74:2416–2422
- Chan WCW, Nic SM (1998) *Science* 281:2016–2019
- Frey M (2002) *Chem Biochem* 3(2–3):153–160
- Kim Y, Park SE, Lee H, Yun JY (2014) *Bioresour Technol* 159:446–450
- Han H, Cui M, Wei L, Yang H, Shen J (2011) *Bioresour Technol* 102:7903–7909
- Zhang T, Wu M-Y, Yan D-Y, Mao J, Liu H, Hu W-B, Du X-W, Ling T, Qiao S-Z (2018) *Nano Energy* 43:103–109
- Johnson AK, Zawadzka AM, Deobald LA, Crawford RL, Paszczynski AJ (2008) *J Nanopart Res* 10:1009–1025
- Sandhu KK, McIntosh CM, Simard JM, Smith SW, Rotello VM (2002) *Bioconjugate Chem* 13:3–6
- Haun JB, Yoon TJ, Lee H, Weissleder R (2010) *WIREs Nanomed Nanobiotechnol* 2(2–10):291–304
- Xu S, Liu H, Fan Y, Schaller R, Jiao J, Chaplen F (2012) *Appl Microbiol Biotechnol* 93:871–880
- Beckers L, Hilgsmann S, Lambert SD, Heinrichs B, Thonart P (2013) *Bioresour Technol* 133:109–117
- Zhu H, Shanks BH, Choi DW, Heindel TJ (2010) *Biomass Bioenerg* 34:1624–1627

23. Abdelsalam E, Samer M, Attia YA, Abdel-Hadi MA, Hassan HE, Badr Y (2016) *Renew Energy* 87:592–598
24. Zhang Y, Shen J (2007) *Int J Hydrogen Energy* 32(1):17–23
25. Zhao W, Zhang Y, Du B, Wei D, Wei Q, Zhao Y (2013) *Bioresour Technol* 142:240–245
26. Cherian E, Dharmendirakumar M, Baskar G (2015) *Chin J Catal* 36:1223–1229
27. Zhang Y, Shen J (2006) *Int J Hydrogen Energy* 31(4):441–446
28. Linville JL, Rodriguez M Jr, Mielenz JR, Cox CD (2013) *Bioresour Technol* 147:605–613
29. Phukoetphima N, Salakkamb A, Laopaiboon P, Laopaiboon L (2017) *J Biotechnol* 243:69–75
30. Dodic JM, Vucurovic DG, Dodic SN, Grahovac JA, Popov SD, Nedeljković NM (2012) *Appl Energy* 99:192–197
31. Khaghani S, Ghanbari B (2016) *J Nanostruct* 6(2):149–155
32. Ma J, Zhu W, Tian Y, Wang Z (2016) *Nanoscale Res Lett* 11:200
33. Prochazkova G, Safarik I, Branyik T (2013) *Bioresour Technol* 130:472–477
34. Zheng B, Zhang M, Xiao D, Jin Y, Choi MMF (2010) *Inorg Mater* 46(10):1106–1111
35. Aruwajoye GS, Faloye FD, Kana EGB (2017) *Energy Convers Manag* 150:558–566
36. Miller GL (1959) *Anal Chem* 31(3):426–428
37. Jaswal VS, Arora AK, Kingler M, Gupta VD, Singh J (2014) *Orient J Chem* 30(2):559–566
38. Li Q, Wang L-S, Hu B-Y, Yang C, Zhou L, Zhang L (2007) *Mater Lett* 61:1615–1618
39. Mohammadyani S, Hosseini SA, Sadrnezhad SK (2012) *Int J Modern Phys Conf Ser* 5:270–276
40. Kumar H, Manisha SP, Sangwan P (2013) *Int J Chem Chem Eng* 3(3):155–160
41. Abdelsalam E, Samer M, Attia YA, Abdel-Hadi MA, Hassan HE, Badr Y (2016) *Energy Convers Manag* 141(2016):108–119
42. Rai MN, Duran NE (2011) *Metal nanoparticles in microbiology*. Springer, Berlin
43. Ban DK, Paul S (2014) *Appl Biochem Biotechnol* 173:155–166
44. El-Kemary M, Nagy N, El-Mehasseb I (2013) *Mater Sci Semicond Process* 16:1747–1752
45. Wang Y, Liu S (2014) *Kinetic Energies*. 7:8411–8426
46. Wimonsong P, Nitisoravut R (2015) *Journal of Clean Energy Technologies* 3(2):128–131
47. Verma A, Stellacci F (2010) *Small* 6(1):12–21
48. Ortiz-Muniz B, Carvajal-Zarrabal O, Torrestiana-Sanchez B, Aguilar-Uscanga MG (2010) *J Chem Technol Biotechnol* 85:1361–1367
49. Ahmad F, Jameel AT, Kamarudin MH, Mel M (2011) *Afr J Biotechnol* 16:18842–18846

Publisher's Note Springer Nature remains neutral with regard to jurisdictional claims in published maps and institutional affiliations.

Affiliations

Isaac A. Sanusi¹ · Funmilayo D. Faloye¹ · E. B. Gueguim Kana¹

✉ E. B. Gueguim Kana
kanag@ukzn.ac.za

¹ Discipline of Microbiology, School of Life Sciences, University of KwaZulu-Natal, Private Bag X01, Scottsville 3209, Pietermaritzburg, South Africa

CHAPTER 4

Impact of Nanoparticle Inclusion on Bioethanol production Process Kinetic and

Inhibitor Profile

This chapter has been published with the title: Impact of Nanoparticle Inclusion on Bioethanol production Process Kinetic and Inhibitor Profile in *Biotechnology Reports* 29 (2021) e00585, <https://doi.org/10.1016/j.btre.2021.e00585>. The published paper is presented in the following pages.

Graphical abstract



Highlights

- NiO nanoparticle (NP) inclusion enhanced bioethanol production up to 59.96%.
- Band energy gap impact NP catalytic performance in bioethanol production.
- Presence of NiO NP improved ethanol productivity by 145%.
- Modified Gompertz model was used to describe ethanol production with NP inclusion.
- Presence of nanoparticles significantly reduced acetic acid concentration by 110%.



Impact of nanoparticle inclusion on bioethanol production process kinetic and inhibitor profile



Isaac A. Sanusi^{a,*}, Terence N. Suinyuy^b, Gueguim E.B. Kana^a

^a Discipline of Microbiology, Biotechnology Cluster, University of KwaZulu-Natal, Pietermaritzburg Campus, South Africa

^b School of Biology and Environmental Sciences, University of Mpumalanga, Mbombela, South Africa

ARTICLE INFO

Article history:

Received 3 October 2020

Received in revised form 8 December 2020

Accepted 31 December 2020

Keywords:

Band energy gap

Inhibitor profile

Nanoparticles

Bioethanol

Saccharomyces cerevisiae

ABSTRACT

This study examines the effects of nanoparticle inclusion in instantaneous saccharification and fermentation (NIISF) of waste potato peels. The effect of nanoparticle inclusion on the fermentation process was investigated at different stages which were: pre-treatment, liquefaction, saccharification and fermentation. Inclusion of NiO NPs at the pre-treatment stage gave a 1.60-fold increase and 2.10-fold reduction in bioethanol and acetic acid concentration respectively. Kinetic data on the bioethanol production fit the modified Gompertz model ($R^2 > 0.98$). The lowest production lag time (t_L) of 1.56 h, and highest potential bioethanol concentration (P_m) of 32 g/L were achieved with NiO NPs inclusion at different process stages; the liquefaction stage and the pre-treatment phase, respectively. Elevated bioethanol yield, coupled with substantial reduction in process inhibitors in the NIISF processes, demonstrated the significance of point of nanobiocatalysts inclusion for the scale-up development of bioethanol production from potato peels.

© 2021 Published by Elsevier B.V. This is an open access article under the CC BY-NC-ND license (<http://creativecommons.org/licenses/by-nc-nd/4.0/>).

1. Introduction

Diminishing fossil resources, in combination with environmental pollution associated with the exploitation of these resources, make it imperative that a transition to bio-based resources is considered [1]. The utilisation of lignocellulosic biomass is desirable both for economic and environmental reasons, as substrate suitability is one of the main cost factors taken into consideration in large scale bioethanol production. It is, therefore, crucial that ethanol production is carried out using inexpensive and carbohydrate-rich feedstocks [2]. Agricultural waste is the most abundant bioresource available for use as a feedstock for biofuel production, thereby contributing to the reduction of

production costs [1]. Different techniques are employed for the production of bioethanol from various bioresources (crops and lignocellulosic) depending on the geographical location, crop and the lignocellulosic biomass availability [3,4]. Potatoes (*Solanum tuberosum*) are the single most prominent vegetable crop in South Africa as the country is the number four producer of potatoes in Africa, producing an estimated 2.3×10^6 tonnes of potatoes, with the top three producing countries being Algeria (4.9×10^6), Egypt (4.8×10^6) and Malawi (4.3×10^6) [5]. Potatoes are also a staple crop across the world, currently, they became the world's fourth-largest food crop after maize, wheat, and rice [6]. The amount of potatoes processed is increasing yearly due to the expansion in the fast-food industry, increase in average income of the populace, increasing urbanisation and the inflow of international investment through international processing companies [5]. This rise in production and processing often leads to an increased generation of large volumes of waste residues such as peels, usually making up between 20–50 % of the entire tuber [6]. Most of the plant is, therefore, underutilised and its disposal has led to environmental concerns [7]. It is, therefore, necessary that an integrated, environmentally friendly solution is identified and developed [8,9].

Potato peels are a starchy, lignocellulosic waste containing intricate structures composed of lignin, hemicellulose and cellulose [10]. This food waste has been reported as one of the sustainable and foremost feedstocks for biofuel production [6]. It is

Abbreviations: NPs, Nanoparticles; wt%, Weight percent; SATP, Soaking assisted thermal pre-treatment; ISF, Instant saccharification and fermentation; SNLISF, SATP + Nano + Liquefaction + ISF; SLNISF, SATP + Liquefaction + Nano + ISF; SLISF, SATP + Liquefaction + ISF; NSLISF, Nano + SATP + liquefaction + ISF; SLIS, SATP + Liquefaction + SS + No Fermentation; NSLIS, Nano + SATP + Liquefaction + SS + No Fermentation; HMF, 5-Hydroxymethyl Furfural; ORP, Oxidation–reduction potential; ATP, Adenosine triphosphate; VICs, Volatile inhibitory compounds; SPR, Surface plasmon resonance; SPA, Surface Plasmon Absorption; UV-vis, Ultraviolet visible; TEM, Transmission electron microscopy; SEM, Scanning electron microscopy; EDX, Energy-dispersive X-ray spectroscopy; EDS, Energy dispersive spectrophotometric; GC-MS, Gas chromatography-Mass spectrometry.

* Corresponding author.

E-mail addresses: Sanusi_isaac@yahoo.com, SanusiA@ukzn.ac.za (I.A. Sanusi).

<https://doi.org/10.1016/j.btre.2021.e00585>

2215-017X/© 2021 Published by Elsevier B.V. This is an open access article under the CC BY-NC-ND license (<http://creativecommons.org/licenses/by-nc-nd/4.0/>).

currently receiving great interest as its bioconversion to high-value products such as renewable fuels do not directly compete with food security [11]. The potential of waste potato material as a feedstock for bioethanol production has recorded some successes [12–14]. For instance, Fadel [15] achieved high alcohol concentration of 13.2 % v/v in a fermentation broth containing 25 % w/v glucose from potato waste. Likewise, Arapoglou et al. [8] obtained 18.5 g/L fermentable sugar from the enzymatic hydrolysis of potato peel waste with a group of three enzymes and produced 7.6 g/L of ethanol after fermentation. Efforts towards the use of starch-based lignocellulosic biomasses for bioethanol production are being challenged by low sugar yield from substrate, high inhibitor production, high production cost and low fermentation efficiency [16], thus highlighting the need for further optimisation.

Despite the vast information available on the use of pre-treated starch-based substrate for bioethanol production, there is a dearth of literature on the kinetics of *Saccharomyces cerevisiae* growth and bioethanol production from potato peels under nanobiocatalyst conditions. Studies on kinetics would provide insights into the impact of process parameters on bioethanol formation [17,18]. Moreover, kinetic modelling can be used to predict the dynamics of substrate utilisation and bioethanol production rate. Usually, these models are employed to improve the yield and the productivity of high-quality product. The release of detrimental and inhibitory can also be minimised using these models [19]. The modified Gompertz model is employed to evaluate production lag time, maximum product production rate, and maximum product concentration on a given substrate [20]. Such model could provide valuable process products knowledge on bioethanol production process using potato peels as feedstock in the presence of a nanobiocatalyst.

Nano-size materials have attracted huge interest for their unique material properties and their corresponding practical applications in biotechnology [21,22]. Nanoparticles (NPs) have been used extensively in biomedicine, drug delivery, biosensors, water purification and environmental remediation [21,23]. Some biological applications include immobilisation of enzymes, microbial cells, as well as biocatalytic agents [23,24]. The strategy of using nanobiocatalytic agents in bioprocesses is to increase process efficiency through increased mass and heat transfer, enzymatic and cell metabolic activities arising from their large surface areas, catalytic properties, growth and enzyme cofactor functionality [25,26]. Besides their importance as cofactor for enzymatic activities, they are also required to aid the structural stability of several proteins and enzymes, many could exert significant control on cellular metabolic processes and ultimately process performance [27]. Furthermore, nano-compounds such as NiO and Fe₃O₄ provide a suitable start-up environment for bioproduct formation due to their ability to modulate oxidation-reduction potential (ORP) values [28]. Yet, the application of this approach is limited because of the poor understanding of the process and the limited available information on nanocatalysed bioethanol fermentation.

Process conditions used for the pre-treatment of lignocellulosic biomass result in the formation of inhibitory compounds [29]. The negative impact of these inhibitors are usually longer microbial lag time and lower cell concentration. In addition, many of these compounds have been reported to influence negatively enzymatic hydrolysis and fermentation processes. Fermentation inhibitors include aliphatic acids, ketones, phenolic compounds, furan-derivatives and alcohols [30]. Their concentrations differ, depending on the structure of the lignocellulosic biomass employed and the pre-treatment techniques implemented [29,30]. Knowledge of profile of inhibitory compounds from various stages of biomass conversion, namely, pretreatment, liquefaction, saccharification

and fermentation in the presence of nanocatalysts would enhance the understanding of the interaction of the biomass and nanoparticles.

The primary biological technique for the production of bioethanol from lignocellulosic feedstock is the instantaneous saccharification and fermentation process. During this process lignocellulosic feedstock is first saccharified by hydrolytic processes to release fermentable sugar, which is simultaneously fermented to produce bioethanol [26]. In instantaneous saccharification and fermentation (ISF), the overall process is limited by the need to optimise enzymatic and cellular activities for maximum sugar release and subsequent ethanol formation as well as to minimise inhibitor formation during the pre-treatment and fermentation processes [16]. Recent studies have examined parameter optimisation as a technique to improve the efficiency of instantaneous saccharification and fermentation process [31,16]. Attempts to include nanoparticles as biocatalytic agents to enhance heat and mass transfer rates, buffering capacity, enzymatic activities and cellular functionality continue to attract great interest [23,24,26,32,33]. Very little is known on the instantaneous saccharification and fermentation process with nanobiocatalyst inclusion at various process namely, liquefaction and pre-treatment stages.

This study therefore examines the impact of nanoparticle inclusion at different stages of ISF, using waste potato peels as substrate and to model the bioethanol production using the modified Gompertz model. In addition, the effect of nanoparticle inclusion on the process volatile compounds profile was also evaluated.

2. Materials and methodologies

2.1. Potato peel powder preparation

Potato peels were collected from food vendors in the Pietermaritzburg metropolis, KwaZulu-Natal province, South Africa. They were immediately oven-dried at 50–55 °C and milled to 1–2 mm particle size using a centrifugal miller. Composition analysis [34] of pulverised waste potato peels show 20 % starch, 14 % structural carbohydrate, 4 % cellulose, 10 % hemicellulose, 6 % lignin and 46 % others (lipids, protein, moisture content and ash contents).

2.2. Soaking assisted thermal pre-treatment (SATP)

The powdered waste potato peels (Fig. 1) were subjected to previously optimised process parameters of pre-treatment [35]. Briefly, 0.92 % (v/v) HCl solution at a solid-to-liquid (S:L) ratio of 10 % solid loading was soaked in a water bath without shaking for 2.34 h at 69.6 °C and followed by 5 min autoclave treatment (121 °C). The pH of the treated potato peel biomass was thereafter brought to neutrality in preparation for the enzymatic hydrolysis (the



Fig. 1. Flowchart of SATP pulverised waste potato peels.

hydrolytic enzymes-amylose and amyloglucosidase used were purchased from Sigma-Aldrich, South Africa).

2.3. Microorganism and inoculum preparation

An Erlenmeyer flask containing 100 mL Yeast-Peptone-Dextrose broth was inoculated with *S. cerevisiae* BY4743 and grown at 120 rpm, 30 °C overnight, to attain an exponential growth phase. This cultivation was subsequently used as seed-culture (10%) source for the instantaneous saccharification and fermentation.

2.4. Preparation of nanomaterials

NiO nanoparticles (NPs) were synthesised by dissolving an appropriate amount of $\text{NiCl}_2 \cdot 6\text{H}_2\text{O}$ in distilled water. Then NH_3 solution is added dropwise to reach a pH of 10. The solution was treated with microwave irradiation operated at a power of 700 W for 180 s, and the culmination of the reaction was signalled by the precipitation of light green NiO NPs. The NiO nanoparticle obtained were washed a few times with deionized water and oven dried for six hours [24].

Iron (III) oxide nanoparticles (Fe_3O_4 NPs) were synthesised by dissolving 1.0 g of $\text{FeSO}_4 \cdot 7\text{H}_2\text{O}$ in distilled water, and the pH was adjusted to 12, then the volume was made up to 200 mL. The solution was heated in a microwave oven at 700 W for 600 s. The obtained black magnetic Fe_3O_4 NPs precipitate was rinsed a few times and dried at 70 °C for a couple of hours [36].

2.5. Characterisation of nanoparticles

The morphology of NiO and Fe_3O_4 NPs was determined by a scanning electron microscope (SEM, ZEISS-EVO/LS15, ZEISS instrument, Germany). Each sample was mounted on an aluminium grid coated with carbon prior to scanning electron microscopy (SEM) analysis. Transmission electron microscopy (TEM) was used to study the shape and the particle size of the NPs. TEM image was captured on JEM-1400 electron microscope operating at 120 kV. The ultra-violet visible (UV-vis) absorption spectral properties of the nanoparticles were investigated by absorption spectroscopy using an ultra-violet visible spectrophotometry (200–700 nm).

2.6. Nanoparticle inclusion in instantaneous saccharification-fermentation (NISF)

The NISF experiments were carried out using hydrolysate from the SATP [32] pre-treatment stage. The NISF process (50 mL) contained pulverised and pre-treated potato peels; 10 % solid loading, 0.212 mL liquefying amylose (at 90 °C, pH 7, for an hour), 0.295 mL saccharifying amyloglucosidase and fermentation nutrients: yeast extract-5 g/L, KH_2PO_4 -2 g/L, MgSO_4 -1 g/L, $(\text{NH}_4)_2\text{SO}_4$ -1 g/L. *S. cerevisiae* inoculum (10 %) was introduced, then, the different NISF set-up in replicates were incubated at 37 °C and 120 rpm over 24 h until glucose concentrations were depleted. Aliquot of 0.5 mL were extracted at regular interval for sample analysis. The NISF designs [24] with nanoparticle supplementation at various process stages are shown below (Fig. 2).

2.7. Analytical methods

2.7.1. Glucose, bioethanol and cell concentration determination

The glucose concentration in the sampled aliquot was determined using D-glucose Assay Kit (Megazyme, Ireland).

The amount of bioethanol produced was determined using a bioethanol vapour sensor (LABQUEST® 2, Vernier, USA) [24].

2.7.2. Kinetic model constants

The bioethanol empirical data were used to fit the modified Gompertz model. The model Eq. (4) is shown below.

$$P = P_m \cdot \exp \left\{ - \exp \left[\frac{r_{p,m} \cdot \exp(1)}{P_m} \cdot (t_L - t) + 1 \right] \right\} \quad (4)$$

where P is the bioethanol concentration, (g/L), P_m is the potential maximum bioethanol concentration, (g/L), $r_{p,m}$ is the maximum bioethanol production rate (g/L/h) and t_L is the lag time of bioethanol production (h).

2.7.3. Calculation of bioethanol yield (wt.%) and bioethanol productivity (g/L/h)

Glucose utilisation, fermentation efficiency, bioethanol yield and bioethanol productivity were obtained using the following

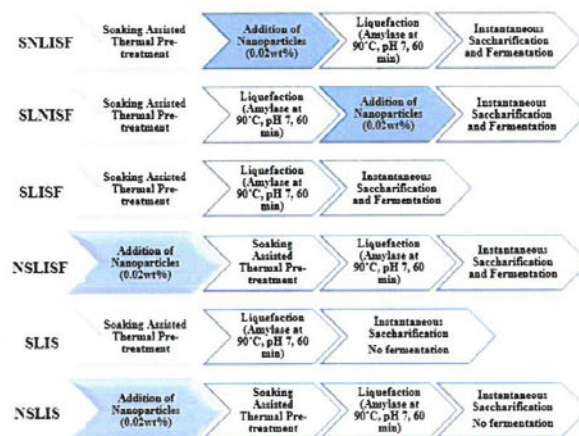


Fig. 2. Process flow diagram showing stages of nanoparticle inclusion in the ISF process. Nanoparticles (0.02 wt.% relative to biomass weight) were added at the pre-treatment (NSLISF), the liquefaction (SNLISF) and the saccharification (SLNISF) stages. The control is without nanoparticle inclusion (SLIS).

Eqs. (5)–(7) respectively.

$$\text{Sugar utilisation (\%)} = \frac{\text{Initial sugar content} - \text{final sugar content}}{\text{Initial sugar content}} \times 100 \quad (5)$$

$$\text{Ethanol yield (g/g)} = \frac{\text{Maximum ethanol concentration (g/L)}}{\text{Utilized glucose (g/L)}} \quad (6)$$

$$\text{Ethanol productivity (g/L/h)} = \frac{\text{Maximum ethanol concentration (g/L)}}{\text{Fermentation time (h)}} \quad (7)$$

2.7.4. Analysis of volatile organic inhibitory compounds

Analysis of inhibitory compounds such acetic acid, furfural, 5-Hydroxymethylfurfural (HMF) and ketones from the fermentation broth was carried out using with Varian 3800 gas chromatography (Varian Palo Alto, California, USA) and Varian 1200 mass spectrometry [30].

3. Results and discussion

3.1. Characterization of NiO and Fe₃O₄ nanoparticles (NPs) with SEM and TEM

In Fig. 3A, SEM-EDS analyses showed the surface morphology and elemental constituent of Fe₃O₄ nanoparticles. Strong signals corresponding to Fe (56.06%), and oxygen (30.19%) were observed. Other elemental constituent of Fe₃O₄ nanoparticles were C (13.40 at %) and Si (0.34 at %). Similarly, the Scanning Electron micrograph showed the aggregated NiO nanoparticle, and the elemental composition obtained using the SEM-EDS machine is Ni (31.46 at %), C (35.04 at %), O (32.53 at %), Cl (0.50 at %) and Si (0.48 at %). The TEM micrograph (Fig. 4A) shows that Fe₃O₄ particles were roughly spherical with particle size in the range of 18–39 nm with a mean

size of 31 nm. Equally, the TEM image of NiO nanoparticle is depicted in Fig. 4B with an average mean size of 29 nm.

Ultraviolet visible (UV) absorption spectra of NiO and Fe₃O₄ NPs were presented in Fig. 5. The UV–vis absorptions showed sharp absorption at 220 and 282 nm due to nickel and iron oxide metal nanoparticles respectively [37]. This can be attributed to the Surface Plasmon Resonance (SPR). The SPR originates from resonance of collective conduction electrons with incident electromagnetic radiations. The frequency and width of the Surface Plasmon Absorption (SPA) usually depends on the size and shape of the nanomaterials. In addition, the dielectric constant of the metal itself and the surrounding medium influences the SPA [38]. Also, the profile of the resonance peak can be qualitatively related to the nature of the NPs. NiO NPs with a small and uniform-sized narrow distribution (23–37 nm) produces a sharp absorbance, however, Fe₃O₄NP with a larger particle size and aggregation shows a broad absorbance [37,38].

3.2. Effect of nanoparticle band gap energy on bioprocessing

From the curve in Fig. 5, the band gap energy of Fe₃O₄ NPs and NiO NPs were 4.04 eV and 4.51 eV, respectively [39]. The inclusion of NiO nanoparticle in the fermentation process resulted in better process efficiency and consequently, higher productivities when compared to Fe₃O₄ NPs supplemented fermentation process (Table 1). This impact by NiO NPs inclusion can be attributed to the size of its band energy gap which is typical of efficient catalyst [40,41]. Activation energy and NPs catalytic potentials are usually dependent on band gap energy. In other words, lower activation energy is associated with higher energy gap, such as obtained in this study. Consequently, band energy gap could impact the interaction/affinity between the nanoparticles, the yeast and the substrate [24]. The process time for nanoparticle supplemented fermentation process achieved peak ethanol production after 16 h. This was two-fold faster than the result obtained in the control experiment. This clearly indicates the presence of the nanoparticles had high catalytic effect on the biochemical processes to improve bioethanol production. This catalytic activity could also be ascribed in part to its band energy gap. Likewise, the efficiency of heat and mass transfer which are vital bioprocess conditions, could

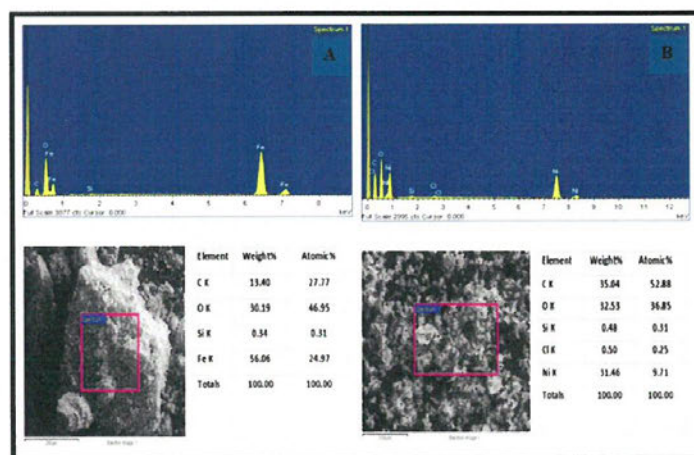


Fig. 3. Scanning electron microscopy (SEM) image and EDX Spectrum of Fe₃O₄ NPs (A) and NiO NPs (B).

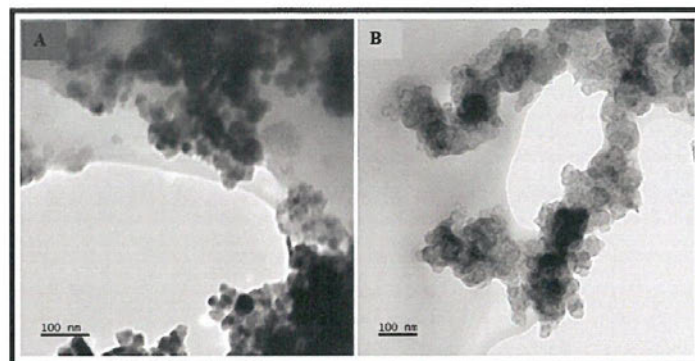


Fig. 4. Transmission electron microscopy (TEM) micrographs of Fe₃O₄ NPs (A) and NiO NPs (B) showing the shape and weak agglomeration of the nanoparticles.

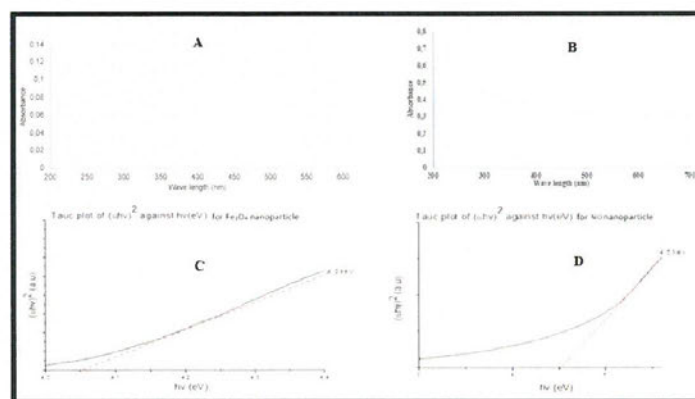


Fig. 5. Fe₃O₄ NPs (A), NiO NPs (B), Tauc plot of Fe₃O₄ NPs (C) and Tauc plot of NiO NPs (D).

Table 1
Performance of ISF processes with nanoparticle inclusion.

| ISF mode with NiO NPs | SNLISF | SLNISF | SLISF (control) | NSLISF |
|--------------------------------------------------|--------|--------|-----------------|--------|
| Glucose utilization (%) | 96.00 | 100.00 | 100.00 | 99.00 |
| Bioethanol yield (g/g) | 0.50 | 0.50 | 0.40 | 0.70 |
| Bioethanol concentration (g/L) | 25.85 | 25.63 | 22.53 | 36.04 |
| Bioethanol productivity (g/L/h) | 0.90 | 0.80 | 0.90 | 2.25 |
| ISF mode with Fe ₃ O ₄ NPs | SNLISF | SLNISF | SLISF | NSLISF |
| Glucose utilization (%) | 97.00 | 100.00 | 100.00 | 96.00 |
| Bioethanol yield (g/g) | 0.93 | 0.60 | 0.46 | 0.79 |
| Bioethanol concentration (g/L) | 23.99 | 25.49 | 22.49 | 23.75 |
| Bioethanol productivity (g/L/h) | 1.99 | 1.60 | 0.90 | 1.98 |

be influenced by band gap size. Mass transfer phenomena are considered under the Poole-Frenkel effect and small-polaron mechanism: these are band energy gap dependent [40,41]. The most remarkable correlation is: the smaller the particle size, the higher the energy gap, that could occasion lower activation energy hence, high process performance. The synthesis of a nanomaterial

with suitable band energy gap would enable the optimal electron transfer and catalytic properties, that could support high process performance.

3.3. Bioethanol production from potato peels

Bioethanol evolution under Fe₃O₄ NIISF (Fig. 6A) and NiO NIISF (Fig. 6B) fermentation processes revealed a short lag time (4 h) for all modes in both nano systems. The NSLISF (NiO NIISF) process showed a sharp increase in bioethanol concentration up to 36.04 g/L, the highest obtained of the NiO NIISF processes which occurred from 4 to 20 h in comparison to 25.13 g/L (Mode SLNISF), the highest of the Fe₃O₄ NIISF processes. Maximum bioethanol concentrations were obtained during the log yeast cell growth stage in the NSLISF (NiO NIISF) and SLNISF (Fe₃O₄NIISF) and were higher than the control experiment (Mode SLISF) in both systems. These were linked with precipitous utilisation of glucose by the yeast and bioethanol formation. Further increment in bioethanol concentration was not observed after the log phase, due to nutrient exhaustion besides fermentable sugar depletion. Ethanol yields of 0.48, 0.48, 0.42 and 0.71 g-ethanol/g-glucose (Table 1)

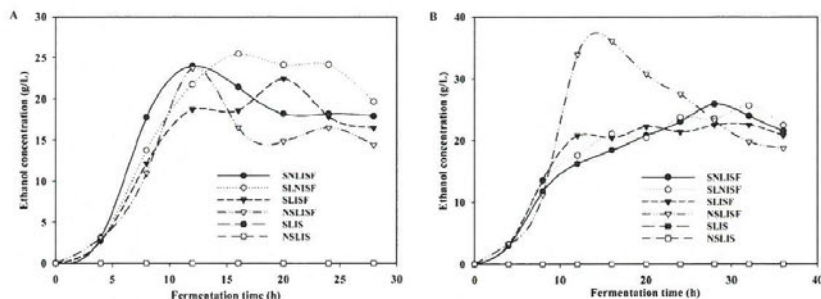


Fig. 6. Production of bioethanol as a function of fermentation time showing the impact of Fe_3O_4 NPs (A) and NiO NPs (B) inclusion.

corresponding to productivities of 0.92, 0.80, 0.92 and 2.25 g/L/h were achieved for NiO NPs ISF Mode SNLISF, SLNISF, SLISF and NSLISF respectively. Similarly, ethanol yield of 0.93, 0.58, 0.46 and 0.79 g/g was obtained, corresponding to 2.00, 1.58, 0.92 and 1.98 g/L/h productivity for Fe_3O_4 NPs ISF Mode SNLISF, SLNISF, SLISF and NSLISF respectively during the same fermentation period. The effect of NiO and Fe_3O_4 NPs inclusion on the processes were substantial. For instance, ethanol yield in the NiO NPs ISF process was 1.69-fold higher than the control set-up while a twofold (2.02-fold) increment in ethanol yield in comparison with the control set-up was observed in the Fe_3O_4 NPs ISF process. Micronutrients such as nickel and iron have a significant impact on *S. cerevisiae* growth and bioethanol formation [2,42]. Additionally, nickel oxide nanoparticles have been reported to exhibit a glucose-nanoparticle electropositive interaction [42], and this is advantageous for substrate to cell contact. Moreover, nanoparticles have stronger affinity for electrons due to their redox potential and small atomic size [43]. Strong affinity within few nanometres distance of microbes and nanoparticles under anaerobic conditions was obtained in previous reported [44]. Furthermore, the possibility of nanoparticles being adsorbed to the cell surface as well as cell adsorption to the surfaces of NPs have been reported [28,33]. Hence, improved *S. cerevisiae* substrate contact, cellular metabolism and process performance were obtained for the nano-fermentation processes [33,45,46].

In comparison, higher bioethanol concentrations were achieved with NPs inclusion in the ISF processes in relation to previous studies using potato wastes as feedstock for bioethanol production. For instance, 1.7-fold increase in the bioethanol concentration was observed in the NiO NPs ISF process compared to the study of Khawla et al. [14]. Likewise, 4.7-fold and 6.5-fold higher ethanol

concentration were achieved in the NiO NPs ISF process compared to studies by Arapoglou et al. [8] and Hashem and Darwish [12], respectively. Similarly, the Fe_3O_4 NPs ISF process had higher bioethanol concentration, 25.49 g/L (4.6-fold increment), compared to previous study on potato starch residue (5.52 g/L, [12]). Again, in another related study, a 3.4-fold increase in bioethanol concentration was also obtained with the Fe_3O_4 NPs ISF process compared to the study by Arapoglou et al. [8], where the authors obtained highest bioethanol concentration of 7.6 g/L from potato peel waste using *Saccharomyces cerevisiae* var. *bayanus*. The higher bioethanol concentration in the current study is desirable and might be ascribed mainly to the nanobiocatalyst employed, which increases the chances of *S. cerevisiae* substrate contact, utilisation and ultimately, enhanced process performance.

Furthermore, the highest bioethanol productivity of 2.25 g/L/h was achieved with NiO NPs inclusion during the pre-treatment stage in the present study (Table 2). By comparison, lower ethanol productivity, in the range of 0.15 to 0.25 g/L/h from previous studies was achieved by Arapoglou et al. [8] and Khawla et al. [14], both also using potato peel as substrate. Similarly, Hashem and Darwish [12] reported ethanol productivity of 0.15 g/L/h which was 15-fold lower than the current study. Additionally, in two different studies, Izmirliglu and Demirci [13] and Izmirliglu and Demirci [47] reported bioethanol productivities of 0.29 and 0.27 g/L/h, respectively using waste potato mash as feedstock. The obtained productivities were 7.8-fold and 8.3-fold, respectively lower when compared to the current study. The reported variations observed in these bioethanol productivities can be attributed mainly to the presence of nano additives as well as the different potato waste feedstock, yeast strain, and the fermentation approach employed [48].

Table 2
Comparison of bioethanol productivity with previous studies.

| Substrate | Yeast | Productivity (g/L/h) | References |
|--------------------|---------------------------------------------------------------------------|----------------------|-------------------------------------------------------------|
| Waste potato peels | <i>S. cerevisiae</i> BY4743 | 0.92 | This study (NiO NP Mode SNLISF) |
| Waste potato peels | <i>S. cerevisiae</i> BY4743 | 0.80 | This study (NiO NP Mode SLNISF) |
| Waste potato peels | <i>S. cerevisiae</i> BY4743 | 0.92 | This study (NiO NP Mode SLISF-control) |
| Waste potato peels | <i>S. cerevisiae</i> BY4743 | 2.25 | This study (NiO NP Mode NSLISF) |
| Waste potato peels | <i>S. cerevisiae</i> BY4743 | 1.99 | This study (Fe_3O_4 NP Mode SNLISF) |
| Waste potato peels | <i>S. cerevisiae</i> BY4743 | 1.59 | This study (Fe_3O_4 NP Mode SLNISF) |
| Waste potato peels | <i>S. cerevisiae</i> BY4743 | 0.92 | This study (Fe_3O_4 NP Mode SLISF-control) |
| Waste potato peels | <i>S. cerevisiae</i> BY4743 | 1.98 | This study (Fe_3O_4 NP Mode NSLISF) |
| Waste potato peels | <i>S. cerevisiae</i> | 0.25 | [15] |
| Waste potato peels | <i>S. cerevisiae</i> var. <i>bayanus</i> | 0.15 | [9] |
| Waste potato peels | <i>S. cerevisiae</i> y-1646 | 0.15 | [12] |
| Waste potato mash | <i>S. cerevisiae</i> (ATCC 24859) | 0.29 | [13] |
| Waste potato mash | <i>Aspergillus niger</i> (NRRL 330) and <i>S. cerevisiae</i> (ATCC 24859) | 0.27 | [45] |

The maximum bioethanol yield of 0.93 g/g was achieved in the current research. This was achieved with Fe₃O₄ NPs inclusion (NIISF Mode SNLISF). Ethanol yields between 0.38 and 0.46 g/g have been reported in previous studies [8,47]. These were 2.4 and 2.0-fold lower than the ethanol yield (0.93 g/g) obtained in present study. These observations further underscore the potential of nanobiocatalyst in the fermentation of waste potato peels and other feedstock for bioethanol production [49].

The high glucose release during the pre-treatment process can be attributed to the enhanced enzymatic hydrolysis of pre-treated waste potato peels [25]. The recovery of fermentable sugars in the nano systems was observed to be slightly higher in comparison to the control experiments (Fig. 7) and this can be ascribed to increased enzyme activities under the nanobiocatalyst conditions [50–54]. In a related study, Ban and Paul [25], reported an increase in intracellular β -glucosidase (BGL) activity up to 28 % with 5 mM ZnO nanoparticle process inclusion. Furthermore, the high glucose availability for immediate utilisation by the yeast cells could promote glycolytic rates and consequently, increase ethanol production instead of cell development, which further explains the higher bioethanol concentration observed in the nano systems.

The depletion of glucose occurred from 0 to 28 h in the Fe₃O₄ NPs inclusion ISF processes (Fig. 7A). The percentage glucose utilisation of 97.00 %, 100.00 %, 100.00 % and 94.00 % were observed under the four fermentation conditions (SNLISF, SLNISF, SLISF and NSLISF, respectively). Similarly, rapid glucose depletion was observed in the NiO NPs inclusion ISF processes from 0 to 36 h (Fig. 7B). And the maximum glucose utilisation of 96.00 %, 100.00 %, 100.00 % and 99.00 % (Table 1), was observed for SNLISF, SLNISF, SLISF and NSLISF processes respectively, further suggesting the nano catalysts favoured glucose uptake and utilisation by *S. cerevisiae*.

3.4. NIISF processes bioethanol production kinetics

The observed data fitted the modified Gompertz model (R^2 value >0.98) for the ISF NiO and Fe₃O₄ NPs inclusion modes, respectively (Table 3). The modified Gompertz kinetic model is widely used for bioproduct formation study [55,56]. This model gives information on the process lag time, the maximum bioethanol production rate, and the potential maximum bioethanol concentration. The kinetic coefficients for the highest maximum potential bioethanol concentration (P_m), maximum bioethanol production rate ($r_{p,m}$), and the lowest lag time obtained in the present study were 32 g/L, 4.50 g/L/h, and 1.56 h, obtained for the ISF NPs inclusion processes, NSLISF (NiO NPs inclusion), SNLISF (Fe₃O₄ NPs inclusion) and SNLISF (NiO NPs inclusion), respectively. All the NIISF results suggest that the presence of these

nanomaterials effectively improved the bioactivity of *S. cerevisiae* and subsequently increase the formation and yield of ethanol from glucose. Also, these metals are bio-active agents such as cofactor enzymes stabilizer and activators that enhance anaerobic bioethanol fermentation [57]. Besides their role as growth factors and enzyme cofactors, they are important in stimulating the formation of cytochromes and ferroxins (Fd) which are vital for cell energy metabolism [42]. Furthermore, NPs have been reported to modulate the oxidation-reduction potential (ORP) values in bioprocessing [28]. Low ORP value enhances bioprocessing, by providing a suitable process environment for bioproduct formation such as bioethanol production [28].

Table 3 shows the comparison of modified Gompertz coefficients obtained in this study with previous studies. In the present study, maximum bioethanol production of 31.84 g/L obtained was 2.77-fold higher compared to the report by [58] and 1.5-fold higher than that achieved by [17]. Similarly, the maximum bioethanol production rate of 4.50 g/L/h was 18.75 times, 8.65 times and 1.03 times that achieved by [58] from oil palm frond juice, Rorke and Gueguim Kana [59] from sorghum leaves and Dodic et al. [19] from sugar beet raw juice, respectively. The highest P_m and $r_{p,m}$ observed in the present work coincided with NPs' presence. This further highlighted the potential of nanoparticles as efficient biocatalyst for starch-based lignocellulosic bioethanol production from ISF processes.

3.5. GC-MS volatile organic inhibitory profile

Fig. 5 shows the profile of obtained volatile organic inhibitory compounds (VOICs) under the various modes of nano inclusion during instantaneous saccharification and fermentation (NIISF) of potato peels. Major VOICs groups found were organic acids, alkanols and ketones. Lower fractions of aldehydes, benzenoids, sulphur-compounds, phenolic compounds, alkanals, amines and amides were also found. Frequently reported volatile inhibitory groups in bioprocessing include aliphatic acid, alcohol, aldehydes, benzenoids, phenolic compounds and ketones [28,30]. Table 4 represents the VOICs distribution observed under different NIISF designs. The largest VOICs part obtained was the aliphatic acids (69 %), with acetic acid making a large part (94 %), corresponding to a concentration of 16.07 g/L (Table 4). The formation of acetic acids has been reported in the pre-treatment of starch-based lignocellulosic biomass due to the release of acetate (acetyl groups of hemicelluloses) upon hemicellulose hydrolysis and fermentation of hexose sugars [35]. Acetic acid within the neutral cell environment dissociates and leads to a decline in pH which consequently impedes cellular activities. Therefore, before proceeding to fermentation, it is important that acid is neutralised,

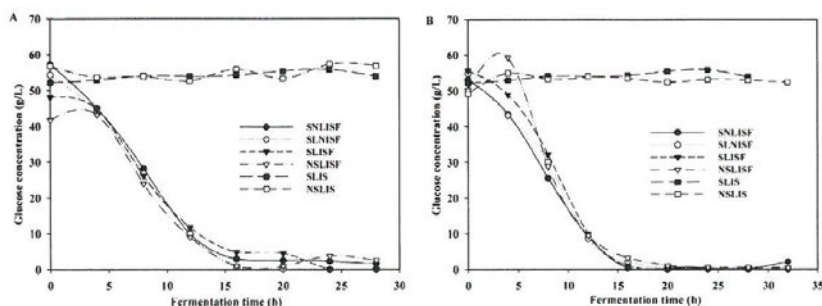


Fig. 7. Effect of inclusion of NPs on glucose utilisation during fermentation process; Fe₃O₄ NPs (A) NiO NPs (B).

Table 3
Modified Gompertz model process parameters for NIISF processes compared to previous studies.

| Feedstock | P_m (g/L) | $r_{p,m}$ (g/L/h) | t_i (h) | Reference |
|------------------------------------|-------------|-------------------|-----------|-------------------------------------------------------------------|
| Waste potato peels | 24.64 | 1.56 | 1.56 | This study (NiO NP Mode SNLISF) |
| Waste potato peels | 24.17 | 1.90 | 1.79 | This study (NiO NP Mode SLNISF) |
| Waste potato peels | 21.85 | 3.02 | 3.18 | This study (NiO NP Mode SLISF-control) |
| Waste potato peels | 31.84 | | | This study (NiO NP Mode NSLISF) |
| Waste potato peels | 23.24 | 4.50 | 3.47 | This study (Fe ₃ O ₄ NP Mode SNLISF) |
| Waste potato peels | 24.83 | 3.26 | 3.59 | This study (Fe ₃ O ₄ NP Mode SLNISF) |
| Waste potato peels | 22.35 | 2.30 | 2.86 | This study (Fe ₃ O ₄ NP Mode SLISF-control) |
| Waste potato peels | 23.59 | | | This study (Fe ₃ O ₄ NP Mode NSLISF) |
| Beet raw juice | 73.30 | 4.40 | 1.00 | [20] |
| Sweet sorghum Juice | 88.48 | 2.17 | 2.98 | [21] |
| Waste sorghum leaves | 17.15 | 0.52 | 6.31 | [49] |
| Oil palm frond juice (10–20 years) | 3.79 | 0.08 | 0.77 | [48] |
| Oil palm frond juice (3–4 years) | 11.50 | 0.24 | 0.12 | [48] |
| Corn cobs waste | 42.24 | 2.39 | 1.98 | [17] |
| Corn cobs waste | 32.09 | 3.25 | 2.68 | [17] |
| Corn cobs waste | 37.87 | 2.14 | 2.66 | [17] |
| Corn cobs waste | 27.62 | 2.33 | 3.12 | [17] |

while during fermentation metabolic shift away from acid formation will favour ethanol production [28]. Other aliphatic acids produced were, among others, propanoic acid (<0.17 g/L), isobutyric acid (<0.13 g/L), lactic acid (<0.20 g/L), formic acid (<0.15 g/L), sorbic acid (<0.20 g/L), hexanoic acid (<0.10 g/L) and levulinic acid (<0.16 g/L). Aliphatic acids such as levulinic acid and formic acid are typically formed upon the degradation of 5-hydroxymethylfurfural and furfural. It has been reported that the presence of these acids affects process performance by reduction of biomass formation and consequent inhibition of ethanol production. This occurs when less ATP is available for biomass formation resulting from intracellular build-up of anions within the fermentative microbes due to dissociation of these acids [30].

The next largest volatile fraction were the ketones, amounting to a maximum of 47 %, with 2,3-dihydro-3,5-dihydroxy-6-methyl-4H-Pyran-4-one being the most prominent, up to 93 % (4.65 g/L). Usually, 2,3-dihydro-3,5-dihydroxy-6-methyl-4H-Pyran-4-one is formed from the intermediate product of Maillard reaction of dextrose, maltose and hexoses such as glucose [60]. Other ketones formed include 1-hydroxy-2-propanone (<2.48 %), 2-Pyrrolidinone (<2.16 %), ethenone (<8.33 %) and 2,5-Dimethyl-4-hydroxy-3 (2H)-furanone (<16.98 %), corresponding to concentrations of 0.21, 0.07, 0.27 and 0.55 g/L respectively. Generally, the formation of ketones occurs due to pentose sugars such as xylose degradation. Similarly, ketones are degradation compounds formed during lignocellulosic biomass pre-treatment and subsequently ethanol fermentation. Like other volatile compounds they have inhibitory effect on enzymes and yeast activities [61].

Phenolics such as 2-methoxy phenol and 2-methoxy-4-vinylphenol observed in this study were formed due to partial degradation of lignin [1]. Phenolic compounds formation can also be due to degradation or protonation of carbohydrates such as D-glucose, D-xylose and L-arabinose [61]. These phenolic compounds impede enzymatic saccharification and can lead to the destruction of cellular electrochemical gradients [30].

Other groups found were aldehydes, amines, amides, lactones, sulphur-containing compounds and alkanal fractions (Table 4). Aldehydes, mainly furfural, 5-Methyl-furfural and 5-Hydroxymethylfurfural (HMF) were detected, which were products of xylose protonation that occurs at elevated pre-treatment conditions [61]. Inhibitory mechanisms of furfural and HMF in bioprocesses include furfuryl alcohol from yeast metabolism of furfural that inhibits anaerobic growth of *S. cerevisiae* and subsequently impedes ethanol production. Similarly, *S. cerevisiae* metabolises HMF to 5-hydroxymethyl furfuryl alcohol, resulting in a prolonged lag phase in microbial growth.

Furthermore, as shown in Fig. 8, aliphatic acids concentration (up to 69 %), was observed to be higher in the control experiment (Mode SLISF) compared to the NiO nano systems: Mode SNLISF (59 %), Mode SLNISF (62 %) and Mode NSLISF (55 %). Likewise, in the Fe₃O₄ nano systems (Mode SNLISF, 58 %; Mode SLNISF, 59 %; Mode NSLISF, 55 %), aliphatic acids concentrations were lower when compared to the control set-up (69 %). This suggests metabolic shift away from ethanol production in the control set-up towards organic acid formation, especially acetic acid formation (Table 4), while the opposite can be suggested for the nano-administered processes. The formation of less acetic acid is of benefit to ethanol production by *S. cerevisiae* [28]. This agrees with the observation in this study, where higher bioethanol concentrations were associated with the NIISF processes, which had lesser acetic acid concentrations when compared to the control experiment (ISF without nanoparticles). Cellular accumulation of acetic acid is detrimental to the cell and the overall fermentation process performance. Also, notable is the lowest acid concentration (55 %) obtained in Mode NSLISF of both nano systems, suggesting the stage of NPs inclusion was vital to its impact on the acid inhibitor formation. Furthermore, in this study, high ethanol yield (>0.93 g/g), lower concentration of aliphatic acids (<69 %), benzenoids (<7 %), lactones (<0.08 %), sulphur-containing compounds (<0.35 %), phenolics (<0.08 %) and alkanal (<0.08 %) were associated with nano supplementation. The distribution of metabolites formed during ethanol production is a crucial signal in assessing the efficiency of the process [43]. To maximise the yield of ethanol, the metabolic activities (by *S. cerevisiae*) must be directed away from these volatile organic inhibitory compounds. In this study, the shift in metabolic pathway away from volatile organic inhibitory compound formation, towards ethanol production can be ascribed to the presence of nanobiocatalyst [62]. Noticeable is the disparity in the concentrations of VOICs obtained in the nano-administered processes and the control experiments. For instance, lower concentrations of acetic acid (<7.837 g/L) and levulinic acid (<0.104 g/L) were observed in the nano system as against the control experiments (>16.073, >0.162 g/L, respectively), representing a 105 % and 56 % reduction in acetic and levulinic acid respectively in the nano system. Similarly ketone, such as 1-Hydroxy-2-propanone (<0.055 g/L), was in lesser concentration in comparison to the control experiments (0.063 g/L), also representing a 15 % reduction in 1-Hydroxy-2-propanone concentration in the nano system. Furthermore, the sulphur compound, dimethyl trisulfide was 7.9-fold less in the nano systems in comparison to the control set-up. These results further vindicate the inclusion of nanoparticles in the ISF process.

Table 4
Relative amounts (g/L) of volatile organic inhibitory compounds from ISF processes with nanoparticle (NiO and Fe₃O₄) inclusion.

| Compounds | NiO NPs ISF | | | | | | Fe ₃ O ₄ NPs ISF | | | | | |
|---------------------------------------------------|-------------|-------|--------|-------|-------|-------|----------------------------------------|-------|-------|-------|-------|-------|
| | 1 | 2 | 3 | 4 | 5 | 6 | 1 | 2 | 3 | 4 | 5 | 6 |
| Amines | | | | | | | | | | | | |
| 3-methyl-pyridine | 0.022 | 0.026 | 0 | 0.010 | 0.013 | 0 | 0 | 0 | 0 | 0 | 0 | 0 |
| Amides | | | | | | | | | | | | |
| Acetamide | 0 | 0 | 0 | 0 | 0 | 0.032 | 0 | 0 | 0 | 0 | 0 | 0 |
| Alcohols | | | | | | | | | | | | |
| 3-Methyl-1-butanol | 0.152 | 0.123 | 0.295 | 0.177 | 0.026 | 0 | 0 | 0.081 | 0.090 | 0.167 | 0 | 0 |
| Pentanol | 0 | 0 | 0 | 0 | 0 | 0 | 0.054 | 0 | 0 | 0 | 0 | 0 |
| 2,3-Butanediol | 0 | 0 | 0 | 0 | 0 | 0 | 0 | 0 | 0 | 0 | 0 | 0 |
| 2-Furanmethanol | 0.293 | 0.125 | 0.114 | 0.203 | 0.105 | 1.137 | 0.105 | 0.076 | 0.151 | 0.141 | 0.210 | 0.598 |
| 5-Methyl-2-furanmethanol | 0.059 | 0.020 | 0 | 0.062 | 0.071 | 0.226 | 0.059 | 0.033 | 0.049 | 0.046 | 0.044 | 0.192 |
| 3-(methylthio)-1-Propanol | 0.056 | 0.047 | 0.090 | 0.053 | 0.047 | 0 | 0.060 | 0.057 | 0.045 | 0.082 | 0 | 0 |
| 2-Methoxy phenol | 0.055 | 0 | 0.018 | 0 | 0.092 | 0 | 0 | 0 | 0 | 0 | 0 | 0 |
| Phenylethyl Alcohol | 0.602 | 0.422 | 0.375 | 0.582 | 0.292 | 0 | 0.374 | 0.498 | 0.353 | 0.667 | 0 | 0 |
| Benzyl alcohol | 0 | 0 | 0 | 0 | 0 | 0.297 | 0.026 | 0 | 0 | 0 | 0 | 0 |
| 4-hydroxy-benzenemethanol | 0 | 0 | 0 | 0 | 0 | 0.061 | 0 | 0 | 0 | 0 | 0.026 | 0.055 |
| Cinnamyl alcohol | 0.092 | 0 | 0.128 | 0.099 | 0.098 | 0 | 0 | 0 | 0 | 0 | 0 | 0.019 |
| 1-(2-Furyl)-2-ethanediol | 1.559 | 1.138 | 1.223 | 1.672 | 0.919 | 0.164 | 1.002 | 1.567 | 0.825 | 1.657 | 0.085 | 0.072 |
| Aldehydes | | | | | | | | | | | | |
| Furfural | 0.098 | 0.098 | 0.107 | 0.228 | 0 | 2.798 | 0.150 | 0.083 | 0.098 | 0.152 | 0.726 | 1.808 |
| 5-Methyl-furfural | 0.263 | 0.278 | 0 | 0.307 | 0.220 | 3.367 | 0.348 | 0.323 | 0.352 | 0.406 | 0.387 | 1.427 |
| 5-Hydroxymethylfurfural | 0 | 0 | 0 | 0 | 0.054 | 5.844 | 0 | 0 | 0 | 0 | 2.509 | 4.781 |
| Aliphatic acids | | | | | | | | | | | | |
| Acetic acid | 7.837 | 7.187 | 16.073 | 7.642 | 2.464 | 7.220 | 6.032 | 6.966 | 7.016 | 7.416 | 1.171 | 4.573 |
| Formic acid | 0 | 0 | 0.127 | 0.022 | 0 | 0 | 0 | 0 | 0.043 | 0 | 0.020 | 0.148 |
| Propanoic acid | 0.090 | 0.064 | 0.162 | 0.111 | 0.044 | 0 | 0 | 0.103 | 0 | 0.170 | 0.023 | 0.038 |
| Isobutyric acid | 0.077 | 0.064 | 0.133 | 0.071 | 0 | 0 | 0.111 | 0.083 | 0.053 | 0.075 | 0.031 | 0.048 |
| 4-Hydroxybutanoic acid | 0 | 0 | 0 | 0 | 0 | 0 | 0.084 | 0.174 | 0.084 | 0 | 0.026 | 0.077 |
| Butanoic acid | 0.055 | 0.046 | 0 | 0.091 | 0.320 | 0 | 0 | 0 | 0 | 0.083 | 0.026 | 0 |
| Isovaleric acid | 0 | 0 | 0 | 0 | 0 | 0 | 0.061 | 0 | 0 | 0 | 0 | 0 |
| 2-Methylhexanoic acid | 0.064 | 0.036 | 0.165 | 0.095 | 0.059 | 0 | 0 | 0.067 | 0.049 | 0.076 | 0 | 0 |
| Valeric acid | 0 | 0 | 0 | 0 | 0 | 0 | 0 | 0 | 0.070 | 0 | 0 | 0 |
| Hexanoic acid | 0.059 | 0.057 | 0.086 | 0.090 | 0.051 | 0 | 0.071 | 0.076 | 0.056 | 0.104 | 0.053 | 0.098 |
| Larixinic acid | 0.063 | 0.062 | 0.198 | 0.082 | 0.059 | 0.084 | 0.075 | 0.068 | 0.075 | 0.090 | 0.013 | 0.065 |
| Sorbic acid | 0.116 | 0.151 | 0 | 0.171 | 0.046 | 0 | 0.070 | 0.123 | 0.054 | 0.202 | 0.036 | 0.198 |
| Octanoic acid | 0 | 0 | 0 | 0 | 0 | 0 | 0 | 0 | 0 | 0 | 0.083 | 0.052 |
| Levulinic acid | 0.078 | 0.097 | 0.162 | 0 | 0.031 | 0.081 | 0.076 | 0.095 | 0.100 | 0.104 | 0.042 | 0.043 |
| Benzenoids | | | | | | | | | | | | |
| Benzeneacetaldehyde | 0.461 | 0.371 | 1.283 | 0.733 | 0.344 | 0.815 | 0.587 | 0.446 | 0.389 | 0.581 | 0.030 | 0.393 |
| Benzoic acid | 0 | 0.155 | 0.497 | 0 | 0 | 0 | 0 | 0.175 | 0.119 | 0.185 | 0.061 | 0.206 |
| Ketones | | | | | | | | | | | | |
| Acetoin | 0 | 0 | 0 | 0 | 0.187 | 0 | 0 | 0 | 0 | 0 | 0 | 0 |
| 1-Hydroxy-2-propanone | 0.034 | 0.037 | 0.043 | 0.028 | 0.051 | 0.213 | 0.055 | 0.048 | 0.063 | 0.027 | 0.076 | 0.133 |
| Ethenone, 1-(2-furanyl) | 0 | 0 | 0.485 | 0.087 | 0.033 | 0.138 | 0 | 0 | 0 | 0.065 | 0.035 | 0.186 |
| 2-Pyrrolidinone | 0.051 | 0.039 | 0.071 | 0.058 | 0.022 | 0 | 0.041 | 0.045 | 0.040 | 0.049 | 0 | 0 |
| Ethenone | 0.198 | 0.140 | 0.268 | 0.255 | 0.130 | 0.158 | 0.136 | 0.173 | 0.145 | 0.207 | 0.054 | 0.061 |
| Furyl hydroxymethyl ketone | 0 | 0 | 0 | 0 | 0 | 0.116 | 0 | 0 | 0 | 0 | 0.019 | 0.051 |
| 2,5-Dimethyl-4-hydroxy-3(2 H)-furanone | 0.242 | 0.260 | 0.555 | 0.339 | 0.140 | 0.247 | 0.247 | 0.223 | 0.200 | 0.315 | 0.105 | 0.144 |
| 2,3-dihydro-3,5-dihydroxy-6-methyl-4H-Pyran-4-one | 1.595 | 1.271 | 1.815 | 1.956 | 1.538 | 7.601 | 1.391 | 1.562 | 1.397 | 2.034 | 4.649 | 6.170 |
| 4-cyclohexene-1,3-dione | 0 | 0 | 0 | 0 | 0 | 0 | 0 | 0 | 0 | 0 | 0.082 | 0.169 |
| Lactones | | | | | | | | | | | | |
| 5-Methyl-2(5 H)-Furanone | 0 | 0 | 0 | 0 | 0 | 0 | 0 | 0 | 0 | 0 | 0 | 0.026 |
| 2(5 H)-Furanone | 0 | 0 | 0 | 0 | 0 | 0 | 0 | 0.008 | 0.010 | 0 | 0.014 | 0.038 |
| Sulphur compounds | | | | | | | | | | | | |
| Dimethyl disulphide | 0 | 0 | 0 | 0 | 0 | 0 | 0 | 0 | 0 | 0 | 0 | 0.031 |
| Dimethyl trisulfide | 0.009 | 0.007 | 0.087 | 0.011 | 0 | 0 | 0 | 0.007 | 0.009 | 0.011 | 0 | 0 |
| Phenolic compounds | | | | | | | | | | | | |
| 2-Methoxy phenol | 0.055 | 0 | 0.018 | 0 | 0.092 | 0 | 0 | 0 | 0 | 0 | 0 | 0 |
| 2-Methoxy-4-vinylphenol | 0.084 | 0.073 | 0.172 | 0.100 | 0.017 | 0.180 | 0.062 | 0.076 | 0.063 | 0.139 | 0.019 | 0.110 |
| Alkanal | | | | | | | | | | | | |
| Methional | 0 | 0 | 0 | 0 | 0 | 0.129 | 0 | 0 | 0.009 | 0.011 | 0 | 0 |

1- SNLISF, 2-SLNISF, 3-SLISF-control, 4-NSLISF, 5-SLIS and 6-NSLIS.

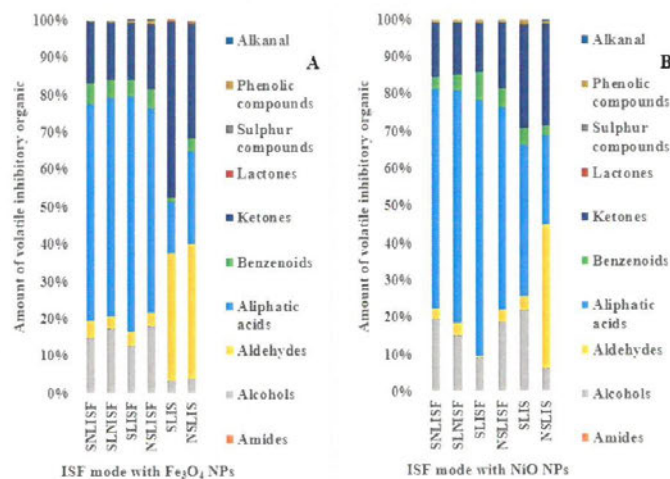


Fig. 8. Profile of volatile organic inhibitory compounds in different modes of ISF processes in the presence of nanocatalysts (A) Fe_3O_4 NPs and (B) NiO NPs.

3.6. Effects of stage of nanoparticle inclusion in the ISF inhibitor compounds profile

There were differences in the concentrations of bioethanol and volatile organic compounds observed in the NIISF processes resulting from the different stages of nanoparticle inclusion in the ISF processes. Inclusion of NiO NPs at the pre-treatment stage (Mode NSLISF), suggests an improved alcoholic metabolic pathway resulting in the highest bioethanol concentration of 36.04 g/L and considerable reduction in acetic acid formation (27%). The results obtained with NPs administered at the liquefaction, saccharification and fermentation stages (Modes SNLISF and SLNISF) indicate the enzymatic and yeast metabolic activities were shifted away from sulphur-containing and phenolic compound formation. Also, the acetic acid was reduced by administering NPs at these stages, but to a lesser extent (10%). The impact of nanoparticles on volatile inhibitory compound formation may be ascribed to the protonation degradation of potato peel biomass during the physicochemical pre-treatment process and the enzymatic activities during the NIISF processes [51]. Protonation site initiating substrate degradation determines the mechanism and degradation pathway, consequently, the degradation products [61]. Similarly, the degradation products depend on operating conditions and could be regulated by controlling the process parameters. In addition, the formation of organic metabolites also occasion by the amounts of enzymes and co-factors such as nickel and iron present, thus, from enzyme regulatory mechanisms, and the need to maintain a relatively steady intracellular pH [63]. Inclusion of metallic supplement in bioprocessing performs various functions such as enzyme activator, enzymes stabilisers, enzymes cofactor, growth factor and chelating of other compounds hence, reducing their toxicity [57]. Moreover, volatile organic inhibitory compounds (VOICs) released due to substrate metabolism have chelating potentials and capacities occasioned by their functional groups [64]. These chelating compounds such as sulphhydryls, amides, carboxylates, hydroxyls, phenols and amines can form ligands and complexes with Fe and Ni metals. The affinity for complexation with VOICs and subsequent bioavailability of these metals are not

the same for various metals; and this is also dependent on operating conditions [27]. Consequently, the VOICs formed, and their chelating activities in bioprocesses play vital roles in metal ions' availability to microorganisms, metabolic activities and ultimately process performance.

4. Conclusions

The impact of inclusion stage of NiO and Fe_3O_4 nanoparticles on bioethanol production and volatile inhibitory organic compound formation in the instantaneous saccharification and fermentation (ISF) of potato peels is elucidated in detail. Addition of NiO NPs at the pre-treatment stage (NSLISF mode) resulted in the production of optimal concentration of bioethanol (36.04 g/L). Likewise, inclusion of Fe_3O_4 NPs during pre-treatment (NSLISCF) and liquefaction (SNLISF) stages lead to the best bioethanol concentration values of 23.99 and 23.75 g/L respectively. Higher ethanol yield (0.93 g/g) with inclusion of Fe_3O_4 NPs during liquefaction and productivity (2.25 g/L/h) with inclusion of NiO NPs during pre-treatment were obtained with the NIISF processes. Moreover, substantial reduction in inhibitory organic compounds was also achieved with the NIISF (nanoparticle inclusion) strategy. Nanoparticle band gap energy property had a pronounced effect on bioethanol bioprocessing. These nano additives are effective biocatalysts; their individual inclusion had significant impact on the biomass conversion processes (pre-treatment, liquefaction, saccharification and fermentation). Hence, NiO and Fe_3O_4 nanoparticles could be an efficient biocatalyst for the industrial bioethanol production from potato peels.

Author contributions

The experiment conceptualization was conceived and designed by Isaac A. Sanusi and Gueguim EB. Kana; experimental investigation and data curation were conducted by Isaac A. Sanusi, while, Terence N. Suinyuy conducted investigation on volatile inhibitory compounds. Isaac A. Sanusi wrote the manuscript for publication under the supervision of Gueguim EB. Kana.

Declaration of Competing Interest

The authors report no declarations of interest.

References

- L.J. Jönsson, C. Martin, Pre-treatment of lignocellulose: formation of inhibitory by-products and strategies for minimizing their effects, *Bioresour. Technol.* 199 (2016) 103–112, doi:<http://dx.doi.org/10.1016/j.biortech.2015.10.009>.
- U. Talasila, R.R. Vechalapu, Optimization of medium constituents for the production of bioethanol from cashew apple juice using doehlert experimental design, *Int. J. Fruit Sci.* 15 (2015) 161–172, doi:<http://dx.doi.org/10.1080/15538362.2014.989134>.
- S. Shanavas, G. Padmaja, S.N. Moorthy, M.S. Sajeev, J.T. Sheriff, Process optimization for bioethanol production from cassava starch using novel eco-friendly enzymes, *Biomass Bioenergy* 35 (2011) 901–909, doi:<http://dx.doi.org/10.1016/j.biombioe.2010.11.004>.
- M. Puri, R.E. Abraham, C.J. Barrow, Biofuel production: prospects, challenges and feedstock in Australia, *Renew. Sustain. Energy Rev.* 16 (2012) 6022–6031, doi:<http://dx.doi.org/10.1016/j.rser.2012.06.025>.
- C.N. Ncobela, A.T. Kanengoni, V.A. Hlatini, R.S. Thomas, M. Chimonyo, A review of the utility of potato by-products as a feed resource for smaller pig production, *Anim. Feed Sci. Technol.* 227 (2017) 107–117, doi:<http://dx.doi.org/10.1016/j.anifeeds.2017.02.008>.
- A.F.S. Maldonado, E. Mudge, M.G. Gänzle, A. Schieber, Extraction and fractionation of phenolic acids and glycoalkaloids from potato peels using acidified water/ethanol-based solvents, *Food Res. Int.* 65 (2014) 27–34, doi:<http://dx.doi.org/10.1016/j.foodres.2014.06.018>.
- M. Kim, J. Kim, Comparison through a LCA evaluation analysis of food waste disposal options from the perspective of global warming and resource recovery, *Sci. Total Environ.* 408 (2010) 3998–4006, doi:<http://dx.doi.org/10.1016/j.scitotenv.2010.04.049>.
- D. Arapoglou, T.H. Vazakas, A. Vlyssides, C. Isralides, Ethanol production from potato peel waste (PPW), *Waste Manag.* 30 (2010) 1898–1902, doi:<http://dx.doi.org/10.1016/j.wasman.2010.04.017>.
- M. Lech, Optimisation of protein-free waste whey supplementation used for the industrial microbiological production of lactic acid, *Biochem. Eng. J.* 157 (2020) 107531, doi:<http://dx.doi.org/10.1016/j.bej.2020.107531>.
- A. Kristiani, H. Abimanyu, A.H.S. Sudiaryanto, F. Aulia, Effect of pretreatment process by using diluted acid to characteristic of oil palm's frond, *Energy Procedia* 32 (2013) 183–189, doi:<http://dx.doi.org/10.1016/j.egypro.2013.05.024>.
- J. Mäder, H. Rawel, L.W. Kroh, Composition of phenolic compounds and glycoalkaloids α -solanine and α -chaconine during commercial potato processing, *J. Agric. Food Chem.* 57 (2009) 6292–6297, doi:<http://dx.doi.org/10.1021/jf901066k>.
- M.S. Hashem, M.I. Darwish, Production of bioethanol and associated by-products from potato starch residue stream by *Saccharomyces cerevisiae*, *Biomass Bioenergy* 34 (2010) 953–959, doi:<http://dx.doi.org/10.1016/j.biombioe.2010.02.003>.
- G. Izmirlioglu, A. Demirci, Ethanol production from waste potato mash by using *Saccharomyces cerevisiae*, *Appl. Sci.* 2 (2012) 738–753, doi:<http://dx.doi.org/10.3390/app2040738>.
- B.J. Khowla, M. Sameh, G. Imen, F. Donyes, G. Dhouha, E.G. Raoudha, N.-E. Ouméma, Potato peel as feedstock for bioethanol production: a comparison of acidic and enzymatic hydrolysis, *Ind. Crops Prod.* 52 (2014) 144–149, doi:<http://dx.doi.org/10.1016/j.indcrop.2013.10.025>.
- M. Fadel, Alcohol production from potato industry starchy waste, *Egypt J. Microbiol.* 35 (2000) 273–287, ISSN: 0022-2704.
- Y. Sewsynker-Sukai, E.B. Gueguim Kana, Simultaneous saccharification and bioethanol production from corn cobs: process optimization and kinetic studies, *Bioresour. Technol.* 262 (2011) 32–41, doi:<http://dx.doi.org/10.1016/j.biortech.2010.04.056>.
- P. Ariyaroenwong, P. Laopaiboon, A. Salakkam, P. Srinophakun, L. Laopaiboon, Kinetic models for batch and continuous ethanol fermentation from sweet sorghum juice by yeast immobilized on sweet sorghum stalks, *J. Taiwan Inst. Chem. Eng.* 66 (2016) 210–216, doi:<http://dx.doi.org/10.1016/j.jtice.2016.06.023>.
- K. Doriya, D.S. Kumar, Solid state fermentation of mixed substrate for L-asparaginase production using tray and in-house designed rotary bioreactor, *Biochem. Eng. J.* 138 (2018) 188–196, doi:<http://dx.doi.org/10.1016/j.bej.2018.07.024>.
- J.M. Dodic, D.G. Vucurovic, S.N. Dodic, J.A. Grahovac, S.D. Popov, N.M. Nedeljkovic, Kinetic modelling of batch ethanol production from sugar beet raw juice, *Appl. Energy* 99 (2012) 192–197, doi:<http://dx.doi.org/10.1016/j.apenergy.2012.05.016>.
- N. Phukoetphim, A. Salakkam, P. Laopaiboon, L. Laopaiboon, Kinetic models for batch ethanol production from sweet sorghum juice under normal and high gravity fermentations: logistic and modified Gompertz models, *J. Biotech* 243 (2017) 69–75, doi:<http://dx.doi.org/10.1016/j.jbiotec.2016.12.012>.
- E. Abdelsalam, M. Samer, Y.A. Attia, M.A. Abdel-Hadi, H.E. Hassan, Y. Badr, Comparison of nanoparticles effects on biogas and methane production from anaerobic digestion of cattle dung slurry, *Renew. Energy* 87 (2016) 592–598, doi:<http://dx.doi.org/10.1016/j.renene.2015.10.053>.
- P.T. Sekoai, C.N.M. Ouma, S.P. du Preez, P. Modisha, N. Engelbrecht, D.G. Bessarabov, A. Ghimire, Application of nanoparticles in biofuels: an overview, *Fuel* 237 (2019) 380–397, doi:<http://dx.doi.org/10.1016/j.fuel.2018.10.030>.
- E. Cherian, M. Dharmendrakumar, G. Baskar, Immobilization of cellulase onto MnO₂ nanoparticles for bioethanol production by enhanced hydrolysis of agricultural waste, *Chin. J. Catal.* 35 (2015) 1223–1229, doi:[http://dx.doi.org/10.1016/S1872-2067\(15\)60906-8](http://dx.doi.org/10.1016/S1872-2067(15)60906-8).
- A.I. Sanusi, F.D. Faloye, E.B. Gueguim Kana, Impact of various metallic oxide nanoparticles on ethanol production by *Saccharomyces cerevisiae* BY4743: screening, kinetic study and validation on potato waste, *Catal. Lett.* 149 (7) (2019) 2015–2031, doi:<http://dx.doi.org/10.1007/s10562-019-02796-6>.
- D.K. Ban, S. Paul, Zinc oxide nanoparticles modulates the production of β -Glucosidase and protects its functional state under alcoholic condition in *Saccharomyces cerevisiae*, *Appl. Biochem. Biotechnol.* 173 (2014) 155–166, doi:<http://dx.doi.org/10.1007/s12010-014-0825-2>.
- Y. Kim, H. Lee, Use of magnetic nanoparticles to enhance bioethanol production in syngas fermentation, *Bioresour. Technol.* 204 (2016) 139–144, doi:<http://dx.doi.org/10.1016/j.biortech.2016.01.001>.
- P.M. Thanh, B. Ketheesan, Z. Yan, D. Stuckey, Trace metal speciation and bioavailability in anaerobic digestion: a review, *Biotechnol. Adv.* 34 (2016) 122–136, doi:<http://dx.doi.org/10.1016/j.biotechadv.2015.12.006>.
- H. Han, M. Cui, L. Wei, H. Yang, J. Shen, Enhancement effect of hematite nanoparticles on fermentative hydrogen production, *Bioresour. Technol.* 102 (2011) 7903–7909, doi:<http://dx.doi.org/10.1016/j.biortech.2011.05.089>.
- A. Cavka, L.J. Jönsson, Detoxification of lignocellulosic hydrolysates using sodium borohydride, *Bioresour. Technol.* 136 (2013) 368–376, doi:<http://dx.doi.org/10.1016/j.biortech.2013.03.014>.
- D.C.S. Rorke, T.N. Suinyuy, E.B. Gueguim Kana, Microwave-assisted chemical pre-treatment of waste sorghum leaves: process optimization and development of an intelligent model for determination of volatile compound fractions, *Bioresour. Technol.* 224 (2017) 590–600, doi:<http://dx.doi.org/10.1016/j.biortech.2016.10.048>.
- N. Cheng, K. Koda, Y. Tamai, Y. Yamamoto, T.E. Takasuka, Y. Uraki, Optimization of simultaneous saccharification and fermentation conditions with amphiphatic lignin derivatives for concentrated bioethanol production, *Bioresour. Technol.* 232 (2017) 126–132, doi:<http://dx.doi.org/10.1016/j.biortech.2017.02.018>.
- Y. Kim, S.E. Park, H. Lee, J.Y. Yun, Enhancement of bioethanol production in syngas fermentation with *Clostridium ljungdahlii* using nanoparticles, *Bioresour. Technol.* 159 (2014) 446–450, doi:<http://dx.doi.org/10.1016/j.biortech.2014.03.046>.
- A.I. Sanusi, T.N. Suinyuy, A. Lateef, E.A. Gueguim Kana, Effect of nickel oxide nanoparticles on bioethanol production: process optimization, kinetic and metabolic studies, *Process Biochem.* 92 (2020) 386–400, doi:<http://dx.doi.org/10.1016/j.procbio.2020.01.029>.
- J.B. Sluiter, R.O. Ruiz, C.J. Scarlata, A.D. Sluiter, D.W. Templeton, Compositional analysis of lignocellulosic feedstocks. 1. Review and description of methods, *J. Agric. Food Chem.* 58 (16) (2010) 9043–9053, doi:<http://dx.doi.org/10.1021/jf1008023>.
- G.S. Aruwajoye, F.D. Faloye, E.B. Gueguim Kana, Soaking assisted thermal pre-treatment of cassava peels wastes for fermentable sugar production: process modelling and optimization, *Energy Convers. Manage.* 150 (2017), doi:<http://dx.doi.org/10.1016/j.jhydene.2014.01.163> 558–566.
- G. Prochazkova, I. Safarik, T. Branyik, Harvesting microalgae with microwave synthesized magnetic microparticles, *Bioresour. Technol.* 130 (2013) 472–477, doi:<http://dx.doi.org/10.1016/j.biortech.2012.12.060>.
- Ritu, Synthesis and characterization of chromium oxide nanoparticles, *IOSR J. Appl. Chem. (IOSR-JAC)* 8 (3) (2015) 05–11, doi:<http://dx.doi.org/10.9790/5736-08310511> Ver. 1.
- D.K. Vizhi, N. Supraja, A. Devipriya, N.V.K.V.P. Tollamadugu, R. Babujanathanam, Evaluation of antibacterial activity and cytotoxic effects of green AgNPs against breast cancer cells (MCF 7), *Adv. Nano Res.* 4 (2) (2016) 129–143.
- M. El-Kemary, N. Nagy, I. El-Mehasseb, Nickel oxide nanoparticles: synthesis and spectral studies of interactions with glucose, *Mater. Sci. Semicond. Process.* 16 (2013) 1747–1752, doi:<http://dx.doi.org/10.1016/j.mssp.2013.05.018>.
- B. Sawicki, E. Tomaszewicz, M. Piatkowska, T. Gróń, H. Duda, K. Górný, Correlation between the band-gap energy and the electrical conductivity in MPr₂W₁₀ tungstates (Where m = Cd, Co, Mn), *Acta Phys. Pol. A* 129 (No. 1-A) (2016), doi:<http://dx.doi.org/10.12693/APhysPolA.129.A-94>.
- A. Mondal, A. Mondal, D. Mukherjee, Room-temperature synthesis of cobalt nanoparticles and their use as catalysts for Methylene Blue and Rhodamine-B dye degradation, *Adv. Nano Res.* 3 (2) (2015) 67–79, doi:<http://dx.doi.org/10.12989/anr.2015.3.2.067>.
- Y.Y. Choong, I. Norli, A.Z. Abdullah, M.F. Yhaya, Impacts of trace element supplementation on the performance of anaerobic digestion process: a critical review, *Bioresour. Technol.* 209 (2016) 369–379, doi:<http://dx.doi.org/10.1016/j.biortech.2016.03.028>.
- Y. Zhang, J. Shen, Enhancement effect of gold nanoparticles on biohydrogen production from artificial wastewater, *Int. J. Hydrogen Energy* 32 (1) (2007) 17–23, doi:<http://dx.doi.org/10.1016/j.ijhydene.2006.06.004>.
- S.K. Lower, M.F. Hochella Jr, T.J. Beveridge, Bacterial recognition of mineral surfaces: nanoscale interactions between *Shewanella* and α -FeOOH, *Science* 292 (5520) (2001) 1360–1363, doi:<http://dx.doi.org/10.1126/science.1059567>.

- [45] A. Verma, F. Stellacci, Effect of surface properties on nanoparticle-cell interactions, *Small* 6 (1) (2010) 2–21, doi:<http://dx.doi.org/10.1002/sml.200901158>.
- [46] S. Faramarzi, Y. Anzabi, H. Fararizadeh-Malmiri, Selenium supplementation during fermentation with sugar beet molasses and *saccharomyces cerevisiae* to increase bioethanol production, *Green Process. Synth.* 8 (1) (2019) 622–628, doi:<http://dx.doi.org/10.1515/gps-2019-0032>.
- [47] G. Izmirlioglu, A. Demirci, Improved simultaneous saccharification and fermentation of bioethanol from industrial potato waste with co-cultures of *Aspergillus niger* and *Saccharomyces cerevisiae* by medium optimization, *Fuel* 185 (2016) 684–691, doi:<http://dx.doi.org/10.1016/j.fuel.2016.08.035>.
- [48] P. Moodley, E.B. Gueguim Kana, Bioethanol production from sugarcane leaf waste: effect of various optimized pre-treatments and fermentation conditions on process kinetics, *Biotechnol. Rep.* 24 (2019) 1–8, doi:<http://dx.doi.org/10.1016/j.btre.2019.e00329>.
- [49] S. Kodhaiyoli, S.R. Mohanraj, M. Engasamy, V. Pugalenthi, Phytofabrication of bimetallic Co-Ni nanoparticles using *Boerhavia diffusa* leaf extract: analysis of phytochemicals and application for simultaneous production of biohydrogen and bioethanol, *Mater. Res. Express* 6 (9) (2019), <https://iopscience.iop.org/article/10.1088/2053-1591/ab2ea8/meta>.
- [50] A. Kumar, S. Singh, R. Tiwar, R. Goel, L. Nain, Immobilization of indigenous holocellulase on iron oxide (Fe₂O₃) nanoparticles enhanced hydrolysis of alkali pre-treated paddy straw, *Int. J. Biol. Macromol.* 96 (2017) 538–549.
- [51] N. Dutta, M.K. Saha, Nanoparticle-induced enzyme pre-treatment method for increased glucose production from lignocellulosic biomass under cold conditions, *J. Sci. Food Agric.* 99 (2) (2019) 767–780, doi:<http://dx.doi.org/10.1002/jsfa.9245>.
- [52] M. Rai, A.P. Ingle, R. Pandit, J.K. Biswas Paralikar, S.S. da Silva, Emerging role of nanobiocatalysts in hydrolysis of lignocellulosic biomass leading to sustainable bioethanol production, *Catal. Rev.-Sci. Eng.* 61 (1) (2019) 1–26, doi:<http://dx.doi.org/10.1080/01614940.2018.1479503>.
- [53] Z.C. Gou, N.L. Ma, W.Q. Zhang, Z.P. Lei, Y.J. Su, C.Y. Sun, G.Y. Wang, H. Chen, S.T. Zhang, G. Chen, Y. Sun, Innovative hydrolysis of corn stover bio waste by modified magnetite laccase immobilized nanoparticles, *Environ. Res.* 188 (2020).
- [54] S. Chamoli, E. Yadav, J.K. Saini, A.K. Verma, N.K. Navani, P. Kumar, Magnetically recyclable catalytic nanoparticles grafted with *Bacillus subtilis* beta-glucosidase for efficient cellobiose hydrolysis, *Int. J. Biol. Macromol.* 164 (2020) 1729–1736, doi:<http://dx.doi.org/10.1016/j.ijbiomac.2020.08.102>.
- [55] A.I. Sanusi, T.N. Suinyuy, A. Lateef, E.B. Gueguim Kana, Effect of nickel oxide nanoparticles on bioethanol production: process optimization, kinetic and metabolic studies, *Process. Biochem.* 92 (2020) 386–400, doi:<http://dx.doi.org/10.1016/j.procbio.2020.01.029>.
- [56] J.L. Linville, M. Rodriguez Jr, J.R. Mielenz, C.D. Cox, Kinetic modeling of batch fermentation for *Populus* hydrolysate tolerant mutant and wild type strains of *Clostridium thermocellum*, *Bioresour. Technol.* 147 (2013) 605–613, doi:<http://dx.doi.org/10.1016/j.biortech.2013.08.086>.
- [57] A. Schattauer, E. Abdoun, P. Weiland, M. Plösch, M. Heiermann, Abundance of trace elements in demonstration biogas plants, *Biosyst. Eng.* 108 (2011) 57–65, doi:<http://dx.doi.org/10.1016/j.biosystemseng.2010.10.010>.
- [58] T. Srimachai, K. Nuithitikul, S. O-thong, P. Kongjan, K. Panpong, Optimization and kinetic modeling of ethanol production from oil palm frond juice in batch fermentation, *Energy Procedia* 79 (2015) 111–118, doi:<http://dx.doi.org/10.1016/j.egypro.2015.11.490>.
- [59] D.C.S. Korke, E.B. Gueguim Kana, Kinetics of bioethanol production from waste sorghum leaves using *Saccharomyces cerevisiae* BY4743, *Fermentation* 3 (2017) 19, doi:<http://dx.doi.org/10.3390/fermentation3020019>.
- [60] Y.P. Teoh, M.M. Don, S. Ujang, Media and antifungal activity, *BioResources* 6 (3) (2011) 2719–2731.
- [61] H. Rasmussen, H.R. Sørensen, A.S. Meyer, Formation of degradation compounds from lignocellulosic biomass in the biorefinery: sugar reaction mechanisms, *Carbohydr. Res.* 385 (2014) 45–57, doi:<http://dx.doi.org/10.1016/j.carres.2013.08.029>.
- [62] P. Wimonsong, R. Nitisoravut, Comparison of different catalysts for fermentative hydrogen production, *J. Clean Energy Technol.* 3 (2) (2015) 128–131, doi:<http://dx.doi.org/10.7763/JOCET.2015.V3.I2.181>.
- [63] K.G. Mackenzie, M.C. Kenny, Non-volatile organic acid and pH changes during the fermentation of distiller's wort, *J. Inst. Brew.* (1985) 71, doi:<http://dx.doi.org/10.1002/j.2050-0416.1985.tb02040.x>.
- [64] W.-C. Kuo, G.F. Parkin, Characterization of soluble microbial products from anaerobic treatment by molecular weight distribution and nickel-chelating properties, *Water Res.* 30 (1996) 915–922, doi:[http://dx.doi.org/10.1016/0043-1354\(95\)00201-4](http://dx.doi.org/10.1016/0043-1354(95)00201-4).

CHAPTER 5

Effect of nickel oxide nanoparticles on bioethanol production: Process optimization, kinetic and metabolic studies

This chapter has been published with the title: Effect of nickel oxide nanoparticles on bioethanol production: Process optimization, kinetic and metabolic studies in *Process Biochemistry* (92 (2020) 386–400) doi.org/10.1016/j.procbio.2020.01.029. The published paper is presented in the following pages.



Effect of nickel oxide nanoparticles on bioethanol production: Process optimization, kinetic and metabolic studies



Isaac A. Sanusi^a, Terence N. Suinyuy^a, Agbaje Lateef^b, Gueguim E.B. Kana^{a,*}

^a School of Life Sciences, University of KwaZulu-Natal, Private Bag X01, Scottsville 3209, Pietermaritzburg, South Africa

^b Laboratory of Industrial Microbiology and Nanobiotechnology, Department of Pure and Applied Biology, Ladoko Akintola University of Technology, PMB 4000, Ogbomoso, Nigeria

ARTICLE INFO

Keywords:
Nickel oxide nanoparticles
Bioprocess modelling
Volatile compound profile
Bioethanol production

ABSTRACT

The present study optimized ethanol yield using nickel oxide (NiO) nanoparticles (NPs) as a biocatalyst. Additionally, *Saccharomyces cerevisiae* BY4743 cell growth and the bioethanol production kinetics were assessed. The Response Surface Methodology (RSM) model showed a coefficient of determination (R^2) value of 0.93. The optimized process gave a biomass concentration and ethanol yield of 2.04 g/L and 0.26 g/g (1.03 and 1.19-fold increment compared to the control experiment), respectively. The process kinetic data showed that the inclusion of NiO NPs improved the affinity of *S. cerevisiae* BY4743 to glucose consumption, carbohydrate and protein accumulation. A significant reduction in volatile fatty acid (VFA) was observed in the presence of NiO NPs. The application of nano biocatalyst in simultaneous saccharification and fermentation of potato peel waste, meaningfully enhanced bioethanol production (> 65 %). The study provided major insights into the use of NiO NPs to enhance the bioprocess of ethanol production.

1. Introduction

The global energy consumption has increased tremendously over the last century and there are environmental concerns associated with the use of fossil fuels. There is a need for alternative sources of energy such as bioethanol, biohydrogen, biomethane and biodiesel which could replace the depleting fossil fuels and alleviate their environmental impacts [1]. Bioethanol has gained global attention as a result of its renewability and environmental benefits [2]. Nevertheless, many of the current bioethanol production technologies are still faced with several challenges. These include the necessity for an enhanced bioactive and stress tolerant ethanol-producing microorganism and an economical fermentation process that will lead to high ethanol yield, enhanced substrate utilisation and shorter fermentation time [3]. A number of studies have reported enhanced bioactivity and metabolic activities of ethanol-producing yeasts under appropriate environmental and nutritional conditions [4,5]. However, higher conversion efficiency of substrates coupled with satisfactory ethanol yields has remained a challenge. Ethanol fermentation performances are influenced by process conditions such as medium constituents, pH, temperature, and substrate concentration [5]. The development of suitable medium constituent and determination of optimum process conditions are crucial steps in obtaining high ethanol yield and productivity [6].

Additionally, enhancing the bioactivity of ethanol-producing yeast as well as reduction in the formation of inhibitory compounds such as acetic acid, ketones, phenolic, alcohols are desirable to achieve high ethanol yield. The significance of trace metals in bioprocess medium formulation for enhanced metabolism is still vastly underestimated [7]. Their availability as micro-nutrients plays a very significant role on the metabolic performance of microorganisms. Although, trace metals is required at very low concentration, their deficiency can impact on the production of enzymes, coenzymes and growth factors required for metabolism and ultimately reduce their metabolic activity [8]. For instance, trace metal deficiency in bioprocesses results in increased build-up of inhibitory volatile fatty acids (VFAs) and subsequently poor fermentation performance [9]. A typical case was reported by Schmidt et al. [9], where precipitous accumulation of VFA compounds in a Fe/Ni-deficient bioprocess was observed.

Metallic nanoparticles (NPs) in culture nutrient formulation have recently been identified as a potential catalytic technique for improving the bioactivity of ethanol-producing microorganisms and fermentation productivity [10,11]. Their ability to alter the rate of reaction coupled with biotechnological potentials have led to their increased application in many fields of research such as biotechnology [12,13,14]. This is due to their exceptional properties (chemical stability, catalytic properties, surface-to-volume ratio, interaction, magnetic separation, and

* Corresponding author.

E-mail address: kanag@ukzn.ac.za (G.E.B. Kana).

<https://doi.org/10.1016/j.procbio.2020.01.029>

Received 23 June 2019; Received in revised form 19 January 2020; Accepted 24 January 2020

Available online 25 January 2020

1359-5113/ © 2020 Elsevier Ltd. All rights reserved.

specificity) which can be implemented in biotechnological processes [15]. Their catalytic properties generally depend on their size, shape, stabilizing agents and operating conditions [15,16].

Data on the use of catalytic nanoparticles for enhancing biological processes such as biomethane, biogas and biohydrogen production currently exist [17,18]. The study by Zhao et al. [18] observed a 1.7-fold increase in biohydrogen yield when silver NPs inclusion in the range of 0–200 nmol/L was implemented. Furthermore, this study reported a higher yield in biohydrogen production when the initial pH was 8.5 compared to pH value of 8.1 (68 % increase). Similarly, Zhang and Shen [19] recorded a 57 % improvement in biohydrogen production using 5 nm particle size gold nanoparticles compared to 20 nm particle size (43 %). Nevertheless, there is a significant knowledge gap on the effect of nanoparticles nutrient supplementation for enhancing bioethanol production using *Saccharomyces cerevisiae*.

Generally, high ethanol yields following fermentation are affected by process conditions such as culture nutrient, pH, temperature and substrate availability [20,21]. Hence, bioprocess can be optimized with these operational conditions such that high productivity could be achieved with their optimum process conditions. Only few studies have reported on the impact of fermenting temperature on the dynamic behaviour of *Saccharomyces cerevisiae* BY4743 during fermentation processes [5]. Metabolic activities of the cell are largely dependent on the pH of the medium and can modify the metabolic pathways as well as the kinetics. Culture nutrient especially the micro-nutrients such as nickel oxide at low concentration have been reported to enhance the bioactivity and growth of yeast during ethanol fermentation [3]. There is dearth of knowledge on the interactive effect of these environmental process conditions on bioethanol fermentation process.

Various bioprocess optimization strategies have been reported [1,22,23]. The 'one-factor at a time' technique is not only time consuming but also often easily misses the interactive effects of the process inputs, and the obtained optimum process set points are not reliable. In contrast, the Response Surface Methodology (RSM) is a modeling technique that combine both mathematical and statistical function to establish the relationship between controllable set of empirical factors and the observed results [24]. RSM has been reported in the optimization process of citric acid production [25,26], biodiesel production, ethanol production [3], yoghurt fermentation [27], biogas generation and biohydrogen production [28]. Knowledge on the dynamics of nanocatalysed ethanol fermentation (NCEF) processes will ease the determination of optimum process conditions.

With increasing interest in the large scale production of ethanol, many kinetic models have been proposed which describe substrate consumption, microbial growth and product formation [29]. Some examples include the logistic, Monod and modified Gompertz models. These kinetic replicas describe bioprocess under different operational input conditions and this can help to enhance productivity, product yield and minimise the formation of undesired by-products (such as inhibitors) [30,31]. Generally, biomass growth with respect to the limiting substrate can be described using Monod model [32]. Similarly, the changes in microbial population as a function of growth rate, initial biomass and maximum biomass concentration, and time, assuming sufficient substrate can be expressed by logistic model [33]; the modified Gompertz model can be used to describe the ethanol production lag time, maximum production rate, and maximum concentration on a given substrate [30]. Despite the availability of data on kinetic models of bioethanol production, very little is known on bioethanol production utilizing nanobiocatalyst.

Agro-industrial wastes are being considered as renewable source of substrate for biofuel production [24,31]. These resources offer numerous advantages which include: local availability, sustainable development of bioenergy, waste management and valorisation. Agricultural waste such as potato waste contains considerable amount of starch, lignin, cellulose, hemicellulose and fermentable sugars that warrant its use as fermentation feedstock. The probable use of potato

peel waste as a potential feedstock for fuel ethanol production has been reported [24]. However, the kinetics of bioethanol production from potato waste in the presence of nanobiocatalyst has not been elucidated.

In this study, the optimum process conditions of NiO NPs concentration, temperature, pH and substrate concentration to achieve high ethanol yield using *S. cerevisiae* BY4743 were investigated. Furthermore, the Monod, logistic and modified Gompertz kinetic models were employed in the current study to describe the microbial growth and ethanol production under the optimized nanobiocatalyst condition. The optimized condition was further validated on simultaneous saccharification and fermentation (SSF) of potato waste.

2. Materials and methods

2.1. Experimental setup

2.1.1. Synthesis of NiO nanoparticles

NiO nanoparticles were prepared by dissolving 4.75 g of Nickel chloride hexahydrate ($\text{NiCl}_2 \cdot 6\text{H}_2\text{O}$) in distilled water (20 mL), and then a dropwise addition of ammonia to $\text{NiCl}_2 \cdot 6\text{H}_2\text{O}$ was made to attain a pH of 10. The mixture was irradiated in a microwave oven at 700 W for 3 min to complete the reaction. The obtained NiO NPs precipitate was washed thoroughly and oven dried at 100 °C for 6 h [13].

2.1.2. Characterization of NiO NPs

The elemental composition, shape and size of the nickel oxide nanoparticles (NiO NPs) were determined using Scanning Electron Microscopy (SEM) and Transmission Electron Microscopy (TEM). The SEM and the TEM operational parameters employed have been previously detailed in Sanusi et al. [17].

2.1.3. Process modelling and optimization

The Box-Behnken design class of Response Surface Methodology (RSM) was employed to generate independent experimental runs (29) with process inputs of NiO nanoparticles concentration (0–0.05 wt%), process temperature (20–50 °C), initial glucose concentration (10–50 g/L) and pH (4–6) (Table 1). The input ranges were chosen based on previous studies (5, 17). The obtained experimental data were then used to fit the polynomial model equations relating the input parameters to the response parameters: biomass concentration and bioethanol yield. The general equation of the model is shown in Eq. (1).

$$Y = \alpha_0 + \alpha_1 X_1 + \alpha_2 X_2 + \alpha_3 X_3 + \alpha_{11} X_1^2 + \alpha_{22} X_2^2 + \alpha_{33} X_3^2 + \alpha_{12} X_1 X_2 + \alpha_{13} X_1 X_3 + \alpha_{23} X_2 X_3 \quad (1)$$

Y represents the response output, α_0 is the intercept, $\alpha_1 X_1$ to $\alpha_3 X_3$ are the linear coefficients, $\alpha_{11} X_1^2$ to $\alpha_{33} X_3^2$ are the quadratic coefficients and $\alpha_{12} X_1 X_2$ to $\alpha_{23} X_2 X_3$ represents the interaction of coefficients.

This model was evaluated using the Analysis of variance (ANOVA). The optimum fermentation set points for the responses (biomass concentration and ethanol yields) were obtained by solving the equations [34] and these set points were hence validated experimentally in duplicate.

2.1.4. Strain and inoculum preparation

The yeast strain used in this study (*Saccharomyces cerevisiae* BY4743) was obtained from the Department of Genetics, University of KwaZulu-Natal, Pietermaritzburg Campus, South Africa. To prepare the inoculum, the yeast was inoculated into a 250 mL Erlenmeyer conical flask containing 100 mL of Yeast Peptone Dextrose medium. The inoculum medium contained; Yeast extract – 10 g/L, Peptone – 20 g/L and Glucose – 20 g/L. The yeast was incubated in a rotary shaker at 120 rpm, 30 °C for 12 h until the exponential growth phase was reached. The culture was then used as the inoculum for the bioethanol production studies.

the lag time (t_l), maximum bioethanol production rate ($r_{p,m}$) and the maximum potential bioethanol concentration (P_m).

$$P = P_m \cdot \exp\left[-\exp\left[\frac{r_{p,m} \cdot \exp(1)}{P_m}\right] \cdot (t_l - t) + 1\right] \quad (5)$$

where P is the ethanol concentration (g/L), P_m is the potential maximum ethanol concentration (g/L), $r_{p,m}$ is the maximum ethanol production rate (g/L h) and t_l is the time (lag phase) from the beginning of fermentation to exponential ethanol production (h).

2.4. Yield and productivity calculation

The ethanol yield and productivity of *S. cerevisiae* BY4743 in the presence of NiO NPs were determined using the following parameters; sugar utilisation, fermentation efficiency, ethanol yield and ethanol productivity were determined using the following Eq.s (6)–(9), respectively:

$$\text{Sugar utilisation (\%)} = \frac{\text{Initial sugar content} - \text{final sugar content}}{\text{Initial sugar content}} \times 100 \quad (6)$$

$$\text{Fermentation efficiency (\%)} = \frac{\text{Actual ethanol yield (g/L)}}{\text{Theoretical yield of ethanol (g/L)}} \times 100 \quad (7)$$

$$\text{Ethanol yield (g/g)} = \frac{\text{Maximum ethanol concentration (g/L)}}{\text{Utilized glucose (g/L)}} \quad (8)$$

$$\text{Ethanol productivity (g/L/h)} = \frac{\text{Maximum ethanol concentration (g/L)}}{\text{Fermentation period (h)}} \quad (9)$$

3. Results and discussion

3.1. Nanoparticles characterization

The morphology of synthesized NiO NPs from SEM analysis is

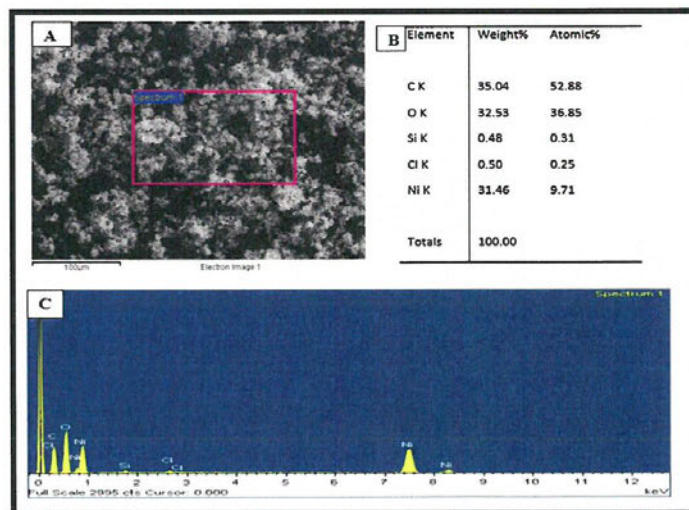


Fig. 1. SEM and EDX images of NiO NPs (A) Scanning electron micrograph of the NiO nano-powder synthesized via microwave-assisted route (B) The percentage weight and atomic composition of the elemental units of NiO NPs. (C) EDX spectrum of NiO NPs on carbon coated grid.

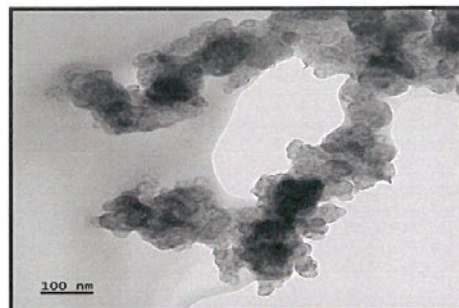


Fig. 2. Transmission electron micrograph of NiO NPs synthesized via microwave-assisted irradiation.

shown in Fig. 1A. The SEM image revealed the spherical structures of NiO NPs that were aggregated. The elemental composition of NiO NPs determined by SEM-EDS shows that NiO NPs comprises of 31.46 % Ni, 35.04 % C, 32.53 % O, 0.50 % Cl, and 0.48 % Si (Fig. 1B and 1C). TEM image (Fig. 2) also confirmed NiO NPs' spherical shape with a narrow size distribution (23–37 nm), an average size of 29 nm, which is comparable to other studies [39]. Similarly, Li et al. [40], obtained spherically shaped nickel oxide nanoparticles with a smaller particle size of 13 nm and a narrow size distribution (8–18 nm). The disparity in the obtained diameter and size distribution compared to other reports, may be attributed to variances in preparation method and the precursors employed.

3.2. RSM Modeling of biomass and ethanol under NiO NPs condition

The observed responses from the experimental design are shown in Table 1. Table 2 shows the fitness of the models as assessed by Analysis

Table 1
Box-Behnken design used for NiO NPs administered fermentation on variables of NiO NPs concentration, glucose concentration, pH and incubating temperature.

| Run | A: Temperature (°C) | B: Glucose (g/L) | C: pH | D: NPs (wt %) | Response 1 Biomass (g/L) | Response 2 Ethanol (g/g) |
|-----|---------------------|------------------|-------|---------------|--------------------------|--------------------------|
| 1 | 20.00 | 30.00 | 6.00 | 0.03 | 2.09 | 0.11 |
| 2 | 20.00 | 30.00 | 5.00 | 0.00 | 2.15 | 0.11 |
| 3 | 50.00 | 30.00 | 4.00 | 0.03 | 0.28 | 0.04 |
| 4 | 35.00 | 50.00 | 5.00 | 0.00 | 2.01 | 0.16 |
| 5 | 50.00 | 10.00 | 5.00 | 0.03 | 0.24 | 0.18 |
| 6 | 50.00 | 50.00 | 5.00 | 0.03 | 0.26 | 0.06 |
| 7 | 35.00 | 30.00 | 4.00 | 0.05 | 1.96 | 0.15 |
| 8 | 50.00 | 30.00 | 5.00 | 0.00 | 0.21 | 0.08 |
| 9 | 20.00 | 50.00 | 5.00 | 0.03 | 2.06 | 0.09 |
| 10 | 35.00 | 30.00 | 4.00 | 0.00 | 1.96 | 0.15 |
| 11 | 35.00 | 30.00 | 6.00 | 0.05 | 1.97 | 0.16 |
| 12 | 20.00 | 30.00 | 5.00 | 0.05 | 2.19 | 0.11 |
| 13 | 50.00 | 30.00 | 5.00 | 0.05 | 0.39 | 0.04 |
| 14 | 35.00 | 30.00 | 5.00 | 0.03 | 1.96 | 0.18 |
| 15 | 35.00 | 30.00 | 5.00 | 0.03 | 1.98 | 0.18 |
| 16 | 20.00 | 30.00 | 4.00 | 0.03 | 2.19 | 0.11 |
| 17 | 35.00 | 10.00 | 5.00 | 0.00 | 1.96 | 0.19 |
| 18 | 35.00 | 10.00 | 6.00 | 0.03 | 1.96 | 0.18 |
| 19 | 35.00 | 30.00 | 5.00 | 0.03 | 1.96 | 0.18 |
| 20 | 50.00 | 30.00 | 6.00 | 0.03 | 0.30 | 0.05 |
| 21 | 35.00 | 10.00 | 5.00 | 0.05 | 2.09 | 0.24 |
| 22 | 20.00 | 10.00 | 5.00 | 0.03 | 2.03 | 0.15 |
| 23 | 35.00 | 50.00 | 6.00 | 0.03 | 1.93 | 0.16 |
| 24 | 35.00 | 30.00 | 6.00 | 0.00 | 1.88 | 0.15 |
| 25 | 35.00 | 50.00 | 5.00 | 0.05 | 1.89 | 0.16 |
| 26 | 35.00 | 30.00 | 5.00 | 0.03 | 1.92 | 0.18 |
| 27 | 35.00 | 50.00 | 4.00 | 0.03 | 1.84 | 0.17 |
| 28 | 35.00 | 10.00 | 4.00 | 0.03 | 1.96 | 0.21 |
| 29 | 35.00 | 30.00 | 5.00 | 0.03 | 1.95 | 0.18 |

2.1.5. Fermentation process

The fermentation experiments as specified in the experimental design (Table 1) were carried out in sterile 250 mL Erlenmeyer flasks with a working volume of 100 mL. The fermentation medium contained; glucose (10–50 g/L), NiO nanoparticles (0–0.05 wt%), nutrients (yeast extract: 5 g/L, (NH₄)₂SO₄: 1 g/L, KH₂PO₄: 2 g/L and MgSO₄: 1 g/L). Then pH values (pH 4–6), were achieved by adjusting the pH of the medium with 1 M HCl and 1 M NaOH. The operating temperature set points were maintained as specified in Table 1. Yeast inoculation were carried out at 10% (v/v). After inoculation, the experiments were incubated at 30 °C and 120 rpm, while 2 mL aliquots were extracted every 3 h for sample analysis.

2.1.6. NiO NPs inclusion in simultaneous saccharification and fermentation of potato waste

The optimized process condition for cell growth and product formation in the presence of NiO NPs obtained using glucose medium were further applied on simultaneous saccharification and fermentation (SSF) of potato peel waste. For the SSF experiments, hydrolysate from the pretreatment stage was employed. The detailed pretreatment protocol has been reported in our previous study (Sanusi et al. [17]). The SSF process (50 mL) contained: 0.05 wt% NiO NPs, pretreated dried potato peel waste with solid loading of 10%, enzyme loading of 0.212 mL amylase for the liquefaction stage at 90 °C, pH 7, for 60 min. Then, 0.295 mL of amyloglucosidase for saccharification and fermentation broth (5 g/L yeast extract, 2 g/L KH₂PO₄, 1 g/L MgSO₄, 1 g/L (NH₄)₂SO₄). After inoculation (*S. cerevisiae* BY4743 inoculum broth (10% (v/v))), the SSF experiment was incubated at 37 °C and 120 rpm over 24 h until glucose concentrations were depleted. For sample analysis, 0.5 mL aliquots were extracted once in every four hours.

2.2. Analytical methods

The glucose content of the enzymatic hydrolysate and fermentation media was determined spectrophotometrically using Megazyme glucose kits (Megazyme, Ireland).

The cell dry weight was obtained by measuring the optical density at 600 nm using SpectroVis plus Spectrophotometer. The biomass concentration (cell dry weight) was determined using a standard calibration curve; a correlation dependence on biomass dry weight as a function of optical density [10,29].

The concentration of ethanol in the medium was determined by means of Vernier ethanol sensor (LABQUEST*2, Vernier, USA). Vernier vapour sensor employs a metallic oxide semiconductor to sense ethanol. Ethanol is consumed in a combustion reaction with the metallic oxide, hence a reduction in the internal resistance of the sensor element occurs. A response voltage corresponding to ethanol concentration results from the change in the internal resistance [29].

Metabolite profile under optimum fermentation conditions (0.05 wt% NiO NPs, 10 g/L glucose concentration, pH 4.86 and incubating temperature of 32.25 °C) was assessed for volatile fatty acids and inhibitory compounds such as acetic acid, butyric acid, succinic acid, 5-methyl-furfural and furfural. Samples were analysed using coupled Varian 3800 Gas Chromatography (California, USA) and Varian 1200 Mass Spectrometry (GC-MS) [35].

The protein content was precipitated from the yeast cells (without the nanoparticles separated from the culture), using the method previously described by Wessel and Fluegge [36]. The protein concentration was then determined by the Bradford method [37], using bovine serum albumin as the standard.

Total carbohydrate content was obtained by pipetting 1 mL sample without the nanoparticles separated from it into 2 mL centrifuge tubes containing saturated mercuric chloride (0.1 mL). Mercuric chloride completely inhibited any further glucose utilisation by the yeast cells. The suspension was centrifuged at 3500 rpm for 15 min. Thereafter, 1 mL aliquot of the suspension was extracted for the total carbohydrate determination using the anthrone reagent with D-glucose as standard at 620 nm (SpectroVis plus Spectrophotometer) [38].

2.3. Kinetic calculations

The specific growth rates (μ) of the fermentation processes were obtained using Eq. (2). The specific growth rate values (μ) and the initial substrate concentration data were then used to estimate the maximum specific growth rate (μ_{max}) and Monod constant (K_s).

$$\text{Specific growth rate } (\mu) = \frac{\ln X_2 - \ln X_1}{t_2 - t_1} \quad (2)$$

where X_2 and X_1 are biomass concentrations (g/L) at t_2 and t_1 , respectively. The linear representation of this equation is expressed as follows:

$$\frac{1}{\mu} = \frac{1}{\mu_{max}} + \frac{K_s}{\mu_{max}} \left(\frac{1}{S}\right) \quad (3)$$

where S represents substrate concentration.

In addition, the integrated logistic function equation (Eq. 4) was used to describe the relationship of biomass (X), at specific times (t) during exponential and stationary phases of cell growth to initial biomass concentration (X_0), maximum biomass concentration (X_{max}) and maximum specific growth rate (μ_{max}). This equation was used to model *S. cerevisiae* BY4743 growth under NiO NPs biocatalyst.

$$X = \frac{X_0 \cdot \exp(\mu_{max} \cdot t)}{1 - \left(\frac{X_0}{X_{max}}\right) \cdot (1 - \exp(\mu_{max} \cdot t))} \quad (4)$$

Furthermore, the experimental data on bioethanol production were used to fit the modified Gompertz model in Eq. 5. This model estimates

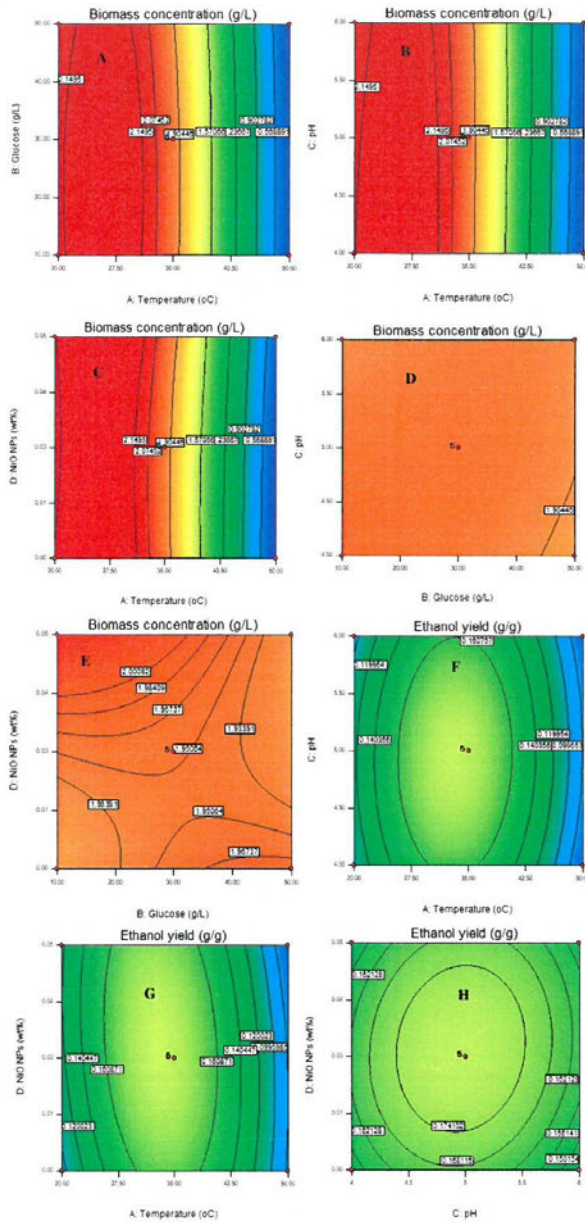


Fig. 3. 2-D contour plots showing the interactive effects of process parameters on biomass concentration and the ethanol yield. (A) The interactive effect of temperature and glucose on biomass concentration (B) Resultant effect of pH and temperature on biomass concentration (C) The impact of the interaction of NiO NPs and temperature on the concentration of cell biomass (D) Biomass concentration from the interactive effect of pH and glucose (E) Resultant influence of the interaction of NiO NPs and glucose on biomass concentration (F) Ethanol yield from the interaction of pH and process temperature (G) Interactive influence of NiO NPs and temperature on ethanol yield (H) Contour plot of the effect of NiO NPs and pH on ethanol yield.

Table 2
Analysis of variance (ANOVA) for biomass and ethanol models.

| Source | Sum of squares | Df | Mean squares | F-value | P-value | R ² |
|---------------------|----------------|------|--------------|---------|----------|----------------|
| Biomass model | 4.00 | 4.00 | 1.00 | 404.40 | < 0.0001 | 0.998 |
| Ethanol yield model | 0.053 | 4.00 | 0.013 | 33.01 | < 0.0001 | 0.925 |

Df: degree of freedom, F-value: Fisher-snedecor distribution value, P-value: probability value, R²: coefficient of determination.

Table 3
Models coefficient of estimates with standard errors.

| Factor | Biomass coefficient estimate | Biomass standard error | Ethanol coefficient estimate | Ethanol standard error |
|----------------|------------------------------|------------------------|------------------------------|------------------------|
| Intercept | 1.95 | 0.022 | 0.18 | 8.977E-003 |
| A | -0.92 | 0.014 | -0.019 | 5.795E-003 |
| B | -0.021 | 0.014 | -0.029 | 5.795E-003 |
| C | -5.000E-003 | 0.014 | -1.667E-003 | 5.795E-003 |
| D | 0.027 | 0.014 | 1.667E-003 | 5.795E-003 |
| AB | -2.500E-003 | 0.025 | -0.015 | 0.010 |
| AC | 0.030 | 0.025 | 2.500E-003 | 0.010 |
| AD | 0.035 | 0.025 | -1.000E-002 | 0.010 |
| BC | 0.022 | 0.025 | 5.000E-003 | 0.010 |
| BD | -0.062 | 0.025 | -0.012 | 0.010 |
| CD | 0.023 | 0.025 | 2.500E-003 | 0.010 |
| A ² | -0.75 | 0.020 | -0.083 | 7.882E-003 |
| B ² | -0.023 | 0.020 | 0.020 | 7.882E-003 |
| C ² | -0.012 | 0.020 | -0.019 | 7.882E-003 |
| D ² | 0.030 | 0.020 | -0.011 | 7.882E-003 |

of Variance (ANOVA). The relatively low p-values of < 0.0001 for both the biomass and ethanol models and the high F values of 404.40 (biomass) and 33.01 (ethanol) elucidate the models' significance (Table 2). The obtained experimental data fitted well to a quadratic model for the models and both exhibited low standard error (Table 3). Coefficient of determination (R²) should be ≥ 0.80 for the good fit of a model [41]. In this case, R² of the models obtained were 0.998 and 0.925 for biomass concentration and ethanol yield respectively, which indicate that the sample variation of 99.8 % for biomass concentration and 92.5 % for bioethanol concentration is ascribed to the independent factors and only 0.2 % (biomass concentration) and 7.5 % (ethanol yield) of the total variation are not explained by the model. It can be implied from these observations that the models are suitable to depict the actual relationship among the selected factors. Consequently, the quadratic model obtained in this study could be employed in the theoretical prediction of biomass concentration and ethanol yield under nanobio-catalyst condition. The final polynomial mode equations in terms of coded factors are depicted below.

$$\text{Biomass (g/l)} = +1.95 - 0.92A - 0.021B - 5.000E-003C + 0.027D - 2.500E-003AB + 0.030AC + 0.035CE + 0.022BCE - 0.062BD + 0.023CD - 0.75A^2 - 0.023B^2 - 0.012C^2 + 0.030D^2 \quad (10)$$

$$\text{Ethanol (g/g)} = +0.18 - 0.019A - 0.029B - 1.667E-003C + 1.667E-003D - 0.015AB + 2.500E-003AC - 1.000E-002CE + 5.000E-003BCE - 0.012BD + 2.500E-003CD - 0.083A^2 + 0.020B^2 - 0.019C^2 - 0.011D^2 \quad (11)$$

3.3. Interactive effect of input parameters on biomass concentration and ethanol yields

The biomass concentration and ethanol yield responses obtained for each experimental run is shown in Table 1 and ranged from 0.21 g/L to 2.19 g/L and 0.04 g/g to 0.24 g/g, respectively. The fermentation process gave higher responses of biomass concentration (2.09 g/L) and

ethanol yield (0.24 g/g) when temperature and pH input variables were maintained at their median values (35 °C and 5), glucose at the lowest value (10 g/L) and NiO NPs concentration at the highest value (0.05 wt %) (run 21) compared to maintaining input variable at low and high values of temperature and pH.

Shown in Fig. 3 (A–H) is the interactive effect of the process inputs on biomass concentration and ethanol yield. It was observed that NiO NPs concentration, glucose concentration, pH and temperature had a linear relationship on biomass concentration (Fig. 3A–E). When glucose concentration and temperature were simultaneously increased from 10 to 50 g/L and 20–50 °C respectively, an increase in biomass concentration from 0.2 to 2.2 g/L (Fig. 3A) was observed. Similar responses were obtained for the interaction of pH (4–6) and temperature (20–50 °C) (Fig. 3B), NiO NPs concentration (0 to 0.05 wt%) and temperature (20–50 °C) (Fig. 3C) when these interacting parameters were concurrently increased. Additional increase in the temperatures from 35 to 50 °C resulted in a sharp decrease in biomass concentration from 2.2 to 0.73 g/L. The noticeable influence of input temperature on biomass concentration may be ascribed to its impacts on the yeast bioactivities and growth kinetics during ethanol fermentation [21,22]. Generally, high temperatures (> 45 °C), negatively impact the process efficiency by denaturing the cells' enzymes, promoting the production of inhibitory compounds and shortening the exponential growth phase. Additionally, extreme temperatures (> 50 °C) were reported to completely inhibit microbial growth [5].

Moreover, shown in Fig. 3D is the interactive effects of pH and glucose concentration on the biomass concentration. Concurrent increase in pH from 4 to 5 and glucose concentration from 10 to 30 g/L resulted in an increase in biomass concentration from 1.84 to 1.96. Additional increase in the pH from 5 to 6 and glucose concentration from 30 to 50 g/L showed a slight reduction in the biomass concentration from 1.96 to 1.91. However, the interactive effect of NiO NPs concentration and glucose concentration in Fig. 3E showed that a simultaneous increase in NiO NPs concentration from 0 to 0.05 wt% and glucose concentration from 10 to 50 g/L led to a sharp increase in biomass concentration from 1.89 to 2.09 g/L with increasing NiO NPs concentration while increasing glucose concentration only resulted in steady increase in biomass concentration from 1.89 to 1.99 g/L. The high biomass concentration observed at high NiO NPs concentration and substrate availability may be attributed to the significance of cell growth largely dependent on substrate concentration [42]. Also, substrate availability might alter the cell's metabolic flux from an ethanol fermentative metabolism using mainly glycolysis, to a respiratory metabolism in which the ethanol formed in the earlier stages of growth is consumed using the tricarboxylic acid, glyoxylate cycles and mitochondrial electron transport chain [43]. And micro-nutrient such as nickel are known to enhance cell metabolic activities and therefore, could have contributed to high ethanol productivity [3].

Looking at the interactive effect of pH and temperature depicted in Fig. 3F, higher ethanol yield (0.04 to 0.15 g/g) was attained with simultaneous increase in pH from 4 to 5 and temperature from 20–35 °C, A further increase in pH (5–6) and temperature (35–50 °C) caused ethanol yield to decrease from 0.15 to 0.096 g/g. Similarly, the interactive effect of NiO NPs concentration and temperature on ethanol yield when the NiO NPs concentration is set at its median value is shown in Fig. 3G. It was observed that an increase in NiO NPs concentration and temperature from 0 to 0.05 wt% and 20–35 °C, respectively led to an increase (350 %) in the ethanol yield from 0.04 to 0.18 g/g. Any further increases in temperature (35–50 °C) showed ethanol yield was drastically reduced from 0.18 to 0.08 g/g. Moreover, the interactive influence of NiO NPs concentration and pH on ethanol yield is shown in Fig. 3H, with simultaneous increase in NiO NPs concentration from 0 to 0.03 wt % and pH from 4 to 5 resulting in an increase (22 %) in ethanol yield from 0.144 to 0.176 g/g. Further increase in NiO NPs concentration (0.03 to 0.05 wt%) and pH (5–6) led to a sharp reduction in ethanol yield from 0.176 to 0.152 g/g.

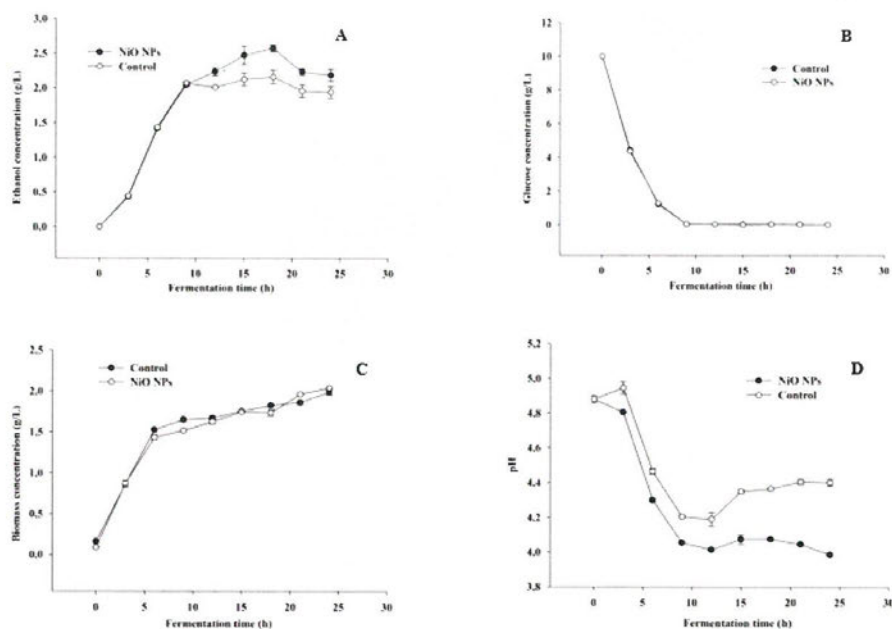


Fig. 4. Bioethanol production process performance under nanobiocatalyst condition. (A) Time course of bioethanol production showing the effect of 0.05 wt% NiO NPs biocatalyst. Bioethanol production reached peak after 18 h corresponding to a 1.18-fold increment over the control experiment (B) Glucose utilisation during fermentation. Initial glucose concentration decreases with increasing process time from 10 – 0.01 g/L and 10 – 0.02 g/L in the nano system and the control experiment after 24 h, respectively. (C) Cell dry weight of *S. cerevisiae* BY4743 in NiO NPs administered system. Under nanobiocatalytic condition 3 % improvement in cell dry weight was observed after 24 h. (D) pH profile during ethanol fermentation. In the presence of NiO NPs, an enhanced buffering capacity was observed. The pH in the nano system remain above 4.2 while the pH in control experiment fell below 4.0 after 24 h.

Table 5
Fermentation performance and kinetic parameters from logistic and modified Gompertz model.

| Fermentation performance | | | | |
|--------------------------|-------------------------|---------------------|------------------------------|-----------------------------|
| Parameter | Glucose utilisation (%) | Ethanol yield (g/g) | Ethanol productivity (g/L/h) | Fermentation efficiency (%) |
| Control | 99.8 | 0.22 | 0.12 | 40 |
| NiO NPs | 99.9 | 0.26 | 0.14 | 60 |
| Kinetic parameters | | | | |
| Logistic Model | | | | |
| | X_0 (g/L) | X_{max} (g/L) | μ_{max} (h^{-1}) | R ² |
| Control | 0.22 | 1.81 | 0.60 | 0.975 |
| NiO NPs | 0.24 | 1.80 | 0.54 | 0.939 |
| Gompertz Model | | | | |
| | P_m (g/L) | $r_{p,m}$ (g/h/L) | t_L (h) | R ² |
| Control | 2.15 | 0.38 | 1.91 | 0.996 |
| NiO NPs | 2.56 | 0.31 | 1.58 | 0.997 |

conversion of glucose to ethanol [55]. Inoculum development with NiO NPs could enhance cell growth rate, biomass concentration and further boost ethanol formation [17].

However, the μ_{max} values obtained from the Monod model differ for the logistic model. The variance in the μ_{max} values between the two types (logistic and Monod) can easily be attributed to the boundaries and inherent parameters employed by each model. For instance, the Monod considers both the biomass concentration and the rate limiting substrate only in log phase whereas the logistic function model employs the biomass concentration from the lag phase to stationary phase

(disregarding the substrate utilisation). Disparities in maximum specific growth rates values from the logistic and Monod models have been previously reported [56]. Shafaghath et al. [56], observed a μ_{max} of 0.65 and 0.45 h^{-1} using the Monod and logistic model, respectively for ethanol production from glucose. The μ_{max} obtained in the current study are comparable to previous studies [29,56]. Growth rates above 0.025 h^{-1} have been shown to linearly increase the fermentative capacity of yeast such as *Saccharomyces* spp, therefore, the obtained μ_{max} values in the current study are highly desirable, particularly for commercial scale up. Moreover, higher growth rates could trigger respirifermentative cellular activities, thus, increasing fermentative capacity and productivity [29].

3.5.3. Kinetics of bioethanol formation using the modified Gompertz model

The experimental data on bioethanol production over time (Fig. 4A) fit the modified Gompertz model with high R^2 values > 0.99 for the NiO NPs supplemented process and the control experiment. A shorter lag time of 1.58 h was observed in the NPs supplemented process compared to 1.91 h for the control experiment. Also, the nano-administered process gave maximum potential ethanol concentration (P_m) of 2.56 g/L as against 2.15 g/L of the control experiment (19 % increment over the control experiment was observed). The observed shorter lag time and higher P_m values in the nano-administered process may be attributed to enhanced metabolic activity under the nanobiocatalyst fermentation [57]. NiO NPs has the potential to trigger metabolic shifts within the cell towards ethanol formation [17]. Additionally, NiO NPs transportation across the cell improves glycolytic rate that go beyond the pyruvate dehydrogenase reaction which generates an overflow

Table 4
Optimum levels of variables during NiO NPs administered glucose fermentation.

| Independent variables | | Predicted optimum levels |
|-----------------------|-----------------|--------------------------|
| NiO NPs concentration | | 0.05 wt% |
| Glucose concentration | | 10 g/L |
| pH | | 4.86 |
| Temperature | | 32.25 °C |
| Response | Predicted value | Observed value |
| Biomass | 2.19 g/L | 2.04 g/L |
| Ethanol yield | 0.23 g/g | 0.26 g/g |

Thus, due to the sensitivity of metabolic fluxes to process input parameters, it is vital to ensure that optimum process conditions are elucidated for maximum ethanol production rate and ethanol yield.

3.4. Experimental validation of the developed models

Experimental validation carried out in duplicate yielded 2.04 g/L and 0.26 g/g for the biomass concentration and ethanol yield, respectively, compared to 1.99 g/L (biomass concentration) and 0.22 g/g (ethanol yield) obtained for the control experiments (Table 4). Consequently, the optimized process under nanobiocatalyst showed a 3 % and 19 % enhancement in the biomass concentration and ethanol yield, respectively over the control experiment. Maximum ethanol concentration was associated with the optimized process conditions employed, NiO NPs presence and stable pH. Bioethanol production requires micronutrients like nickel for the yeast optimum metabolic activities during ethanol fermentation [3]. Nickel form the metal content at the active site of alcohol dehydrogenase enzyme, thus activating and enhancing anaerobic ethanol production [44a,b]. In addition, the impact of NiO NPs on the process can also be ascribed to the oxidation–reduction potential (ORP), that provide a relatively good start-up environment for ethanol formation. Reports have shown that low ORP value benefits bioprocessing [45,46]. Ethanol concentration was observed to show no additional increment after the exponential phase (> 18 h) and this can be attributed to glucose and nutrient been used up along with change in pH of the system [47].

The higher ethanol yield obtained for the nano-administered process (0.26 g/g) in this study could be of interest considering that fermentation efficiency and ethanol yield were improved by 50 % and 18 % over the control experiment. *S. cerevisiae* BY4743 growth in the nano-fermentation process and the control experiment are presented in Fig. 4C, with apparently no lag phase and an exponential phase that occurred for 6 h in both processes. Though the growth patterns observed in the lag and exponential phases were comparable the nano-administered process resulted in a higher biomass concentration (2.04 g/L) compared to the control experiment (1.99 g/L). Higher biomass accumulation in the nano-administered processes can be ascribed to the impact of NiO NPs on *S. cerevisiae* BY4743 (as microorganisms require metals like Ni that are essential for microbial metabolism and growth) and the employed optimum conditions. The influencing impacts of NiO NPs may as well be due to their cellular uptake and integration with the metabolic intermediates and key enzyme activities [48].

Maximum glucose utilisation of 99.9 and 99.8 % (Table 5) were observed for the nano-administered process and the control experiment, respectively. At the initial fermentation phase, the glucose concentration decreased from 10 g/L to 4.44 g/L and 10 g/L to 4.36 g/L for the control and the nano-administered processes respectively (Fig. 4B). Furthermore, as glucose concentration reduces, there was no substantial ethanol production throughout this period. Presumably, glucose was channelled for cells adaptive metabolism and synthesis of key nutrients required for biomass and product formation [30].

The pH was observed to be stable in the nano-administered process with values maintained around 4.19 throughout the fermentation

period (Fig. 4D), while the pH in the control experiment decreased to 3.99 after 24 h. Both the pH of the system and the cell internal pH influence the rate of Ni^{2+} cation uptake by *S. cerevisiae* [49]. The uptake of ion is reduced at pH value below 5, due to the reduction in the net negative charge of plasma membrane. This result suggests a close relation between NiO NPs uptake and *S. cerevisiae* metabolic activities which subsequently influences the pH in the nano-administered system [45,50]. The pH stability resulting from nano-enhanced buffering capacity also kept the yeast in optimum physiological state for optimum metabolic activities. Similarly, a stable pH would enhance enzymatic activities [51,52].

3.5. Kinetic studies of *S. cerevisiae* growth and bioethanol formation in the presence of NiO NPs biocatalyst

3.5.1. *S. cerevisiae* BY4743 growth using the Monod model

The specific growth rate (μ) were determined from the log phase of *S. cerevisiae* BY4743 growth. The specific growth rate when nanoparticle was included were 0.222, 0.282, 0.279, 0.297, and 0.305 h^{-1} at initial substrate concentrations of 2.00, 4.00, 6.00, 8.00, and 10.00 g/L, respectively. Alternatively, lower μ values of 0.198 h^{-1} (2.00 g/L), 0.252 h^{-1} (4.00 g/L), 0.265 h^{-1} (6.00 g/L), 0.265 h^{-1} (8.00 g/L) and 0.271 h^{-1} (10.00 g/L) were obtained for the control experiments (Fig. 5A). The higher μ values achieved for the nano-administered process suggests the impact of NiO NPs on glucose uptake and *S. cerevisiae* growth [51]. NiO NPs has been reported to have a positive interaction with glucose, where the hydrophobic unit of glucose is adsorbed onto the surface layers of NiO NPs by van der Waals forces [52]. Likewise, a strong affinity within few nanometre distance between microbes and nanoparticles has been reported [53]. This affinity is influenced by various factors which include; electrostatic considerations of the process, degree of electrochemical heterogeneity on the surface of cell and the amine groups on cell surface proteins. Additionally, the adherence of NPs to the cell surface was observed in the present study (Fig. 6) [45,54]. The adhesion between yeast and nickel nanoparticles is presumed to be due, at least in part, to processes associated with metal dissimilation by the cell, that they localize and/or produce reactive membrane biomolecules to congregate at the metal interface. The aforementioned interactions enhanced substrate uptake by the cells and improved process productivity.

Estimated Monod constant (K_s) and maximum specific growth rate (μ_{max}) from the specific growth rate values and initial glucose concentrations are shown in Fig. 5B and 5C. A maximum specific growth rate (μ_{max}) value of 0.33 and 0.30 h^{-1} were observed for the nano-administered and control processes, respectively. The K_s value obtained for NiO NPs (at 0.05 wt%) inclusion was 1.00 g/L while the K_s value of 1.11 g/L was obtained for the control experiment. Furthermore, *S. cerevisiae* BY4743 had higher affinity constant ($1/K_s$) for glucose in the nano-administered process (1.0) compared to the control experiment (0.9). The higher μ_{max} and $1/K_s$ values observed for the NiO NPs supplemented process demonstrates the suitability of this NPs as a potential catalytic supplement to improve glucose uptake and improve cell metabolic activities.

3.5.2. *S. cerevisiae* BY4743 growth using the Logistic model

The empirical data from the biomass concentration over the fermentation period were used to fit the logistic function models with correlation coefficients (R^2) > 0.93. An indication that the model could proficiently describe *S. cerevisiae* BY4743 growth under these fermentation conditions. Slightly lower maximum cell concentration (X_{max}) and maximum specific growth rate (μ_{max}) were obtained with NiO NPs administered process in comparison with the control experiment (Table 5). Though insignificant lower X_{max} and μ_{max} were obtained in the nano-administered process, higher ethanol concentration was observed in comparison to the control experiment, thus suggesting that the presence of NiO nanoparticles largely enhanced *S. cerevisiae*

Table 6
Comparison in the fermentation performance and kinetic parameters with previous studies.

| Fermentation performance | | | | | |
|--------------------------|---------------------------------|--------------------------------|--------------------------------|-----------------------------|------------|
| Substrate | Glucose utilisation (%) | Ethanol yield (g/g) | Ethanol productivity (g/L/h) | Fermentation efficiency (%) | References |
| Glucose | 99.9 | 0.26 | 0.14 | 60 | This study |
| OPFJ (10-20Yrs) | 89.5 | 0.39 | 0.04 | 76 | [61] |
| OPFJ (20-25Yrs) | 95.2 | 0.37 | 0.02 | 73 | [61] |
| Sugar beet juice | 100.0 | 0.43 | 0.77 | 79 | [60] |
| Monod model | | | | | |
| Substrate | Strain | μ_{max} (h ⁻¹) | K _s (g/L) | R ² | References |
| Glucose | <i>S. cerevisiae</i> BY4743 | 0.21 | 1.0 | 0.900 | This study |
| Xylose | <i>Scheffersomyces stipitis</i> | 0.23 | 1.67 | 0.945 | [64] |
| OPFJ (20-25Yrs) | <i>S. cerevisiae</i> | 0.11 | 1.82 | > 0.950 | [61] |
| OPFJ (10-20Yrs) | <i>S. cerevisiae</i> | 0.15 | 10.21 | > 0.950 | [61] |
| Glucose | <i>S. cerevisiae</i> | 0.13 | 3.70 | ND | [62] |
| Glucose | <i>S. cerevisiae</i> | 0.65 | 11.39 | ND | [56] |
| Glucose | <i>S. cerevisiae</i> | 0.08 | 213.60 | 0.957 | [63] |
| Sorghum leaves | <i>S. cerevisiae</i> BY4743 | 0.18 | 10.11 | 0.980 | [31] |
| Logistic model | | | | | |
| Substrate | X ₀ (g/L) | X _{max} (g/L) | μ_{max} (h ⁻¹) | R ² | References |
| Glucose | 0.24 | 1.80 | 0.54 | 0.939 | This study |
| Corn cobs (PSSF) | 0.56 | 3.65 | 0.22 | 0.893 | [2] |
| Corn cobs (OSSF) | 0.29 | 3.52 | 0.27 | 0.927 | [2] |
| Gompertz model | | | | | |
| Substrate | P _m (g/L) | r _{p,m} (g/h/L) | t _i (h) | R ² | References |
| Glucose | 2.56 | 0.31 | 1.58 | 0.997 | This study |
| OPFJ (10-20Yrs) | 3.79 | 0.08 | 0.77 | 0.996 | [61] |
| OPFJ (20-25Yrs) | 2.34 | 0.05 | 0.85 | 0.990 | [61] |
| Sorghum leaves | 17.15 | 0.52 | 6.31 | 0.980 | [31] |

Footnote: OPFJ-oil palm frond juice, PSSF-simultaneous saccharification and fermentation with prehydrolysis, OSSF-simultaneous saccharification and fermentation without prehydrolysis, ND-not determined.

substrates, fermentation condition and strain of yeast employed. Furthermore, the maximum specific growth (μ_{max}) of 0.067 h^{-1} was obtained in the present study. Using waste sorghum leaves as substrate, μ_{max} of 0.18 h^{-1} was obtained by Rorke and Gueguim-Kana [31], while Srimachai et al. [61] and Singh and Sharma [62], reported μ_{max} in the range of $0.11\text{--}0.15\text{ h}^{-1}$ using oil palm frond juice and glucose, respectively. Likewise, using *S. cerevisiae* and glucose as substrate, Shafaghat et al. [56] and Ahmad et al. [63] obtained maximum specific growth (μ_{max}) of 0.65 h^{-1} and 0.08 h^{-1} respectively (Table 6).

Furthermore, by comparison, higher maximum cell concentration (X_{max}), in the range of 3.65 to 3.52 g/L from different modes of SSF studies were obtained by Sewsynker-Sukai and Gueguim-Kana [2], as against the 1.80 g/L obtained in the present study. Variations in the maximum cell concentration (X_{max}) observed for the prehydrolysis (PSSF), without prehydrolysis (OSSF) and the present study can be attributed to the different initial cell concentration (X_0) and substrate concentration [42].

The modified Gompertz model in this study exhibited R^2 value of 0.997, which is higher than those reported in many previous studies (Table 6). Higher maximum potential ethanol concentration (P_m) was also achieved with the NiO NPs inclusion compared to some recent reports (Table 6). For instance, the maximum potential ethanol concentration (P_m) was 1.1-fold higher compared to that obtained in a batch fermentation study on oil palm frond juice by Srimachai et al. [61]. Maximum ethanol production rate ($r_{p,m}$), obtained was 3.9-folds higher compared to the study by Srimachai et al. [61]. Additionally, Srimachai et al. [61], in the same study, using palm oil frond juice obtained $r_{p,m}$ value of 0.05 g/L/h , which was 6.2-folds lower than the NiO NPs administered process in the present study. The model by Srimachai et al. [61], had a lower lag time (0.85 h) compared to the current study on fermentation with NiO NPs (1.58 h), while the lag time in the current study was 4 times lesser than that obtained by Rorke and Gueguim-Kana [31] (Table 6). These further demonstrated that the inclusion of NiO NPs in the ethanol fermentation process had considerable impact on bioethanol production lag time, production rate and maximum potential bioethanol production and can be applied to ethanol fermentation for enhanced process performance.

3.7. *S. cerevisiae* carbohydrate and protein accumulation in the presence of NiO NPs

The carbohydrate accumulation profile by *S. cerevisiae* BY4743 under different process conditions is presented in Fig. 7. Cellular carbohydrate fractions formed during bioprocessing by the yeast has the potential to influence the yeast productivity [64]. The total cellular carbohydrate obtained for the control sample increased from 1.37 g/L to 2.22 g/L after 24 h (Fig. 7A). While in the NiO NPs administered process, the total carbohydrate content initially increased from 1.36 g/L (0 h) to 1.57 g/L (12 h) followed by a decline. This decline stretched for 6 h thereafter a sharp increment was observed in the cellular carbohydrate fraction till the 24 h mark (2.29 g/L). 1.03-fold higher cellular carbohydrate was observed in the nano-administered process compared to the control experiment. This suggests *S. cerevisiae* growth in the presence of nanoparticles improved both glucose uptake, cellular carbohydrate synthesis and accumulation. Accumulated cellular carbohydrates are classified as alkali-labile, alkali-soluble and alkali-insoluble carbohydrate, all playing different roles during fermentation [65,66]. For instance, alkali-insoluble cellular carbohydrate has been identified as the most important energy source during endogenous fermentation by the yeast cells. They are synthesized at a faster rate than the carbohydrates of other fractions and subsequently broken down to provide additional carbon source which enhances the yeast overall metabolic processes [65,67]. Moreover, the final period is marked by a continued synthesis of the alkali-soluble carbohydrates and the conversion of the alkali-insoluble reserve to other carbohydrate products. This phenomenon may account for the carbohydrate accumulation pattern observed in the nano-administered process.

The total cellular protein in the nano-administered process was 1.6-fold higher compared to the control experiment (Fig. 7B). This can be attributed to the growth medium and the protein cellular machinery [38]. Nickel ion (Ni^{2+}) can be taken up by *S. cerevisiae* at different growth stages. Ni^{2+} is absorbed by a non-exchangeable pool but the uptake process has been shown to deteriorate at low pH values (< 4) [49,68]. The pH range (4.19–4.86) in the present study favoured the absorption of Ni and subsequently enhanced the *S. cerevisiae* BY4743

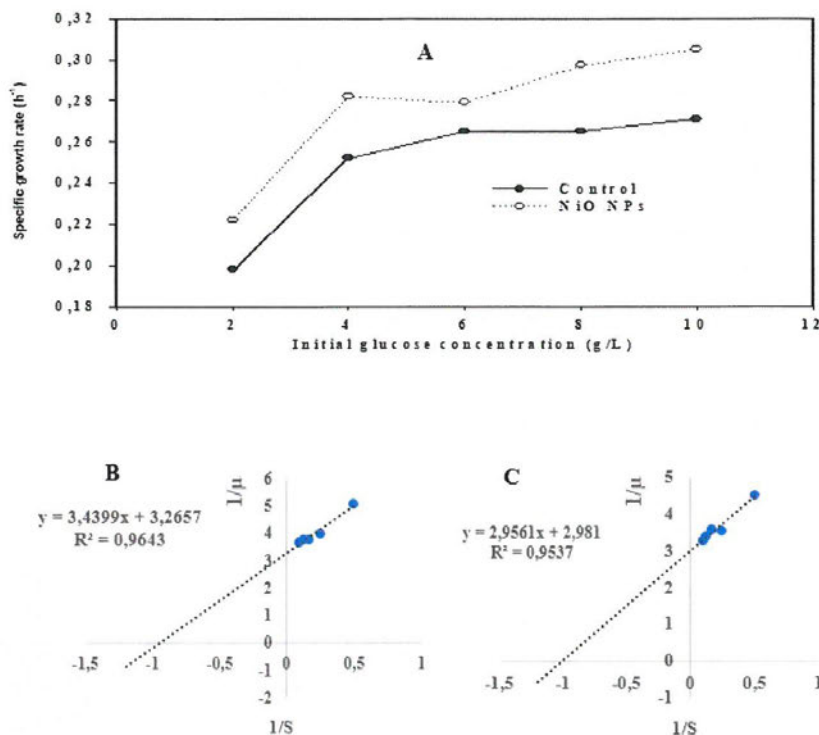


Fig. 5. Profile of specific growth rate (μ) of *S. cerevisiae* in the presence of NiO NPs. (A) *S. cerevisiae* BY4743 specific growth rates at varied initial glucose concentrations increases with increase in initial glucose concentration. The specific growth rate in all the nano fermentation runs was higher compared to the control experiments. Lineweaver–Burk plot estimating Monod constants for batch ethanol production using glucose as substrate ($B_{control}$) and ($C_{NiO NPs}$).

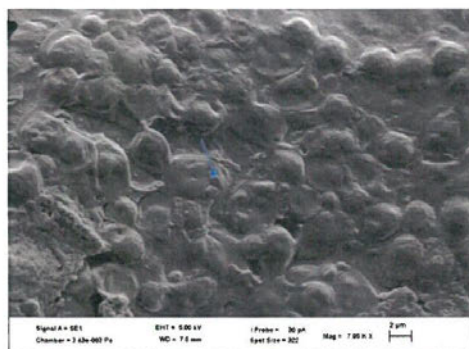


Fig. 6. Scanning electron micrograph of Nano-yeast interaction. NiO nanoparticles adhered to the cell surface.

towards pyruvate decarboxylase, thus increasing *S. cerevisiae* affinity for glucose and invariably increasing ethanol production. Pyruvate decarboxylase and alcohol dehydrogenase convert pyruvate into ethanol and carbon (IV) oxide to reoxidize two molecules of NADH that

was produced from the glycolytic pathway under anaerobic conditions [58].

3.6. Comparison of the developed NPs based bioethanol production with previous studies

Ethanol yield of 0.26 g/g was obtained in the present study, corresponding to 60 % fermentation efficiency (Table 6). Similar to other studies, Linville et al. [59] reported ethanol yield of 0.12 g/g, while ethanol yield of 0.43 g/g and fermentation efficiency of 79 % was obtained by Pavleic et al. [60]. A productivity of 0.14 g/L/h and 99.9 % glucose utilisation was observed in this study, while glucose utilisation and ethanol productivities between 89.5 % and 95.2 %, 0.02 g/L/h and 0.04 g/L/h, respectively were reported by Srimachai et al. [61], using oil palm frond juice as substrate.

The coefficient of determination (R^2) (0.950) obtained for the Monod model was similar to earlier reports (R^2 range; 0.980–0.957) on different substrates (Table 6). This suggests that Monod model can efficiently describe yeast-substrate affinity under different fermentation conditions. The K_S value obtained (1.0 g/L) was the least compared with values reported from studies on lignocellulosic substrates, xylose, and glucose (Table 6). The high value of $1/K_S$ obtained in the present study can be ascribed to the impact of NiO-biocatalyst [52]. Variations in K_S values (1–213.6 g/L) can be attributed to substrate type for defined substrate, sugar composition and concentration of lignocellulosic

NPs biocatalyst in the process probably shift acid-forming pathway to gradually reduce in the metabolic flow. Additionally, the production of benzoic acid, propanoic acid, octanoic acid, acetic acid and butanoic acid were in agreement with the trend of bioethanol formation, a probable suggestion that enzyme metabolic pathway that produced these acids contributed to the majority of ethanol production. The lower concentration of acidic metabolites in the nano system also lessens acid effect on the buffering capacity of the medium (pH value remains above 4.19). In the control experiment, with the pH value falling to 3.99, higher concentrations of by-products were observed (Fig. 8), which, subsequently, impacted ethanol yield and the fermentation efficiency (Table 5). While in the nano system, the pH was above 4.19 and the concentration of by-products was lesser (Fig. 8), resulting in an enhanced ethanol production efficiency [19].

The second largest fraction of the volatile compound profile is the alcohols (excluding ethanol), with phenylethyl alcohol (over 80 % of the other alcohols produced in both system) being the most prominent. Alcohols are the by-products of different processes such as carbohydrate metabolism and degradation of acetic acid and acetaldehyde [77]. For instance, acetic acid condenses to form acetoacetate, which undergoes decarboxylation to acetone. The latter can either be reduced to isopropanol or condensed with acetaldehyde to β -methylcrotonaldehyde which gets further converted to 3-methyl-1-butanol [77]. Increased formation of other alcohols can result to reduction in ethanol formation by deviation of metabolic pathway from ethanol formation as observed in the control experiment.

The other large groups present were the benzenoids and the aldehydes. The control experiment had higher concentration of both groups compared to the nano system. Benzene acetaldehyde is the major fraction of benzenoids in both systems, amounted to 5.54 g/L and 3.08 g/L for the control experiment and nano system, respectively. While the aldehydes main fraction is attributed to 5-methyl-furfural, up to 2.04 g/L in control experiment and 0.24 g/L in the nano-administered system corresponding to 93 % and 88 % fraction of the total aldehydes, respectively. Aldehydes such as furfural and its derivatives are formed upon hexose degradation [75]. Furfural is another by-product that has been reported to be inhibitory to bioprocesses. For example, *S. cerevisiae* under aerobic, oxygen-limited and anaerobic conditions could metabolized furfural to produce additional inhibitory product (furfuryl alcohol). Furfuryl alcohol hampers ethanol production by impeding anaerobic growth of *S. cerevisiae* [78]. Additionally, furfural causes reactive oxygen species to accumulate within the yeast, which causes damage to cell organelles such as vacuole, mitochondrial membranes, chromatin and actin [77,75]. Consequently, furan and its by-products hinder bioethanol production by: redirecting energy used for ethanol production to fix damage caused by furans; enzymatic inhibition or use of necessary cofactors and growth factors [78].

Furthermore, volatile metabolic compounds (VMCs) have chelating capacities due to their functional groups, these include carboxylates, hydroxyls, phenols, sulphydryls, and amines. These chelating factions can act as ligands and complex metals available during fermentation. Kuo and Parkin [79], reported that 0.3 g/L of volatile compounds in an anaerobic system can chelate up to 0.75 mM of Ni. Thus, natural chelating agents such as VMCs in bioprocessing play a significant role in metal ions bioavailability and consequently the overall process performance [7].

3.9. Potential of NiO NPs as biocatalyst in simultaneous saccharification and fermentation of potato peel waste

The optimized process conditions for bioethanol formation in the presence of nanobiocatalyst using glucose medium were further applied on simultaneous saccharification and fermentation of potato peel waste. NiO NPs administered hydrolysis, liquefaction and saccharification gave glucose concentration of 49.09 g/L compared to 46.71 g/L for the control experiment (Fig. 9a). Furthermore, glucose concentration in the

NiO NPs supplemented process was consistently higher throughout the fermentation time compared to the control experiment (Fig. 9a). These results indicate that inclusion of biocatalyst in the hydrolysis, liquefaction, saccharification and fermentation of starch-based lignocellulosic biomass such as potato peel waste might be desirable, as enhanced sugar recovery (1.05-fold increment compare to the control experiment) and ethanol yield were observed. This may be attributed to improved hydrolytic process as well as an enhanced activity of liquefying and saccharifying enzymes in the presence of NiO NPs [17,51].

Bioethanol production on this substrate in the presence of NiO NPs gave a peak concentration of 31.58 g/L which was 65.96 % improvement over the control experiment and decreased thereafter (Fig. 9b). This decrease in ethanol concentration can be ascribed to fermentable sugar and nutrient depletion [2,17]. Although a similar bioethanol production pattern was observed in control experiment, the maximum bioethanol concentration observed was 19.03 g/L (Fig. 9b). The sugar utilisation, ethanol yield and ethanol productivity in the NiO NPs administered process was 98 %, 0.66 g/g and 1.97 g/L/h respectively. This corresponds to 1.03, 1.53 and 1.66-fold improvement, respectively over the control experiment. NiO NPs have the potential to reduce the oxidation-reduction potential of the process [45], enhanced buffering capacity [17], reduce inhibitor concentration to a favourable extent and consequently improving the bioactivity of ethanol-producing yeast [17]. Furthermore, NiO NPs are bioactive agent such as cofactor, enzymes stabilizer and activators that enhances anaerobic ethanol production [44a,b]. In addition, they form the metal content at the active site of enzymes such as alcohol dehydrogenase, pyruvate decarboxylase that catalyze the conversion of pyruvic acid to ethanol [44a,b].

The modified Gompertz model fit the experimental data with a coefficient of determination (R^2) > 0.98 (Table 7). A potential maximum bioethanol concentration (P_m) of 29.14 g/L was obtained in the nano-system and 18.02 g/L in the control experiment. Considering the aforementioned factors that contributed to enhanced process performance in the nano-system, the higher P_m obtained for NiO NPs administered process was expected. Maximum ethanol production rate ($r_{p,m}$) of 7.96 g/L/h was obtained under NiO NPs supplemented process, this is 2.43-fold increment over the control experiment (3.27 g/L/h). This was also higher than those reported in other studies [6,29,30,61]. For instance, maximum ethanol production rate of 0.24 and 2.44 g/L/h were reported by Srimachai et al. [61] from oil palm frond juice and Moodley and Gueguim Kana [29] from sugarcane leaf waste, respectively. The high $r_{p,m}$ obtained in the current study with the nanoparticle inclusion is desirable since higher production rates are preferred at large scale. However, a higher lag time (6.43 h) was obtained in the nano-system compared to the control experiment (3.27 h), thereby implying the yeast cells needed a longer period to adapt to the presence of NiO NPs.

4. Conclusion

This study optimized biomass concentration and ethanol yield using NiO NPs as a biocatalyst. Three kinetic models (i.e. Monod, logistic and the modified Gompertz) were employed to describe *S. cerevisiae* growth and ethanol production under the nanobiocatalyst process condition. All models fit the experimental data with high accuracy (R^2 > 0.94). Additionally, under nanobiocatalyst fermentation condition, *S. cerevisiae* showed improved glucose consumption, cellular protein and carbohydrate accumulation. Furthermore, substantial reduction in the VFA formation in the presence of NiO NPs was observed. The study provides major insights into the use of NiO NPs to reduce the formation of fermentation process inhibitors and enhance product formation. An improved bioethanol production was also observed with potato peel waste in the presence of NiO NPs, thus underscoring the potential of using nanoparticle to enhance biofuel production on starch-based agricultural residues such as potato peel waste.

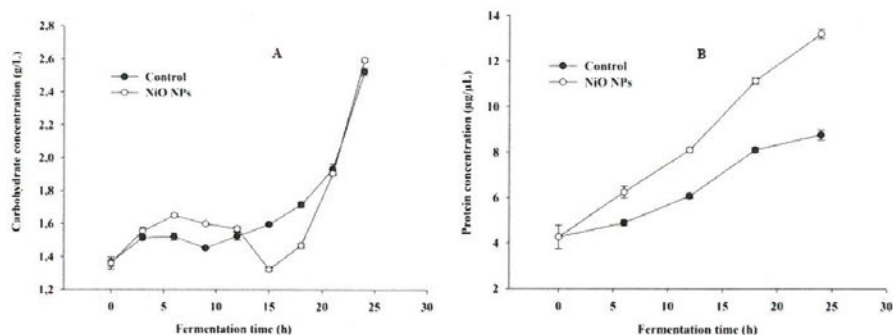


Fig. 7. Carbohydrate and protein accumulation profile in the presence of NiO NPs by *S. cerevisiae*. (A) *S. cerevisiae* BY4743 total carbohydrate accumulation (TCA) as shown Fig. 7B, reveal an undulating pattern with lower TCA (g/L) in the first 18 h and thereafter increased sharply till 24 h mark in both systems. The TCA (g/L) was higher in the nano system, up to 1.03-fold increment over the control experiment after 24 h. (B) Comparison of *S. cerevisiae* BY4743 total cellular protein composition under nanobiocatalytic condition and the control experiment. Protein concentration profile in both systems showed an increasing pattern in relation to the process time with higher protein concentration observed in the nano system.

metabolic and enzymatic activities. Ni ions play two major roles: (1) acting as enzyme activators and (2) a structural role in cell membrane formation [69]. Furthermore, they form the functional components of proteins, growth factors and protein stabilisers [70,71]. The total protein content of *S. cerevisiae* in the current study differs from the study by Usatii et al. [38], where a 10–15 % decrease in cellular protein was observed when 1.0–5.0 mg/L ZnO NP was administered. This variance may be due to the variations in the operating conditions, fermenting yeast, type of nanoparticles and concentration employed.

3.8. Volatile metabolites distribution

Aliphatic acids, alkanols, benzenoids and aldehydes were the main factions of metabolites obtained, as well as lower fractions of ketones, amines and amides (Fig. 8). Formation of organic metabolites usually results from the concentrations of enzymes and co-factors present, hence, from enzyme control mechanisms, and the need to maintain a relatively constant intracellular pH [72]. As shown in Fig. 8, the largest volatile fraction observed was the aliphatic acids (up to 60 %), of which acetic acid makes up a large portion (up to 78 %) in the control experiment. Comparable fraction of aliphatic acid was observed under the nanobiocatalytic condition but the acetic acid fraction to a lesser extent

(75 %). The formation of less aliphatic acids in the nano system especially acetic acid improved ethanol production. Acetic acid is usually the main volatile fatty acid in ethanol fermentation and is formed early in fermentation, this accounted for its present and high concentration observed in the present study. The rate of pyruvate decarboxylase activity in relation to that of alcohol and acetaldehyde dehydrogenases controls acetic acid accumulation [73]. This acetic acid undergoes dissociation within the relatively neutral cell environment leading to a drop in pH which ultimately inhibits cellular activity [74].

Acid-forming pathway evidently dominated the metabolic flow in both systems (Fig. 8). Acetic acid (45 %), propanoic acid (3 %), 2-methyl propanoic acid (4 %), octanoic acid (0.7 %) and butanoic acid (3 %) were the major acidic metabolites in the nano system, while acetic acid (47 %), propanoic acids (3 %), 2-methyl propanoic acid (3 %), octanoic acid (0.8 %) and butanoic acid (3 %) were the dominant acids in the control experiment. The presence of these acidic metabolites could inhibit bioethanol formation by the reduction of biomass formation [75]. This results from the accumulation of anions owing to acid dissociation; a detrimental intracellular condition [76]. Moreover, the production of benzoic acid, propanoic acid, octanoic acid, acetic acid and butanoic acid decreased obviously by 2.71, 2.29, 1.40, 1.37 and 1.16-fold, respectively in the presence of NiO NPs. The presence of NiO

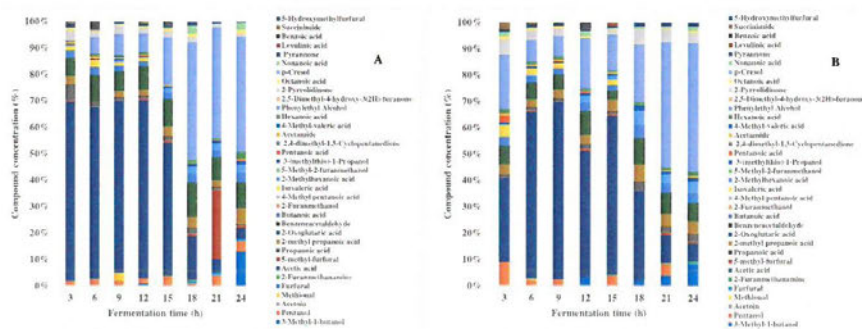


Fig. 8. Comparison between the nano system and the control experiment for volatile metabolic compound distribution. (A) Volatile compounds profile in the control experiment. This was dominated by acetic acid up to 78 % over half the fermentation period. (B) Volatile compounds profile in the nano system. The acetic acid fraction was to a lesser extent (75 %) compared to the control experiment.

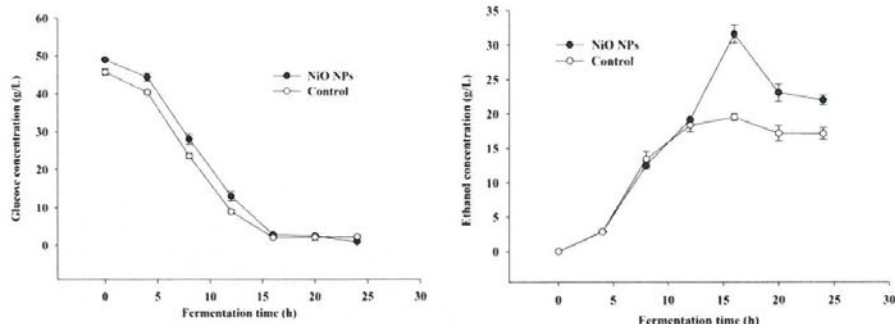


Fig. 9. Fermentable sugar release and bioethanol production of simultaneous saccharification and fermentation of pretreated potato peel waste under NiO NPs biocatalyst condition and the control experiment. (A) Comparison of fermentable sugar release in the nano system and the control experiment. Sugar recovery was better under NiO NPs biocatalytic condition compared to the control experiment. (B) Evolution pattern of bioethanol production in the presence of NiO NPs biocatalyst and the control experiment.

Table 7

| Process performance | NiO NPs | Control | Process kinetic | NiO NPs | Control |
|------------------------------|---------|---------|-------------------|---------|---------|
| Sugar utilisation (%) | 98 | 95 | P_m (g/L) | 29.14 | 18.02 |
| Ethanol yield (g/g) | 0.66 | 0.43 | $r_{p,m}$ (g/L/h) | 7.96 | 3.27 |
| Ethanol productivity (g/L/h) | 1.97 | 1.19 | t_l (h) | 6.43 | 3.27 |
| Fermentation time (h) | 24 | 24 | R^2 | 0.98 | 0.99 |

P_m = maximum potential bioethanol concentration, $r_{p,m}$ = maximum bioethanol production rate, t_l = bioethanol production lag time, R^2 = coefficient of determination.

Author contributions

Isaac A. Sanusi and Gueguim EB. Kana conceived and designed the experiments; Terence N. Suinyuy conducted analysis on volatile inhibitory compounds, while Isaac A. Sanusi performed every other experiment, and analysed the data. Isaac A. Sanusi wrote the manuscript for publication with the help and guidance of Agbaje Lateef and Gueguim EB. Kana.

Conflict of Competing Interest

The authors; Isaac Sanusi, Terence Suinyuy Agbaje Lateef and Gueguim EB. Kana, declare there are no conflict of interest in this work.

Acknowledgement

This work is financially supported by National Research Foundation (NRF), South Africa, Grant-81331:2016.

References

- E. Betiku, S.O. Ajala, Modeling and optimization of *Thevetia peruviana* (yellow oleander) oil biodiesel synthesis via *Musa paradisiacal* (plantain) peels as heterogeneous base catalyst: a case of artificial neural network vs. Response surface methodology, *Ind. Crops Prod.* 53 (2014) 314–322, <https://doi.org/10.1016/j.biombioe.2013.02.034>.
- Y. Sewsynker-Sukai, E.B. Gueguim-Kana, Simultaneous saccharification and bioethanol production from corn cobs: process optimization and kinetic studies, *Bioresour. Technol.* 262 (2018) 32–41, <https://doi.org/10.1016/j.biortech.2018.04.056>.
- U. Talasila, R.R. Vechalapu, Optimization of medium constituents for the production of bioethanol from cashew apple juice using doehlert experimental design, *Int. J. Fruit Sci.* 15 (2) (2015) 161–172, <https://doi.org/10.1080/15538362.2014.989134>.
- L. Laopaiboon, S. Nuanpeng, P. Srinophakun, P. Klanrit, P. Laopaiboon, Selection of *Saccharomyces cerevisiae* and investigation of its performance for very high gravity ethanol fermentation, *Biotechnology* 7 (2008) 493–498, <https://doi.org/10.1016/j.biortech.2009.03.046>.
- Y. Lin, W. Zhang, C.L.K. Sakakibara, S. Tanaka, H. Kong, Factors affecting ethanol fermentation using *Saccharomyces cerevisiae* BY4742, *Biomass Bioenergy* XXX (2012) 1–7, <https://doi.org/10.1016/j.biombioe.2012.09.019>.
- N. Phuokeophim, A. Salakkam, P. Laopaiboon, L. Laopaiboon, Kinetic models for batch ethanol production from sweet sorghum juice under normal and high gravity fermentations: logistic and modified Gompertz models, *J. Biotech.* 243 (2017) 69–75, <https://doi.org/10.1016/j.jbiotec.2016.12.012>.
- P.M. Thanh, B. Ketheesan, Z. Yan, D. Stuckey, Trace metal speciation and bioavailability in anaerobic digestion: a review, *Biotechnol. Adv.* 34 (2016) 122–136, <https://doi.org/10.1016/j.biotechadv.2015.12.006>.
- F. Fermo, G. Collins, J. Bartacek, V. Oflaherty, P. Lens, Role of nickel in high rate methanol degradation in anaerobic granular sludge bioreactors, *Biodegradation* 19 (2008) 725–737, <https://doi.org/10.1007/s10532-008-9177-3>.
- T. Schmidt, M. Nelles, F. Scholwin, J. Pröter, Trace element supplementation in the biogas production from wheat stillage — optimization of metal dosing, *Bioresour. Technol.* 168 (2014) 80–85, <https://doi.org/10.1016/j.biortech.2014.02.124>.
- Y. Kim, S.E. Park, H. Lee, J.Y. Yun, Enhancement of bioethanol production in syngas fermentation with *Clostridium ljungdahlii* using nanoparticles, *Bioresour. Technol.* 159 (2014) 446–450, <https://doi.org/10.1016/j.biortech.2014.03.046>.
- Y. Kim, H. Lee, Use of magnetic nanoparticles to enhance bioethanol production in syngas fermentation, *Bioresour. Technol.* 204 (2016) 139–144, <https://doi.org/10.1016/j.biortech.2016.01.091>.
- K.K. Sandhu, C.M. McIntosh, J.M. Simard, S.W. Smith, V.M. Rotello, Gold nanoparticle-mediated transfection of mammalian cells, *Bioconjugate Chem.* 13 (2002) 3–6, <https://doi.org/10.1021/bc015545c>.
- E. Abdelsalam, M. Samer, Y.A. Attia, M.A. Abdel-Hadi, H.E. Hassan, Y. Badr, Comparison of nanoparticles effects on biogas and methane production from anaerobic digestion of cattle dung slurry, *Renew. Energy* 87 (2016) 592–598, <https://doi.org/10.1016/j.renene.2015.10.053>.
- I.A. Adelere, A. Lateef, A novel approach to the green synthesis of metallic nanoparticles: the use of agro-wastes, enzymes and pigments, *Nanotechnol. Rev.* 5 (6) (2016) 567–587, <https://doi.org/10.1515/ntrev-2016-0024>.
- R. Lakshmanan, Application of Magnetic Nanoparticles and Reactive Filter Materials for Wastewater Treatment, Doctoral thesis (2013), pp. 26–28.
- A. Lateef, S.A. Ojo, J.A. Elegbede, The emerging roles of arthropods and their metabolites in the green synthesis of metallic nanoparticles, *Nanotechnol. Rev.* 5 (6) (2016) 601–622, <https://doi.org/10.1515/ntrev-2016-0049>.
- I.A. Sanusi, F.D. Faloye, E.G. Kana, Impact of various metallic oxide nanoparticles on ethanol production by *Saccharomyces cerevisiae* BY4743: screening, kinetic study and validation on potato waste, *Catal. Letters* 149 (7) (2019) 2015–2031, <https://doi.org/10.1007/s10562-019-02796-6>.
- W. Zhao, Y. Zhang, B. Du, D. Wei, Q. Wei, Y. Zhao, Enhancement effect of silver nanoparticles on fermentative biohydrogen production using mixed bacteria, *Bioresour. Technol.* 142 (2013) 240–245, <https://doi.org/10.1016/j.biortech.2013.05.042>.
- Y. Zhang, J. Shen, Enhancement effect of gold nanoparticles on biohydrogen production from artificial wastewater, *Int. J. Hydrogen Energy* 32 (1) (2007) 17–23, <https://doi.org/10.1016/j.ijhydene.2006.06.004>.
- S. Xu, H. Liu, Y. Fan, R. Schaller, J. Jiao, F. Chaplen, Enhanced performance and mechanism study of microbial electrolysis cells using Fe nanoparticle decorated anodes, *Appl. Microbiol. Biotechnol.* 93 (2012) 871–880, <https://doi.org/10.1007/s00253-011-3643-2>.
- M.J. Torija, N. Rozes, M. Poblet, J.M. Guillamon, A. Mas, Effects of fermentation

- temperature on the strain population of *Saccharomyces cerevisiae*. *Int. J. Food Microbiol.* 80 (2003) 47–53, [https://doi.org/10.1016/S0168-1605\(02\)00144-7](https://doi.org/10.1016/S0168-1605(02)00144-7).
- [22] E.B. Gueguim-Kana, J.K. Oloke, A. Lateef, Novel feeding strategies for *Saccharomyces cerevisiae* DS2155, using glucose limited exponential fed batch cultures with variable specific growth rates (μ), *Afr. J. Biotechnol.* 6 (9) (2007) 1122–1127, <https://doi.org/10.5897/AJB2007.000-2146>.
- [23] A.C.M. Souza, M. Mousaviraad, K.O.M. Mapoka, A. Kurt, Rosentrater, Kinetic Modeling of Corn Fermentation with *S. cerevisiae* Using a Variable Temperature Strategy, *Bioengineering* 5 (2018) 34, <https://doi.org/10.3390/bioengineering5020034>.
- [24] G. Izmirlioglu, A. Demirci, Ethanol production from waste potato mash by using *Saccharomyces cerevisiae*, *Appl. Sci. Basel (Basel)* 2 (2012) 738–753, <https://doi.org/10.3390/app2040738>.
- [25] E.B. Gueguim-Kana, J.K. Oloke, A. Lateef, A. Oyejani, Comparative evaluation of artificial neural network coupled genetic algorithm and response surface methodology for modelling and optimization of citric acid production by *Aspergillus niger* MCBN 297, *Chem. Eng. Trans.* 27 (2012) 397–402 <http://www.aidic.it/cet/12/27/000.html>.
- [26] A.O. Adeoye, A. Lateef, E.B. Gueguim-Kana, Optimization of citric acid production using a mutant strain of *Aspergillus niger* on cassava peel substrate, *Biocatal. Agric. Biotechnol.* 4 (4) (2015) 568–574, <https://doi.org/10.1016/j.beab.2015.08.004>.
- [27] E.B. Gueguim-Kana, J.K. Oloke, A. Lateef, M.G. Zehaze-Kana, Novel optimal temperature profile for acidification process of *Lactobacillus bulgaricus* and *Streptococcus thermophilus* in yogurt fermentation using Artificial Neural Network and Genetic Algorithm, *J. Ind. Microbiol. Biotechnol.* 34 (7) (2007) 491–496, <https://doi.org/10.1007/s10295-007-0220-x>.
- [28] Y. Sewsynker, E.B. Gueguim-Kana, A. Lateef, Modelling of biohydrogen generation in microbial electrolysis cells (MECs) using a committee of artificial neural networks (ANNs), *Biotechnol. Biotechnol. Equip.* 29 (6) (2015) 1208–1215, <https://doi.org/10.1080/13102818.2015.1062732>.
- [29] P. Moodley, E.B. Gueguim-Kana, Bioethanol production from sugarcane leaf waste: effect of various optimized pretreatments and fermentation conditions on process kinetics, *Biotechnol. Rep.* 24 (2019), <https://doi.org/10.1016/j.btre.2019.e00329> xxx–xxx.
- [30] J.M. Dodic, D.G. Vuc'urovic, S.N. Dodic, J.A. Grahovac, S.D. Popov, N.M. Nedeljkovic, Kinetic modelling of batch ethanol production from sugar beet raw juice, *Appl. Energy* 99 (2012) 192–197, <https://doi.org/10.1016/j.apenergy.2012.05.016>.
- [31] D.C.S. Rorke, E.B. Gueguim-Kana, Kinetics of bioethanol production from waste Sorghum Leaves using *Saccharomyces cerevisiae* BY4743, *Fermentation* 3 (2017) 19, <https://doi.org/10.3390/fermentation3020019>.
- [32] E. Imamoglu, F.V. Sukan, Scale-up and kinetic modeling for bioethanol production, *Bioresour. Technol.* 144 (2013) 311–320, <https://doi.org/10.1016/j.biortech.2013.06.118>.
- [33] Y. Mu, G. Wang, H.Q. Yu, Response surface methodological analysis on bio hydrogen production by enriched anaerobic cultures, *Enzyme Microbiol. Technol.* 38 (2006) 905–913, <https://doi.org/10.1016/j.enzmictec.2005.08.016>.
- [34] R.H. Myers, D.C. Montgomery, *Response Surface Methodology: Process and Product Optimization Using Designed Experiments*, 1st ed., Wiley-Interscience, USA, 1995.
- [35] T.N. Suinyuy, J.S. Donaldson, S.D. Johnson, Patterns of odour emission, thermogenesis and pollinator activity in cones of an African cycad: what mechanisms apply? *Ann. Bot.* 112 (2013) 891–902, <https://doi.org/10.1093/aob/mct159>.
- [36] D. Wessel, U.I. Flügge, A method for the quantitative recovery of protein in dilute solution in the presence of detergents and lipids, *Anal. Biochem.* 138 (1984) 141–143, [https://doi.org/10.1016/0003-2697\(84\)90782-6](https://doi.org/10.1016/0003-2697(84)90782-6).
- [37] M.M. Bradford, A rapid and sensitive method for the quantitation of microgram quantities of protein utilizing the principle of protein-dye binding, *Anal. Biochem.* 72 (1976) 248–254, [https://doi.org/10.1016/0003-2697\(76\)90527-3](https://doi.org/10.1016/0003-2697(76)90527-3).
- [38] A. Usati, N. Chiselita, N. Eferemova, The evaluation of nanoparticles ZnO and TiO₂ effects on *Saccharomyces cerevisiae* CNMN-Y-20 yeast strain, *Acta Univ. Cibiniensis Ser. E Food Technol.* 85 XX (1) (2016) 85–92, <https://doi.org/10.1515/auetf-2016-0007>.
- [39] S. Mohammadyani, S.A. Hosseini, S.K. Sadrezhaad, Characterization of Nickel oxide nanoparticles synthesized via rapid microwave-assisted route, *Int. J. Mod. Phys. Conf. Ser.* 5 (2012) 270–276, <https://doi.org/10.1142/S2010194512002127>.
- [40] Q. Li, L.-S. Wang, B.-Y. Hu, C. Yang, L. Zhou, L. Zhang, Preparation and characterization of NiO nanoparticles through calcination of malate gel, *Mater. Lett.* 61 (2007) 1615–1618, <https://doi.org/10.1016/j.matlet.2006.07.113>.
- [41] E. Betiku, A.E. Taiwo, Modeling and optimization of bioethanol production from breadfruit starch hydrolysate vis-à-vis response surface methodology and artificial neural network, *Renew. Energy* 74 (2015) 87–94, <https://doi.org/10.1016/j.renene.2014.07.054>.
- [42] G.C. Okpokwasili, C.O. Nweke, Microbial growth and substrate utilization kinetics, *Afr. J. Biotechnol.* 5 (2005) 305–317 <http://www.academicjournals.org/AJB>.
- [43] J.R. Dickinson, M. Schweizer, *The Metabolism and Molecular Physiology of Saccharomyces cerevisiae*, 2nd ed., CRC Press, Florida, 2004, pp. 13–66.
- [44] (a) A. Schattauer, E. Abdoun, P. Weiland, M. Plo'chl, M. Heiermann, Abundance of trace elements in demonstration biogas plants, *Biosyst. Eng.* 108 (2011) 57–65, <https://doi.org/10.1016/j.biosystemseng.2010.10.010>;
(b) M.S. Romero-Guiza, J. Vila, J. Mata-Alvarez, J.-M. Chimenos, S. Astal, The role of additives on anaerobic digestion: a review, *Renewable Sustainable Energy Rev.* 58 (2016) 1486–1499, <https://doi.org/10.1016/j.rser.2015.12.094>.
- [45] H. Han, M. Cui, L. Wei, H. Yang, J. Shen, Enhancement effect of hematite nanoparticles on fermentative hydrogen production, *Bioresour. Technol.* 102 (2011) 7903–7909, <https://doi.org/10.1016/j.biortech.2011.05.089>.
- [46] C.J. Stephanson, G.P. Flanagan, Non-toxic hydride energy source for biochemical and industrial venues: ORP and NAD⁺ reduction analyses, *Int. J. Hydrogen Energy* 29 (5) (2004) 459–464, [https://doi.org/10.1016/S0360-3199\(03\)00123-X](https://doi.org/10.1016/S0360-3199(03)00123-X).
- [47] S. Mazzeoni, G. Landi, F. Carteni, E. de Alteris, F. Giannino, L. Paciello, P. Parascandola, A novel process-based model of microbial growth: self-inhibition in *Saccharomyces cerevisiae* aerobic fed-batch cultures, *Microb. Cell Fact.* 14 (2015) 109, <https://doi.org/10.1186/s12934-015-0295-4>.
- [48] J. Bartacek, F.G. Feroso, A.M. Baldo-Urrutia, E.D. Van Hullebusch, P.N.L. Lens, Cobalt toxicity in anaerobic granular sludge: influence of chemical speciation, *J. Ind. Microbiol. Biotechnol.* 35C (2008) 1465–1474, <https://doi.org/10.1007/s10295-008-0448-0>.
- [49] G.W.J. Colm, Magnesium and Control of Yeast Growth and Metabolism, Master thesis (1987), pp. 9–12.
- [50] P. Wimonsoong, R. Nitisoravut, Comparison of different catalysts for fermentative hydrogen production, *J. Clean Energy Technol.* 3 (2) (2015) 128–131, <https://doi.org/10.7763/JOCET.2015.V3.181>.
- [51] D.K. Ban, S. Paul, Zinc oxide nanoparticles modulates the production of β -Glucosidase and protects its functional state under alcoholic condition in *Saccharomyces cerevisiae*, *Appl. Biochem. Biotechnol.* 173 (2014) 155–166, <https://doi.org/10.1007/s12010-014-0825-2>.
- [52] M. El-Kemary, N. Nagy, I. El-Mehasseb, Nickel oxide nanoparticles: synthesis and spectral studies of interactions with glucose, *Mater. Sci. Semicond. Process.* 16 (2013) 1747–1752, <https://doi.org/10.1016/j.mssp.2013.05.018>.
- [53] S.K. Lower, M.F. Hochella Jr., T.J. Beveridge, Bacterial recognition of mineral surfaces: nanoscale interactions between *Shewanella* and α -FeOOH, *Science* 292 (5520) (2001) 1360–1363, <https://doi.org/10.1126/science.1059567>.
- [54] H. Yang, J. Shen, Effect of ferrous iron concentration on anaerobic biohydrogen production from soluble starch, *Int. J. Hydrogen Energy* 31 (15) (2006) 2137–2146.
- [55] S. Ozmihci, F. Kargi, Effects of feed sugar concentration on continuous ethanol fermentation of cheese whey powder solution (CWP), *Enzyme Microb. Technol.* 41 (2007) 876–880, <https://doi.org/10.1002/jctb.2013>.
- [56] H. Shafaghat, G.D. Najafpour, P.S. Rezaei, M. Sharifzadeh, Growth kinetics and ethanol productivity of *Saccharomyces cerevisiae* PTCC 24860 on various carbon sources, *World Appl. Sci. J.* 7 (2) (2009) 140–144.
- [57] I.S.I. Snook, H.Y. Steensma, Factors involved in anaerobic growth of *Saccharomyces cerevisiae*, *Yeast* 24 (2007) 1–10, <https://doi.org/10.1002/yea.1430>.
- [58] J.L. Wang, W. Wan, Effect of Fe²⁺ concentrations on fermentative hydrogen production by mixed cultures, *Int. J. Hydrogen Energy* 33 (4) (2008) 1215–1220, <https://doi.org/10.1016/j.ijhydene.2008.07.010>.
- [59] J.L. Linville, M. Rodriguez Jr, J.R. Mielenz, C.D. Cox, Kinetic modeling of batch fermentation for *Populus hydrolyzate* tolerant mutant and wild type strains of *Clostridium thermocellum*, *Bioresour. Technol.* 147 (2013) 605–613, <https://doi.org/10.1016/j.biortech.2013.08.086>.
- [60] M. Pavlecic, I. Vrana, K. Vibovec, M.I. Santek, P. Horvat, B. Santek, Ethanol production from different intermediates of sugar beet processing, *Food Technol. Biotechnol.* 48 (2010) 362–367.
- [61] T. Srimachai, K. Nuihitikul, S. O-thong, P. Kongjan, K. Panpong, Optimization and kinetic modeling of ethanol production from Oil Palm Frond Juice in batch fermentation, *Energy Procedia* 79 (2015) 111–118, <https://doi.org/10.1016/j.egypro.2015.11.490>.
- [62] J. Singh, R. Sharma, Growth kinetic and modeling of ethanol production by wilds and mutant *Saccharomyces cerevisiae* MTCC 170, *Eur. J. Exp. Biol.* 5 (2015) 1–6 www.pelagiaresearchlibrary.com.
- [63] F. Ahmad, A.T. Jameel, M.H. Kamarudin, M. Mel, Study of growth kinetic modeling of ethanol production by *Saccharomyces cerevisiae*, *Afr. J. Biotechnol.* 16 (2011) 1884–1886, <https://doi.org/10.5897/AJB11.2763>.
- [64] F.W. Fales, The assimilation and degradation of carbohydrates by yeast cells, *J. Biol. Chem.* 193 (1951) 113–124 <http://www.jbc.org/content/193/1/113>.
- [65] P.M. Holligan, D.J. Jennings, Carbohydrate metabolism in the fungus *Dendryphiella salina*. II. The influence of different carbon and nitrogen sources on the accumulation of Mannitol and arabinol, *New Phytol.* 71 (4) (1972) 583–594 <https://about.jstor.org/terms>.
- [66] D. Cheng, D. Li, Y. Yuan, L. Zhou, X. Li, T. Wu, L. Wang, Q. Zhao, W. Wei, S. Yuhuan, Improving carbohydrate and starch accumulation in *Chlorella* sp. AE10 by a novel two-stage process with cell dilution, *Biotechnol. Biofuels* 10 (2017) 75, <https://doi.org/10.1186/s13068-017-0753-9>.
- [67] M.E. Van der Rest, A.H. Kamminga, A. Nakano, Y. Anraku, B. Poolman, W.N. Konings, The plasma membrane of *Saccharomyces cerevisiae*: structure, function, and biogenesis, *Microbiol. Rev.* 59 (2) (1995) 304–322 <https://doi.org/10.1146/annurev-micro.1995.0504.0101>.
- [68] R.P. Jones, P.F. Greenfield, A review of yeast ionic nutrition. Part I: growth and fermentation requirements, *Process. Biochem.* (1984) 48–60.
- [69] M.J. Lewis, A. Sommer, P.C. Patel, Association of divalent ions with proteins of the yeast plasma membrane, *J. Food Biochem.* 2 (1978) 169–184.
- [70] G. Diekert, U. Konheiser, K. Piechulla, R.K. Thauer, Nickel requirement and factor F430 content of methanogenic Bacteria, *J. Bacteriol.* 2 (148) (1981) 459–464 <http://doi.org/10.1128/JB.148.2.459-464.1981>.
- [71] K.G. Mackenzie, M.C. Kenny, Non-volatile organic acid and pH changes during the fermentation of distiller's wort, *J. Inst. Brew.* 71 (1985) (1985), <https://doi.org/10.1002/j.2050-0416.1985.tb02040.x>.
- [72] G.C. Whiting, Organic acid metabolism of yeasts during fermentation of alcoholic beverages—a review, *J. Inst. Brew.* 82 (1976) 84–92, <https://doi.org/10.1002/j.2050-0416.1976.tb03731.x>.
- [73] P.F.H. Harmsen, W.J.J. Huijgen, L.M.B. López, R.R.C. Bakker, Literature review of physical and chemical pretreatment processes for lignocellulosic biomass, *Food & Biobased Research*, Wageningen (2010), <https://www.ecn.nl/docs/library/report/2010/e10013.pdf>.

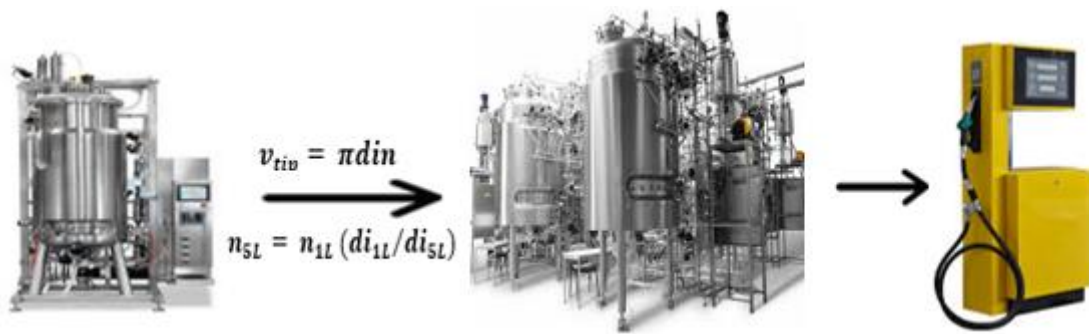
- [74] S. Larsson, E. Palmqvist, B. Hahn-Hägerdal, C. Tengberg, K. Stenberg, G. Zacchi, N. Nilvebrant, The generation of fermentation inhibitors during dilute acid hydrolysis of softwood, *Enzyme Microb. Technol.* 24 (3–4) (1999) 151–159, [https://doi.org/10.1016/S0141-0229\(98\)00101-X](https://doi.org/10.1016/S0141-0229(98)00101-X).
- [75] D.C.S. Rorke, T.N. Suinyuy, E.B. Gueguim-Kana, Microwave-assisted chemical pretreatment of waste sorghum leaves: process optimization and development of an intelligent model for determination of volatile compound fractions, *Bioresour. Technol.* 224 (2017) 590–600, <https://doi.org/10.1016/j.biortech.2016.10.048>.
- [76] M. Pietruszka, K. Pielech-przybylska, J.S. Szopa, Synthesis of higher alcohols during alcoholic fermentation of rye mashes, *Food Chem. Biotechnol.* 1081 (74) (2010) 51–7464 <http://hdl.handle.net/11652/258>.
- [77] E. Palmqvist, B. Hahn-Hägerdal, Fermentation of lignocellulosic hydrolysates. I: inhibition and detoxification, *Bioresour. Technol.* 74 (1) (2000) 17–24, [https://doi.org/10.1016/S0960-8524\(99\)00169-1](https://doi.org/10.1016/S0960-8524(99)00169-1).
- [78] J.R.M. Almeida, T. Modig, A. Petersson, B. Hahn-Hägerdal, G. Lidén, M.F. Gorwa-Grauslund, Increased tolerance and conversion of inhibitors in lignocellulosic hydrolysates by *Saccharomyces cerevisiae*, *J. Chem. Technol. Biotechnol.* 82 (2007) 340–349, <https://doi.org/10.1002/jctb.1676>.
- [79] W.-C. Kuo, G.F. Parkin, Characterization of soluble microbial products from anaerobic treatment by molecular weight distribution and nickel-chelating properties, *Water Res.* 30 (1996) 915–922, [https://doi.org/10.1016/0043-1354\(95\)00201-4](https://doi.org/10.1016/0043-1354(95)00201-4).

CHAPTER 6

Preliminary scale-up studies of nano-catalysed simultaneous saccharification and bioethanol production from waste potato peels

This chapter has been submitted for publication in a peer review journal-*Process Biochemistry* with the title: Preliminary scale up studies of nano-catalysed simultaneous saccharification and bioethanol production from waste potato peels. The manuscript is presented in the following pages.

Graphical abstract



Highlights

- Preliminary scale-up for bioethanol production from potato wastes with nanoparticles
- Improved productivity was achieved using constant power consumption criterion
- Gompertz and logistic models were used to describe process kinetics
- Reduced inhibitory compounds formation and lower shear stress were achieved

Preliminary scale-up studies of nano-catalysed simultaneous saccharification and bioethanol production from waste potato peels

Isaac A. Sanusi*, Gueguim E. B. Kana

Discipline of Microbiology, Biotechnology Cluster, University of KwaZulu-Natal, Private Bag X01, Scottsville 3209, Pietermaritzburg Campus, South Africa

Abstract

Preliminary scale-up of bioethanol production was carried out using waste potato peels supplemented with NiO nanoparticles from 2 to 10 L bioreactors. The considered criteria were constant power consumption (P/V) and impeller tip speed (V_{tip}). Scale-up using constant P/V showed an increase in ethanol concentration and productivity up to 1.02 and 1.38 folds respectively. Process kinetic data fit the modified Gompertz and logistic models with $R^2 > 0.98$. Potential maximum bioethanol concentrations (P_m) of 25.29 gL^{-1} and 23.97 gL^{-1} were observed in the 10 L and 2 L bioreactors respectively. A 0.79 fold decrease in shear stress was achieved with constant P/V which resulted in low cell damage, and a substantial reduction in the production of process inhibitors was observed. These findings highlight the potential of industrial valorisation of waste potato peels supplemented with NiO nanoparticles for bioethanol production.

Keywords: Bioreactor, bioethanol, power consumption, nanobiocatalyst, potato peels, scale-up

*Correspondence to: Sanusi_isaac@yahoo.com; Tel.: +27616181662

6.0 Introduction

Amidst the growing demand for alternative and renewable biofuels as well as for the development of sustainable bio-economy and environment, yeast fermentations by means of renewable feedstocks such as starch based potato peel waste have become increasingly important [1]. The bioconversion of starch based lignocellulosic wastes to biofuel such as bioethanol, biohydrogen, biomethane have continue to receive global attention in the last few decades [2, 3, 4, 5]. Great efforts have been attempted for enhanced bioethanol process performance, improved bioethanol yields and achieving production scale, through various bioprocess approaches. These include; nutrient formulation, process optimization, scaling up and microbial engineering strategies [6, 7, 8, 9].

In principle, bioprocess capacity depends primarily on gene functions, enzyme kinetics (cellular machinery) and fluid-dynamics in the bio-reactor [1]. For these reasons, it is crucial to gain additional knowledge on cellular machinery and bio-reactor fluid-dynamics in order to fast-track the transition from the bench-top scale to its industrial scale [10]. The fundamental problem of bioprocess scale-up is its negative impact on the cell kinetic mechanism resulting from heterogeneous condition in the large scale bioreactor [1]. Large scale bioreactors constantly face different challenges such as mixing problem, heterogeneous environment, contamination and variability [1, 7]. One of the problematic incidents in scaling up is insufficient mixing. Mass and heat transfer can be adversely affected leading to local substrate-nutrient concentration and unfavourable temperature-gradients in the bio-reactor [6, 7]. The cell's immediate microenvironment and the cell physiology might be influenced, resulting to critical metabolic alterations. Microbial cells have the tendency to transform their genetic footprint due to the changing environmental conditions which could cause lose in vital metabolic features required for the process optimal performance. Impeller system in stirred tank bioreactors are used to enhance homogeneous mixing of reacting species. The ultimate aim of obtaining effective mixing regime from suitable combination of parameters is to achieve

substrate-nutrient concentration and temperature-gradient homogeneity at each instant of the reaction volume in the shortest practicable time to the fermenting cells [6, 7]. These parameters; mixing-time, pumping-capacity and circulation-time are three essential mixing properties used to describe mixing behaviour [7]. This requires appropriate energy being transferred to fermentation system through the stirrer power-input. Impeller tip speed has some advantages in bioprocessing with shear stress sensitive microorganisms, as it regulates the optimum shear stress in the bio-reactor, the probable cell destruction and the size of gas-bubbles. For instance, impeller tip speed $>3.0 \text{ ms}^{-1}$ could lead to cell damage [6]. Conversely, it involves a decrease in the power-input and in the agitation speed, which leads to a notable decline in the rate of gas transfer, this can impact negatively on the process performance [11].

Usually the most preferable criteria for scaling up is to sustain the volumetric power-input or the volumetric mass transfer coefficient constant. Hence, knowledge on the relationship between the fluid movement, the impeller velocity, and the power consumption will be required to achieved the optimum energy input. Consequently, experimental investigation on scaling up processes is necessary to provide more insights on these issues.

Scaling up from laboratory scale to a production-scale could be challenging because of various important but different aspects involved [7]. The main aspects which require precise compromise between intrinsically contradictory desirable characteristics are the engineering, metabolic processes and economic implications needed for an industrial scale production at the best-economic proficiency [7].

Four techniques are widely recognized in scaling up [12]. These include, fundamental-methods; semi-fundamental methods; dimensional-analysis; and rules of thumb. The rule of thumb method is the most commonly used technique. The scale-up criterion largely employed in the fermentation processes are: constant power consumption input, constant volumetric mass transfer, constant impeller tip speed and constant mixing time [12]. These factors are

diametrically related to mass transfer, mixing activity, power consumption, bulk rheology, cell viability, substrate and products concentration, micro-conditions, nutrients constituent and availability in the bioreactor [6, 7]. Thus, application of the rule of thumb technique, though a very delicate technique, can result in an overall alteration in the limiting regime beyond a certain degree, is very simple but effective [12].

The design of industrial-scale microbial fermentation process depends on the growth conditions, nutrient formulation, target product, microbial strain, bioreactor geometry and fluid dynamics. Consequently, for a certain product, an adequate and comprehensive process parameters which directly linked to improved product yield and scaling-up potentials has to be established. To the best of our knowledge there is a dearth of reports on the scaling up of bioethanol production from potato peels under nano-biocatalytic condition. The existing literature has focused mostly on the potential utilization of potato waste for value-added bioproduct such as bioethanol [13, 2, 3, 8, 5, 9], however, there is a paucity of data on scale up studies of this bioprocess in the presence of NiO nanoparticles. Previously, we reported that nanobiocatalytic conditions improved ethanol bioprocessing from waste potato peel through promoting sugar recovery, utilization, metabolic activities and inhibitory compound reduction [8, 9]. This approach of nano inclusion in nutrient formulation has shown potential high process performance which makes it a feasible strategy for large-scale bioethanol production from potato waste using simultaneous saccharification and fermentation bioprocessing (SSF).

Simultaneous saccharification and fermentation process involve lignocellulosic feedstock saccharification by hydrolysis to release reducing sugar, which is simultaneously fermented to produce bioethanol [14]. This process is considered an effective strategy to reduce the overall operational costs, increase bioethanol concentration and bioethanol conversion within shorter period due to the exclusion of separate, long saccharification steps. Moreover, SSF processes are operated in a single bioreactor with the same operational condition and the fermentable

sugar that is released is concurrently metabolized to ethanol by fermenting microbe. Additionally, the inhibitory impacts of process inhibitors and high glucose yields during the enzymatic-hydrolysis stage are considerably lowered [15].

Furthermore, scaling up could considerably impact the process kinetics and consequently, the process productivity. Kinetic models have been employed in this regard to understand, predict, and optimize the properties and behaviour of cells in bioprocessing [16].

This study examines the scale-up of simultaneous saccharification and bioethanol production from waste potato peels by *Saccharomyces cerevisiae* BY4743 in the presence of NiO nanoparticles biocatalyst. The suitability of constant power consumption and impeller tip speed as scale-up criteria for this bioprocess are assessed; the process kinetics and inhibitors profile are examined.

6.1 Materials and Methods

6.1.0 Inoculum development

S. cerevisiae BY4743 strain was provided courtesy of Dr Che Pillay (Discipline of Genetic), Pietermaritzburg Campus, University of KwaZulu-Natal, South Africa. Seed culture of *S. cerevisiae* BY4743 were maintained on double strength Yeast-Peptone-Dextrose (YPD) agar slant containing yeast extract (10 g/L⁻¹), peptone (20 g/L⁻¹), glucose (20 g/L⁻¹), agar (20 g/L⁻¹) and kept in the fridge at 4 °C.

For inoculum cultivation, colonies of *S. cerevisiae* were introduced into 500 mL flask containing 250 mL broth YPD medium. This was incubated under shaking conditions (at 120 rpm) overnight, at 30 °C to achieve exponential growth phase.

6.1.1 Substrate preparation

The waste potato peels used as bioethanol production feedstock in this study were initially dried at 50–55 °C to remove bound-water and was grinded to 1-2 mm particle size using a centrifugal miller (Retsch ZM-1, Durban, South Africa). The compositional content of the dried

potato peels gave starch (20%), carbohydrate (14%), hemicellulose (10%), cellulose (4%), acidified detergent lignin (6%) and others (36%).

The detailed synthesis and description of nickel oxide nanoparticles (NPs) with particle size of 29 nm used for the current study has been described in our previous work [8]. NiO NPs of 0.05 wt% was added to the fermentation process at the point of milled potato peel substrate pretreatment. This was informed by the significant impact of nanometric nickel oxide supplement on bioethanol production in our previous studies [8, 9].

Milled waste potato peels were pretreated under previously optimised conditions with slight modification [17]. Briefly, HCl solution (0.92% (v/v)) at a solid-to-liquid ratio of 5.08% milled potato peels and NiO NPs (0.05 wt%) were placed in a 500 mL Schott bottle. The mixture was transferred to a static water bath for 2.34 h at 69.6 °C, This was followed by 5 min autoclave heat treatment (at 121 °C). Afterwards, 125 Unit/g amylase (Sigma-Aldrich, South Africa) was added for the liquefaction of starch at 90 °C, neutral pH of 7, for 1 h and, sugar saccharification was achieved using amyloglucosidase (Sigma-Aldrich, South Africa) (15 Unit/g).

6.1.2 Fermentation parameters

Fermentation processes were carried out in 2 L (Bio/CelliGen 115, New Brunswick, USA) and 10 L (Labfors-INFORS HT, Switzerland) bioreactors under anaerobic environments with working volumes of 1 L and 5 L, respectively. Hydrolysate from the pretreated milled potato peels (500 mL containing 100 g of pretreated substrate) and nutrient broth (400 mL containing nutrient for a litre working volume) were fed to the sterilized bioreactor and then inoculated with the seed culture (10% v/v). The nutrient broth contains; yeast extract (5 gL⁻¹), KH₂PO₄ (2 gL⁻¹), MgSO₄ (1 gL⁻¹) and (NH₄)₂SO₄ (1 gL⁻¹). This was followed by fermentation process carried out at pH 5, 37 °C and 120 rpm for 36 h. Samples were withdrawn routinely for analytical purpose. The fermentation broth was centrifuge (10000 rpm, 5 min, 4°C) and the

supernatant was then used for bioethanol and glucose determinations. The schematic design of the process is shown below (Fig. 6.0).

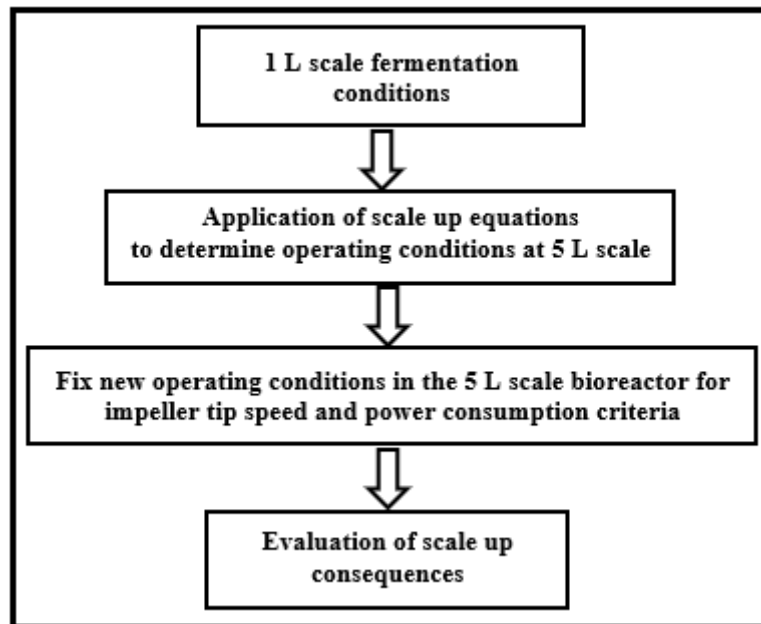


Fig. 6.0: Process scale-up schematic based on constant impeller tip speed and power consumption

6.1.3 Scale up parameter determination

Two scale up approaches namely, constant power consumption per unit volume (P/V) and impeller tip speed (V_{tip}) were used to determine the most suitable operational parameters at a semi-pilot scale production of bioethanol from waste potato peels by *S. cerevisiae*. The changes of constant impeller tip speed and constant power consumption in the fermentation broth were carried out by varying the agitation rate which was set to 120 rpm in 2 L control bioreactor.

6.1.4 Scale up parameters

6.1.4.0 Constant impeller tip speed (V_{tip})

When the V_{tip} is employed as scale-up criterion, it provides more insights on the relationship between shear stress and microbial cell [11]. The tip speed impacts on the shear stress in the bioreactor with potential damage to the cell [18]. It is directly proportionate to the stirrer

velocity and the stirrer (impeller) diameter. In this study, it was determined using Eq. 1, while, the stirrer speed in the 5 L scale bioreactor, was computed according to Eq. 2 [19].

$$v_{tip} = \pi d i n \quad (1)$$

$$n_{5L} = n_{1L} (d i_{1L} / d i_{5L}) \quad (2)$$

6.1.4.1 Constant power consumption

The constant power consumption per unit of volume was performed according to Eq. 3-6, while Eq. 7 was employed to compute the stirring speed in the 5 L scale bioreactor [19].

$$\text{Power consumption} = P/V \quad (3)$$

$$P = N_p \rho n^3 d i^5 f_c N \quad (4)$$

$$V = \frac{\pi D^2 H}{4} \quad (5)$$

$$f_c = \frac{(DH)^{1/2}}{3di} \quad (6)$$

where, P is the non-gassed power, N_p the power number, N the number of impellers, D the bioreactor vessel diameter and H is the static height of fermentation broth and f_c is the geometric factor (Eq. 6).

$$n_{5L} = n_{1L} (d i_{1L} / d i_{5L})^{5/3} (D_{5L} / D_{1L})^{2/3} [(H_{5L} / H_{1L})(N_{1L} / N_{5L})(f_{c1L} / f_{c5L})]^{1/3} \quad (7)$$

6.1.4.2 Reynold's number

For an efficient mixing to be achieved in the bioreactor a turbulent condition must be attained. The intensity of turbulence is denoted by the impeller's Reynolds number, which is a function of the system geometry (stirrer speed and impeller diameter) and the fluid properties (viscosity and density) [19]. The correlation of these parameters to Reynolds number was expressed using Eq. 8. where ρ is the broth density and η is the viscosity of the broth.

$$Re = \frac{\rho n d i^2}{\eta} \quad (8)$$

6.1.4.3 Pumping capacity

The impeller pumping capacity (V_p), was obtained using Eq. 9 [7]. This is the liquid volume that is given-off from the stirrer per unit time (m^3s^{-1}).

$$V_p = N_f n d_i^3 \quad (9)$$

Where N_f is the flow number ($N_f = 0.72$ for Rushton turbine and low viscosity fluid), d_i is the impeller diameter and n is the impeller speed.

6.1.4.4 Fluid circulation time

The fluid circulation time (t_c), is a function of the volume of the liquid phase (V_L) and pumping capacity (V_p) [7]. This was determined by Eq. 10 below;

$$t_c = V_L / V_p \quad (10)$$

6.1.4.5 Scale of turbulence determination

Broth homogeneity and fluid material transfer are two variables whose influence are proportionate to eddies bulk liquid break up and it is a function of input power. The breaking up of eddies bulk liquid or scale of turbulence was computed by Kolmogorov scale of turbulence, λ using Eq. 11.

$$\lambda = \left(\frac{V^3}{\varepsilon}\right)^{1/4} \quad (11)$$

where:

λ = size of eddies

V = viscosity

ε = turbulence energy per unit mass of liquid

$\varepsilon = N \rho n^3 d_i^2$

6.1.4.6 Shear stress

The shear stress resulting from the mixing system was obtained by Eq. 12, where n is the mixing speed and k is the empirical constant for a standard Rushton impeller ($k = 10$ for Rushton turbine) [6].

$$\gamma = kn \quad (12)$$

6.1.4.7 Non dimensional bioreactor configuration

This set of dimensionless numbers was computed using Eq. 13-16 [20]. Dimensionless number; Froude number expresses the ratio of centrifugal to gravitational forces, while the Volume number and the Geometric number depict the ratio of impeller diameter (agitation diameter) to bioreactor diameter in relation to the filling volume and the Galilei number relates the height of the liquid surface during agitation as a function of the ratio of gravitational force to the liquid kinematic viscosity.

$$Froude\ number = \frac{n^2 \cdot d_o}{g} \quad (13)$$

$$Volume\ number = V_L/d^3 \quad (14)$$

$$Geometric\ number = d_o/d \quad (15)$$

$$Galilei\ number = \frac{d^3 \cdot g}{v^2} \quad (16)$$

Where d (m) is the bioreactor diameter, d_o (m) the agitation diameter, n (s^{-1}) the shaking frequency, V_L (m^3) the liquid volume, v (m^2/s) the kinematic viscosity and g (m/s^2) the gravitational acceleration.

Table 6.0: Bioreactor geometry employed in the scale-up fermentation processes

| Bioreactor configurations | 2 L scale | 10 L scale |
|-----------------------------------------------|------------------------|------------------------|
| Bioreactor capacity (m ³) | 0.002 | 0.010 |
| Working volume (m ³) | 0.001 | 0.005 |
| Bioreactor height [h] (m) | 0.237 | 0.427 |
| Bioreactor diameter [D] (m) | 0.125 | 0.200 |
| Static height of broth [H] (m) | 0.084 | 0.162 |
| Number of impellers (N) | 1 | 2 |
| Impeller diameter [di] (m) | 0.054 | 0.070 |
| Impeller thickness (m) | 0.001 | 0.002 |
| Geometric factor (fc) | 0.633 | 0.857 |
| Geometric number | 0.432 | 0.350 |
| Geometric ratio (h/D) | 1.9:1 | 2.1:1 |
| Power number (Np) | 5.20 | 10.40 |
| Broth density [ρ] (kg/m ³) | 1013 | 1013 |
| Broth viscosity [η] (Pa s) | 9.173×10^{-5} | 9.173×10^{-5} |
| Volume number | 512000 | 625000 |
| Galilei number | 2.28×10^{-6} | 9.33×10^{-6} |
| Impeller type | Rushton turbine | Rushton turbine |

Table 6.1: Rheology and hydrodynamic parameters of scale-up fermentation criteria

| | 2 L control bioreactor | 10 L bioreactor | |
|------------------------------|-------------------------------|--------------------------------------|-----------------------|
| Parameters | | Constant v_{tip} | Constant P/V |
| n (rpm/rps) | 120/2 | 93/1.55 | 95/1.58 |
| V_{tip} (m/s) | 0.34 | 0.34 | 0.35 |
| Re | 3.86E + 06 | 5.03E + 06 | 5.14E + 06 |
| P (W) | 0.012 | 0.057 | 0.012 |
| P/ V_L (W/m ³) | 12 | 11 | 2.4 |
| V_P (m ³ /s) | 2.3×10^{-4} | 3.8×10^{-4} | 3.9×10^{-4} |
| t_c (s) | 4 | 13 | 12.8 |
| λ (m) | 4.25×10^{-4} | 3.80×10^{-4} | 3.75×10^{-4} |
| γ (1/s) | 1200 | 930 | 950 |
| Froude number | 0.022 | 0.017 | 0.018 |

6.2 Analytical Methods

The glucose concentration of both the enzymatic hydrolysate and the fermentation medium were obtained spectrophotometrically using standard Megazyme glucose kits (Megazyme Ltd, Ireland, United Kingdom).

Biomass dry weight (biomass concentration) was determined using a calibration standard curve; a correlation dependence on cell dry weight as a function of cell count [21].

Fermentation broth viscosity was determined as described by Pérez *et al.* [19]. While, the broth density was obtained as depicted by Deniz *et al.* [6]. The obtained viscosity and density values were used for the computation of non-gassed power (P), Reynold's number (Re), Kolmogorov scale (λ) and Galilei's number.

Bioethanol concentrations in broth samples were obtained using a Gas Chromatograph (Perkin Elmer GC Clarus 500, Auto sampler) equipped with a flame ionization detector. Instrument conditions: injector temperature; 200 °C, detector temperature; 250 °C, oven temperature; 150 °C (Isothermal), flowrate; 2.0 mL/min, split ratio; 1:50, injection volume; 0.5 μ L and 3 min run time.

Bioethanol productivity during the fermentation process was obtained as stated in Equation 18 below.

$$\text{Bioethanol productivity (g/L/h)} = \frac{\text{Maximum ethanol concentration (g/L)}}{\text{Time (h)}} \quad (17)$$

The specific growth rates (μ) of *S. cerevisiae* were calculated using Equation 19, where X_2 and X_1 are biomass dry weights (g/L) at t_2 and t_1 , respectively.

$$\text{Specific growth rate } (\mu) = \frac{\ln X_2 - \ln X_1}{t_2 - t_1} \quad (18)$$

Additionally, the logistic model equation (Eq. 20) was used to define the correlation of cell dry weight (X), at definite time (t) in the course of active cell growth (log phase) and static phases

of cell growth to initial cell dry weight (X_0), maximum cell dry weight (X_{max}) and maximum specific growth rate (μ_{max}) during the scale up process.

$$X = \frac{X_0 \cdot \exp(\mu_{max} \cdot t)}{1 - \left(\frac{X_0}{X_{max}}\right) \cdot (1 - \exp(\mu_{max} \cdot t))} \quad (19)$$

While, the empirical data on ethanol production were used to fit the modified Gompertz model. This kinetic model relate the production lag time, the maximum bioethanol production rate, and the potential maximum bioethanol concentration as shown in Eq. 20.

$$P = P_m \cdot \exp \left\{ - \exp \left[\frac{r_{p,m} \cdot \exp(1)}{P_m} \right] \cdot (t_L - t) + 1 \right\} \quad (20)$$

where P represent the bioethanol concentration (g/L), P_m is the potential highest bioethanol concentration (g/L), $r_{p,m}$ is the highest bioethanol production rate (g/L/h) and t_L is the period from the start of the fermentation process to the log phase of bioethanol production (h).

Inhibitory volatile compounds of the fermentation broth were analysed using Varian 3800 gas chromatography (California, USA) coupled Varian 1200 mass spectrometry (GC–MS). Gas chromatography operational conditions: column of 30 m x 0.25 mm internal diameter x 0.25 μ m film thickness, injector temperature; 40 $^{\circ}$ C, detector temperature; 240 $^{\circ}$ C, oven temperature; 200 $^{\circ}$ C (Isothermal), flowrate; 1.0 mL/min, split ratio; 1:20, injection volume; 0.4 μ L and 3 min run time [22].

6.3 Results and Discussion

6.3.1 The effects of scaling-up on process performance

The experimental profiles for glucose consumption, process pH, biomass concentration and ethanol concentration in the 5 L scale fermentation with constant impeller tip speed (V_{tip}) and power consumption (P/V) as scale-up criteria are presented in Fig 6.1, 6.2, 6.3 and 6.4. As shown in Fig 6.1, *S. cerevisiae* BY4743 effectively utilise glucose within 36 h of fermentation for both constant V_{tip} and P/V , reflecting the impact of a suitable reactor mixing on substrate utilization. A good mixing regime favours mass transfer and nutrients consumption rate [7]. The rate of cellular glucose uptake and utilisation is a regulating step in the optimal functioning

of the Embden-Meyerhof-Parnas pathway, thus impact on the efficiency of ethanol fermentation and productivity. The pH silhouettes for both scales are depicted in Fig. 6.2. Higher ethanol concentrations were achieved above pH 4.86, which occurred between the 24 h and 36 h in the 5 L scale reactors. This also corresponded with the efficient glucose utilization mentioned above. Moreover, yeast especially *Saccharomyces cerevisiae* is well-known to produce bioethanol optimally at pH of 4.5-5.5. A pH beyond this range might affect the optimal functioning of plasma membrane-bound proteins, this includes enzymes and transport proteins [21]. Bioethanol fermentation process results from a sequence of organised enzymatic reactions. This process is thermodynamically balance and required provided that cellular-enzymes use up the net phosphorylated nucleotide produced from substrate level phosphorylation [7]. Additionally, pH plays a vital role in ethanol production by regulating cell metabolic activities. Volatile metabolite formation usually results in the reduction of the buffering capacity of the system with a concurrent change in pH leading to process inhibition. In the current study, the buffering capacity was enhanced due to the inclusion of NiO nanoparticles, and the pH was maintained above 4.86. The presence of nanoparticles potential influences the volatile metabolite pathways through the system buffering capacity. This phenomenon has been observed in other studies [23, 24, 8]. Furthermore, the biomass dry weight (gL^{-1}) increased precipitously in the early hours (3-12 h) of fermentation, this coincided with ethanol production during this period and then proceeded a little until the 36 h (Fig. 6.3). The maximum dry-cell mass of 4.57 and 4.77 gL^{-1} were obtained for constant P/V and V_{tip} respectively, which were slightly lower than that obtained in the 1 L scale (5.07 gL^{-1}). The difference in dry-cell mass was presumably caused by the variation in the fermentation environment which might be detrimental to cell viability and growth [6, 25]. Meanwhile, the ethanol concentration was higher in the 5 L scale for P/V (25.10 gL^{-1}) and V_{tip} , (24.60 gL^{-1}), compared to the 1 L scale (24.50 gL^{-1}). Bioethanol production increased from zero hour till the

24th h, afterwards there was a decline in bioethanol concentration for all the systems (Fig. 6.4). The decrease in bioethanol production could be ascribed to the depletion of fermentable sugar (glucose), nutrient, formation of inhibitory compounds and reduction in the pH of the system. The disparity in bioethanol response under various scales may be ascribed to differences in rheological characteristics within the reactor at different scales (Tables 6.0 and 6.1). The rheological characteristics of fermenting broth changes during fermentation process, as biomass and products accumulate [19]. Thus, the velocity and turbulence of fluid send-off the stirrer need to be adequate to transport material into the most remote sections of the reactor to ensure and maintain effective mixing regime. Mixing effects on metabolic activities and productivity could be pronounced, in a very considerable extend, determines the performance of a reactor.

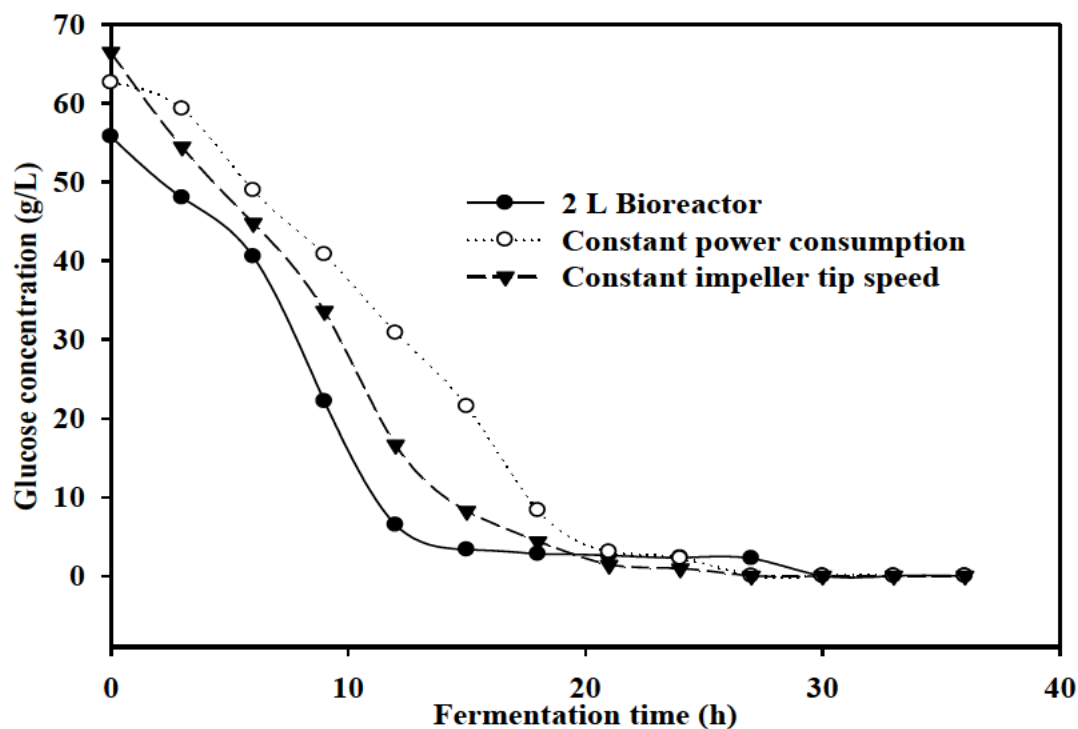


Figure 6.1: Schematic description of glucose consumption from the scale-up variations using constant P/V and V_{tip}

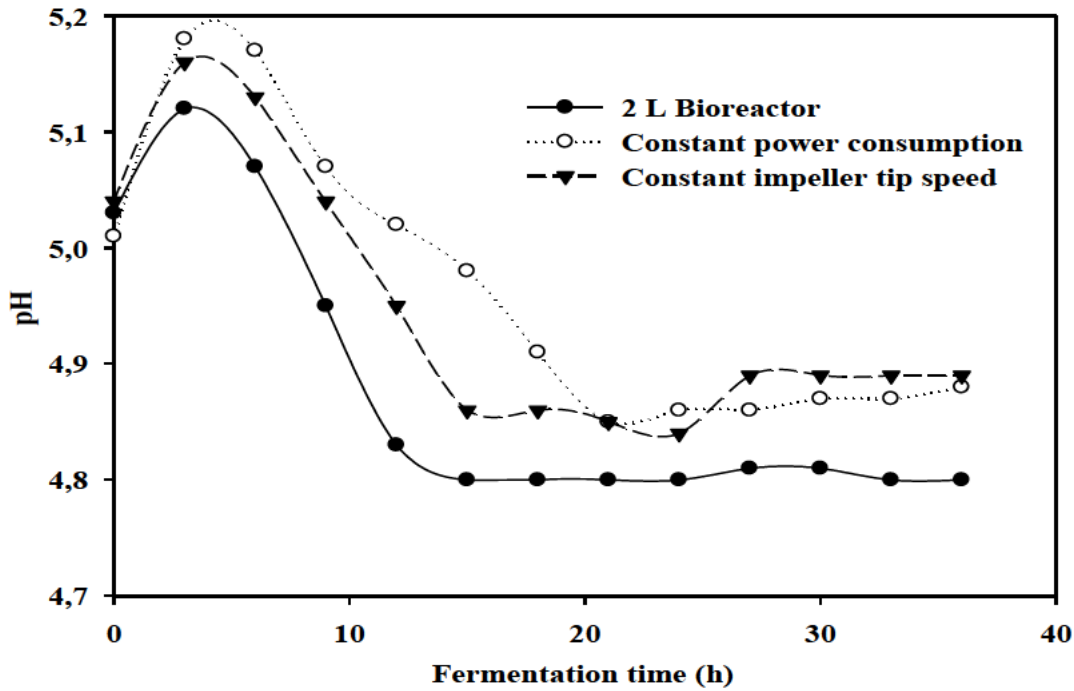


Figure 6.2: pH evolution profile during the bioethanol fermentation at 1 L and 5 L scale

6.3.2 Scaling-up based on constant power consumption (P/V)

In the present study, using the constant power consumption criterion, the size of eddies was computed to be 3.75×10^{-4} m which was considerably bigger than an average *S. cerevisiae* size. When the Kolmogorov eddy size equals the cell diameter or gets smaller, as a rule of thumb, the flow lines pattern could shear fermenting cells [6]. On the other hand, smaller eddies, facilitates rapid transfer of material, which is proportionate to the power input. The greater the power input (ϵ) to the fermenting broth, the smaller the eddies, the better the mixing regime and consequently, the better the system productivity [7]. Similarly, the power number for the current scale up was 5.20 at fully turbulent flow for Rushton-turbine impeller design and 10 for the typical experiential constant (k) for a conventional Rushton-turbine impeller [6]. Power consumption per unit volume (P/V_L) is the degree of mixing intensity and mass transfer rate. The increase in impeller tip speed from the 1 L scale control reactor to 5 L scale bioreactor was

considered negligible, since the P/V_L ratio in the constant P/V system was lesser than the constant V_{ip} system (Table 6.1). The observed outcome was in agreement with the studies of Deniz *et al.* [6] and Perez *et al.* [19]. For instance, scale-up based on maintaining P/V occasioned an increase of the shear rate of 2.2%, as compared to keeping impeller tip speed constant. This increase in the shear stress may be associated with an increase in the probable cell impairment and consequently, decrease in ethanol productivity of desired interest. Although, excess shear stress could result in the loss of cell viability and disruption, a certain degree of shear rate is necessary to achieve appropriate transfer of materials and energy within the bioreactor. These aforementioned parameters offer specific information concerning the mixing system, suggesting the optimum hydrodynamic regime and predicting the modification of mixing efficiency induced by the scale-up strategy employed [26]. Additionally, the liquid volume that was dismissed from the stirrer per unit time (V_p) (Table 6.1) and the circulation time (t_c), another important quantitative mixing characteristics were apparent sufficient and efficient to obtain good mixing. This must have contributed to the process performance using constant P/V .

Furthermore, based on constant P/V , maximum ethanol concentration of 25.10 gL^{-1} was obtained after 24 h. This was 1.02 fold higher in comparison to the 1 L scale stirred bioreactor. Moreover, a significant difference in ethanol productivity was observed in the 5 L and 1 L scales when constant P/V was implemented. The productivity ($1.10 \text{ gL}^{-1}\text{h}^{-1}$) was 1.38 fold higher and the fermentation period to achieve this was shorter compared to the 1 L scale control experiment (Fig. 6.4). These can be elucidated from the mixing view point of the homogenization level: macromixing, mesomixing, and micromixing [27]. Regardless of the flow regime achieved in the 5 L scale set up, the flow will remain laminar at micromixing scale, due to its larger surface area and double impeller system employed [28]. Moreover, meso and micromixing are known to be important processes for bioprocesses biochemical reactions.

Hence, it attained a mixing regime needed for optimal process parameters (pH, temperature, absorption, nutrient distribution and uptake) to reach a beneficial productive level. Furthermore, the current observed ethanol productivity could be attributed to the synergistic effect of NiO nano-additives and the mixing regime (mixing intensity, pumping capacity and the circulation time) on *S. cerevisiae* metabolic activities. This in turn impacts cell growth and overall fermentation performance. A suitable mixing regime will promote a wide distribution of nano-glucose composite within the bioreactor [25, 29, 30]. NiO nanoparticle has the potential to positively bond with glucose [31, 9], and enhanced cell to glucose contact could improve the process performance [32, 8]. Additionally, nanoparticles are known to promote the cell affinity for glucose, efficient sugar utilization, cellular growth and metabolic activities [32, 9].

Deniz *et al.* [6], using *Escherichia coli* K011 and quince pomace as substrate for scaling up from 2 L to 8 L bioreactor, reported maximum ethanol productivity of 0.49 gL⁻¹h⁻¹ based on constant mixing time which was 2.24 fold lower in ethanol productivity in comparison to the current study. Similarly, de la Roza *et al.* [33], obtained a lower volumetric ethanol productivity (0.015 g/L/h) by *S. cerevisiae* in a 13 L semi-pilot scale production. This is 73 fold lower compared to the current study. Usually bioprocessing productivity is a significant factor to assess the cost-effectiveness of a large scale production. The obtained bioethanol productivity in this study is highly desirable, particularly for industrial bioethanol production from potato peel waste.

Table 6.2: Parameters for scale-up studies of ethanol production from potato peels

| 2 L control bioreactor | | 10 L bioreactor | |
|-----------------------------------------------------------|-------|--------------------|----------------|
| Parameters | | Constant V_{tip} | Constant P/V |
| Fermentation performance | | | |
| Bioethanol concentration (gL^{-1}) | 24.50 | 24.60 | 25.10 |
| Bioethanol productivity ($\text{gL}^{-1}\text{h}^{-1}$) | 0.80 | 0.70 | 1.10 |
| Kinetic performance | | | |
| Logistic function Model | | | |
| X_o (gL^{-1}) | 0.48 | 0.54 | 0.54 |
| X_{\max} (gL^{-1}) | 5.07 | 4.77 | 4.57 |
| μ (h^{-1}) | 0.14 | 0.16 | 0.14 |
| μ_{\max} (h^{-1}) | 0.31 | 0.24 | 0.24 |
| R^2 | 0.99 | 0.98 | 0.98 |
| Modified Gompertz Model | | | |
| P_m (gL^{-1}) | 23.97 | 23.81 | 25.29 |
| $r_{p,m}$ ($\text{gh}^{-1}\text{L}^{-1}$) | 2.12 | 2.01 | 2.00 |
| t_L (h) | 2.58 | 3.00 | 3.89 |
| R^2 | 0.99 | 0.97 | 0.98 |

6.3.3 Scaling-up based on constant impeller tip speed (v_{tip})

The ethanol concentration of 24.6 gL^{-1} was obtained based on constant V_{tip} experiment which was 2% lower than the value obtained with constant P/V experiment (Table 6.2). The volumetric ethanol productivity based on constant V_{tip} was also considerably lower when compared to the 1 L scale bioreactor and the constant P/V experiment, 14% and 57%, respectively. This result may be ascribed to the lower mixing rate employed due to constant V_{tip} at 5 L scale. Though, the stirrer tip speed scale-up parameter has some benefits in the instance of processes with shear susceptible microbes, nonetheless it is also disputed that it is not a suitable parameter for scaling up. This is in agreement with the current study. The intensity of agitation reduces with the increase of the production scale [19]. Unfortunately it is physically impracticable to sustain similar process parameters for laboratory scale, pilot scale and industrial scale reactors due to the fact that physical processes are dimensionally related while metabolic processes are circuitously scale dependent. This in some cases might lead to improper mixing regime, resulting in lower concentrations of cell dry-weight and ethanol concentration as obtained with constant V_{tip} in this study. In a related study, Obonna *et al.* [34],

also, reported similar or lesser mixing speed employed in a 2 L stirred-bioreactor was not appropriate for 8 L stirred-bioreactor. Hence, the cells and the substrate were not homogeneously dispersed leading to declined bioethanol productivity. Mixing rate could influence the mass transfer and temperature gradient homogeneity negatively for viscous fermentation broth of ethanol production [6]. This lower productivity based on constant V_{tip} can further be elucidated by the reduction of turbulent-flow which was confirmed by the decrease in P/V_L value (Table 6.1). Also, studies have shown, when a scale-up approach occasioned a higher Reynolds number as observed in the present study, a low P/V_L value is achieved. This is not adequate for efficient admixing, hence, productivity rate is adversely affected. In other words, a longer mixing-time might be achieved with constant V_{tip} experiment that subsequently affected ethanol productivity unfavourably. This effect might be due to the phenomena that longer mixing-time may possibly influenced the mass transfer unfavourably, leading to apparent death regions within the bioreactor [6]. The probable occurrence of death regions in the 5 L scale bioreactor could have resulted in lower cell biomass and product yield upon scaling-up based on constant V_{tip} (Table 6.2). The biomass dry weight based on constant V_{tip} experiment was 6% lower than the 1 L control reactor experiment (Fig. 6.3). This decreased level of biomass growths in the 5 L scale bioreactor based on constant V_{tip} experiment may further be ascribed to poor gaseous–liquid diffusion observed at the lower stirrer speed with the higher Kolmogorov eddy size (Table 6.1). It is worth mentioning that, as impeller speed declined in scaling up process, eddy size increased for bioethanol production by *S. cerevisiae*. Furthermore, the observed low productivity when constant V_{tip} was employed, can also be ascribed to the fluctuating pH during the fermentation process (Fig. 6.2), given that, microbial ethanol production is a pH sensitive process [32].

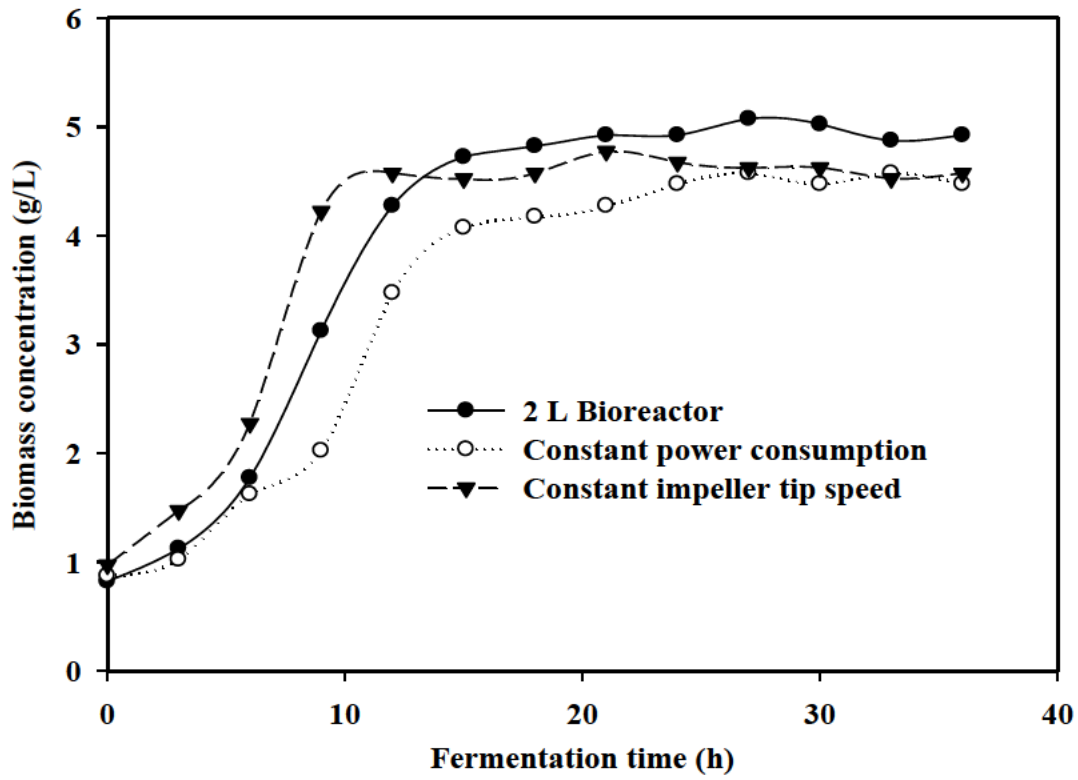


Figure 6.3: *Saccharomyces cerevisiae* biomass dry weight based on constant P/V and V_{tip}

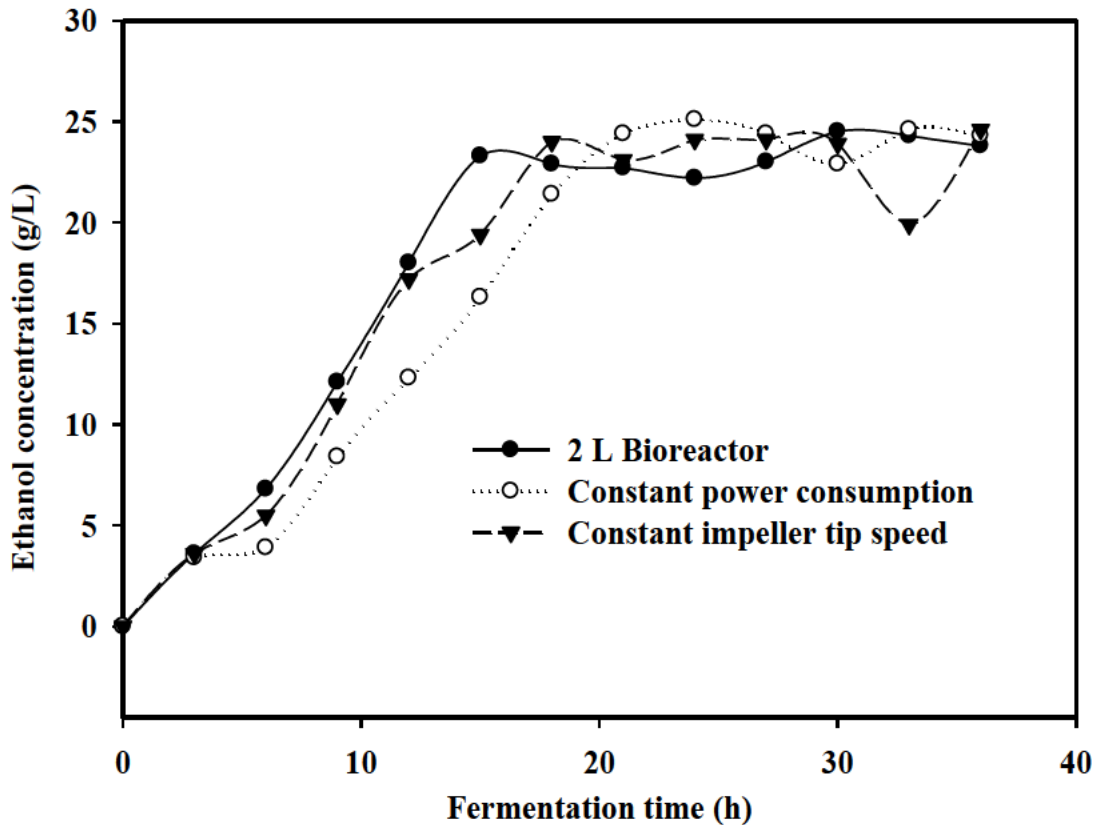


Figure 6.4: Representation of bioethanol production depicting the impact of constant P/V and V_{tip}

6.3.4 Logistic function growth kinetics of *S. cerevisiae*

Experimental data from the cell dry weight over time for both scales were fitted into the logistic function model with a high correlation coefficients (R^2) >0.98 . This shows the suitability of logistic function to describe the growth of *S. cerevisiae* BY4743 employing these scale-up criteria. A little lower maximum biomass dry weight (X_{max}) and maximum specific growth rate (μ_{max}) were achieved with V_{tip} and P/V when compared to the control set-up (Table 6.2). Even though insignificant lesser value of X_{max} and μ_{max} were achieved in the 5 L scale bioreactor, higher bioethanol concentration and productivity were observed in contrast with the 1 L scale control experiment. Suggesting the scale up criteria largely provide suitable process condition that favoured *S. cerevisiae* BY4743 ethanol production [1]. Scale up criteria that favour both

S. cerevisiae BY4743 growth and ethanol formation could improve cell growth rate, cell dry weight and further increase bioethanol production.

6.3.5 Modified Gompertz function kinetics of bioethanol production

Empirical data on ethanol formation over the fermentation period (Fig. 6.4) fit the modified Gompertz function with R^2 values > 0.97 for V_{tip} , P/V and the 1 L scale control experiment. The shortest lag period of 2.58 h was observed in the 1 L scale bioreactor compared to 3.00 h and 3.89 h for the V_{tip} , and the P/V respectively. The differences in ethanol production lag time could be ascribed to changing microenvironment surrounding the cell [25, 7]. An actively growing cell with hundreds enzyme-catalysed reactions, structured into organized sequences-metabolic pathways, are likely to be influenced due to the fluctuating environment and might affect vital cell traits require for optimal process performance [1, 7, 25]. On the other hand, P/V gave highest potential bioethanol concentration (P_m) of 25.29 gL⁻¹ as against 23.97 gL⁻¹ of the 1 L scale control system. The observed higher P_m value in the 5 L scale bioreactor may be attributed to good mixing that resulted in a suitable mixing regime and subsequently desirable process performance based on P/V . This has the capacity to cause metabolic-shifts within the cell towards bioethanol formation.

Table 6.3: Comparative amount (g/L) of the profile of volatile compounds obtained scaling up using P/V and V_{tip}

| Compounds | Concentration (g/L) | | | Concentration (%) | | |
|---------------------------------------------------|---------------------|-----------|---------|-------------------|-----------|---------|
| | P/V | V_{tip} | Control | P/V | V_{tip} | Control |
| Amines | | | | | | |
| 2-methyl-pyridine | 0 | 0 | 0.043 | 0 | 0 | 0.390 |
| 3-methyl-pyridine | 0.084 | 0 | 0.157 | 0.629 | 0 | 1.408 |
| 3-Hydroxy-6-methylpyridazine | 0.039 | 0 | 0.094 | 0.295 | 0 | 0.844 |
| Amides | | | | | | |
| Acetamide | 0 | 0.021 | 0.058 | 0 | 0.107 | 0.520 |
| Alcohols | | | | | | |
| 3-Methyl-1-butanol | 0.306 | 0.304 | 0.360 | 2.305 | 1.571 | 3.235 |
| 2-Furanmethanol | 0.211 | 0.094 | 0.155 | 1.585 | 0.484 | 1.391 |
| 5-Methyl-2-furanmethanol | 0.029 | 0 | 0 | 0.220 | 0 | 0 |
| 3-(methylthio)-1-Propanol | 0.050 | 0.348 | 0.034 | 0.376 | 1.795 | 0.309 |
| 1-(2-Furyl)-1,2-ethanediol | 0.841 | 0.880 | 0.272 | 6.332 | 4.540 | 2.447 |
| Phenylethyl Alcohol | 0.265 | 0.191 | 0.144 | 1.994 | 0.984 | 1.294 |
| Maltol | 0.208 | 0.314 | 0.188 | 1.562 | 1.622 | 1.688 |
| Aldehydes | | | | | | |
| Fufural | 0.032 | 0.053 | 0.030 | 0.240 | 0.275 | 0.268 |
| 5-Methyl-fufural | 0.306 | 0.020 | 0.383 | 2.300 | 0.104 | 3.441 |
| Aliphatic acids | | | | | | |
| Acetic acid | 8.042 | 13.463 | 7.167 | 60.517 | 69.483 | 64.429 |
| Propanoic acid | 0.056 | 0.137 | 0.046 | 0.425 | 0.708 | 0.411 |
| 4-Hydroxybutanoic acid | 0.074 | 0.104 | 0.060 | 0.558 | 0.535 | 0.542 |
| 4-Oxo-pentanoic acid | 0.080 | 0.022 | 0.065 | 0.604 | 0.113 | 0.580 |
| Butanoic acid | 0 | 0.508 | 0 | 0 | 2.621 | 0 |
| 2-Methylpropanoic acid | 0.014 | 0 | 0 | 0.107 | 0 | 0 |
| Hexanoic acid | 0.024 | 0.053 | 0.029 | 0.183 | 0.276 | 0.258 |
| Sorbic acid | 0.176 | 0.109 | 0.054 | 1.324 | 0.563 | 0.488 |
| Octanoic acid | 0 | 0.106 | 0 | 0 | 0.545 | 0 |
| Pentanoic acid | 0 | 0.071 | 0 | 0 | 0.364 | 0 |
| Benzenoids | | | | | | |
| Benzeneacetaldehyde | 0.260 | 0.271 | 0.221 | 1.960 | 1.399 | 1.986 |
| Benzoic acid | 0.122 | 0.073 | 0.094 | 0.918 | 0.378 | 0.849 |
| Ketones | | | | | | |
| 1-Hydroxy-2-propanone | 0.032 | 0.036 | 0 | 0.237 | 0.187 | 0 |
| Ethenone, 1-(2-furanyl) | 0.047 | 0.014 | 0.048 | 0.357 | 0.075 | 0.429 |
| 2-Pyrrolidinone, 1-methyl | 0.020 | 0.021 | 0.013 | 0.149 | 0.106 | 0.118 |
| 2,5-Dimethyl-4-hydroxy-3(2H)-furanone | 0.203 | 0.295 | 0.147 | 1.529 | 1.521 | 1.320 |
| 2,3-dihydro-3,5-dihydroxy-6-methyl-4H-Pyran-4-one | 1.199 | 1.237 | 0.854 | 9.024 | 6.382 | 7.674 |
| 4,5-Dimethyl-1,3-dioxol-2-one | 0.322 | 0.292 | 0.168 | 2.423 | 1.507 | 1.508 |
| 2-Hydroxy-5-methylacetophenone | 0 | 0.045 | 0.023 | 0 | 0.234 | 0.202 |
| Dihydro-4-hydroxy-2-(3H)-furanone | 0.216 | 0.273 | 0.187 | 1.623 | 1.410 | 1.684 |
| Lactones | | | | | | |
| 2(5H)-Furanone | 0.030 | 0.021 | 0.032 | 0.225 | 0.111 | 0.285 |

6.3.6 Volatile compound distribution

Organic acids, alcohols and ketones were the major groups of volatile metabolite compound observed, as well as lower portions of aldehydes, benzenoids, lactones, amino group and amide functional group (Table 6.3). Presence of volatile metabolic compounds generally results from the classes and concentrations of enzymes and co-factors present, thus, from enzyme control mechanisms, and the necessity to maintain a constant pH intracellularly [35, 9]. This enzymatic activity could be affected by the scaling up process conditions [7]. As mentioned earlier, an actively growing cell with hundreds enzyme-catalysed reactions, are likely to be influenced due to changing process environment [7]. The largest metabolite portion observed was the aliphatic acids, up to 63% and 75% in the P/V and V_{tip} bioreactors respectively, and 67% in the 1 L scale control bioreactor. Acetic acid constitutes a substantial fraction of 61, 69, and 64% in the P/V , V_{tip} bioreactors and the control set up respectively. Comparable portion of acetic acid was observed based on constant P/V but to a lesser extent (61%). This accounted for the high ethanol productivity, which was probably achieved due to good mixing effect attained using P/V as a scale up criterion. As aforementioned above, good mixing results in suitable process condition, hence desirable process performance. Typically, the major organic acid in yeast bioethanol fermentation process is the acetic acid and it is formed early in process. This agrees with the result obtained in the current study, where high concentration of acetic acid was observed. Its dissociation could lead to decline in the pH which could eventually impede cellular and metabolic activity and process productivity [36]. Moreover, acid-forming pathway obviously dominated the fermenting yeast metabolic flow in all the bioreactors in the present study (Table 6.3). Acetic acid (61%), Sorbic acid (1.3%) in the P/V bioreactor, and acetic acid (69%), Propanoic acid (0.71%) in the V_{tip} bioreactor were the main acidic compounds in these systems, with acetic acid (64%), 4-Oxo-pentanoic acid (0.58%) being the dominant organic acid in the 1 L scale control set up. The occurrence of these organic acids could result in the

build-up of anions owing to their dissociation; a harmful intra-cellular state, that affects biomass formation and consequently, inhibit bioethanol formation [37, 36].

The next highest portion of the volatile metabolite silhouette is the organic-alcohols (keeping out ethanol), with 1-(2-Furyl)-1,2-ethanediol (in both P/V (0.841 g/L) and V_{tip} (0.880 g/L) bioreactor) being the foremost. Alcohols are the derivatives of various bioprocesses, this includes carbohydrate metabolism, acetic acid degradation and breaking down of acetaldehyde [38]. Increase in the formation of other organic-alcohols could also occasion the decline in bioethanol formation via deviance of metabolic pathway from bioethanol formation. Therefore, the choice of suitable scale up criterion that favours ethanol formation pathway is important. In this case constant P/V , where the rheological and the hydrodynamic characteristic as well as the inclusion of NiO nanoparticles attained this condition. This was evident in the higher ethanol concentration and productivity (1.02 and 1.57 fold increase, respectively) observed in comparison to constant V_{tip} criterion employed.

The other large group present was the ketones. The constant P/V system had highest percentage of ketones (15%, 2.039 g/L) compared to V_{tip} system (11%, 2.213 g/L) and the 1 L scale control experiment (13%, 1.440 g/L). This probably account for the highest lag time observed when constant P/V was employed (Table 6.2). Ketones like other volatile metabolites, could cause an elongated lag period in microbial growth. Therefore, hampering ethanol production and consequently overall process performance.

6.4 Conclusion

This study has provided a coherent mathematical model for translating an optimized laboratory scale bioethanol fermentation to a pilot scale successfully. It was demonstrated that the application of constant P/V is a better approach in scaling up bioethanol production from potato peels fermentation supplemented with NiO nano-biocatalyst. This was due to the importance of suitable mixing regime and homogeneity. Evidently, by maintaining constant P/V , higher

productivity (1.10 g/L/h) and significant reduction in the formation of process inhibitors were achieved. These findings highlight the potential of industrial valorisation of waste potato peels supplemented with NiO nanoparticles for bioethanol production.

References

- [1] J. Xia, G. Wang, J. Lin, Y. Wang, J. Chu, Y. Zhuang S. Zhang, Advances and Practices of Bioprocess Scale-up. *Advances in Biochemical Engineering/Biotechnology*, (2015), https://doi.org/10.1007/10_2014_293.
- [2] G. Izmirliloglu, A. Demirci, Ethanol Production from Waste Potato Mash by Using *Saccharomyces Cerevisiae*, *Applied Science*, 2, (2012) 738-753, <https://doi.org/10.3390/app2040738>.
- [3] B.J. Khawla, M. Sameh, G. Imen, F. Donyes, G. Dhouha, E.G. Raoudha, N-E. Oumèma, Potato peel as feedstock for bioethanol production: A comparison of acidic and enzymatic hydrolysis. *Industrial Crops and Products*, 52 (2014) 144–149, <http://dx.doi.org/10.1016/j.indcrop.2013.10.025>.
- [4] F.D. Faloye, E.B. Gueguim Kana, S. Schmidt, Optimization of biohydrogen inoculum development via a hybrid pH and microwave treatment technique - Semi pilot scale production assessment. *International Journal of Hydrogen Energy*, 39 (2014) 5607-5616, <http://dx.doi.org/10.1016/j.enconman.2017.08.046>.
- [5] N.A. Chohan, G.S. Aruwajoye, Y. Sewsynker-Sukai, E.B. Gueguim Kana, Valorisation of potato peel wastes for bioethanol production using simultaneous saccharification and fermentation: Process optimization and kinetic assessment, *Renewable Energy*, 146 (2020) 1031-1040, <https://doi.org/10.1016/j.renene.2019.07.042>.
- [6] I. Deniz, E. Imamoglu, F. Vardar Sukan, Evaluation of scale-up parameters of bioethanol production from *Escherichia coli* KO11, *Turkish Journal of Biochemistry*, 40 (1) (2015) 74–80, <https://doi.org/10.5505/tjb.2015.33603>.
- [7] M.E. Qazizada, Design of a batch stirred fermenter for ethanol production, *Procedia Engineering*, 149 (2016) 389–403, <http://creativecommons.org/licenses/by-nc-nd/4.0/>.

- [8] A.I. Sanusi, F.D. Faloye, E.B. Gueguim Kana, Impact of Various Metallic Oxide Nanoparticles on Ethanol Production by *Saccharomyces cerevisiae* BY4743: Screening, Kinetic Study and Validation on Potato Waste, *Catalysis Letters*, 149 (7) (2019) 2015–2031, <https://doi.org/10.1007/s10562-019-02796-6>.
- [9] A.I. Sanusi, T.N. Suinyuy, A. Lateef, E.A. Gueguim Kana, Effect of nickel oxide nanoparticles on bioethanol production: Process optimization, kinetic and metabolic studies, *Process Biochemistry*, 92 (2020) 386–400. <https://doi.org/10.1016/j.procbio.2020.01.029>.
- [10] W. Babel, U. Brinkmann, R. Müller, The auxiliary substrate concept—an approach for overcoming limits of microbial performances, *Acta Biotechnologica*, 13 (3 (1993) 211–242, <https://doi.org/10.1002/abio.370130302>.
- [11] M.P. Marques, J. Cabral, P. Fernandes, Bioprocess scale-up: quest for the parameters to be used as criterion to move from microreactors to lab-scale. *Journal of Chemical Technology and Biotechnology*, 85 (2010) 1184–98. <https://doi.org/10.1002/jctb.2387>.
- [12] F. Garcia-Ochoa, E. Gomez, Bioreactor scale-up and oxygen transfer rate in microbial processes: An overview. *Biotechnology Advances*, 27 (2009) 153–176, <https://doi.org/10.1016/j.biotechadv.2008.10.006>.
- [13] D. Arapoglou, Th. Varzakas, A. Vlyssides, C. Israilides, Ethanol production from potato peel waste (PPW), *Waste Management*, 30 (2010) 1898–1902, <https://doi.org/10.1016/j.wasman.2010.04.017>.
- [14] Y. Kim, H. Lee, Use of magnetic nanoparticles to enhance bioethanol production in syngas fermentation. *Bioresource Technology*, 204 (2016) 139–144, <https://doi.org/10.1016/j.biortech.2016.01.001>.
- [15] F.A. Gonçalves, H.A. Ruiz, E.S. dos Santos, J.A. Teixeira, G.R. de Macedo, Bioethanol production by *Saccharomyces cerevisiae*, *Pichia stipitis* and *Zymomonas mobilis* from

- delignified coconut fibre mature and lignin extraction according to biorefinery concept. *Renewable Energy*, 94 (2016) 353–365, <https://doi.org/10.1016/j.renene.2016.03.045>.
- [16] K.E.J. Tyo, K. Kocharin, J. Nielsen, Toward design-based engineering of industrial microbes. *Current Opinion Microbiology*, 13 (3) (2020) 255–262, <https://doi.org/10.1016/j.mib.2010.02.001>.
- [17] G.S. Aruwajoye, F.D. Faloye, E.B. Gueguim Kana, Soaking assisted thermal pre-treatment of cassava peels wastes for fermentable sugar production: Process modelling and optimization, *Energy Conversion and Management*, 150 (2017) 558–56, <http://dx.doi.org/10.1016/j.ijhydene.2014.01.163>.
- [18] P.M. Bonvillani, P. Ferrari, E.M. Ducrós, J.A. Orejas, Theoretical and Experimental Study of the Effects of Scale-Up on Mixing time for a Stirred-Tank Bioreactor, *Brazilian Journal of Chemical Engineering*, 23 (1) (2006) 1-7, <http://doi.org/10.1590/S0104-66322006000100001>.
- [19] R.P. Pérez, J.G. Suárez, E.N. Diaz, R.S. Rodríguez, E.C. Menéndez, H.D. Balaguer, A.M. Lasa, Scaling-up fermentation of *Escherichia coli* for production of recombinant P64k protein from *Neisseria meningitidis*, *Electronic Journal of Biotechnology*, 33 (2018) 29–35, <https://doi.org/10.1016/j.ejbt.2018.03.004>.
- [20] W. Klöckner, R. Gacem, T. Anderlei, N. Raven, S. Schillberg, C. Lattermann, J. Büchs, *Journal of Biological Engineering*, 7 (2013) 28, <http://www.jbioleng.org/content/7/1/28>.
- [21] P. Moodley, E.B. Gueguim Kana, Bioethanol production from sugarcane leaf waste: Effect of various optimized pre-treatments and fermentation conditions on process kinetics, *Biotechnology Reports*, 24 (2019) xxx–xxx, <https://doi.org/10.1016/j.btre.2019.e00329>.

- [22] T.N. Suinyuy, J.S. Donaldson, S.D. Johnson, Patterns of odour emission, thermogenesis and pollinator activity in cones of an African cycad: what mechanisms apply? *Annals of Botany*, 112 (2013) 891–902, [http://doi: 10.1093/aob/mct159](http://doi:10.1093/aob/mct159).
- [23] H. Han, M. Cui, L. Wei, H. Yang, J. Shen, Enhancement effect of hematite nanoparticles on fermentative hydrogen production, *Bioresource Technology*, 102 (2011) 7903–7909, <http://doi:10.1016/j.biortech.2011.05.089>.
- [24] P. Wimonsong, R. Nitorisavut, Comparison of Different Catalysts for Fermentative Hydrogen Production, *Journal of Clean Energy Technologies*, 3 (2) (2015) 128–131, [http://doi: 10.7763/JOCET.2015.V3.181](http://doi:10.7763/JOCET.2015.V3.181).
- [25] T. Ma, A-C. Tsai, Y. Liu, Biomanufacturing of human mesenchymal stem cells in cell therapy: Influence of microenvironment on scalable expansion in bioreactors, *Biochemical Engineering Journal*, 108 (2016) 44-50, <https://doi.org/10.1016/j.bej.2015.07.014>.
- [26] C. Oniscu, A-L. Galaction, D. Cascaval, F. Ungureanu, Modeling of mixing in stirred bioreactors 2. Mixing time for non-aerated broths. *Biochemical Engineering Journal* 12 (2002) 61–69, PII: S1369-703X(02)00042-6.
- [27] W. Bujalski, Z. Jaworski, A.W. Nienow, CFD Study of Homogenization with Dual Rushton Turbines—Comparison with Experimental Results: Part II: The Multiple Reference Frame, *Chemical Engineering Research and Design*,. 80 (1) (2002) 97-104, <https://doi.org/10.1205/026387602753393402>.
- [28] A. Vincent, M. Meneguzzi, The dynamics of vorticity tubes in homogeneous turbulence. *Journal of Fluid Mechanics*, 258 (1994) 245-254, <https://doi.org/10.1017/S0022112094003319>.

- [29] K. Doriya, D.S. Kumar, Solid state fermentation of mixed substrate for l-asparaginase production using tray and in-house designed rotary bioreactor. *Biochemical Engineering Journal*, 138 (2018) 188–196, <https://doi.org/10.1016/j.bej.2018.07.024>.
- [30] T. Lawson, D.E. Kehoe, A.C. Schnitzler, P.J. Rapiejko, K.A. Der, K. Philbrick, S. Punreddy, S. Rigby, R. Smith, Q. Feng, J.R. Murrell, M.S. Rook, Process development for expansion of human mesenchymal stromal cells in a 50 L single-use stirred tank bioreactor. *Biochemical Engineering Journal*, 120 (2017) 49–62, <http://dx.doi.org/10.1016/j.bej.2016.11.020>.
- [31] M. El-Kemary, N. Nagy, I. El-Mehasseb, Nickel oxide nanoparticles: Synthesis and spectral studies of interactions with glucose. *Materials Science in Semiconductor Processing*, 16 (2013) 1747–1752, <http://dx.doi.org/10.1016/j.mssp.2013.05.018>.
- [32] D.K. Ban, S. Paul, Zinc Oxide Nanoparticles Modulates the Production of β -Glucosidase and Protects its Functional State Under Alcoholic Condition in *Saccharomyces cerevisiae*. *Applied Biochemistry and Biotechnology*, 173 (2014) 155–166, <http://doi.org/10.1007/s12010-014-0825-2>.
- [33] C. de la Roza, A. Laca, L.A. García, M. Díaz, Ethanol and ethyl acetate production during the cider fermentation from laboratory to industrial scale. *Process Biochemistry*, 38 (2003) 1451-6.
- [34] J.C. Ogbonna, H. Mashima, H. Tanaka, Scale up of fuel ethanol production from sugar beet juice using loofa sponge immobilized bioreactor. *Bioresource Technology*, 76 (2001) 1-8, PII: S 0 9 6 0 - 8 5 2 4 (0 0) 0 0 0 8 4 – 5.
- [35] G.C. Whiting, Organic acid metabolism of yeasts during fermentation of alcoholic beverages—A review. *Journal of the institute of Brewery*, 82 (1976) 84-92, <https://doi.org/10.1002/j.2050-0416.1976.tb03731.x>.

- [36] D.C.S. Rorke, T.N. Suinyuy, E.B. Gueguim Kana, Microwave-assisted chemical pre-treatment of waste sorghum leaves: Process optimization and development of an intelligent model for determination of volatile compound fractions, *Bioresource Technology*, 224 (2017) 590–600, <http://dx.doi.org/10.1016/j.biortech.2016.10.048>.
- [37] M. Pietruszka, K. Pielech-przybylska, J.S. Szopa, Synthesis of higher alcohols during alcoholic fermentation of rye mashes. *Food Chemistry and Biotechnology*, 1081 (74) (2010) 51-64, <http://hdl.handle.net/11652/258>.
- [38] E. Palmqvist, B. Hahn-Hägerdal, “Fermentation of lignocellulosic hydrolysates. I: inhibition and detoxification,” *Bioresource Technology*, 74 (1) (2000) 17–24, [https://doi.org/10.1016/S0960-8524\(99\)00160-1](https://doi.org/10.1016/S0960-8524(99)00160-1).

Chapter 7

7.0 Conclusions and recommendations for future studies

The application of nanobiotechnology in bioprocessing offers significant advantages over other nutrient supplement approaches in terms of efficient process performance due to nanoparticles' biotechnological properties. The ultimate goal of a fermentative bioethanol production system is to achieve high yield and contribute to an economically viable renewable energy system. Bioethanol production technology from renewable feedstock will contribute to the development of the global economy by facilitating a sustainable energy supply alongside the reduction in environmental pollution. In response to the rising demand for waste-based energy sources as green alternatives to fossil fuel energy sources, meaningful efforts to realise high yielding bioethanol production from waste using various techniques have been implemented. However, there is a significant knowledge gap on the effect of nanoparticle nutrient supplementation on the metabolic activities and kinetics of bioethanol production by *Saccharomyces cerevisiae*.

Thus, this study was undertaken with the aim of synthesising various metallic oxide nanoparticles and assessing their potential to improve bioethanol production on glucose and waste potato peel substrates. The research explored the impact of nanoparticles on the kinetic and metabolic activities as well as the inhibitory metabolite profile of fermentative bioethanol production using *S. cerevisiae* BY4743. Additionally, the viability of a preliminary scale-up of the optimized process was evaluated. This research has extensively explore nano-biocatalyst potential in fermentative bioethanol production from waste potato peels. The major findings of this study and their significance are summarised below:

Nine metallic oxide nanoparticles were synthesised, characterised and evaluated for their catalytic potential to promote bioethanol production by *S. cerevisiae* BY4743. Upon analysis, five of these nano oxides employed positively impacted bioethanol fermentation. The obtained data proved that the inclusion of nanoparticles in batch fermentative bioethanol production with

glucose as substrate does indeed improve process performance and thus bioethanol productivity. The inclusion of NiO NPs, Fe₃O₄ NPs, CuO NPs, CoO and ZnO NPs had a significant impact on bioethanol productivity and yield. Much of the biocatalytic potential demonstrated by these nanoparticles is attributed to higher chemical reactivity associated to their high surface area, providing a greater number of reaction sites. The desirable outcome obtained was also linked to the pH stability resulting from nano-enhanced buffering capacity which maintained the culture under optimum physiological state of the fermenting yeast for efficient metabolic and enzymatic activities. An additional reason might be ascribed to nanoparticles' positive interaction with glucose – glucose hydrophobic unit is adsorbed onto the surface layers of NPs by Van der Waals forces, coupled with strong affinity of microbes and nanoparticles influenced by electrostatic considerations of the process. A degree of electrochemical heterogeneity and the amine groups on cell surface proteins enhanced substrate uptake by the cells and ultimately improved process productivity as observed in this study. In addition, the impact of nanoparticles on the process may be ascribed to reduced oxidation-reduction potential (ORP) in the fermentation processes with nanoparticle inclusion, providing a relatively good start-up environment for bioethanol formation.

From a techno-economical perspective, there is a need to consider low-cost substrate source for the nano-fermentation process. Compared to lignocellulosic waste feedstock, a substrate such as pure glucose is an expensive option for the industrial production of bioethanol. The use of starchy lignocellulosic waste feedstock such as waste potato peels could lower the cost of bioethanol production due to their abundance, sustainability and renewability. Hence, waste potato peels were assessed as feedstock in the simultaneous saccharification and fermentation with nanoparticle inclusion as a biocatalyst. Nanoparticles were included at different stages of simultaneous saccharification and fermentation (SSF) of waste potato peels for bioethanol production. The productivity and the yield were substantially enhanced with NiO NPs inclusion

from the pre-treatment stage, as well as Fe₃O₄ nanoparticle inclusion at the liquefaction stage.

These might be attributed to the following:

1. improved activities of liquefying and saccharifying enzymes resulting in an enhanced fermentable sugar recovery;
2. increased fermentative capacity and productivity due to higher growth rates due to improved respirofermentative cellular activities in the presence of these nanobiocatalysts;
3. nanoparticles transportation across the cell improving glycolytic rate that goes beyond the pyruvate dehydrogenase reaction which generates an overflow towards pyruvate decarboxylase, thus increasing *S. cerevisiae* affinity for glucose and invariably increased bioethanol production.

The presence of metallic oxide nanoparticle in the hydrolysis of waste potato peels promotes substrate hydrolysis and the overall efficiency of bioethanol production processes observed from the results compared to fermentation process without nanoparticle inclusion. High conversion efficiency on substrates coupled with desirable bioethanol yields made nanoparticle inclusion in bioethanol fermentation process a suitable and promising approach for industrial application. However, to further improve the process performance and the industrial production viability, process optimization, metabolic and inhibitory metabolite profiling of the nano supplemented fermentation is needed. This is necessary due to the sensitivity of metabolic fluxes to process input parameters. Hence, it is vital to ensure that optimum process conditions are determined for maximum bioethanol production rate and yield.

The combined nanoparticle concentration, substrate concentration, pH and temperature on bioethanol production was therefore, modelled and optimized using the Response Surface Methodology (RSM), a modelling technique that combines both mathematical and statistical

functions to establish the relationship between a controllable set of empirical factors and the observed response. RSM provides information on the relationship between the experimental variables and the process response. The model suggested optimal process set points of 0.05 wt%, 10 g/L, 4.86 and 32.25 °C respectively that promoted *S. cerevisiae* metabolic activities and bioethanol productivity. Analysing the pairwise interactive effects of the process inputs (nanoparticle concentration, pH, temperature and substrate concentration) and the obtained optimum process set points, clearly, resulted in increased bioethanol yield – an indication that the set points were suitable to achieve high bioethanol yield. Model validation gave 0.26 g/g bioethanol yield resulting in a 19% increase. These findings could pave the way for large-scale bioethanol production process by offering reliable nano-catalysed fermentation data. The scaling-up of bioethanol production process will accelerate its commercialisation and contribute to the global sustainable bioenergy supply. Hence, it is crucial to conduct findings on scale-up viability to fully understand the process complexities of bioethanol-producing fermentation processes from these optimized process conditions.

Moreover, process modelling tools such as kinetic models employed in this study provided significant knowledge on the biochemical kinetics of bioethanol production in the presence of nanobiocatalyst. The logistic function, Monod and modified Gompertz kinetic models gave coefficient of determination (R^2) values ≥ 0.88 , which indicated that the sample variation of 88% was attributed to the independent factors and only 12% of the total variation was not explained by these models. This observation shows that the models were suitable to adequately describe the actual relationship among the different operational input conditions.

Furthermore, the kinetic data showed a significant improvement in *S. cerevisiae* affinity for available substrate and growth rate with nano-sized metallic oxide inclusion in the fermentation process. Higher values of maximum specific growth (μ_{max}) and affinity constant ($1/K_s$) observed for the nanoparticle-supplemented process further demonstrated the suitability of NPs

as potential biocatalytic additives to improve glucose uptake and improve cell metabolic activities. The obtained μ_{max} (0.33 h^{-1}) values in the current study were desirable, particularly for commercial scale-up, since growth rates above 0.025 h^{-1} have been shown to linearly increase the fermentative capacity of *Saccharomyces* spp. Moreover, the influencing impacts of nanoparticles on *S. cerevisiae* metabolic activity are ascribed to their cellular uptake and integration with the metabolic intermediates and key enzyme activities.

Additionally, the protein and the carbohydrate accumulation resulting from *S. cerevisiae* metabolic activity showed an elevation in the protein content build-up. This could be related to nanoparticle-nutrient supplement shock protein formation as well as increase in the presence of specific enzymes to promote bioethanol production. Similarly, increase in cellular carbohydrate- alkali-labile, alkali-soluble and alkali-insoluble accumulation and availability might be related to the cells metabolic pathway and cells' metabolic flux from nanoparticle metallic ion interaction with biological macromolecules of the fermenting cells.

Nanoparticle inclusion in fermentative bioethanol production resulted in significant repression of volatile metabolite compound formation. This repression can be ascribed to metal complex formation from chelating of metallic-nano by microbial metabolites released in the nano-supplemented fermentation, preventing the accumulation of inhibitory metabolites. These metabolite compounds profile includes inhibitors such as dimethyl trisulfide, acetic acid, furfural, 1-Hydroxy-2-propanone, furfural, 5-Methyl-fufural, 5-Hydroxymethylfufural (HMF), phenol, levulinic acid and formic acid. Likewise, this inhibitory metabolite repression can be attributed to the impact of nanoparticles on the enzymatic degradation of carbohydrates and bioethanol formation metabolic pathway of *S. cerevisiae* BY4743. Hence, a nano-based bioethanol production approach could be a vital strategy for the implementation of industrial bioethanol production from renewable waste feedstock.

Techno-economically viable bioethanol production from lignocellulosic biomass remains the main goal of renewable energy system development. Scaling up bioethanol production from lignocellulosic biomass from laboratory-scale to a production-scale could be challenging because of various important but different aspects involved. The main aspects of scaling up needed for an industrial scale production are the engineering, metabolic processes and economic implications. For these reasons, it is imperative to gain additional knowledge on cellular machinery, bio-reactor fluid-dynamics and engineering in order to accelerate the transition to industrial application. Consequently, experimental investigation on scaling-up processes is essential to provide more insights on these issues.

Hence, this research work undertook preliminary scale-up assessment of nanoparticle inclusion in simultaneous saccharification and fermentation of waste potato peels. Scaling up intricacies could considerably impact the process kinetics, process performances and consequently the process productivity. Scaling-up criteria of constant impeller tip speed (V_{tip}) and constant power consumption (P/V) were employed in this regard to obtain optimum process conditions towards high productivity. In this study constant power consumption (P/V) provided the most desirable process conditions and performance that favoured high bioethanol production. The intrinsic constant power consumption (P/V) scale-up criterion with a process condition of 95 rpm, Reynold number (Re) $5.14E + 06$, Power (P) 0.012 W, Power to Volume ratio (P/V_L) 2.4 W/m^3 , shear stress (γ) 950 S^{-1} and at $37 \text{ }^\circ\text{C}$, pH 5 gave a maximum bioethanol productivity of 1.10 g/L/h . High productivity was obtained due to the efficiency of the chosen criteria and the suitability of the implemented process conditions as well as optimum mixing efficiency attained in this research. Insufficient mixing has been identified as a major challenge in bioprocess scaling up. Desirable pumping capacity ($V_P = 3.9 \times 10^{-4} \text{ m}^3/\text{s}$) and circulation time ($t_c = 12.8 \text{ s}$) were attained in this study to achieve considerable process performance. Pumping capacity and circulation time are essential mixing properties that have been used to describe

efficient mixing behaviour in bioprocess. Thus, the scale-up results in this study provided significant insights on bioethanol production from waste potato peels with nanoparticle inclusion as biocatalyst towards achieving its commercialisation.

7.1 Recommendations for future studies

Screening a number of nanoparticles for biocatalytic potential in bioethanol fermentation process is an intricate process that requires the evaluation of many parameters. In this study it was demonstrated that the inclusion of nanoparticles as biocatalyst in bioethanol fermentation process improved metabolic and kinetic process performances and consequently bioethanol productivity. In order to improve on the catalytic efficiency of nanoparticles employed in this research, different surface modification could be evaluated to enhance their surface functional properties; biocompatibility, bioavailability and catalytic efficiency.

Additional research into the interaction of nanoparticles with biocomponents such as cellular carbohydrate and protein in this study would provide knowledge on the impact of nanoparticles on *S. cerevisiae* metabolic activities. For example to expand high-throughput knowledge on nanoparticles' interaction with cellular enzymes and other biocomponents such as glycerolipids, lysophospholipids, phospholipids, sphingolipid, sterols and plasma membrane fatty acids would be helpful in improving bioethanol formation and productivity.

Moreover, a broad screening of various lignocellulosic waste substrates for bioethanol production in the presence of nano additives would aid in identifying suitable feedstocks for industrial bioethanol production. Feedstock that requires less pre-treatment cost with high yield on substrate is desirable for industrial implementation of bioethanol production.

Furthermore, bioethanol fermentation process in the presence of nanoparticles as biocatalyst using continuous fermentation mode would promote the industrial desirability of this approach.

Finally, technoeconomic studies will provide data for strategic research and development investment and knowledge on the economic viability of bioethanol fermentation in the presence of nanobiocatalyst.